# Novel pDNA Particles for Pulmonary Administration.

A Thesis submitted to Cardiff University in accordance with the requirements for the degree of

**DOCTOR OF PHILOSOPHY**

Presented by

**Baljinder Kaur Bains M.Pharm., M.R.Pharm.S.**

Department of Drug Delivery

Welsh School of Pharmacy

Cardiff University

June 2010





ProQuest LLC
789 East Eisenhower Parkway
P.O. Box 1346
Ann Arbor, MI 48106-1346

*To my family*

## Acknowledgments

First and foremost, I would like to express my sincere appreciation to my academic supervisors Dr James Birchall and Dr Glyn Taylor for their insight, guidance, continued enthusiasm, advice and encouragement throughout this PhD study especially during the writing of this thesis. I am very grateful to my industrial supervisor Dr Richard Toon for his enthusiasm, comments and kind support.

I extend my gratitude to Cardiff University Welsh School of Pharmacy and 3M Healthcare Ltd. for the provision of funding for this research. I would also like to thank 3M Healthcare Ltd. for their generous gifts of valves, actuators and canisters and for the advice offered by the 3M staff during our meetings.

I am very appreciative of all the technical support given by Julian Menai-Purnell and the staff at the Welsh School of Pharmacy. I would like to thank Dr Cuong Hoa Tran for his assistance and practical advice especially at the start of the study.

I am indebted Dr A. Hann and Mr Guy Pitt for their assistance with the electron microscopy studies.

I must also acknowledge the numerous colleagues and friends I have made throughout my three years both inside and outside of the department, especially Anja Schermann, Barbara Torrisi, Federica Pinto, Hanif Zulfakar, Jeff James, Keng Wooi Ng, Lau Wing Man, Marc Pearton, Rebecca Price-Davies and Tina Kamma-Lorger. It has been a pleasure working and socialising with you.

Finally, the completion of this PhD would not have been possible without the emotional support of my family (Team Bains) their unwavering patience and belief in me truly got me through the darkest of days. I am forever grateful.

## Summary

Aerosolised DNA administration could potentially advance the treatment of inheritable lung diseases and lung malignancies and provide genetic immunisation against infection. Pressurised metered dose inhalers (pMDIs) offer a potentially efficacious and pragmatic, although unexplored, means for pDNA delivery. The aim of this thesis was to investigate the potential of a novel low-energy nanotechnology process, to prepare surfactant-coated pDNA particles for pulmonary gene delivery via pMDI technology.

Following process optimisation using salbutamol sulphate as the model drug, water-in-oil microemulsions containing pEGFP-N1 reporter plasmid were investigated using carbohydrate lyoprotectants in aqueous solution, lecithin:propan-2-ol (surfactant) and iso-octane (organic phase). Resultant microemulsions were snap-frozen in liquid nitrogen and lyophilised. Agarose gel electrophoresis with ethidium bromide staining revealed that pDNA integrity was retained after lyophilisation and reduction of excess surfactant by organic solvent. pDNA particles were incorporated into pMDI formulations containing hydrofluoroalkane 134a (HFA134a) propellant and ethanol as co-solvent. A549 human lung epithelial cells were exposed to pMDI aerosolised pDNA particles with dioleoyl-trimethylammonium propane (DOTAP) in the culture medium. Cellular gene expression studies demonstrated that pDNA biological functionality was maintained whilst an *in vitro* toxicity (MTT) assay showed no significant loss of cell viability following pMDI aerosolised pDNA treatment. Subsequent investigations incorporating DOTAP transfection agent into pDNA pMDI formulations demonstrated a proof-of-concept that aerosolised pMDI DOTAP-pDNA formulations can confer significant cellular gene expression with the potential for pulmonary gene delivery.

Methods have been successfully developed and evaluated to aerosolise surfactant-coated pDNA particles and maintain pDNA viability. Furthermore, investigations have demonstrated that the pDNA particles and a transfection agent (DOTAP) can be incorporated into a generic HFA134a formulation and successfully aerosolised using a standard valve and actuator. Further studies demonstrated the performance of these formulations after four week accelerated stability conditions.

## Table of Contents

## List of Figures

## List of Tables

## Abbreviations

| | |
|---|---|
| µg | Micrograms |
| µl | Microlitres |
| µm | Micrometres |
| AAT | α-1 antitrypsin |
| ACI | Andersen-type cascade impactor |
| ANOVA | Analysis of variance |
| AUC | Area under the curve |
| AVS | Andersen viable sampler |
| AAVS | Abbreviated Andersen viable sampler |
| bp | Base pairs |
| cDNA | Chromosomal deoxyribonucleic acid |
| CFC | Chlorofluorocarbons |
| cm | Centimetres |
| CMV | Human cytomegalovirus promoter |
| CPP | Critical packing parameter |
| CTAB | Cetyltrimethylammoniumbromide |
| DMEM | Dulbecco's Modified Eagle's Medium |
| DNA | deoxyribonucleic acid |
| DOSPA | 2,3-dioleyloxy-*N*-[2(sperminecarboxaminino)ethyl]-*N*,*N*-dimethyl-1-propanaminium |
| DOTAP | 1,2 dioleoyloxypropyl-3 (trimethylammonium)- propane |
| DOTMA | N-[1-(2,3-dioleoyloxy)propyl]-N,N,N-trimethylammonium chloride |
| DPI | Dry powder inhaler(s) |
| dsDNA | Double stranded deoxyribonucleic acid |
| *E. coli* | *Escherichia coli* |
| ECD | Effective cut-off diameter |
| ED | Emitted dose |
| EDTA | Ethylenediaminetetraacetic acid |
| EGFP | Enhanced green fluorescent protein |
| EHD | Electrohydrodynamic |

| | |
|---|---|
| EPF | Extra fine particle fraction |
| EtBr | Ethidium bromide |
| FEP | Fluorinated ethylene propylene |
| FPF | Fine particle fraction |
| g | Grams |
| GFP | Green fluorescent protein gene |
| GSD | Geometric Standard Deviation |
| HFA | Hydrofluoroalkane |
| HLB | Hydrophile-lipophile balance |
| HPLC | High performance liquid chromatography |
| hr | Hours |
| IS | Internal standard |
| kb | Kilobase pairs |
| l | Litres |
| LB | Luria-Bertani |
| Lipoplex | Lipid-DNA complex |
| LPD | Lipid:protamine:pDNA |
| MCS | Multiple cloning site |
| mg | Milligrams |
| min | Minutes |
| ml | Millilitres |
| MLV | Multilamellar vesicles |
| mm | Millimetres |
| MMAD | Mass Median Aerodynamic Diameter |
| MMI | Marple-Miller impactor |
| mN | Milli Newtons |
| MOUDI | Micro-orifice uniform deposit impactor |
| MSLI | Multi-stage liquid impinger |
| MTT | 3-[4, 5–dimethylthiazol-2-yl]-2, 5-diphenyl tetrazolium bromide |
| n | Number of replicates |
| ng | Nanograms |
| NGI | Next generation impactor |

| | |
|---|---|
| nm | Nanometres |
| o/w | Oil-in-water |
| PBS | Phosphate buffered saline |
| pDNA | Plasmid deoxyribonucleic acid |
| pEGFP-N1 | Plasmid enhanced green fluorescent protein |
| PEG | Polyethyleneglycol |
| PET | Polyethylene terephthalate |
| pg | Picograms |
| pMDI | Pressurised metered dose inhaler(s) |
| RNA | Ribonucleic acid |
| rpm | Revolutions per minute |
| RSD | Relative standard deviation |
| sd | Standard deviation |
| sec | Seconds |
| SEM | Scanning electron microscopy |
| SS | Salbutamol sulphate |
| SOC | Super optimal broth with catabolite repression medium |
| SUV | Small unilamellar vesicles |
| T25 | 25 $cm^2$ angled neck, cell culture flasks |
| TBE buffer | Tris-borate EDTA buffer |
| TE buffer | Tris-EDTA buffer |
| TEM | Transmission electron microscopy |
| Tg | Glass transition temperature |
| TGLD | Task group on lung dynamics |
| TSI | Twin stage impinger |
| USP | United States of America pharmacopoeia |
| UV-vis | Ultraviolet-visible |
| v/v | Volume/volume |
| VS | Andersen six stage viable sampler |
| w/o | Water-in-oil |
| w/v | Weight/volume |
| w/w | Weight/weight |

# CHAPTER ONE

# Introduction

Pulmonary administration of nucleic acids may be particularly relevant for treating localised lung disorders of genetic origin (Driskell and Engelhardt 2003; Birchall 2007). Disease states such as cystic fibrosis and α-1 antitrypsin (AAT) deficiency have been favoured as early targets for treatment by inhaled gene therapy as both are monogenic disorders, therapy would therefore involve correction of the single malfunctioning gene by the introduction and expression of its correct copy to restore normal function (Riordan *et al* 1989; Brantly *et al* 2006). Other possible candidates for pulmonary gene therapy include lung malignancies. Gene therapy for lung cancer would involve for example, blockade of activated tumour-promoting oncogenes or replacement of inactivated tumour-suppressing genes (Zou *et al* 2007; Choi *et al* 2008). The pulmonary route would also be appropriate for the delivery of inhaled DNA vaccines, as this would follow the natural route of infection for many common airborne diseases (Bivas-Benita *et al* 2005; Lu and Hickey 2007), such as measles (Fennelly *et al* 1999), *Mycobacterium tuberculosis* (Bivas-Benita *et al* 2004) and respiratory syncytial virus (Harcourt *et al* 2004). The advantage of gene therapy includes its potential for treating diseases for which there is no effective treatment to date, such as cystic fibrosis (Riordan 2008; Griesenbach and Alton 2009). Additionally, gene therapy offers the ability to selectively recognise molecular targets. This specificity of action offers the possibility for reduced toxicity and side effects (Patil *et al* 2005). Aerosolised gene therapy provides a direct, non-invasive means for targeted delivery to the lung, with the potential for delivering a high dose to the target site of pulmonary based disorders (Birchall 2007).

The success of therapeutic strategies using genetic material depends on the efficiency of systems for the delivery of nucleic acids into the target cells. Whilst it is established that nucleic acid therapy can correct genetic defects in diseased cells (Rich *et al* 1990), cellular uptake of naked deoxyribonucleic acid (DNA) in its native form remains relatively inefficient (Zabner *et al* 1997; Remaut *et al* 2006). Thus, therapy is a formulation and delivery quandary where success requires optimisation of both transfection and drug delivery

strategies. As a consequence, gene transfer vectors are employed to promote cellular uptake and processing of the nucleic acid cargo (Remaut *et al* 2006; Davies *et al* 2008; Jiang *et al* 2008). Gene transfer vectors fall into two groups, viral gene vectors and non-viral gene vectors.

Viruses have the natural ability to infect cells efficiently and consequently a number of recombinant viruses, which carry the therapeutic chromosomal DNA within their genome, have been exploited for delivering genes into eukaryotic cells (Kay *et al* 2001). Examples of such viral vectors include the lentivirus (Limberis *et al* 2002), adenovirus (Perricone *et al* 2001), and adeno-associated virus (Moss *et al* 2004, 2007). Although viral gene delivery systems are often very efficient at stimulating cell transfection and can be modified to reduce both their pathogenicity and ability to replicate, they still face inherent safety and immunogenicity issues and are sometimes inappropriate for repeated use (Thomas *et al* 2003).

As an alternative, non-viral gene vectors employ synthetic carriers that complex with plasmid DNA (pDNA) to form particulates that are generally regarded as safer and less immunogenic (Li and Huang 2007), although not as efficient as viral vectors (Ferrari *et al* 2003; El-Aneed 2004). In this category of non-viral agents, cationic lipids and liposomes have demonstrated proof-of-principle for gene transfer to the airway for over two decades (Stribling *et al* 1992; Alton *et al* 1993; McDonald *et al* 1998). Whilst impressive results have been achieved in some animal models including mice (Alton *et al* 1993; Hyde *et al* 1993), rats (Rosenfeld *et al* 1992; Logan *et al* 1995), rabbits (Canonico *et al* 1994), monkeys (McDonald *et al* 1998) and pigs (Cunningham *et al* 2002), non-viral gene transfer has yet to deliver a clear therapeutic benefit in human studies. For example, although correction of the chloride transport defect in cystic fibrosis has been demonstrated to some extent in a number of clinical trials (Alton *et al* 1999; Moss *et al* 2007), the level of effect has been found to be variable, usually lasting for less than 15 days (Hyde *et al* 2000; Ruiz *et al* 2001). Clinical trials using gene therapy have also been undertaken in an

attempt to restore normal AAT function. This involved either nasal instillation of the AAT gene with a cationic liposome (Brigham *et al* 2000), or intramuscular injection of the gene with a viral vector (Brantly *et al* 2006). As with the cystic fibrosis trials, although proof-of-principle of successful gene expression has been demonstrated, there was a notable lack of significant functional correction.

It is accepted, therefore, that the development of more efficient vectors is essential for the progression of gene delivery science towards the clinic (Ferrari *et al* 2002; Moss *et al* 2007; Ratjen 2008). Equally, however, the administration method selected to deliver the therapeutic material to the cellular target is of paramount importance, yet is often overlooked. The efficiency of delivery to the cell targets, the avoidance of biological barriers and clearance mechanisms (Agu *et al* 2001), the physical and chemical durability of the nucleic acid cargo during delivery (Birchall 2007) and the manageable dose are all critical parameters that require optimisation (Robinson *et al* 2000).

## 1.1 Pulmonary Delivery Devices

Pulmonary drug delivery devices can be broadly classified into three main categories; (i) Nebulisers convert aqueous drug solutions or micronized suspensions into aerosols by the use of compressed air or ultrasonic energy, (ii) Dry powder inhalers (DPI) deliver solid aerosolised particles of the drug, produced most commonly from the action of the patient inhaling deeply with the inspiratory air flow passing through a powder mixture of micronised drug and a carrier such as lactose, (iii) Pressurised metered dose inhalers (pMDI) produce aerosolised drug from the evaporation of propellant.

pMDI systems, the delivery method utilised in this thesis, typically contain a drug formulated as a solution or suspension within a propellant or blend of propellants maintained under pressure as liquefied gases. The basic components of a pMDI inhaler include a canister, a metering valve and

actuator (Figure 1.1). The canister is sealed by the metering valve, the stem of which sits in the body of the actuator. On depression of the metering valve stem, the metering chamber undergoes a pressure drop due to exposure with atmospheric pressure. This initiates the propulsion of a fixed volume of formulation from the metering chamber into the expansion chamber, where the propellant flash boils causing a mixture of vapour and liquid to form before passing through the actuator spray orifice. The aerodynamic shear between the liquid and vapour phases of the mixture as they exit the spray orifice result in the formation of droplets (Clark 1996). As the aerosolised droplets move away from the actuator, the heat of the surrounding air causes the propellant to evaporate leaving aerosolised drug particles.

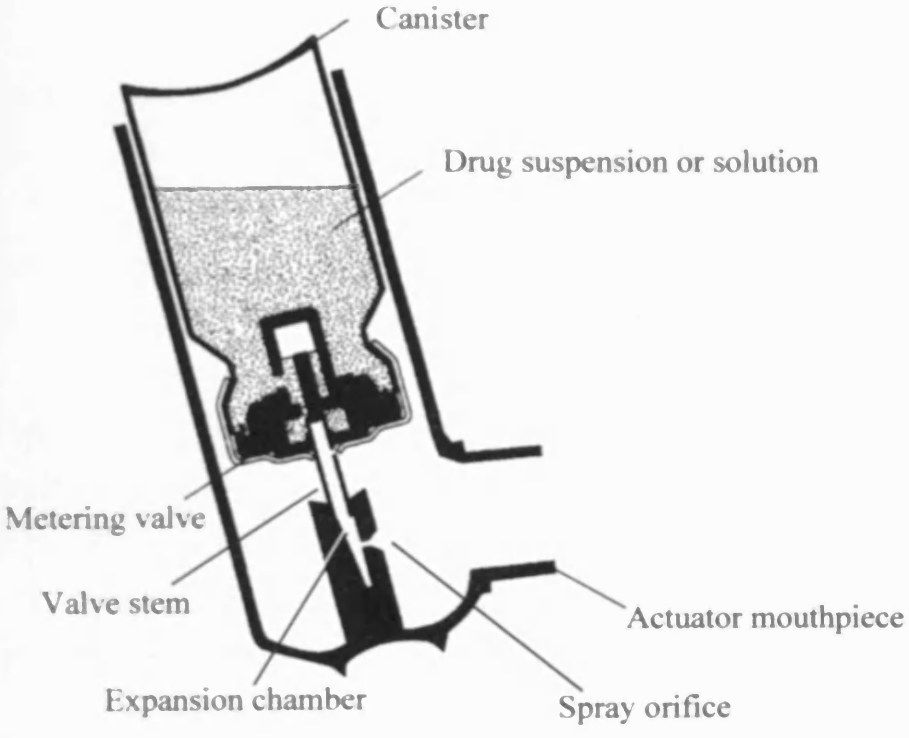


**Figure 1.1 A schematic representation of a typical pMDI.** Adapted from O'Callaghan and Wright (2002).

## 1.2 Pulmonary Gene Therapy

To date, most pre-clinical and clinical research studies in pulmonary gene therapy have used nebulisers to deliver the gene 'cargo' in liquid suspension (Alton *et al* 1999; Moss *et al* 2004, 2007). Nebulisation is, however, an

inherently inefficient process for the delivery of large charged macromolecules (Arulmuthu *et al* 2007; Lu and Hickey 2007) due to; adhesion of the formulated therapeutic agent to the device components, large residual dead volume, limitations on suspension concentration without causing precipitation, chemical degradation through high shearing forces (Birchall *et al* 2000; Lentz *et al* 2006a; Arulmuthu *et al* 2007) and evaporation (Hyde *et al* 1993).

Conventional jet and ultrasonic nebulisers have both been reported to extensively damage naked pDNA due to the shearing forces generated on creation of the aerosol (Kleemann *et al* 2004; Lentz *et al* 2005; Lentz *et al* 2006a). Relatively newer nebuliser technologies have claimed greater pDNA aerosolisation efficiency (Davies *et al* 2005). Aerosolisation, based on electrohydrodynamic (EHD) delivery for example, has been found to cause no detectable pDNA degradation or loss in transfection efficiency in plasmids up to 15 kb in size (Davies *et al* 2005; Lentz *et al* 2006b). Additionally the eFlow® electronic nebuliser has also shown potential for delivering nucleic acids (Bitterle *et al* 2006). Whilst these encouraging new generation nebuliser technologies are under development, DPIs have shown promise in gene delivery. Aerosolised gene based DPI formulations have been shown to produce powders of a respirable size range whilst maintaining significant *in vitro* transfection (Li *et al* 2005a; Li and Birchall 2006). However, DPI formulations can succumb to hygroscopic and agglomeration issues which can result in reduced inhaler performance, drug degradation and changes in the particle size distribution (Byron 1990).

pMDIs offer a sparsely investigated alternative to nebulisers and DPI. Potential advantages of pMDIs over other pulmonary delivery systems include their portability, low cost, rapid drug administration and disposability (Dolovich *et al* 2005). Many doses can be stored in a relatively small canister and the metering valve ensures reproducible dose delivery. pMDIs offer a more convenient alternative to nebulisers, especially for therapies requiring repeated administration.

To date, there has been very little published research on methods for incorporating pDNA into pMDIs. Brown and Chowdhury (1997), demonstrated that pDNA, lyophilised in the presence of a both non-ionic (Tween 40) and ionic surfactant (lipofectin or lipofectamine), could be incorporated into a metered-dose inhaler resulting in suspended pDNA particles in dimethylether propellant. In addition, they demonstrated that gene expression could be obtained in the lungs of mice following exposure to the aerosolised pDNA formulation (Brown and Chowdhury 1997). Clearly, further investigations in this area are warranted.

## 1.3 Macromolecule Particle Preparation Methods

Macromolecule particles have been prepared for DPI or pMDI systems using a variety of methods used to dehydrate the formulation including; spray-drying (Li and Seville 2009), freeze-drying (Maitani *et al* 2008), spray freeze drying (Maa *et al* 1999) and supercritical drying (Bustami *et al* 2003). However, although a variety of methods are available, macromolecule powders are generally manufactured using one of two methods;

Spray-drying, a one step process, involves the atomisation of a liquid sample into a spray of droplets and evaporation of the droplets using hot air conditions to form dried particles. The process of spray-drying has been used in the food industry to prepare spices and flavourings. In the context of the pharmaceutical industry, spray-drying has been applied to the preparation of dry powder antibiotics (Broadhead *et al* 1992). This process has attracted some interest as a technique to prepare macromolecules such as proteins (Maa *et al* 1999; Liao *et al* 2005) and DNA for inhaled therapy (Li *et al* 2005a). Spray-drying has been found to offer potential advantages as the process has been shown to generate stable, efficient and potentially respirable protein and DNA/lipid powders (Seville *et al* 2002; Colonna *et al* 2008; Li and Seville 2009). However, large quantities of the drug are required to produce a sufficient powder yield, leading to high costs (Bosquillon *et al* 2004; Li *et al* 2005a). There is also potential for shear-induced and thermal degradation of macromolecules (Mumenthaler *et al*

1994; Ståhl *et al* 2002).

Freeze-drying, also known as lyophilisation, is a dehydration process which comprises three stages, freezing, primary drying and secondary drying. Briefly, the process of freeze-drying involves initially freezing the sample often by submersion into liquid nitrogen. Following freezing the sample is then dried by applying temperatures and pressures to promote sublimation and subsequent removal of solvent from the solid phase directly into the gaseous phase.

In the past, the process of freeze-drying has been used in the food industry to prepare instant coffee and preserve foods such as dried fruit. In the context of the pharmaceutical industry, freeze-drying is the most commonly used method to increase the shelf life of injectables such as vaccines by dehydrating the samples which can be later reconstituted prior to use (Amorij *et al* 2008; Prego *et al* 2010).

Freeze-drying is a commonly employed manufacturing strategy for thermolabile macromolecules. It is particularly suited to the preparation of thermolabile powders as the process avoids denaturation caused through heating the thermolabile product, by working on the principle of sublimation using low temperatures and reduced pressures (Seville *et al* 2002; Prego *et al* 2010).

The method of freeze-drying has been used to prepare macromolecules such as proteins for inhaled therapy (Brown and George 1997; Williams III and Liu 1999; Nyambura *et al* 2009a, b). More recent studies have shown lyophilised DNA/lipid systems, in the presence of a lyoprotectant, to preserve their physicochemical properties and *in vitro* transfection activity after rehydration (Seville *et al* 2002; Maitani *et al* 2008).

However, lyophilised powders are often found to be unsuitable for pulmonary delivery due to inadequate control of particle size distribution achieved during

the freeze-drying process (Seville *et al* 2002). Further processing using a milling step, necessary to render particles into dimensions suitable for inhalation, is potentially damaging to macromolecules due to localised heat generation and destructive of the solid state properties of many pharmaceuticals (Shoyele and Cawthorne 2006; Murnane *et al* 2008).

### 1.3.1 Preparation of Particles for pMDI

The lyophilisation technique has been previously reported to produce particles outside the respirable size range. Dickinson *et al* (2001), however, proposed an alternative approach, comprising a lyophilisation step, to produce nanoparticles suitable for incorporation into pMDI systems. Their nanotechnology process utilised the nanoparticle size range of water droplets dispersed in the oil phase of a reverse microemulsion as a 'template'. These swollen reverse micelles containing a low molecular weight drug were then reduced to surfactant-coated nanoparticles using the process of lyophilisation. The technology proposed by Dickinson *et al* (2001) offers potential advantages as it is able to 'capture the microemulsion template, dehydrate and form the nanoparticle in one step' without the use of additional milling steps. This technique has a relatively low risk of toxicity, is ideal for formulating thermolabile drugs for the reasons mentioned earlier and offers the potential for industrial scale-up and development.

More recently the lyophilisation of carefully prepared emulsions has been used to formulate macromolecules into nanoparticles suitable for pMDI systems (Nyambura *et al* 2009a, b). However, emulsions inherently require a larger input of energy to form than microemulsions (Schulman and Cockbain 1940; Capek 2004). The energy input in the form of mechanical agitation required to prepare emulsions can expose macromolecules to high shear stress with the potential for their degradation. This limitation is not encountered when working with microemulsions which spontaneously form thermodynamically stable systems (Gillberg *et al* 1970). For these reasons, the process proposed by Dickinson *et al* (2001) is worthy of further investigation to ascertain its

potential in preparing macromolecule nanoparticles, such as pDNA, suitable for incorporation into pMDI systems. Such investigations were carried out in this thesis.

### 1.3.2 Nanoparticles

Nanoparticles are generally regarded as colloidal particles which range in size from 10 nm to 1000 nm. They offer the potential to act as carriers for macromolecular drugs or biologically active materials which can be encapsulated, entrapped, dissolved or attached to the nanoparticle (Dickinson *et al* 2001; Grenha *et al* 2005; Cui *et al* 2006; de Martimprey *et al* 2009).

Particle size, density and hence aerodynamic diameter play a crucial role in governing the particle deposition within the respiratory tract (Figure 1.2) (Task group on lung dynamics 1966; Taylor and Kellaway 2001). Research has shown that as the particle size decreases the likelihood of deep lung penetration increases (Task group on lung dynamics 1966), and so it would follow that nanoparticles offer a great potential for improved pulmonary delivery. In fact, such properties have already been exploited as nanoparticles have been proposed for use as radiolabelled aerosols in lung ventilation scanning, where they offer deep penetration in the lung (Burch *et al* 1986).

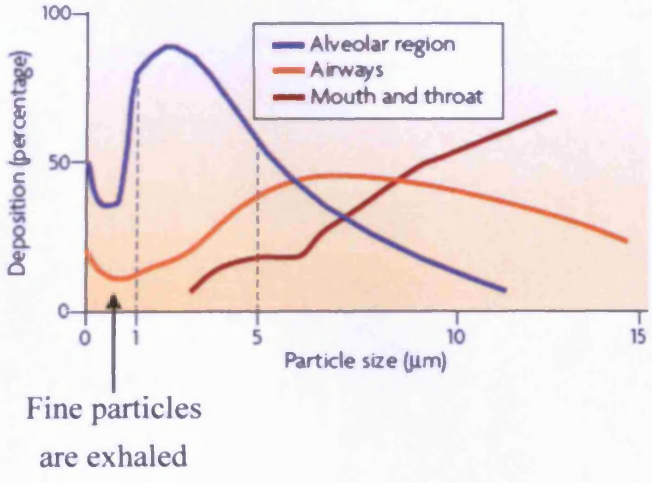


**Figure 1.2 The effect of particle size on the deposition of aerosol particles in the human respiratory tract following inhalation and a 5 sec breath hold.** Adapted from Patton and Byron (2007).

However although smaller particles can penetrate deeper into the lung, the effect of exhalation plays an important role on particle deposition (Figure 1.2). The utility of pulmonary delivered nanoparticles can therefore be hindered because of their low inertia, due to their small dimensions and mass, preventing the particle from depositing and making the particles prone to exhalation. The TGLD (Task group on lung dynamics 1966) reported dust particles ranging from 2-3 μm diameter have higher deposition values than smaller particles ranging from 0.2-0.5 μm. The work conducted by the TGLD emphasises that when designing a formulation, a balance between particle size and the effects of exhalation is required.

Nevertheless nanoparticles do offer potential advantages for achieving prolonged drug deposition in the alveolar region of the lung. A reason for this being that alveolar macrophages, which are responsible for engulfing 'foreign substances', can often reduce the particle retention time in the alveolar region. However, as phagocytic activity has been reported to decrease for particles smaller than 1 μm in size (Makino *et al* 2003), nanoparticles offer the potential of deep lung penetration, reduced macrophage uptake and potentially increased lung retention time.

Although the use of nanoparticles for inhalation offers significant advantageous, there is growing concern regarding the potential toxicity of these particles. It has been suggested that some nanoparticles are more toxic than their larger chemical forms due to the increase in their surface area leading to a greater biological activity (Donaldson *et al* 2000; Oberdorster 2000). The mechanism of action of nanoparticles in the lung is yet to be fully understood. Reports have suggested that poorly soluble nanoparticles such as ultrafine polymer fumes and asbestos retained in the lungs can cause oxidative stress, due to the presence of free radicals on the nanoparticles surface or by triggering the influx of defence cells and the release of various mediators such as chemokines and cytokines, leading to inflammation, fibrosis and cancer (Maynard and Kuempel 2005; Muller *et al* 2006). However, it is important to

note that toxicity data available so far on inhaled nanoparticles does not primarily concern therapeutic molecules and, therefore, is not directly applicable to inhalation therapies (Oberdorster *et al* 2005; Rogueda and Traini 2007a).

## 1.4 Particle Sizing

Particle sizing of aerosolised nanoparticle formulations is important for predicting pulmonary deposition. There are a variety of techniques available for aerosol particle sizing analysis in the pharmaceutical industry some of which are based on light scattering or inertial impaction.

Laser diffraction, a light scattering technique, can offer a rapid particle size analysis of aerosolised formulations (Ziegler and Wachtel 2005; Mitchell *et al* 2006). However, this technique has been criticised as it quantifies the droplet size distribution without reference to the drug mass content within the droplets of aerosolised suspensions (de Boer *et al* 2002; Mitchell *et al* 2006).

Inertial impaction techniques, however, directly measure aerodynamic particle diameter. The aerodynamic particle diameter is considered a relevant parameter used to indicate the likely deposition of a particle in the respiratory tract as it takes into account the influence of particle size, shape and density (Mitchell and Nagel 2003). The aerodynamic diameter of a particle is defined as the diameter of a sphere with unit density ($\rho = 1$), having the same terminal settling velocity in still air as the particle in consideration;

$$D_A = D_S \times \rho_\rho^{0.5}$$

Where $D_A$ = Aerodynamic diameter; $D_S$ = Stokes diameter;

$\rho_\rho$ = particle density

Inertial impactors, which are used to measure the aerodynamic particle diameter, are made up of a throat (and induction port) and one or more stages which contain particle collection plates. During testing, aerosol clouds

discharged from an inhaler are drawn through the impactor, with the aid of a vacuum set at a fixed flow rate which is connected to the outlet of the impactor. Impaction techniques rely on the separation of particles present in the aerosol plume by differences in their inertia. Once the inhaler is actuated, the aerosolised particles generated become entrained into the air stream. Large particles are likely to become disentrained and impact on the throat. The aerosol cloud is then drawn through successively smaller jets and at progressively increasing velocities, projected towards the adjacent impaction stages. As the larger particles at any particular velocity have greater inertia they are unable to remain entrained in the diverging air stream, caused by the 90 degree geometry between air-jet and collection plates and they impact on the plate. Smaller particles with a lower inertia remain in the air stream until their velocity increases and their inertia overwhelms entrainment. As the velocity of these smaller particles increases further down the impactor, the smaller particles begin to impact on the plates. Although the term impactor is reserved for instruments where particles impact on a dry impaction plate and the term impinger is used if the collection surface is liquid, the general principal of inertial impaction described above applies to both types of instruments.

A variety of impaction apparatus are available which include the twin stage impinger (TSI), multi-stage liquid impinger (MSLI), Marple-Miller impactor (MMI), next generation impactor (NGI), Micro-orifice uniform deposit impactor (MOUDI), Andersen cascade impactor (ACI) and Andersen viable sampler (AVS). Some of these apparatus are mentioned in more detail below.

The TSI comprises of a throat and two impingement chambers. Prior to testing 7 ml of solvent is dispensed into the upper impingement chamber and 30 ml into the lower chamber. The TSI divides the emitted dose from an inhaler into respirable and non-respirable fractions. During testing the proportion of aerosolised particles which impact on the throat and in the upper chamber (collectively termed Stage 1) are considered the non-respirable dose, whilst the

remaining particles which collect in the lower impingement chamber (Stage 2) are the respirable dose. After the test is complete, the drug collected in the lower impingement chamber is assayed and expressed as a respirable fraction of the delivered dose.

The TSI has value as a simple and inexpensive tool which offers the ability for rapid screening and quality assessment of aerosol products (Hallworth and Westmoreland 1987). However, although the TSI can characterise particles in terms of the non-respirable and respirable fraction, the apparatus is unable to provide particle size distribution data as more impaction stages are required.

Multi-stage cascade impaction apparatus such as the MSLI, NGI and ACI are extensively used for the *in vitro* determination of the aerosol particle size distribution and play an important role in product development, comparison of formulations and quality control of medicinal inhalers (Mitchell and Nagel 2003).

The MSLI comprises four impingement stages with cut-off diameters ranging from 1.7 to 13 μm. The MSLI can be used for determining the aerodynamic size distribution of particles aerosolised from pMDI, DPI and nebulisers (British Pharmacopoeia 2010b). Each stage of the MSLI, except the final filter stage, holds 20 ml of a suitable solvent termed the impaction medium. During testing, aerosolised particles will deposit on the impaction medium at various stages depending on their aerodynamic diameter based on the principle of inertia described earlier. The use of an impaction medium for particle collection is deemed advantageous as particle bounce and re-entrainment effects, often observed for particles impacting directly onto an impaction plate, are minimised (Ranz and Wong 1952). After the test is complete, the drug collected at the various stages can be assayed in order to determine the formulation particle size distribution profile.

The NGI comprises three main parts, a bottom frame which holds the cup tray containing particle collection cups, the seal body which holds the nozzles with successively smaller diameters and the lid that contains the inter-stage passageways (British Pharmacopoeia 2010b). The NGI has seven impaction stages with the cut-off diameters ranging from 0.23 to 11 μm. During testing, aerosolised particles will deposit on the collection cups at various stages depending on their aerodynamic diameter. Deposited particles are then collected by adding approximately 10 ml of a suitable solvent to each of the collection plates.

An ACI is an alternative multi-stage cascade impaction apparatus to the MSLI and NGI. The ACI which comprises eight stages can provide a higher resolution (or increased number of stages) than both the TSI and MSLI to characterise the emitted aerosol and for this reason was the choice apparatus for use in this thesis (Marple *et al* 1998; Van Oort and Truman 1998).

### 1.4.1 Andersen Cascade Impactor

The eight stage ACI, is a standard particle sizing device recognised in compendia (British Pharmacopoeia 2010b) and by regulatory authorities (EMEA 2002). Originally used to measure air-borne dust particles (Andersen 1966), the ACI is now widely used to characterise the aerodynamic particle size distribution of particles and droplets emitted from inhalers.

The Westech Andersen-type Mark II non-viable cascade impactor comprises eight stages that are used for separating the spectrum of aerosolised particles into two categories above 5.8 μm aerodynamic diameter and six categories below 5.8 μm aerodynamic diameter. The eight stages of the compactor each contain multiple precision drilled orifices, the holes becoming successively smaller from Stage 0 to Stage 7. Each stage holds a removable stainless steel plate, the plates used in Stage 0 and Stage 1 having a hole in the centre. Below the eight stages is a final filter stage which is used to capture particles which have escaped impaction. The eight stages are held together in a stack by three

spring clamps and sealed at each stage with rubber o-rings. A 90° aluminium USP-2 induction port (throat) is located at the top of the ACI and acts as an inlet to the device. The effective cut-off diameters for each stage of the ACI system are given in Table 1.1.

Table 1.1 Particle cut-off diameters using Mark II eight stage ACI at a flow rate of 28.3 l/min adapted from Andersen (1985).

| Stage | Effective cut-off diameter (μm) |
|---|---|
| 0 | 9.0 |
| 1 | 5.8 |
| 2 | 4.7 |
| 3 | 3.3 |
| 4 | 2.1 |
| 5 | 1.1 |
| 6 | 0.7 |
| 7 | 0.4 |

The ACI is well suited for characterising aerosols emitted from pMDIs as it is an efficient size-separator of particles in the range of 9.0 μm to 0.4 μm (Table 1.1). Particles that impact on the metal plates, found at each stage, can be collected and assayed. Testing with the ACI allows for the mass and particle size distribution of the aerosolized drug to be determined directly through analysis of each impaction stage.

Although ACIs are frequently used for *in vitro* particle size analysis, the data they generate can be limited when predicting *in vivo* deposition. Evidence that ACIs can be poor simulators of the respiratory tract has been presented by superimposing the collection efficiency curves for each stage of a ACI with that of the corresponding regions of the respiratory tract (Dunbar and Mitchell 2005). The results showed that the collection efficiency curves for the respiratory tract were relatively shallow compared to the ACI stages.

Parameters such as FPF can, therefore, often overestimate the true percentage deposition in the respiratory tract (Newman 1998). The disparity between the two sets of data is due to a number of differences. The stages of an ACI are more size selective compared to the various regions of the lung. Additionally the 90° inlet throat typically used in an ACI has been criticised as failing to reflect the 'complex geometry of the upper airways, which will have a significant "filtering" effect on the particles and droplet' (Miller and Purrington 1996; Newman 1998). Also ACIs do not simulate the temperature and relative humidity that exists in the respiratory tract. Both humidity and temperature are known to affect particle deposition, by influencing droplet growth and evaporation (Stein and Myrdal 2006). The differences in temperature and relative humidity between *in vitro* and *in vivo* models can therefore lead to inconsistency between the particle deposition data.

ACIs should not be considered as *in vitro* lung simulators for the aforementioned reasons. Nevertheless they can provide information on the size of particles based on their aerodynamic diameter which may be indicative of the likely deposition of particles in the lung. Additionally ACIs are a useful tool in product development where comparisons can be drawn between various devices and pMDI formulations' deposition profiles (Smyth 2003).

### 1.4.2 Andersen Viable Sampler (AVS)

The AVS offers a possible alternative to the ACI to measure the aerodynamic particle diameter of biological aerosols. The six stage AVS was first developed in 1958 (Andersen 1958) and was originally designed to measure the concentration and particle size distribution of viable aerobic bacteria and fungi. As the AVS directly measures aerodynamic particle diameter it is therefore able to indicate the likely deposition of biological aerosols in the respiratory tract (Mitchell and Nagel 2003). For this reason, this *in vitro* model has been utilised in predicting and assessing the health hazard or infection potential of biological aerosols to humans (Wendt *et al* 1980; Weis *et al* 2002; Fennelly *et al* 2004).

The AVS used for particle distribution analysis is available with either six or eight stages. The six stage AVS used in this thesis is constructed with six aluminium stages used for separating a spectrum of aerosolised particles. The sampler is often referred to as a multi-orifice impactor as each stage of the sampler contains 400 precision drilled orifices which are successively smaller from Stage 1 to Stage 6. Each stage holds a removable petri dish containing an impaction medium. The six stages are held together in a stack by three spring clamps and sealed at each stage with rubber o-rings. The effective cut-off diameters for each stage of the AVS are given in Table 1.2.

Table 1.2 Particle cut-off diameters using Andersen six stage viable sampler at a flow rate of 28.3 l/min adapted from Andersen (1958).

| Stage | Effective cut-off diameter (μm) |
|---|---|
| 1 | 7.00 |
| 2 | 4.70 |
| 3 | 3.30 |
| 4 | 2.10 |
| 5 | 1.10 |
| 6 | 0.65 |

To date the use of an AVS for characterising aerosolised particles emitted from an inhaler system has not been reported in published work. However the AVS offers a number of potential advantages for sizing biological particles such as aerosolised pDNA. As the viable sampler is based on particle impingement onto a liquid collection surface, it is ideal for collecting particles whilst minimising particle bounce and re-entrainment, effects which can be observed for particles impacting directly onto an impaction plate (Ranz and Wong 1952). Also judicious selection of the impaction media means that aerosolised particles can deposit directly into the media used to treat cells during cellular gene expression studies, minimising the possibility of sample loss through insufficient plate washing a possibility faced with the ACI. The AVS offers advantageous over alternative impingers as it comprises a larger number of

collection stages than for example the TSI and MSLI, offering a higher resolution of particle characterisation. Additionally the total volume of impaction media used in the AVS (48 ml) is lower than that used in the MSLI (80 ml) which is crucial to prevent any dilution effect during quantification of deposited pDNA particles using cellular transfection methods.

## 1.5 Scope of Thesis

Nebulisers and DPIs are currently the most used devices for aerosolising pDNA in pre-clinical and clinical studies. As limitations for both of these devices have been reported, the pMDI offers a potential alternative. The incorporation of pDNA into a pMDI system for pulmonary administration is a sparsely investigated area of research due to the inherent challenges of formulating and maintaining pDNA stability. A novel approach to preparing pMDI formulations proposed by Dickinson *et al* (2001) has been demonstrated to produce surfactant-coated nanoparticles suitable for incorporation into a pMDI system. As this formulation technology has only been proven with a low molecular weight drug, this thesis will aim to research the potential of developing the technology to formulate surfactant-coated pDNA particles suitable for incorporation into a pMDI system. Since the native structure of macromolecules is susceptible to damage during processing conditions, utilising the nanotechnology process will bring about new formulation challenges previously not faced when dealing with small molecular weight drugs. The work carried out in this thesis will attempt to address these challenges and investigate whether it is viable to aerosolise and deliver biologically active surfactant-coated pDNA particles via a pMDI with potential for pulmonary gene delivery.

These overall aims of the thesis will be addressed through the experimental work divided into the following chapters;

Chapter 2: This chapter will aim to validate, optimise and develop stages of the nanotechnology process using a model drug. Investigations will be carried out to develop an optimised surfactant microemulsion system based on HLB and HFA solubility to confer drug stability and dispersion in a pMDI system. The potential for achieving effective pulmonary delivery from the aerosolised pMDI formulation will be predicted using an *in vitro* cascade impaction model.

Chapter 3: The utility of the developed technology will be investigated for

preparing surfactant-coated pDNA particles. Attempts to maximise pDNA integrity during processing through the use of lyoprotectants and freezing rates will be explored.

Chapter 4: The feasibility of incorporating surfactant-coated pDNA particles into a pMDI system to deliver biologically active pDNA following aerosolisation will be examined. The biological efficiency of the aerosolised pDNA formulation will be assessed by quantifying gene expression in an *in vitro* cellular model.

Chapter 5: As gene transfer vectors are commonly utilised to promote pDNA cellular transfection, this chapter will investigate the feasibility for incorporating a transfection agent into the pDNA pMDI formulation and will assess formulation stability during storage. Further to this, aerosolised particles will be characterised through aerodynamic particle size distribution profiles generated using an *in vitro* cascade impaction model.

# CHAPTER TWO

# Process Optimisation

## 2.1 Introduction

A novel process for preparing hydrophilic drug nanoparticles, from small molecular weight drugs, suitable for dispersion in hydrofluoroalkane (HFA) propellant was originally outlined as a proof-of-principle by Dickinson *et al* (2001). The approach utilised a reverse microemulsion as a 'template' (Figure 2.1), where the hydrophilic drug, for example salbutamol sulphate (SS), was incorporated into the water phase of a water in oil (w/o) microemulsion. Reverse micelles containing the drug were subsequently reduced to solid surfactant-coated nanoparticles using lyophilisation, prior to pressure filling with HFA 134a propellant into a pMDI. In this chapter we aim to further optimise this process and evaluate its potential for achieving effective pulmonary drug delivery from pMDIs.

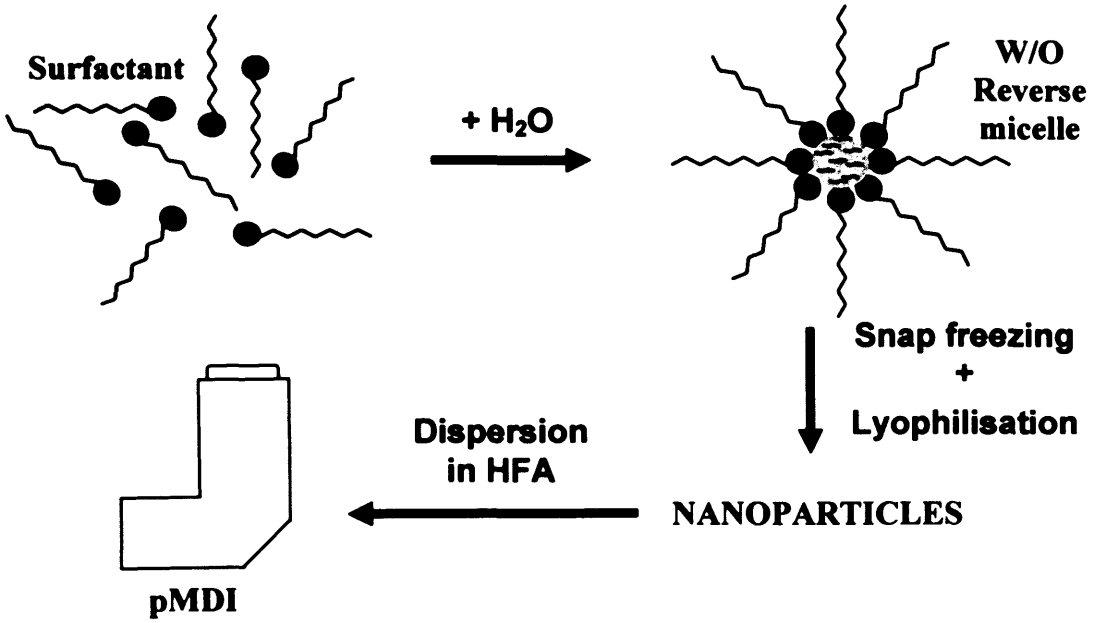


**Figure 2.1 Schematic illustration of the novel process involved in the formulation of a nanoparticulate pMDI.**

### 2.1.1 W/O Microemulsion System

Microemulsions are typically regarded as 'a system of water, oil and amphiphile which is a single optically isotropic and thermodynamically stable liquid solution', as defined by Danielsson and Lindman (1981). Surfactants are amphiphilic as they are characteristically made up of two groups, the hydrophobic group (tail) and the hydrophilic group (head). When two immiscible liquids such as oil and water are added together, any surfactant

present will reside at the oil/water interface due to its amphiphilic properties and will reduce the interfacial tension of the system. The orientation of the surfactant will optimise its solvation requirements and the free energy of the system overall (Attwood 2008).

Although both microemulsions and emulsions are dispersions of oil and water stabilised by an amphiphilic molecule, the two systems should not be confused. Microemulsions are only formed when the interfacial tension at the oil/water interface is brought to a very low level and the interfacial layer is kept highly flexible and fluid (Schulman *et al* 1959; Shinoda and Lindman 1987). These two conditions are usually met by a careful and precise choice of the microemulsion components and of their respective proportions. The surfactant plays a key role in forming stable microemulsions. If the surfactant molecule possesses the correct characteristics such as hydrophile-lipophile balance (HLB) (Griffin 1949) (mentioned in more detail on page 26) to match the relative oil and water substrates used, the surfactant will reside at the oil/water interface; causing a reduction in the interfacial tension to spontaneously form a thermodynamically stable microemulsion (Gillberg *et al* 1970). However in order to sufficiently minimise the interfacial tension and form a highly flexible stable system, co-surfactants are often used to augment the surfactant (Schurtenberger *et al* 1993). Polar organic liquids such as short chain alcohols are incorporated into the microemulsion to reside at the interfacial surfactant layer in order to stabilise and facilitate the dispersion of the surfactant along the oil-water interface (Shinoda *et al* 1991; Mendonça *et al* 2009). The co-surfactant also ensures that the interfacial film is flexible enough to deform readily around each droplet by intercalating between the surfactant molecules to decrease interactions associated with both the polar head group and the hydrocarbon chain (De Gennes and Taupin 1982).

Conversely emulsions are not thermodynamically stable and require a relatively large input of energy to form (Schulman and Cockbain 1940; Capek 2004). During dispersion of immiscible liquids, an input of energy, by for

example mechanical agitation, will eventually cause one immiscible liquid to disperse (disperse phase) throughout the other (continuous phase) in the form of droplets. The surface free energy of the system, which is dependent on the interfacial area and the interfacial tension, is increased by the increase in the surface area produced during dispersion (Schulman and Cockbain 1940). If the surfactant used is unable to lower the interfacial tension to a degree where the system is stable, as in a microemulsion, the droplets will collide with one another and coalesce (Boyd *et al* 1972). Eventually the emulsion will bulk-phase separate in order to reduce the interfacial area between the immiscible liquids so that the system is in a state of minimum free energy (Wennerstrom *et al* 1997). Prior to their phase separation, most emulsions will comprise droplets with diameters of 0.1-100 μm and are cloudy in appearance, whereas in microemulsions the droplet size of the disperse domain is much smaller (usually 5-140 nm) resulting in their transparent or translucent appearance (Saint Ruth *et al* 1995; Attwood 2008).

Whether a microemulsion forms an oil-in-water (o/w) or water-in-oil (w/o) micelle system is determined by a number of factors including the relative volumes of the microemulsion components and more importantly the nature of the surfactant. In general, o/w microemulsions are favoured when there is a smaller volume of oil than water and w/o systems are favoured in the presence of a smaller volume of water. In a system where the volumes of water and oil are equivalent, a bicontinuous microemulsion may result (illustrated in Figure 2.2).

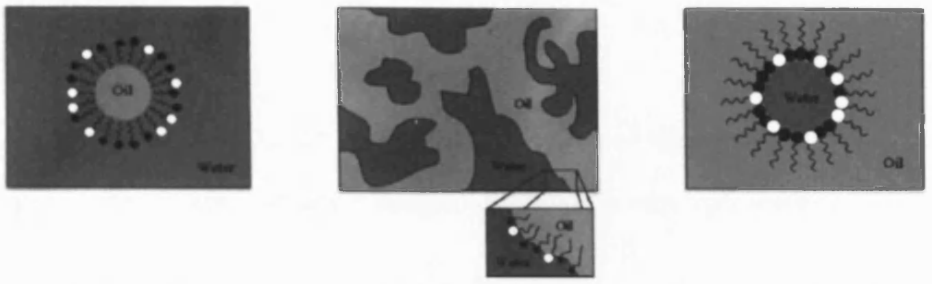

Oil-in-water microemulsion. Spherical micelle

Bicontinuous microemulsion

Water-in-oil microemulsion. Reversed micelle

**Figure 2.2 Schematic representation of the three common microemulsion systems adapted from Lawrence and Rees (2000).** Black head groups ( ~●) indicate the surfactant and white head groups (~○ ) indicate the co-surfactant.

The type of microemulsion system formed has been reported to be related to the surfactant hydrophile-lipophile balance (HLB) (Griffin 1949). The HLB is a value expressing the simultaneous attraction of a surfactant for the water and oil phases. As surfactants are made up of both hydrophilic and lipophilic regions, it is the balance of the size and strength of these regions that is termed the HLB and assigned a numerical value between the range of 0 to 20 for non-ionic surfactants. A surfactant that is lipophilic in character will have a low HLB and a surfactant that is more hydrophilic will have a high HLB. The Bancroft rule states that "The phase in which an emulsifier is more soluble constitutes the continuous phase" (Bancroft 1912). Therefore oil soluble surfactants which tend to have a low HLB will stabilise w/o systems and surfactants with a high HLB will stabilise o/w systems. Although both the HLB and Bancroft rule were originally formulated to explain surfactant behaviour in emulsions, the applicability of these rules has also been demonstrated for use in determining the system formed in microemulsions (Shinoda *et al* 1991; Ruckenstein 1996).

In addition to HLB, the behaviour of surfactants has also been rationalised in terms of the critical packing parameter (CPP). The CPP relates to the ability of the surfactant to form particular aggregates governed by the geometry of the surfactant (Israelachvilli *et al* 1976). The CPP can be calculated using the

following equation:

$$CPP = v/l.a_0$$

Where $v$ = volume of the hydrophobic portion of the surfactant; $a_0$ = optimal head group area; $l$ = length of the surfactant hydrocarbon tail.

As the CPP is a measure of the preferred orientation adopted by a surfactant, surfactants with a CPP < 1 (larger head group area compared to the hydrophobic portion) have a tendency to form o/w microemulsions and a CPP > 1 (smaller head group area compared to the hydrophobic portion) have a tendency toward w/o microemulsion. Surfactants with a CPP = 1 have a tendency to form lamellar structures (Mitchell and Ninham 1981).

Both HLB and CPP can be used to predict the microemulsion system formed using the surfactant of choice, lecithin, for the work carried out in this thesis. Lecithins, are complex mixtures of phospholipids and fatty acids, but are composed mainly of the twin-tailed phospholipid phosphatidylcholine (Figure 2.3). They are naturally occurring surfactants that form components of the cell membrane and are consumed as a normal part of diet. Lecithin is an ideal surfactant for this study in the sense that it is relatively non-toxic and has been approved for pulmonary administration (Fowler 2006). Although, as it is composed of a mixture of lipids there is a degree of batch to batch variation which could lead to potential differences in its ability to stabilise a microemulsion system (Attwood *et al* 1992).

Lecithin has a HLB of approximately 8 and favours the formation of w/o microemulsions (Griffin 1949; Shinoda *et al* 1991) which is one of the required features for the success of this proposed technology (Figure 2.1). However as the twin-tailed surfactant has a CPP close to 1, it tends to form highly rigid lamellar structures (Aboofazeli and Lawrence 1993). A co-surfactant such as propan-2-ol is often used to enhance the flexibility of the interfacial surfactant film, by reducing the interactions between the surfactant molecules (De Gennes and Taupin 1982), therefore promoting the formation of a w/o microemulsion.

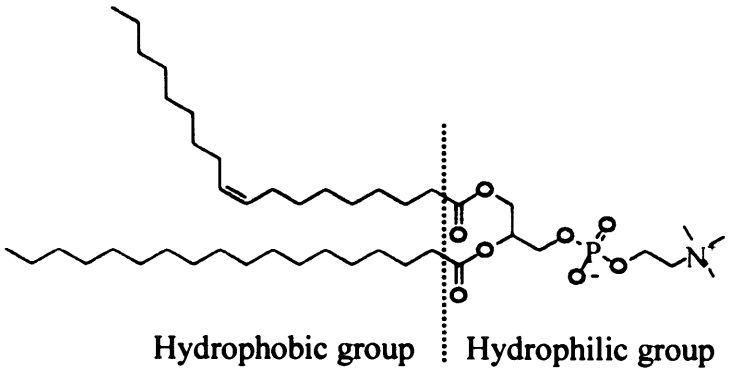


**Figure 2.3 Schematic illustration of the chemical structure of phosphatidylcholine.** Highlighting the hydrophilic head-group and hydrophobic tail-group.

The capacity of w/o microemulsions to act as drug carriers of water soluble molecules has been reported for a number of delivery routes including topical (Chen *et al* 2006) and ocular (Lv *et al* 2005; Chan *et al* 2007). Although the possibility for the formation of microemulsions prepared in HFAs for the pulmonary route has been explored (Patel *et al* 2003; Chokshi *et al* 2009), as yet no data has been published on the incorporation of drugs into these systems.

The technology proposed by Dickinson *et al* (2001) (Figure 2.1) utilises the microemulsions capability to incorporate water soluble medicament, and the nanometre size range of microemulsion droplets to generate surfactant-coated drug nanoparticles suitable for aerosolised delivery in pMDI. The use of microemulsions to form nanoparticles appropriate for pulmonary delivery is an uncluttered area of research with the potential for delivering macromolecules (Rogueda and Traini 2007b).

### 2.1.2 pMDI Formulation Excipients

During the production of surfactant-coated drug nanoparticles (Figure 2.1), apart from their role in generating microemulsions, surfactants also play an integral role in stabilising the pMDI dispersion. Due to their amphiphilic nature surfactants; minimise the adhesion of drug particles to canister walls, stabilise

drug dispersions and prevent irreversible caking through sterically conferred repulsive forces between the surfactant tails which extend into the propellant (Vervaet and Byron 1999).

Suitable surfactant for pMDIs should not only have FDA approval of safety but also have a HLB that assures propellant compatibility. Selecting such a surfactant poses a formulation challenge as, to date, FDA approved surfactants are generally only compatible in chlorofluorocarbons (CFC) propellants. CFCs are however being phased out in response to concerns raised over their detrimental effects on the ozone layer (United Nations Environment Programme 2006). Due to this, hydrofluoroalkanes (HFA) propellants have been identified and used as an alternative to replace CFCs as they do not deplete ozone, are non-flammable and they are considered as non-toxic as the CFCs (Alexander and Libretto 1995; Donnell *et al* 1995). However, although they may seem to be a good alternative, HFAs are not a direct replacement for CFCs in pMDIs. HFAs are relatively polar compared to CFCs, and have insufficient capacity to solubilise low HLB surfactants traditionally used in CFC formulations (Blondino and Byron 1998; Vervaet and Byron 1999). As most of the FDA-approved surfactants have a low HLB, such as lecithin and oleic acid, they can only be used effectively in HFA propellants containing an additional co-solvent excipient such as ethanol which facilitate their dissolution (Tzou *et al* 1997; Smyth 2003).

Apart from improving the solubility of surfactants, ethanol is also known to exert an effect on a pMDI formulation as a vapour pressure modifier (Gupta *et al* 2003; Stein and Myrdal 2006). The vapour pressure of a propellant is critical in influencing the performance of a pMDI in terms of the aerosol droplet velocity and the dose delivery characteristics (Morén 1978; Stein and Myrdal 2006). The presence of a less volatile solvent such as ethanol in a pMDI formulation can reduce the propellant vapour pressure to confer pMDI formulations which emit a slower velocity plume minimising particle impaction at the throat (Gabrio *et al* 1999). However, a careful balance is

required as ethanol may cause excessive reduction in the vapour pressure resulting in larger droplets which evaporate slowly and tend to impact in the upper respiratory tract leading to a decrease in the respirable fraction (Steckel and Müller 1998; Smyth *et al* 2002).

The formulation technology previously outlined in this chapter (Figure 2.1) will be used to produce salbutamol sulphate (SS) nanoparticles. pMDI formulations incorporating these nanoparticles should confer smaller aerosolised particle sizes than commercially available SS pMDI which utilise micronised SS. In order to assess this, the aerodynamic particle size distribution of the novel formulation will be compared against commercial formulations Ventolin Evohaler® and Proventil® HFA. The Ventolin Evohaler® comprises SS suspended in HFA 134a propellant. Proventil® HFA comprises SS in a formulation containing oleic acid surfactant and ethanol co-solvent.

### 2.1.3 Specific Aims and Objectives of the Chapter

The aim of this chapter is to validate, optimise and develop stages of the nanotechnology process originally proposed by Dickinson *et al* (2001) to better understand its technological limitations and determine its potential for the effective pulmonary delivery of medicaments from pMDIs. Optimised parameters of the technology will be translated into later studies whereby the technology will be adapted for delivering pDNA to the lung using a pMDI.

The experimental objectives are to:

1. Use ternary phase diagrams to identify optimised constituent ratios to form stable isotropic microemulsions, with a maximum aqueous volume and minimum surfactant volume.
2. Incorporate salbutamol sulphate (SS), as a model drug, into surfactant-coated nanoparticles.
3. Develop washing procedures to remove excess surfactant from the surfactant-coated freeze-dried SS particles.
4. Characterise the engineered nanoparticles prior to incorporation into a pMDI and after aerosolisation from a pMDI, using scanning electron microscopy (SEM).
5. Quantify the ratio of SS and surfactant present in solvent washed freeze-dried SS particles using a high performance liquid chromatography (HPLC) assay method.
6. Characterise solvent-washed freeze-dried SS particle dispersion behaviour in pMDI canisters.
7. Determine deposition patterns of aerosolised solvent-washed freeze-dried SS particle pMDI formulations and compare with commercially available SS pMDI formulations.

## 2.2 Materials and Methods

All reagents were used as received and were purchased from Fisher Scientific UK Ltd. (Loughborough, UK) unless otherwise stated.

Deionised water was obtained from an Elga reservoir (High Wycombe, UK). Iso-octane (2,2,4 trimethylpentane 99+ %) and Bamethane sulphate were purchased from Sigma-Aldrich Ltd. (Poole, UK). Micronised salbutamol sulphate (mean diameter of 50% particle population $\leq 3.07$ μm) was purchased from Micron Technologies Ltd. (Dartford, UK). Ventolin Evohaler® was purchased from AAH Hospital Service (Coventry, UK). Proventil® HFA was a generous gifts from 3M Healthcare Ltd. (Loughborough, UK). HFA 134a (Zephex 134a) was a generous gift from INEOS Fluor Ltd. (Runcorn, UK). Liquid nitrogen was purchased from BOC Gases Ltd. (Manchester, UK).

### 2.2.1 Optimisation of Microemulsion Formulation Parameters

Water-in-oil microemulsions were prepared at ambient temperatures using distilled water (aqueous phase), egg lecithin (~ 90%) in propan-2-ol (1:3 w/w) (stabilising surfactant system) and iso-octane (organic phase). Iso-octane was added to the surfactant: co-surfactant mixture in a 15 ml centrifuge tube and gently agitated using a vortex mixer. Distilled water was then pipetted into the centrifuge tube containing the surfactant-iso-octane mixture. The formulation was inverted five times to completely mix the components. Nineteen formulations were investigated with component proportions ranging from; surfactant system 36% to 71% (w/w), organic phase 7% to 41% (w/w) and aqueous phase 6% to 32% (w/w). The water content was sequentially increased to determine the phase boundary between a clear micellar (isotropic) phase and an opaque (non-isotropic) multiphase system. Samples that were potentially isotropic were visually inspected at 10 min and 24 hr, after the final water addition, to ensure that equilibrium had been fully established. Any visual changes over this period were noted. A pseudoternary phase diagram was constructed to show the phase boundary and identify optimum microemulsion formulation constituent ratios.

### 2.2.2 Preparation of Nanoparticles

As the preparation of pDNA is a labour intensive and relatively expensive process, these preliminary studies used commercially available salbutamol sulphate (SS) as an accessible and easily identifiable model drug.

Drug-loaded microemulsions were prepared as outlined in Section 2.2.1. SS, to produce a concentration previously successfully incorporated into a microemulsion system (Dickinson *et al* 2001), (17% w/v) was added to the aqueous phase and agitated using a vortex mixer to form a solution prior to addition into the surfactant-iso-octane mixture of an optimised microemulsion system. The centrifuge tubes containing SS-loaded microemulsions were sealed with perforated Parafilm and snap-frozen by submersion in liquid nitrogen. Snap-frozen microemulsions were placed into a tray filled with dry ice in order to maintain their solid state, ensuring sublimation rather than melting occurred, and lyophilised for 24 hr using a Heto Drywinner freeze-drier (Heto-Holten, Alleroed, Denmark) with the condenser chamber set at -110°C.

### 2.2.3 Microscopic Characterisation of SS Nanoparticles

Excess surfactant in the microemulsion and resulting particulates could potentially cause particle aggregation, hinder surface morphology characterisation of resulting particles and potentially adversely affect particulate dispersibility and physical stability in a pMDI. Methods were therefore developed to remove excess surfactant from the formulation.

Method One

A sequential wash method, adapted from Dickinson *et al* (2001) was used to remove excess surfactant from the freeze-dried SS formulation. 300 µl of iso-octane or propan-2-ol was pipetted into microcentrifuge tubes containing lyophilised microemulsions (0.5 g). The samples were centrifuged at 13,000 rpm for 10 min using a Sanyo MSE Micro Centaur microcentrifuge (Sanyo Electric Co., Ltd., Hertfordshire, UK). The resulting supernatant was

gently removed using a pipette ensuring minimal disturbance of the pellet. The pellet was resuspended with either 300 µl iso-octane or propan-2-ol and recentrifuged. This wash cycle was repeated a total of six times. In order to remove residual solvent, microcentrifuge tubes containing washed lyophilised SS were sealed with perforated Parafilm, snap-frozen by submersion in liquid nitrogen and lyophilised for 24 hr using a Heto Drywinner freeze-drier (Heto-Holten, Alleroed, Denmark) with the condenser chamber set at -110°C.

The extent of removal of excess surfactant from the iso-octane washed samples was compared against propan-2-ol washed samples by visual assessment using scanning electron microscopy (SEM).

Solvent-washed SS formulations were placed onto double-sided carbon tape mounted on SEM aluminium stubs using a microspatula. Samples were sputter coated with gold (gold sputter coater, EM Scope, Kent, UK), to form a thin conductive layer, before being viewed using a Philips XL-200 Scanning Electron Microscope (TEI Company, Eindhoven, The Netherlands).

Method Two

As in Method One 300 µl of iso-octane or propan-2-ol was pipetted into microcentrifuge tubes containing lyophilised microemulsions (0.5 g). At this stage an additional vortexing step was incorporated into the wash cycle. Samples were gently agitated using a vortex mixer for 5 min in an attempt to maximise dispersion of excess surfactant into the solvent. Post-vortexing, samples were then centrifuged to form a pellet which was subsequently resuspended with 300 µl iso-octane or propan-2-ol as outlined in wash Method One. This wash cycle was repeated a total of six times. Samples were then prepared for freeze-drying and visualised using SEM as outlined in Method One.

### 2.2.4 HPLC Assay to Quantify SS

A HPLC assay was used to quantify SS present in a specific quantity of the solvent-washed freeze-dried SS sample and thus determine the SS: surfactant ratio. Solvent-washed freeze-dried SS particles were assessed for SS: surfactant ratio using a calibration curve constructed from data generated from HPLC assays using known dilutions of micronised SS.

Preparation of Standard Solutions:

Internal Standard

A fresh stock of internal standard (IS) solution was prepared consisting of bamethane in methanol 400 ml, made up to 1000 ml with de-ionised water to a final concentration of 8 μg/ml. The internal standard was used to prepare a series of micronised SS dilutions from which a calibration curve would be generated.

A reference internal standard was also prepared containing equal concentrations of SS and bamethane (8 μg/ml). The reference internal standard was periodically injected during HPLC assays to ensure the assay remained consistent.

Mobile phase

A fresh stock of mobile phase was prepared consisting of 1-heptane sulphonic acid 0.83 mg/ml in deionised water to form an aqueous buffer. The aqueous buffer solution was adjusted to pH 3.2 using drop-wise additions of glacial acetic acid. Methanol was mixed into the aqueous buffer at a 40:60% v/v methanol: buffer ratio. The mobile phase was then filtered though a 0.2 μm Whatman® nylon membrane filter (Whatman International Ltd., Maidstone, UK).

A calibration curve was constructed from micronised SS diluted in 10 ml IS to form a series of final concentrations ranging from 0.2-1 mg/ml. Samples were analysed using a HPLC system model p 2000 pump, AS 3000 autosampler, UV

2000 detector and Chem Quest® 4.1 software (Thermo Electron Corporation, Altrincham, UK) under the assay conditions outlined in Table 2.1, using a Genesis C18 chromatography column 120 Å 4 um 15 cm x 4.6 mm (Grace Vydac, Illinois, USA).

Solvent-washed freeze-dried SS was diluted in 10 ml IS to form a final concentration of 1 mg/ml and assayed using the same HPLC method as the micronised SS (Table 2.1). The concentration of SS in the sample of solvent-washed freeze-dried SS particles was calculated by using the linear equation generated from the calibration curve.

Table 2.1 Chromatographic conditions for the analysis of SS.

| Condition | Parameter |
|---|---|
| Flow rate of mobile phase | 1 ml/min |
| Injection volume | 100 µl |
| UV Wavelength | 278 nm |
| Retention time: SS | 6 min |
| Bamethane | 10 min |

### 2.2.5 Production of SS pMDI Formulations

A quantity of solvent-washed lyophilised SS particles, sufficient to deliver 100 µg of salbutamol, ex-valve (including a 10% overage to compensate for potential SS losses that could occur through factors such as drug adherence to the canister) was added directly to fluorinated ethylene propylene (FEP) coated aluminium canisters (3M Drug Delivery Systems, Loughborough, UK) and dispersed in absolute ethanol a co-solvent (8% v/v) using a vortex mixer. Spraymiser™ 50 µl retention valves (3M Drug Delivery Systems, Loughborough, UK) were crimped onto the aluminium canisters and 6 ml HFA 134a was pressure filled through the valve using a Pamasol® semi-automatic filling and crimping machine model P2005/2 (Pamasol Willi Mäder AG, Pfäffikon SZ, Switzerland). The formulation was dispersed in the propellant by vortexing the canister for 5 min. The dose of SS expelled per actuation from

the washed SS formulation was selected to permit comparison with marketed SS formulations (Ventolin Evohaler® and Proventil® HFA) during the impactor studies (Section 2.2.6).

Washed SS formulations were also prepared in plastic polyethylene terephthalate (PET) pMDI vials (3M Drug Delivery Systems, Loughborough, UK), for visual assessment of physical stability and dispersion homogeneity. pMDI vials were stored at room temperature with visual observation at 1 min and 1 month.

### 2.2.6 Assessment of SS pMDI Formulations

Aerodynamic Particle Size Distribution profiles were generated for three SS formulations; the washed SS formulation (as above), Ventolin Evohaler® and Proventil® HFA so that a comparison of the novel pMDI formulation could be made with commercially available pMDIs.

Aerosol performance of the three formulations was assessed using an eight stage non-viable Andersen-type cascade impactor (ACI) (Westech Instrument Services Ltd., Bedfordshire, UK) fitted with a 90° aluminium USP-2 induction port (throat), to act as an inlet to the device, and operated at 28.3 l/min. As impaction results may be affected by variations in temperature, operator technique and the impactor used (Stein 1999) these studies were carried out in a 20°C temperature controlled room, using the same apparatus and a standard operating procedure. The ACI stainless steel collection plates were evenly spray-coated with 2% v/v polyethylene glycol (PEG) in acetone to reduce particle bounce and re-entrainment. Once coated the plates were carefully placed into the stages of the ACI using tweezers. A Whatman® glass microfiber filter (Whatman International Ltd., Maidstone, UK) was placed into the filter holder.

Prior to testing, each canister was initially primed by actuating five shots to waste using an actuator with a 0.25 mm orifice diameter of (3M Drug Delivery

Systems, Loughborough, UK). The initial priming actuations were required to eliminate the low dose first-spray effect (Cyr *et al* 1991). Canisters were also assessed for valve functionality issues such as blockages. Valve functionality was monitored by calculating the canister shot weight from weight measurements taken of canisters before and after testing.

During priming and testing pMDIs were shaken for 5 sec between actuations, as specified in compendia procedures (British Pharmacopoeia 2010b). Once primed, each inhaler was weighed and fixed into the testing position using a rubber mouthpiece attached to the throat of the ACI. The vacuum pump was then turned on and the canister was depressed and held for 5 sec. Two actuations were delivered from each canister, and three canisters of each formulation were used for this assessment (n = 3). Following actuation, the canisters were then re-weighed. The number of actuations used in this assessment were minimised as close to the patient dose as possible as recommended by the European agency for the evaluation of medicinal products (EMEA 2002). Flow through the ACI was maintained for an additional 30 sec following the final actuation.

Once the pMDI formulation had been actuated the ACI was disassembled and the amount of SS was recovered quantitatively from the components of the ACI using a washing step. The collection plates and filter were each placed in separate sterile petri dishes and washed with 10 ml of IS (prepared in Section 2.2.4) using a pipette. The actuator and inlet stage (inlet and Stage 0) were each washed in 25 ml IS and the throat was washed in 50 ml of IS. The differences in the volumes of IS used was accounted for when quantifying the SS recovered from the various points of ACI. Each piece of apparatus was vortexed, using a minishaker, in its corresponding volume of IS to ensure impacted SS had been effectively removed from the apparatus. Washings were then placed into 2 ml mini vials and sealed with a septa and screw lid. A Minisart® single use filter unit (0.2 μm) non-pyrogenic (Sartorius Stedim UK Ltd., Surrey, UK) attached to a syringe was used to remove the washings from

the filter stage. This was to ensure that washings were free from any fibres picked up from the filter. The washings were then assessed for SS concentration by the HPLC-UV method outlined in Section 2.2.4.

Several parameters were derived from the ACI deposition data and used to quantify inhaler performance;
The emitted dose (ED) (μg) is the total amount of drug collected from all the parts of the impactor (Throat and Stages), excluding the amount recovered in the actuator, from one shot of the pMDI.

The fine particle fraction (FPF) (%) is the ratio of the aerosolised fine particle mass to the total mass of drug recovered from the various parts of the ACI excluding the actuator. The FPF is defined as the fraction of particles of an aerosol with an aerodynamic diameter less 5.8 μm (particles deposited on Stage 2 and below of the ACI). This ratio is often used as a guide to understanding the portion of the aerosolised drug that is likely to reach the lung (the respirable portion).

Extra fine particle fraction (EPF) (%) is the ratio of the aerosolised extra fine particle mass to the total mass of drug recovered from the various parts of the ACI (ex-actuator). The EPF is defined as the fraction of particles of an aerosol with an aerodynamic diameter less 1.1 μm (particles deposited on Stage 6 and below of the ACI).

Mass Median Aerodynamic Diameter (MMAD) (μm) is a statistical measure of central tendency of the particle size distribution of aerosolised particles emitted from an inhaler. The MMAD denotes the diameter that divides the particle size distribution into two halves with respect to mass. Of the total mass of particles found on the impactor plates, 50% resides with particles above and below the MMAD. Most orally inhaled pharmaceutical aerosols have a MMAD of between 1 and 5 μm (Hickey 1993).

Geometric Standard Deviation (GSD): In addition to the MMAD, the GSD is a useful measure as it is a single parameter that quantifies the spread of the aerosol particle size distribution. In a logarithmic-normal (log-normal) distribution, the GSD is the measure of the polydispersity of the aerosol (Gonda 2000). An ideal monodisperse formulation should therefore have a GSD of 1, however as it is virtually impossible to prepare mondisperse aerosols a GSD of 1.2 is generally considered the limit above which an aerosol would be classed as polydisperse (Gonda 2000).

The MMAD and GSD can be calculated using the following method which utilises an Excel™ spreadsheet. Probit values, determined from the particle deposition cumulative percentage undersize can be plotted against the log effective cut-off diameters (ECD) of the ACI stages. A probit value of 5 corresponds to the cumulative percentage undersize of 50%, probit values of 4 and 6 correspond to 15.87% and 84.13% respectively. Linear regression can be applied to the resulting line using the points plotted between the probit value of 4 and 6. The MMAD and GSD can be calculated using the straight line equation generated. The log ECD is calculated at the probit value of 5 using the straight line equation. The inverse of the log ECD value results in the MMAD. The GSD is then calculated by dividing the inverse of log ECD calculated from the probit value 6 (cumulative percentage undersize 84%) by the MMAD.

#### 2.2.6.1 Microscopic Characterisation of Aerosolised SS Formulation

The solvent-washed SS pMDI formulation was actuated 60 times into a Volumatic™ spacer (Allen and Hanburys, Middlesex, UK) connected to an ACI operating at 28.3 l/min. Double sided carbon tape was attached at various points on the wall of the spacer and the plates in the ACI using tweezers. Particles that had deposited on the carbon tape, were mounted onto SEM aluminium stubs and sputter coated with gold (gold sputter coater, EM Scope, Kent, UK) before being viewed using a Philips XL-200 Scanning Electron Microscope (TEI Company, Eindhoven, The Netherlands).

### 2.2.7 Statistical Analysis

Statistical analysis was carried out using a statistical package, SPSS 16®. One-way analysis of variance (ANOVA) was followed by a Duncan's multiple range test, to compare multiple groups, with significant differences indicated by p values $<0.05$. Results are summarised as mean ± sd.

## 2.3 Results

### 2.3.1 Optimisation of Microemulsion Formulation Parameters

Initial studies aimed to identify optimised constituent ratios that form stable isotropic w/o microemulsions (Figure 2.4). Generally microemulsions to the right of the phase boundary formed stable monophasic systems (Figure 2.5) which had a surfactant to water ratio of approximately 2.0 and greater (Figure 2.4). Microemulsions to the left of the phase boundary formed unstable biphasic systems (Figure 2.5) with a surfactant to water ratio below 2.0. Stable microemulsion systems with the lowest surfactant to water ratio were deemed as optimal from a drug loading and surfactant content perspective. The optimum microemulsion (identified by the arrow in Figure 2.4) with the lowest surfactant to water ratio comprised water phase: surfactant: organic phase, 26:52:22 w/w/w.

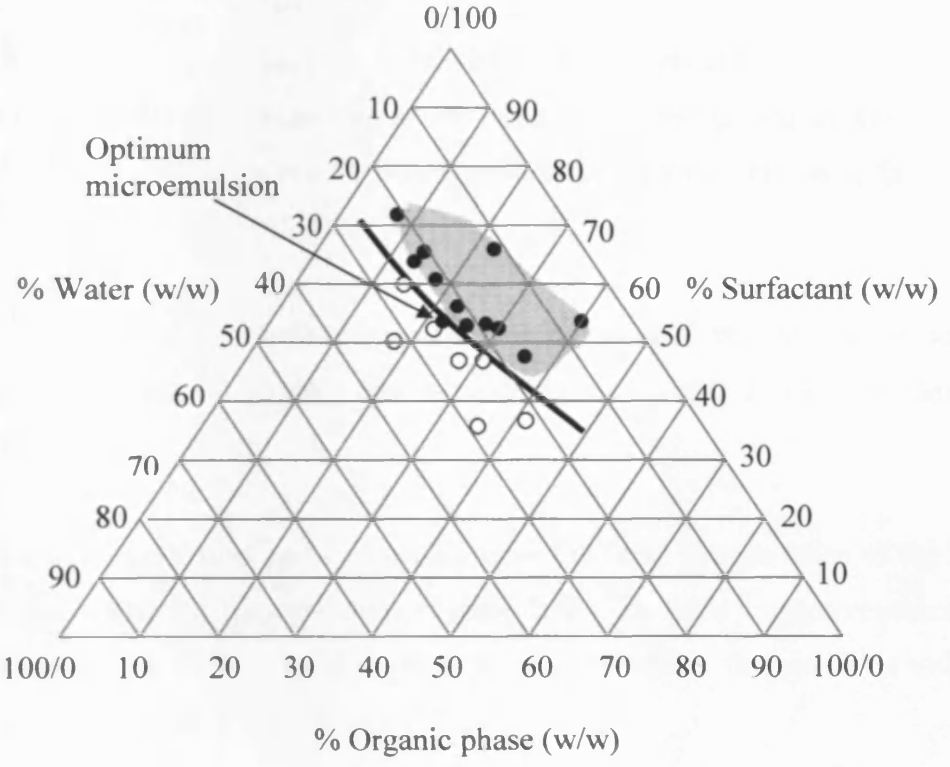


**Figure 2.4 Pseudoternary phase diagram of lecithin: Propan-2-ol (1:3 (w/w))/ iso-octane/ water at room temperature.** ( ● ) indicates a stable microemulsion. ( ○ ) indicates phase separation. The black line (——) indicates the phase boundary. ( ▒ ) indicates anticipated boundaries for w/o microemulsion.

Figure 2.5 displays a typical stable monophasic microemulsion system and an unstable biphasic system. The stable microemulsion is isotropic, with the water, oil and amphiphile dispersed throughout the whole system. Conversely the unstable system displays phase separation between the oil and the water.

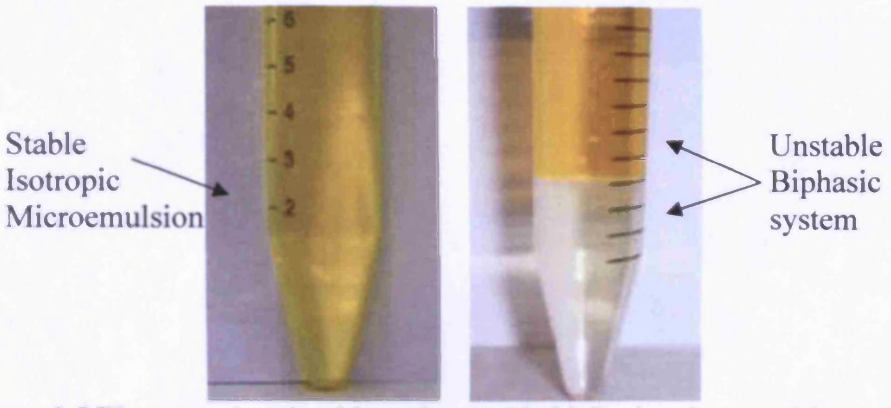


**Figure 2.5 Photographs of stable and unstable biphasic microemulsion systems.**

### 2.3.2 Microscopic Characterisation of SS Nanoparticles

SEM was utilised to characterise SS particles following one of two wash methods to ascertain the most efficient method for removing excess surfactant.

Method One

In wash Method One, either iso-octane or propan-2-ol was used to remove excess surfactant from the freeze-dried surfactant-coated SS formulation (Section 2.2.3).

There were no distinct particles visible from the SEM images taken of the SS particles washed using iso-octane (Figure 2.6). The SEM images revealed a continuous matrix with no clear particle outlines within the matrix at either magnification used (Figure 2.6A or B).

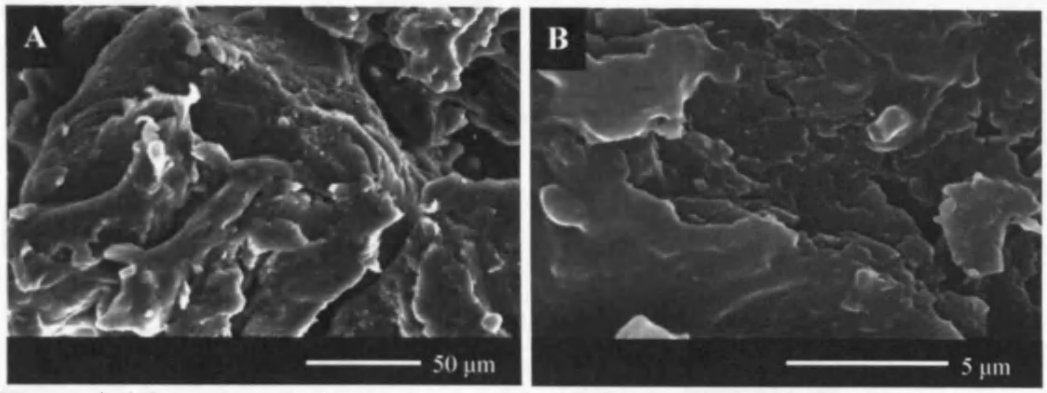


**Figure 2.6 Scanning electron micrographs of the freeze-dried SS microemulsion formulation washed in iso-octane using Method One.** Scale bar = 50 µm (A) and 5 µm (B).

SEM images of surfactant-coated SS particles washed using propan-2-ol revealed the presence of aggregated structures (Figure 2.7). Although distinct particles cannot be viewed in either micrograph (Figure 2.7A and Figure 2.7B), the lack of any visible continuous matrix indicates that some of the excess surfactant has been removed. Micrograph Figure 2.7B displays a heterogeneous population with structures ranging in size but predominantly smaller than 5 µm.

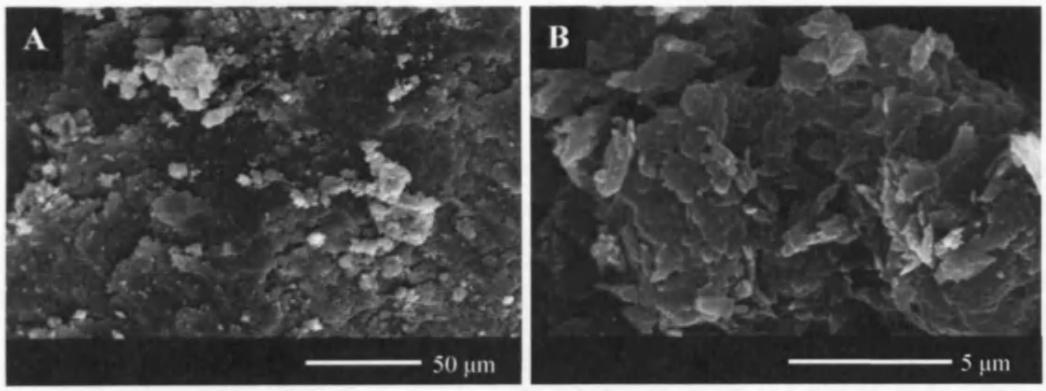


**Figure 2.7 Scanning electron micrographs of the freeze-dried SS microemulsion formulation washed in propan-2-ol using Method One.** Scale bar = 50 µm (A) and 5 µm (B).

Method Two

Wash Method Two, (Section 2.2.3) was based on wash Method One but incorporated an additional vortexing step prior to centrifugation in an attempt

to optimise surfactant removal.

Figure 2.8A reveals a general population of particle clusters residing on an amorphous surface. On closer inspection, Figure 2.8B reveals an amorphous matrix interspersed with aggregates made up of a heterogeneous particle population. Particles appear asymmetric in shape and although particles vary in size the majority are smaller than 5 μm.

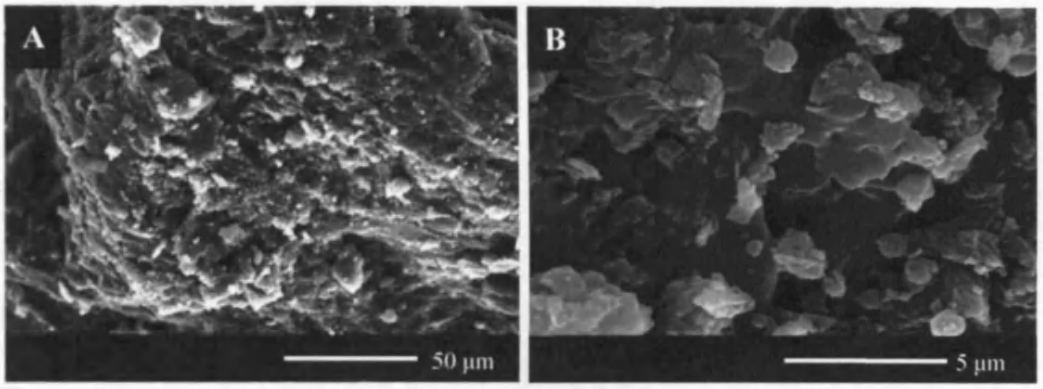


**Figure 2.8 Scanning electron micrographs of the freeze-dried SS microemulsion formulation washed in iso-octane using Method Two.** Scale bar = 50 μm (A) and 5 μm (B).

Figure 2.9A displays an extensive population of particle clusters. Closer inspection of the particle population (Figure 2.9B) generally revealed particles with a plate-like appearance. Although particles appear aggregated and variable in size, all particles were less than 5 μm.

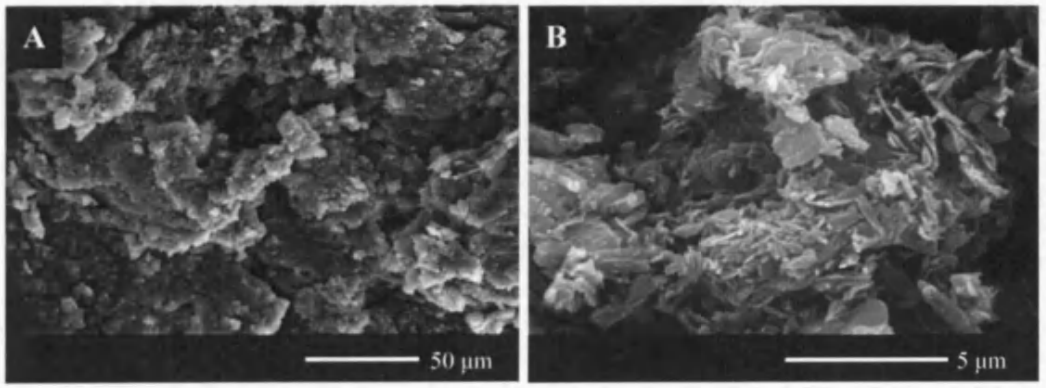


**Figure 2.9 Scanning electron micrographs of the freeze-dried SS microemulsion formulation washed in propan-2-ol using Method Two.** Scale bar = 50 μm (A) and 5 μm (B).

### 2.3.3 HPLC Assay to Quantify SS

A calibration curve was generated from HPLC data using the area under the curve (AUC) ratios between known concentration of SS and bamethane internal standard (Figure 2.10).

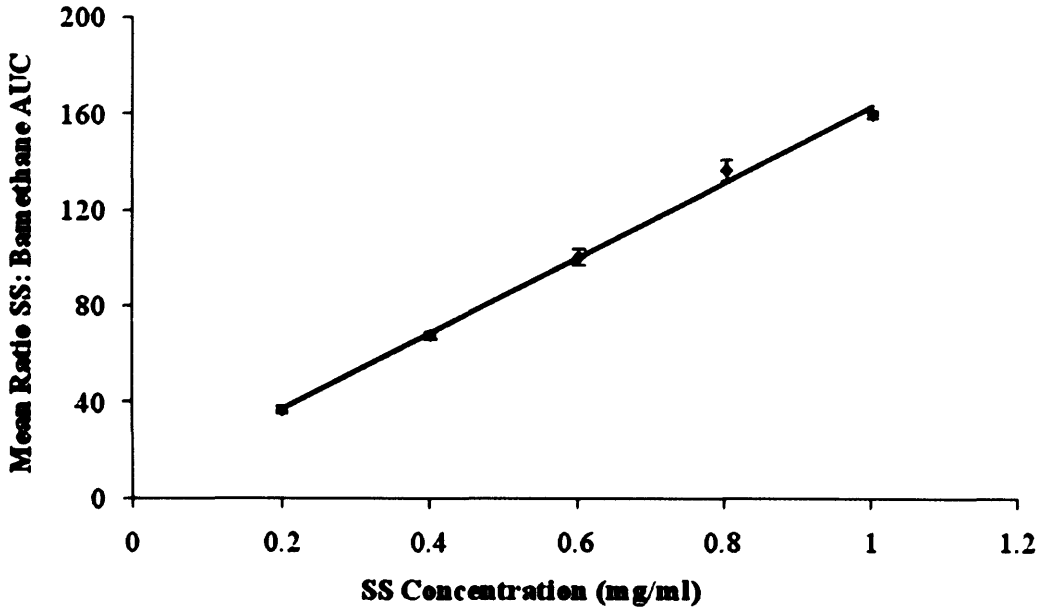


**Figure 2.10 Calibration curve for the quantification of SS** (linear equation: y = 158.49x+ 5.7816, $R^2$ = 0.9963). Data are presented as mean ± sd; n = 3.

The $R^2$ is a measure of the accuracy of the goodness of fit of the line to the plotted data points. An $R^2 > 0.90$ is generally considered a good fit, as the $R^2$ generated from this calibration curve was 0.9963 the linear equation was taken as valid for calculating the concentration of SS present in a known quantity of solvent-washed freeze-dried SS (Figure 2.10).

The final amount of SS present in 1.00 mg of solvent-washed freeze-dried SS was 0.82 ± 0.05 mg; therefore the SS:surfactant ratio was 0.8:0.2. This data demonstrates that, even after the solvent wash, surfactant still remained which accounted for approximately 1/5 of the solvent-washed freeze-dried SS formulation mass. However, as the SS to surfactant ratio used during the production of the microemulsion was 1.0:2.94, the wash procedure resulted in a 10-fold reduction in the surfactant content.

### 2.3.4 Assessment of SS pMDI Formulations

Visual observations of the washed SS particulate formulation, in transparent PET pMDI vials, provided a simple indication to the physical stability of the formulation.

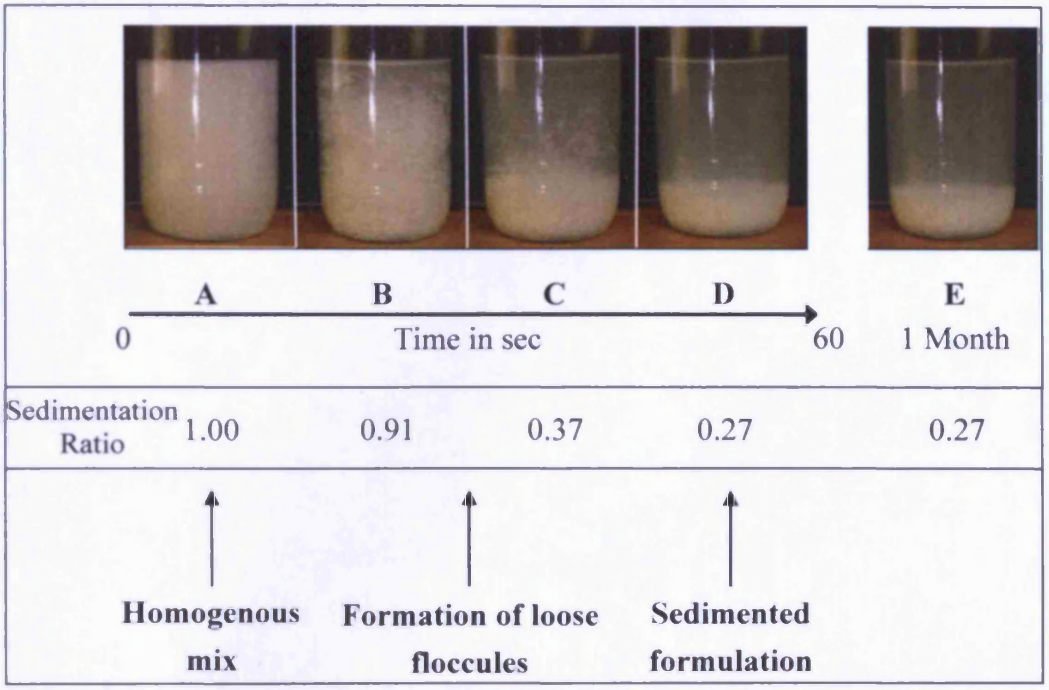


**Figure 2.11 Sedimentation behaviour of washed SS pMDI formulations.** HFA 134a is used as propellant with absolute ethanol as a co-solvent. Images and sedimentation ratios were taken during 60 sec and after 1 month of producing the formulation.

The addition of HFA 134a propellant to the SS formulation led to the formation of an opaque dispersion with particles suspended throughout the propellant where the sediment volume was equal to that of the propellant (Figure 2.11 photograph A). Within 20 sec the suspension had begun to sediment (Figure 2.11 photographs B and C), visual observations showed an inelegant (non–homogenous) formulation. At 60 sec (Figure 2.11 photograph D) the SS formulation had almost completely sedimented, with few visible suspended particles, leaving a distinct boundary between a larger volume of supernatant and the sediment. After this point there was no further visible change in the sedimentation height for up to 1 month after pMDI formulation production, as the sedimentation ratio appeared to plateau at 0.27 (Figure 2.11

photograph E). Up to a period of 1 month, suspended particles were still visible, although most particles had formed loose sedimented floccules which were easily dispersed by one inversion of the PET vial.

### 2.3.4.1 Assessment of SS Deposition Following Aerosolisation from a pMDI

To enable comparison of aerosol deposition characteristics between the novel washed SS formulation and commercially available pMDIs the aerodynamic particle size distribution profiles of Ventolin Evohaler®, Proventil® HFA and the washed SS formulation were determined using an ACI method (Section 2.2.6).

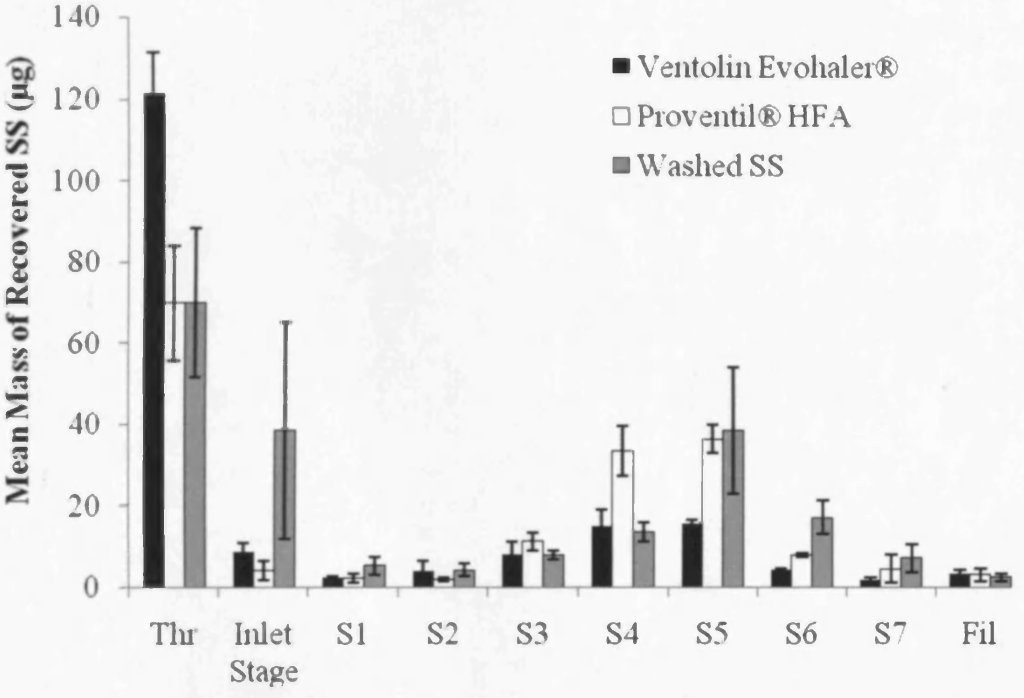


**Figure 2.12 Comparison of aerodynamic particle size distribution of two commercially available SS inhalers and a novel SS formulation. Thr:** throat, **Inlet stage:** inlet and Stage 0, **S1 to S7:** Stages 1 to 7, **Fil**: final filter. Data are presented as mean ± sd; n = 3, each individual measurement is the sum of two actuations.

Figure 2.12 highlights how the deposition pattern of aerosolised particles within the impactor can differ for different formulations. Although all of the SS formulations generally display a bimodal mass distribution of particles

following aerosolisation, a difference between the mass of deposited SS between the three formulations using equivalent doses can be observed. Deposition data generated from the Ventolin Evohaler® displayed a relatively large deposition of SS in the throat, with a secondary peak on Stages 4 and 5. The mass distribution of deposited particles for the Proventil® HFA formulation followed a similar pattern to the Ventolin Evohaler but with a decreased throat deposition and an increased deposition on Stages 4 and 5. The novel washed SS formulation displayed a primary deposition of particles at the throat and inlet stages, similar in total to the throat deposition from Ventolin Evohaler® with a secondary peak at Stage 5 which was greater than that for either Ventolin Evohaler® or Proventil® HFA. Indeed the novel formulation had greatest deposition at Stages 5, 6 and 7 of the impactor, indicative of a significant proportion of smaller aerosolised particles.

The MMAD is a statistical measure of central tendency of the particle size distribution on impaction plates of the ACI. The difference in MMAD between the three formulations is highlighted in Figure 2.13. The aerosol emitted from the washed SS formulation resulted in particles with a significantly lower ($p< 0.05$) MMAD (1.90 ± 0.06 μm) than particles emitted from the Ventolin Evohaler® (2.32 ± 0.06 μm) but statistically comparable ($p> 0.05$) to Proventil® HFA (2.00 ± 0.10 μm).

A significant difference ($p<0.05$) between the $FPF_{5.8\ \mu m}$ of all three formulations was found (Figure 2.13). The washed SS formulation resulted in a $FPF_{5.8\ \mu m}$ (ex-actuator) of (45.0 ± 2.58%) which was significantly higher than that measured for Ventolin Evohaler® (27.7 ± 4.07%) but lower than for Proventil® HFA (56.6 ± 6.89%).

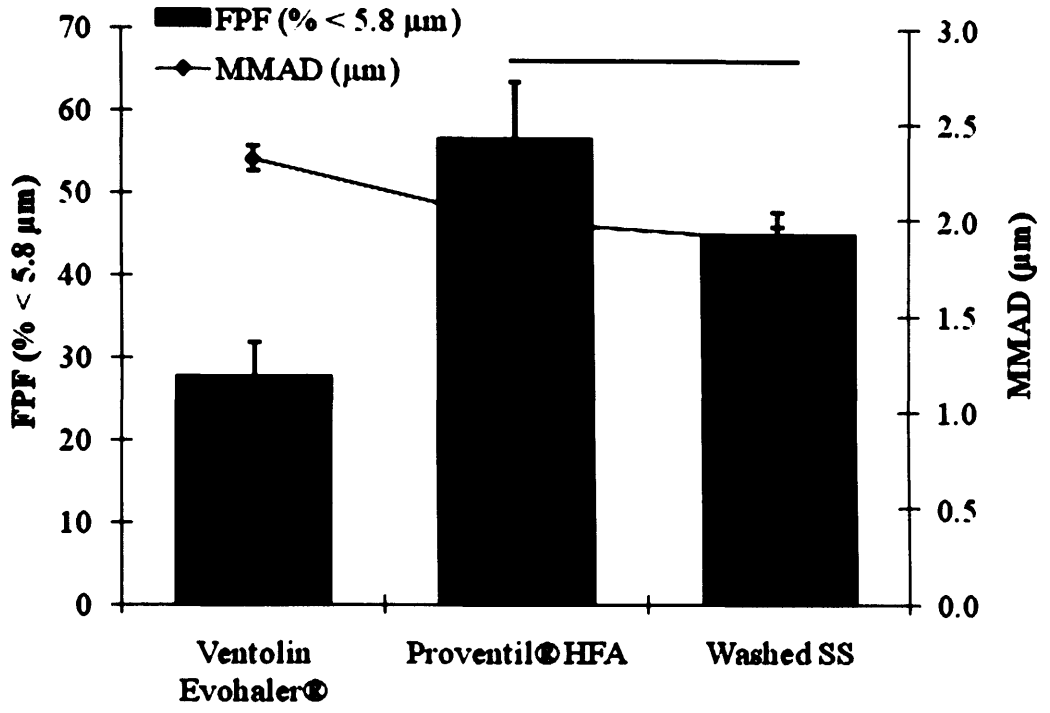


**Figure 2.13 A comparison of fine particle fraction ($FPF_{5.8\ \mu m}$, ex-actuator) and mass median aerodynamic diameter (MMAD) between two commercially available SS inhalers and a novel SS formulation.** Data are presented as mean ± sd; n = 3. Bar represents no significant MMAD difference ($p>0.05$).

The geometric standard deviation (GSD) measures the spread of the particle size distribution within the ACI (Table 2.2). The actuated washed SS formulation produced an aerosolised particle population with a significantly greater degree of polydispersity (2.76 ± 0.15) compared to Ventolin Evohaler (2.06 ± 0.12) and Proventil HFA (1.77 ± 0.11).

Extra fine particle fraction ($EPF_{1.1\ \mu m}$) measures the fraction of particles depositing on and below Stage 6 of the ACI. The washed SS formulation showed a significantly higher EPF (13.8 ± 1.66% $p< 0.05$) compared to both the Proventil® HFA (8.76 ± 1.68%) and Ventolin Evohaler® (4.83 ± 0.99%) (Table 2.2).

The mean emitted dose (ED) was calculated from the cumulative particle deposition in the ACI (Throat and Stages). The dose of SS emitted into the ACI

from the washed SS formulation revealed a relatively high relative standard deviation (RSD) (102.52 ± 31.75%) (Table 2.2). Although the sample number was n = 3, the high RSD was a result of one of the washed SS formulation canisters tested emitting a lower SS dose (65.90 μg) compared to the other two canisters (128.16 μg and 113.50 μg).

Table 2.2 Comparison of aerosol characteristics, using geometric standard deviation (GSD), Extra fine particle fraction (EPF) and emitted dose (ED) per actuation, between two commercially available SS inhalers and a novel SS formulation. Data are presented as mean ± sd/ % rsd; n = 3.

| Formulation | GSD | $EPF_{1.1\ \mu m}$ (%) (ex-actuator) | ED per actuation (μg) (± % rsd) (ex- actuator) |
|---|---|---|---|
| Ventolin Evohaler® | 2.06 ± 0.12 | 4.83 ± 0.99 | 91.24 ± 5.96% |
| Proventil® HFA | 1.77 ± 0.11 | 8.76 ± 1.68 | 87.01 ± 6.90% |
| Washed SS | 2.76 ± 0.15 | 13.8 ± 1.66 | 102.52 ± 31.75% |

### 2.3.4.2 Microscopic Characterisation of Aerosolised SS Formulation

SEM images taken of SS particles aerosolised from the washed SS pMDI formulation and collected using an ACI showed the presence of SS aggregates (Figure 2.14). The micrographs in Figure 2.14A to D indicate the presence of an amorphous population of particles. Particles deposited on Stage 5 (Figure 2.14A and Figure 2.14B) revealed amorphous bridged structures, whereas particles deposited on Stage 6 (Figure 2.14C and Figure 2.14D) revealed a continuous matrix interspersed with protrusions of amorphous structures with an agglomerated appearance. Although particle size was variable, all particles were less than 10 μm. Microscopic observations showed that ACI Stages 5 (Figure 2.14A and Figure 2.14B) and Stage 6 (Figure 2.14C and Figure 2.14D) with cut-off diameters of 1.1 μm and 0.7 μm respectively had the greatest particle deposition. This potentially indicates that the majority of the aerosolised particles were within the respirable size range. However, SEM images (Figure 2.14B and Figure 2.14D) revealed the presence of particles

deposited on Stages 5 and 6 that were larger than the quoted cut-off diameters.

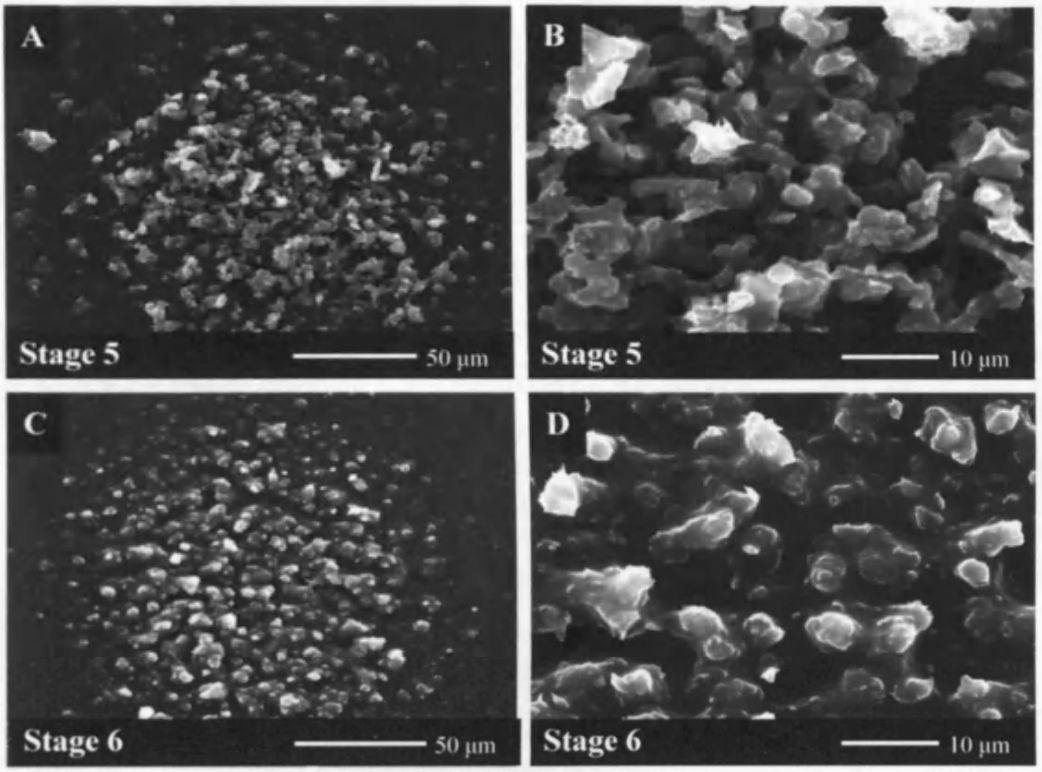


**Figure 2.14 Scanning electron micrographs of a solvent-washed freeze-dried pMDI formulation containing SS collected at Stage 5 (A and B) and 6 (C and D) of an ACI.** Scale bar = 50 µm (A and C) or 10 µm (B and D).

## 2.4 Discussion

### 2.4.1 Optimisation of Microemulsion Formulation Parameters

In order to maximise the loading capacity of a water-soluble therapeutic molecule such as SS, an optimum w/o microemulsion should consist of a large aqueous phase and a small volume of surfactant.

In this study an optimum microemulsion was found to have a surfactant to water ratio of approximately 2.0. At this ratio, the concentration of surfactant was sufficient to reduce the interfacial tension at the oil/water interface to form a stable, isotropic, monophasic microemulsion (Schulman *et al* 1959; Shinoda and Lindman 1987). Attempts to reduce the surfactant to water ratio below 2.0 by increasing the quantity of water or decreasing the quantity of surfactant resulted in an unstable biphasic system. The reason for this being that there was insufficient surfactant at the oil-water interface, which can lead to an increase in the interfacial tension, causing the collapse of the microemulsion resulting in a phase separation (Gillberg *et al* 1970).

Having said this, Dickinson *et al* (2001) who used the same microemulsion components as this study reported stable systems with surfactant to water ratios as low as 1.5. The difference between the surfactant to water ratio reported and the ratio quoted in this study could be attributed to impurities in the egg lecithin (which was quoted as approximately 90% pure by the manufacturer) or unreported variations in the microemulsion preparation conditions (Attwood *et al* 1992; Cilek *et al* 2006).

### 2.4.2 Microscopic Characterisation of SS Nanoparticles

Microscopic characterisation of freeze-dried SS particles, having undergone Wash Method One (Section 2.2.3) with iso-octane, revealed insufficient removal of excess surfactant which hindered surface morphology characterisation and potentially caused particle aggregation. A typical feature of a microemulsion is the submicron size of the disperse domains (Schulman *et al* 1959; Saint Ruth *et al* 1995). This is advantageous as freeze-drying a drug

solubilised in the disperse phase of a microemulsion can lead to the formation of surfactant-coated nanoparticles, a feature exploited by Dickinson *et al* (2001). However, stabilising such a microemulsion system requires a relatively large quantity of surfactant due to the large interfacial area between the disperse phase and the continuous phase (Shinoda *et al* 1991; Zarur *et al* 2000), which explains the microscopic observation of excess surfactant coating the lyophilised SS particles. The excess surfactant invariably required to formulate a stable microemulsion system, in addition to hindering particle characterisation, could also potentially adversely affect particulate dispersibility and physical stability of the formulation in a pMDI due to the poor solubility of surfactants in HFA propellants (Blondino and Byron 1998) a feature further explored in Section 2.4.3.

Visual inspection using SEM of the freeze-dried SS particles after solvent washing using Method One (Section 2.2.3) revealed differences in the extent of surfactant removal between the two solvents. The presence of a continuous matrix, which may be the sticky surfactant system, and the lack of any visible distinct SS particles (Figure 2.6) exemplifies that 6 wash cycles using iso-octane (Method One) is not sufficient in removing excess surfactant for successful particle visualisation.

Replacing the iso-octane solvent with propan-2-ol which has a higher dipole moment and confers lower lipophilicity than iso-octane resulted in SEM micrographs with more discrete structures without the coverage of a continuous matrix (Figure 2.7). The apparent differences in the appearance of iso-octane and propan-2-ol washed particles demonstrates the superiority of propan-2-ol in removing excess surfactant after 6 wash cycles compared to the iso-octane solvent. The rationale for this increased surfactant removal is dependent upon the chemistry of the two solvents. Propan-2-ol is composed of a polar hydroxyl group which can interact with the polar head group of the surfactant, whilst the non-polar hydrocarbon portion of the alcohol can interact with the hydrophobic tail group of the surfactant (Fowler 2006). As iso-octane is composed solely of

non-polar hydrocarbons it can only interact with the hydrophobic portion of the surfactant. This increased interaction conferred by the alcohol propan-2-ol explains its increased efficiency, and use in the past, in surfactant removal compared to the lipophilic iso-octane solvent (Lang and Tuel 2004; Nyambura *et al* 2009b). However, as these particles were still highly aggregated a secondary wash method, wash Method Two (Section 2.2.3), was developed in an attempt to optimise removal of excess surfactant.

Wash Method Two involved the addition of a vortexing step to dramatically increase shear and enhance surfactant removal. In contrast to previous micrographs generated from SS particles washed using iso-octane which revealed a continuous matrix without any discrete particles (Figure 2.6), the addition of a vortexing step revealed that some of the excess surfactant had been successfully removed to reveal an amorphous matrix (the sticky surfactant system) interspersed with an aggregated particle population (Figure 2.8). This increased removal of surfactant using vortexing was also observed when comparing SS particles washed in propan-2-ol, although to a lesser extent than with iso-octane.

General observations of the micrographs revealed that the best method to remove excess surfactant from the freeze-dried SS particles utilised propan-2-ol as the solvent and Wash Method Two, i.e. sample vortexing. This method resulted in the greatest visibility of SS particles than any other solvent method combination. However, in all micrographs particles remained aggregated which could adversely affect the deposition profiles of these particles during particle characterisation of aerosolised particles (Berry *et al* 2004; Traini *et al* 2007) further discussed in Section 2.4.3.1.

Although the technology explored was originally reported to generate particles of the nanoparticle size range (Dickinson *et al* 2001), SEMs revealed that such particles were not detected. A possible reason for this may due to the observed aggregation caused by the presence of a sticky surfactant. Nevertheless the

particles generated from the developed technology was a significant advancement, as previous reports of lyophilised powders have often shown particles with diameters unsuitable for pulmonary delivery and generally require further processing using a milling step prior to incorporation into an inhaler (Seville *et al* 2002; Shoyele and Cawthorne 2006). It is generally acknowledged that particles require an aerodynamic diameter $\leq 5$ μm to allow efficient penetration and deposition in the peripheral pulmonary regions (Hickey 1993). Solvent-washed lyophilised particles, although not in the nanoparticle size range, are still in the respirable size range for deposition in the bronchiolar and alveolar region.

### 2.4.3 Assessment of SS pMDI Formulations

Visual observation of solvent-washed SS formulations loaded into PET vials was used to determine gross visual changes in the properties of the dispersion. Solvent-washing the surfactant-coated SS particles removed excess surfactant to produce an off-white powder which initially dispersed in the propellant-cosolvent mixture. Sedimentation of the particles began to occur after 20 sec and was complete by 60 sec but the sedimented particles were readily redispersed by one inversion of the vial confirming the presence of loose floccules which showed no signs of caking following 1 month's storage. The presence of surfactant excipient coating the drug particles may have stabilised the drug dispersion to prevent any irreversible sedimenting. Surfactants are often incorporated into suspension formulations to decrease the drug interparticle attractive forces through sterically conferred repulsive forces between the surfactant tails which extend into the propellant (Hickey *et al* 1988; Vervaet and Byron 1999).

Observations of the dispersibility of the flocculated system indicate that particle aggregation of the formulation was suitably controlled within the 1 month time span. The lack of solubility of the hydrophobic surfactant lecithin in HFA 134a propellant resulting in aggregation is well documented and commonly requires the use of a co-solvent in commercial formulations

(Blondino and Byron 1998). The observations of a dispersed system suggest that the quantity of surfactant in the solvent-washed formulation fell within the range of that which can be solubilised into the propellant with the aid of ethanol as co-solvent (8% v/v).

A flocculated system is deemed advantageous, rather than for example a deflocculated system, as it is readily re-dispersible upon sedimentation. Rapid sedimentation, conferred from a flocculated system, can however often lead to poor dose reproducibility (Byron 1994, 1997). Dose reproducibility was one of the parameters measured during the assessment of the SS formulation aerosol performance (Section 2.3.4.1).

#### 2.4.3.1 Assessment of SS Deposition Following Aerosolisation from a pMDI

Emitted dose reproducibility was measured as one of the means for assessing aerosolised formulation performance. Poor emitted dose reproducibility translating into a high RSD value (± 32.55%) was observed for the washed SS formulation. To put this data into context, compendial guidelines (British Pharmacopoeia 2010a) state that the emitted dose for 9 out of 10 canisters should be within ± 25% in order to assume uniformity of dose. Possible reasons for the poor dose reproducibility include the presence of a rapidly sedimenting formulation (Byron 1994) observed during the assessment of the formulation in PET vials (Section 2.3.4). As there was only a small delay between shaking the formulation and actuation of the formulation, it is perhaps more likely that the erratic dosing was caused by partial actuator blockage due to the presence of aggregated particles (Traini *et al* 2007).

Closer inspection of the ED data generated from each canister revealed that the poor RSD was due to one canister emitting a relatively small dose in relation to the 100 μg salbutamol sulphate target dose (from the mouthpiece). A possible reason for this could be due to a faulty valve. Additionally, the valve and actuators used for the commercial formulations have been carefully optimised.

As the valve and actuators used for the washed SS formulations have yet to be optimised they are therefore prone to the possibility of for example actuator blockage if the actuator orifice is too small (Ecanow *et al* 1986; Dalby and Byron 1988). This could explain the low emitted dose in one of the washed SS canister resulting in a relatively high RSD compared to values generated from the commercial formulations.

Aerosol deposition profiles generated using an ACI illustrated the difference in aerosol performance between the SS formulations, both bespoke and commercially available. Both the Ventolin Evohaler® and Proventil® HFA formulations displayed a broad mean mass SS particle deposition peak at Stage 4 and 5. The novel washed SS formulation, however, displayed a deposition profile skewed towards the smaller particle size range relative to the commercial formulations. This said, the washed SS formulation displayed an increased ACI inlet particle deposition, a phenomenon also reported by Dickinson *et al* (2001).

There are a number of possible reasons for this increased ACI inlet particle deposition. The presence of aggregated particles, observed during microscopic particle characterisation (Section 2.3.2), which are not broken up through the shearing forces of aerosolisation may have led to the observed impaction in the upper stage of the ACI (Berry *et al* 2004; Traini *et al* 2007). Conversely particle aggregation may have occurred post-aerosolisation. Gonda (1985) reported that in concentrated non-aqueous suspension formulations there is often more than one particle in a single aerosolised propellant droplet. Due to this, after droplet evaporation, the particles tend to aggregate resulting in a particle distribution which does not match the original size distribution of the particles. Also the presence of surfactant in the washed SS formulation may have caused particle deposition in the upper stages of the ACI including the inlet stage (Dalby and Byron 1988; Hickey *et al* 1988). During aerosolisation, surfactant has a tendency to associate at the droplet-air interface, as surfactant is non-volatile the presence of surfactant can retard propellant evaporation

resulting in larger droplets and consequently an increased deposition in the upper stages of the ACI (Snead and Zung 1968; Otani and Wang 1984).

Apart from the inlet stage, the washed SS formulation deposition profile revealed a larger mass of particles deposited at the lower stages of the ACI (Stages 5 to 7) which suggests the presence of smaller and more dispersible particles compared to the two commercially available formulations. Compendially recognised parameters such as the MMAD, GSD and FPF (British Pharmacopoeia 2010b), were used as a means to quantify aerosol performance and draw statistically significant conclusions between the aerosols emitted from the three pMDI formulations.

It is generally acknowledged that an aerosol with a MMAD of between 1 and 5 μm is acceptable for pulmonary delivery (Hickey 1993). The MMAD for all three formulations was found to be within this respirable range. However, both the novel washed SS and Proventil® HFA formulations generated a significantly smaller MMAD and significantly higher percentage of particles within the respirable size range ($FPF_{5.8\ \mu m}$) compared to the Ventolin Evohaler®. Although there is little published literature on the performance of the Ventolin Evohaler® and Proventil® HFA formulations, the data generated in this chapter is generally typical of a previous report (Harris *et al* 2006).

The washed SS particles had been carefully manufactured in an attempt to produce nanoparticles using the nanotechnology process (Figure 2.1). Although, as explained earlier, nanoparticles were not observed (Section 2.2.3) the technology may have produced smaller particles than those used in the commercial formulations. This may have been reflected in the smaller MMAD and larger $FPF_{5.8\ \mu m}$ generated from the aerosolised particles emitted by the washed SS compared to the Ventolin Evohaler®. In addition to this the washed SS formulation generated aerosolised particles with significantly greater $EPF_{1.1\ \mu m}$ than both the commercially available SS formulations. In a suspension formulation, the aerosolised drug output cannot be smaller than the

original particles used to prepare the formulation (Gonda 1985; Berry *et al* 2004). The aforementioned data was therefore able to confirm that the technology used to generate the novel washed SS particles had successfully produced particles with a smaller aerodynamic diameter than both the Ventolin Evohaler® (washed SS formulation demonstrated superior MMAD, $FPF_{5.8\ \mu m}$ and $EPF_{1.1\ \mu m}$) and Proventil® HFA (washed SS formulation demonstrated superior $EPF_{1.1\ \mu m}$). Additionally the $FPF_{5.8\ \mu m}$ standard deviation generated from the washed SS formulation was less variable than for the commercially available formulations. As the experimental technique used to generate this data was standardised throughout aerosol testing, this difference in variability was most likely a feature of the formulations used. The lower $FPF_{5.8\ \mu m}$ variability for the washed SS formulation could allude to the consistent performance of this formulation however as the sample number was small (n = 3) such results cannot be taken as conclusive.

Factors other than the particle manufacturing process may have also played a part in the significantly superior data profiles achieved from the aerosolised washed SS formulation. Formulation excipients such as surfactant, present in both the washed SS (lecithin) and Proventil® HFA (oleic acid) but not the Ventolin Evohaler®, may have played a role in reducing the MMAD of particles emitted from pMDI when compared to a formulation containing no surfactant. As salbutamol sulphate is well known for its cohesive nature, surfactants incorporated in pMDI formulations can play an integral role in stabilising the drug dispersion, and preventing particle aggregation (Hickey *et al* 1988; Vervaet and Byron 1999), which may be a possible reason for their ability to maintain a reduced MMAD.

Ethanol is often used as a co-solvent to improve the solubility of surfactants in HFA based formulations (Tzou *et al* 1997; Smyth 2003) and was used as an excipient in both the Proventil® HFA and washed SS formulations. Ethanol is also known to exert its effect as a vapour pressure modifier (Gupta *et al* 2003; Stein and Myrdal 2006). The vapour pressure of a propellant is critical in

influencing the performance of a pMDI in terms of the aerosol droplet velocity and the dose delivery characteristics (Morén 1978; Stein and Myrdal 2006). The reduction of the propellant vapour pressure by the addition of a less volatile solvent such as ethanol will cause the aerosolised formulation to exit the atomisation nozzle at a reduced speed and can consequently minimise impaction in the throat (Gabrio *et al* 1999). Reduced vapour pressure is a possible rationale as to why aerosolisation of both SS formulations containing ethanol, Proventil® HFA and washed SS, resulted in a reduced impaction at the ACI throat and generated significantly larger $FPF_{5.8\ \mu m}$ than the Ventolin Evohaler®. Although the washed SS formulation did display a deposition of particles at the throat and inlet stages similar in total to the throat deposition from Ventolin Evohaler®, this is likely to be a feature of the presence of particle aggregation (explained earlier) rather than the vapour pressure.

The Ventolin Evohaler® formulation has been reported to generate a larger spray plume force upon actuation, 95.4 mN, compared to Proventil® HFA, 29.3 mN (Gabrio *et al* 1999). As the Ventolin Evohaler® formulation does not contain ethanol, the relatively higher vapour pressure caused the aerosolised Ventolin Evohaler® droplets to exit the atomisation nozzle at high speeds leading to increased ACI throat deposition observed in the deposition profiles. An increased impaction at the upper stages of the ACI would consequently reduce the mass of particles reaching the lower stages leading to the reduced $FPF_{5.8\ \mu m}$ observed.

Although the aerosolised particles emitted from the washed SS formulation had a MMAD that was lower than the Ventolin Evohaler® and comparable to the Proventil® HFA, the GSD is another important parameter that should be considered. The GSD measures the spread of the particle size distribution. Although all formulations were observed to generate polydisperse aerosols (GSD > 1.2) the actuated washed SS formulation had the greatest degree of polydispersity when compared to the two commercial SS formulations. An increased GSD can have detrimental effects on the respirable fraction of

aerosolised drug particles although this was not seen with the washed SS formulation.

### 2.4.3.2 Microscopic Characterisation of Aerosolised SS Formulation

Visual observations of ACI plates showed the largest deposition of drug particles on Stages 5 and 6. This observation was supported by the aerodynamic particle size distribution profiles (Figure 2.12), which indicated that a relatively large degree of aerosolised particles were within the respirable size fraction and deposited at the lower stages of the ACI.

Scanning electron microscopy of the aerosolised, washed SS formulation deposited on Stage 5 revealed amorphous bridged structures (possibly surfactant-coated SS particles). Stage 6 SEMs revealed a continuous matrix (which may be the sticky surfactant system) interspersed with protrusions of a heterogeneous population (possibly the surfactant-coated SS particles).

Although micrographs showed particle deposition at Stage 5 and 6 of the ACI (cut-off diameter 1.1 μm and 0.7 respectively), the observed larger particle dimensions suggest that particle agglomeration was still prevalent. Whilst particles were solvent-washed to remove excess surfactant, the presence of the surfactant, even at a minimal quantity, may have caused the particles to agglomerate as they impacted on the ACI plate. It is also possible that sample heating during SEM processing and analysis may have caused particle agglomeration. As discrete particles could not be seen from the SEM images, the 60 actuations of the formulation into the ACI could have resulted in particle overload on the ACI stages, another significant reason as to why particle agglomeration may have been observed. The difference in appearance between the particles deposited on Stages 5 and 6 could be a feature of the larger mass of SS depositing on Stage 5 (Figure 2.12), causing a greater degree of ACI stage overload resulting in more agglomeration than on Stage 6. Further characterisation of discrete particles may have been possible at higher magnifications. However, due to the magnifying limitations of the SEM the

particles could not be viewed at higher magnifications without a significant loss in the image resolution.

## 2.5 Conclusion

This chapter aimed to further test and develop the nanotechnology process proposed by Dickinson *et al* (2001) and evaluate its potential for achieving effective pulmonary drug delivery from pMDIs.

Optimum microemulsions, comprising water phase: surfactant: organic phase 26:52:22 w/w/w, were lyophilised in the presence of SS to confer surfactant-coated SS particles. Particle characterisation using SEM and quantification using HPLC assays revealed that the developed washing procedure served to successfully remove some of the excess surfactant from the SS particles with a 10-fold reduction in surfactant content. However, the SS particles remained aggregated, rendering sizing of discrete particles difficult.

Incorporation of solvent-washed SS particles into a pMDI revealed an easily dispersed flocculated system that, upon aerosolisation, displayed deposition profiles skewed towards the smaller particle size range relative to commercial SS formulations. Aerodynamic particle size data confirmed that the developed nanotechnology process had generated smaller SS particles than the commercially available formulations. These studies highlight the potential for the use of this novel low-energy microemulsion process technology in delivering macromolecules to the lower respiratory tract.

# CHAPTER THREE

# Preparation of pDNA Particles

## 3.1 Introduction

The previous chapter focussed on developing a process (Figure 2.1) used to generate particles for incorporation into pMDI systems using small molecular weight drugs. This chapter will concentrate on advancing this technology to incorporate macromolecules and assessing the suitability of the technology for such use. As the native structure of macromolecules is susceptible to damage during processing conditions, applying the technology to pDNA will introduce new formulation challenges previously not faced when dealing with small molecular weight drugs. Some of these challenges and other strategies which have been investigated to overcome them are included in this introduction.

The novel process used for preparing pDNA particles in this project included a freeze-drying step. Freeze-drying consists of two major steps, freezing of the pDNA microemulsion and drying of the frozen solid under a vacuum. Although freeze-drying is particularly suited to formulating thermolabile drugs (Anchordoquy *et al* 1997; Cherng *et al* 1997; Talsma *et al* 1997), as solvents are eliminated by applying pressures as well as temperature, the process itself can often induce destabilising stresses for the pDNA. Both the pDNA formulation and the design of the freeze-drying process play an important role in pDNA stabilisation.

Maintenance of pDNA biological function is dependent upon preserving its native structure after the freeze-drying process. As the structure and conformational states of DNA are critically dependent on the hydration level, the removal of water as either ice (during the freezing stage) or gas (during the drying stage) can cause pDNA to concentrate, consequently promoting aggregation (Anchordoquy *et al* 1997; Allison and Anchordoquy 2000) and pDNA degradation (Poxon and Hughes 2000). Previous studies on lyophilised pDNA have demonstrated that preservation of pDNA integrity and prevention of aggregation are critical in maintaining pDNA function, assessed through maintenance of the plasmid supercoiled conformation (Ando *et al* 1999) and transfection rates (Anchordoquy *et al* 1997; Allison and Anchordoquy 2000) respectively. Two accepted methods for reducing pDNA degradation are by

controlling the rate of freezing and by incorporating a lyoprotectant into the pDNA formulation.

pDNA function (damage) can be affected by the rate of cooling during the freeze-drying process (Anchordoquy *et al* 1998). The time between the start of the freezing process and the point at which the product is frozen is critical (Woelders and Chaveiro 2004). Rapid freezing of macromolecules by liquid nitrogen has been shown to minimise damage when compared to slow freezing (Anchordoquy *et al* 1998; Heller *et al* 1999). The reason for this being that as the freezing process begins the aqueous media in which the macromolecule is suspended begins to crystallise into ice. During this freezing process, the unfrozen fraction of the media progressively reduces. As the macromolecule resides in the unfrozen fraction, the progressive reduction of this fraction causes the macromolecule to concentrate into a small area eventually leading to macromolecule aggregation (Anchordoquy *et al* 1998). Contrary to rapid freezing, the process of slow freezing allows macromolecules such as pDNA sufficient time to diffuse away from the ice crystals causing the pDNA to aggregate in the progressively reduced unfrozen fraction.

The use of sugar excipients has proven to be critical in maintaining macromolecule function during both the freezing and drying stages (Talsma *et al* 1997; Carpenter and Crowe 1988a; Poxon and Hughes 2000). The mechanism by which excipients exert their protective effect on pDNA has yet to be clearly elucidated, although several mechanisms have been put forward. Two mechanisms, which are by no means exclusive, are explained below.

Vitrification is a process of converting a material into a glass-like amorphous solid. The process of vitrification is dependent on glass transition temperature (Tg), which is the temperature below which an amorphous material is in a glassy state and above which it is a viscous liquid. This process of glass formation has been proposed as responsible for the stabilisation of macromolecules during freeze-drying (Franks *et al* 1991). Macromolecules trapped in a glassy matrix, i.e. vitrified, during freezing will have limited

mobility so that the rates of reactions, including macromolecule unfolding, aggregation and chemical degradation, are reduced relative to the rates which can occur in a rubber state (Levine and Slade 1992). Sugars have been found to cause glass formation (Crowe *et al* 1994). Rapid freezing of a sample in the presence of a sugar is therefore found to maintain pDNA integrity as the pDNA would not have sufficient time to aggregate before glass formation occurs (Zelphati *et al* 1998).

The shortcomings of vitrification as a mechanism to explain the protection conferred by sugars is exemplified when looking at dextran and trehalose. Dextran exists as a glass at a higher temperature than trehalose. Although dextran is capable of causing glass formation which should, according to the vitrification hypothesis, confer greater stability of macromolecules than trehalose, the converse has been found to be true (Crowe *et al* 1994; Allison *et al* 1999). This example highlights that although an important mechanism, vitrification alone is insufficient in preventing loss of macromolecule function during freeze-drying (Crowe *et al* 1994).

The replacement of hydrogen bonding between water and macromolecules such as protein, by that of sugar and protein, known as the "water replacement hypothesis" is considered to be a key factor by which sugars stabilise macromolecules during freeze-drying (Carpenter and Crowe 1988b, 1989). Protection conferred through hydrogen bonding would therefore indicate that the sugar moiety plays a critical role (Carpenter *et al* 1987). Sugars, such as the disaccharides sucrose and trehalose which posses a greater number of hydroxyl groups than monosacharrides such as glucose should and do result in conferring greater macromolecule stability (Carpenter *et al* 1987; Allison and Anchordoquy 2000).

Although the degree of structural protection conferred by sugars correlates with the extent of hydrogen bonding between sugar and protein, the excipient molecular size must also be taken into account. Potential steric hindrance due to the molecular size has been reported to dictate the hydrogen bonding

capacity of sugars (Allison *et al* 1999). Dextran, for example, a relatively large complex branched polysaccharide is testament to this. Although dextran has many hydroxyl groups, its size results in its inability to hydrogen bond adequately to the protein. This steric hindrance results in its failure to inhibit dehydration-induced protein unfolding (Crowe *et al* 1994; Allison *et al* 1999).

### 3.1.1 Plasmid EGFP-N1

The pEGFP-N1 reporter plasmid was selected as an appropriate candidate gene for incorporation into pDNA particles. pEGFP-N1 contains the commonly used reporter gene enhanced green fluorescent protein (EGFP). EGFP is a mutant variant of green fluorescent protein gene (GFP) native to the bioluminescent jellyfish *Aequorea Victoria* (Prasher *et al* 1992). GFP was first identified as a marker for gene expression by Chalfie *et al* (1994). The GFP gene codes for the GFP protein which exhibits green fluorescence when exposed to blue light. The ability of GFP to fluoresce in cells without the need for exogenous substrates makes it an ideal marker for gene expression in living cells, an important requirement for the scope of this project.

pEGFP-N1 has several important sites critical to its function and identification indicated on Figure 3.1.

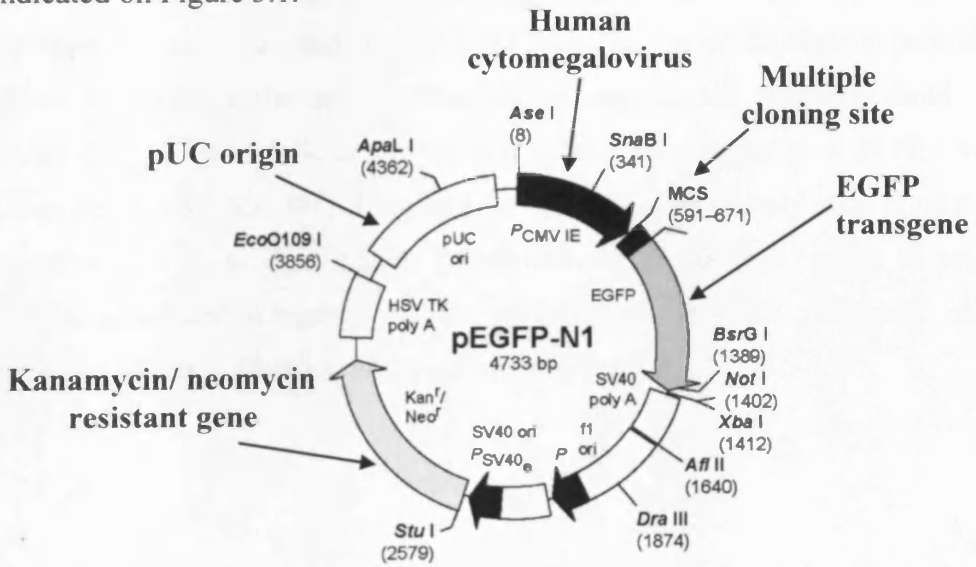


**Figure 3.1 Schematic diagram of plasmid enhanced green fluorescent protein construct.** Adapted from Clontech (1999).

The EGFP transgene utilises a cells transcription and translation apparatus to biosynthesise the EGFP protein marker. The human cytomegalovirus (CMV) promoter provides for efficient expression of the transgene in mammalian cells through binding with transcription factors during the initiation of gene transcription. The multiple cloning site (MCS) located on the N terminus of the EGFP gene contains restriction sites that only occur once within a given plasmid. The MCS plays an important role in plasmid identification during restriction digest assays.

The kanamycin/ neomycin resistant gene confers host resistance to kanamycin and neomycin antibiotics. This gene therefore permits selection of pEGFP-N1 transformed bacteria host cells during plasmid propagation. The pUC origin is the origin at which DNA replication is initiated. As the pDNA will replicate within the host cell independently of the host cell's own replication cycle, the pUC origin determines the number of copies of the plasmid which can be made, i.e. the vector copy number, in each host cell.

pDNA can exist as three main conformations, supercoiled, nicked circular/ open circular and linear. Processing pDNA can lead to degradation of its native structure. Although linear DNA forms have also been found to be transfection competent (Chancham and Hughes 2001; von Groll *et al* 2006) most published literature supports the opinion that pDNA supercoiled structure should be retained to optimise cellular transfection efficiency (Cherng *et al* 1999; Even-Chen and Barenholz 2000; Remaut *et al* 2006) and to comply with regulatory requirements on product quality (Arulmuthu *et al* 2007). In order to assess pDNA structural integrity, pDNA samples are typically analysed using ethidium bromide (EtBr) agarose gel electrophoresis.

### 3.1.2 Specific Aims and Objectives of the Chapter

The overall aim of this chapter is to research the potential for developing a nanotechnology process, originally used for small molecular weight drugs (Dickinson *et al* 2001), to prepare surfactant-coated pDNA particles. The development of this technology to prepare macromolecule particles will invariably face new challenges due to the susceptibility of the macromolecule native structure to damage during processing.

The primary aim of this chapter is to develop an approach to optimise retention of pDNA integrity by investigating the use of lyoprotectants and freezing rates. This chapter will also aim to compare the freeze-drying procedure with spray-drying, another process widely used in forming pDNA particles for pulmonary delivery (Seville *et al* 2002; Li *et al* 2005a). Subsequent aims of this chapter are to investigate the transferability of the wash procedure developed in the previous chapter to remove excess surfactant from pDNA particles without reducing pDNA integrity.

The experimental objectives are to:

1. Amplify and purify pEGFP-N1 from DH5α *Escherichia coli* (*E. coli*) and confirm pEGFP-N1 identity and integrity through the use of restriction endonucleases and ethidium bromide agarose gel electrophoresis.
2. Optimise pDNA integrity during freeze-drying by investigating the effect of freezing rate and the lyoprotection conferred by various sugar excipients.
3. Identify the optimum pDNA concentration incorporated into the aqueous phase of a microemulsion.
4. Compare the effectiveness of freeze-drying and spray-drying as methods to produce pDNA particles from pDNA incorporated microemulsions.
5. Remove excess surfactant from the surfactant-coated pDNA particles using washing procedures.
6. Verify pDNA stability in solvent-washed pDNA particles through maintenance of the supercoiled fraction.
7. Characterise the engineered nanoparticles using SEM and particle sizing techniques.

## 3.2 Materials and Methods

All reagents were used as received and were purchased from Fisher Scientific UK Ltd. (Loughborough, UK) unless otherwise stated.

Deionised water was obtained from an Elga reservoir (High Wycombe, UK). Iso-octane (2,2,4 trimethylpentane 99+ %), Luria agar (Miller's LB agar), Luria broth, *Not I*, 10x buffer SH, sucrose 99+ %, D-lactose monohydrate and D- (+)-glucose 99.5% minimum were purchased from Sigma-Aldrich Ltd. (Poole, UK). D-Trehalose anhydrous 99% was purchased from ACROS Organics (Geel, Belgium). Agarose (LE analytical grade) *EcoR I*, 10x buffer H and Wizard® DNA Clean-Up System product A7280 were purchased from Promega Ltd. (Southampton, UK). 2-Log DNA ladder (0.1–10.0 kb) 1000 μg/ml was purchased from New England Biolabs (Hertfordshire, UK). Library efficiency® DH5α™ competent cells kit containing pUC19 and super optimal broth with catabolite repression medium (SOC), kanamycin (100 mg/ml) and ampicillin (100 mg/ml) were purchased from Invitrogen Ltd. (Paisley, UK). pEGFP-N1 (4.7 kb) reporter pDNA was purchased from Clontech Laboratories Inc. (Palo Alto, USA). 5x coloured loading buffer blue was purchased from Bioline Ltd. (London, UK). Qiagen Plasmid Mega Kit® was purchased from Qiagen Ltd. (Crawley, UK). Liquid nitrogen was purchased from BOC Gases Ltd. (Manchester, UK).

### 3.2.1 Bacterial Transformation

Bacterial transformation is a process whereby foreign pDNA is introduced into a bacterial vector to amplify the quantity of pDNA.

All apparatus were sterilised or purchased as sterile prior to use.

Transformation:

The process of transformation (as outlined in the Invitrogen protocol, (Invitrogen 2003) involved transforming the DH5α strain of *Escherichia coli* (*E. coli*) bacteria with pEGFP-N1, using kanamycin to ensure selective growth of transformed bacteria (Figure 3.1).

Library efficiency® DH5α™ competent cells were gently thawed to 4°C after which 100 µl of the competent cell suspension was aliquoted into a pre-chilled polypropylene tube (Falcon® 2059 Becton, Dickinson Biosciences, Oxford, UK). For the transformation, 1 µl of pEGFP-N1 (10 ng/µl) in Tris-EDTA buffer (Tris-Cl, EDTA) (TE buffer) pH 8.0 was pipetted into the tube, mixed gently and then placed on ice for 30 min. Competent cells were heat shocked by placing in a water bath set at 42°C for 45 sec, after which the cells were immediately returned to ice for a further 2 min. At that point 900 µl of room temperature sterile SOC medium was pipetted into the heat shocked cell suspension. The tube was capped and incubated in an orbital shaker (100 rpm and 37°C) for 1 hr. The cell suspension mixture was then diluted with 250 µl of sterile Luria broth (2.5% w/v).

A sterile Luria agar plate was prepared by adding 25 µl of kanamycin (100 mg/ml) to 25 ml of autoclaved Luria agar in deionised water (4% w/v). The inoculated Luria agar was gently poured into a plastic petri dish in the presence of a Bunsen burner flame. Once the agar had set, 100 µl of the diluted cell suspension mixture was pipetted onto the plate and spread over the surface of the agar using a sterile cell spreader. The agar plate was then covered with a lid, inverted and incubated for 16 to 18 hr in a humidified incubator (37°C/ 5% $CO_2$).

During the process of bacterial transformation three controls were also prepared alongside the pEGFP-N1 transformed *E. coli.* The controls were used as a way of validating the bacterial transformation process.

Control A (positive control):
A Luria agar (4% w/v) plate containing no antibiotic was streaked with 100 µl of the heat shocked DH5α *E. coli* cells transformed with pEGFP-N1 (prepared as above). The agar plate was then covered with a lid, inverted and incubated for 16 to 18 hr in a humidified incubator (37°C/ 5% $CO_2$).

This agar plate should serve as a positive control, bacterial colonies should be

visible in order to demonstrate that the heat shock process has not resulted in cell death.

Control B (positive control):
A Luria agar (4% w/v) plate containing 25 µl of ampicillin (100 mg/ml) and 31.3 µl of X-gal (40 mg/ml) was prepared in the presence of a Bunsen burner flame.

DH5α competent cells were gently thawed as above and 100 µl was aliquoted into a pre-chilled polypropylene tube using a pipette. pUC19 was used as the control plasmid, 5 µl (10 pg/µl) of which was pipetted into the competent cell suspension. The sides of the polypropylene tube were then gently tapped to ensure sufficient mix of the cells with the plasmid. The cells were then heat shocked and incubated in the orbital shaker using the procedure outlined above. The reaction mixture was diluted by pipetting 9 ml of Luria broth (2.5% w/v) and 100 µl was spread onto the surface of the ampicillin-X-gal impregnated Luria agar gel plate. The agar plate was then covered with a lid, inverted and incubated for 16 to 18 hr in a humidified incubator (37°C/ 5% $CO_2$).

pUC19 is a plasmid vector containing the lacZ gene coding for β-galactosidase. In the presence of X-gal, the substrate is cleaved by β-galactosidase to yield a blue product. Control B acts as a visual marker used to identify *E. coli* cells successfully transformed with pUC19.

Control C (negative control):
A sterile Luria agar (4% w/v) plate prepared using 25 µl of kanamycin (4% w/v) was streaked with non-transformed DH5α *E. coli* cells using a sterile inoculation loop. The agar plate was then covered with a lid, inverted and incubated for 16 to 18 hr in a humidified incubator (37°C/ 5% $CO_2$).

This agar plate should serve as a negative control in which bacterial growth should be inhibited by the antibiotic.

Propagation:

*E. coli* bacteria successfully transformed using pEGFP-N1 was propagated for further experimental use.

A McCartney bottle was prepared containing 10 ml of sterile Luria broth (2.5% w/v) and 10 µl of kanamycin (100 mg/ml) in the presence of a Bunsen burner flame. A single colony of the pEGFP-N1 transformed *E. coli* was removed from the agar plate and placed into the McCartney bottle using a sterile inoculation loop. The McCartney bottle was then covered using a loosely screwed cap and incubated in an orbital shaker (100 rpm and 37°C) for 16 to 24 hr.

Storage:

A sterile pipette was used to remove 50 µl of incubated bacterial culture from the McCartney bottle and placed into a pre-chilled microcentrifuge tube. An equal volume of glycerol in deionised water (30% v/v) was pipetted into the microcentrifuge tube and mixed gently by tapping the sides of the tube. The microcentrifuge tube containing the glycerol-cell mix was immersed in an ethanol-dry ice bath for 5 min and then stored in -80°C for future use.

### 3.2.2 pDNA Amplification and Purification

Preparation of Luria agar plate:

A Luria agar plate containing 25 ml sterile Luria agar (4% w/v) in water and 25 µl kanamycin (100 mg/ml) was prepared using the methods described in Section 3.2.1 (Bacterial Transformation). DH5α *E. coli* glycerol stocks of pEGFP-N1, prepared in Section 3.2.1, were gently thawed on ice after removal from -80°C storage and streaked over the surface of the agar plate using a sterile inoculation loop in the presence of a Bunsen burner flame. The agar plate was then covered with a lid, inverted and incubated for 16 to 24 hr in a humidified incubator (37°C/ 5% $CO_2$).

Amplification of pDNA:

A McCartney bottle was prepared containing 5 ml of sterile Luria broth

(2.5% w/v) and 5 µl of kanamycin (100 mg/ml) in the presence of a Bunsen burner flame. A single colony of the pEGFP-N1 transformed *E. coli* was removed from the agar plate and placed into the McCartney bottle using a sterile inoculation loop. The McCartney bottle was then covered using a loosely screwed cap and incubated in an orbital shaker (300 rpm and 37°C) for 8 hr.

After the initial propagation, 1 ml of the bacterial suspension was sub-cultured into 500 ml conical flasks each containing 125 ml of sterile Luria broth (2.5% w/v) and 125 µl of kanamycin (100 mg/ml). The tops of the flasks were covered with foil; flasks were then incubated in an orbital shaker (300 rpm and 37°C) for 16 hr. The bacterial cultures were split equally between two 250 ml Sorvall® polypropylene centrifuge bottles (Sorvall®, North Carolina, USA) and centrifuged at 6000 x g for 15 min (4°C).

Purification of pDNA:

pEGFP-N1 was harvested and purified using Qiagen Plasmid Mega Kit®. The process, detailed in the Qiagen® plasmid purification handbook (Qiagen® 2005), briefly involved lysing the bacteria, complexing and discarding cell debris and chromosomal DNA (cDNA), adsorbing the pDNA onto the column, washing through impurities (degraded RNA) and eluting the pDNA. Propan-2-ol and ethanol were then used to precipitate the pDNA resulting in pure pDNA. Finally the pDNA precipitated pellets were dissolved in 1 ml of warmed TE buffer pH 8.0 and stored in a sterile eppendorf.

Samples were removed at set stages of the purification procedure in order to monitor the procedure on an analytical level (Qiagen® 2005). Samples were analysed using gel electrophoresis (Section 3.2.3.1).

### 3.2.3 Assessment of pDNA Quality

#### 3.2.3.1 Gel Electrophoresis – Analysis of pDNA Purification Procedure

Samples removed during the purification of pDNA (Section 3.2.2) were analysed as a means of assessing the purification procedure.

A 1% (w/v) agarose gel was prepared by boiling 1 g of agarose in 100 ml of 1x Tris-borate EDTA buffer (Tris-Borate, EDTA) (TBE buffer) pH 8.0 until the agarose was fully dissolved. The solution was then left to cool at room temperature. Once the solution had cooled to approximately 55°C, 80 µl of EtBr solution (a fluorescent probe) was added to the agarose solution. The solution was swirled to ensure a sufficient mix and was then poured into an electrophoresis plate containing an 8-well comb. Once the gel had solidified, it was placed into an electrophoresis tank and submerged under 1x TBE buffer.

Aliquots of 15 µl were removed from each of the four samples taken throughout the purification procedure (Section 3.2.2) and made up to 20 µl using 5x coloured loading buffer blue. A sample of the purified pDNA diluted to 2 µg/ 15 µl using TE buffer pH 8.0 was also prepared and made up to 20 µl using 5x coloured loading buffer blue. A 20 µl aliquot of each sample was then carefully pipetted into the wells of the agarose gel.

The gel was developed for 30 min at 200 volts using an electrophoresis power supply and analysed using Molecular Analyst® software and Bio-Rad Gel Doc 1000 (Bio-Rad Laboratories Ltd., Hertfordshire, UK).

### 3.2.3.2 Determination of pDNA Yield and Purity

pDNA concentration was determined by the UV absorbance at 260 nm using an Eppendorf Biophotometer (Eppendorf Ltd., Cambridge, UK). An aliquot of pDNA stock solution was diluted x50 using TE buffer pH 8.0 and transferred to an Eppendorf Uvette® (Eppendorf Ltd., Cambridge, UK). The diluted aliquot was analysed for double stranded DNA (dsDNA) concentration. The purity of the dsDNA was calculated from the absorbance ratios given at $A_{260}/A_{280}$.

### 3.2.3.3 pEGFP-N1 Restriction Enzyme Double Digest – Determination of Plasmid Identity

A restriction enzyme double digest was used to confirm pDNA identity with the aid of a restriction map of pEGFP-N1 (Figure 3.2).

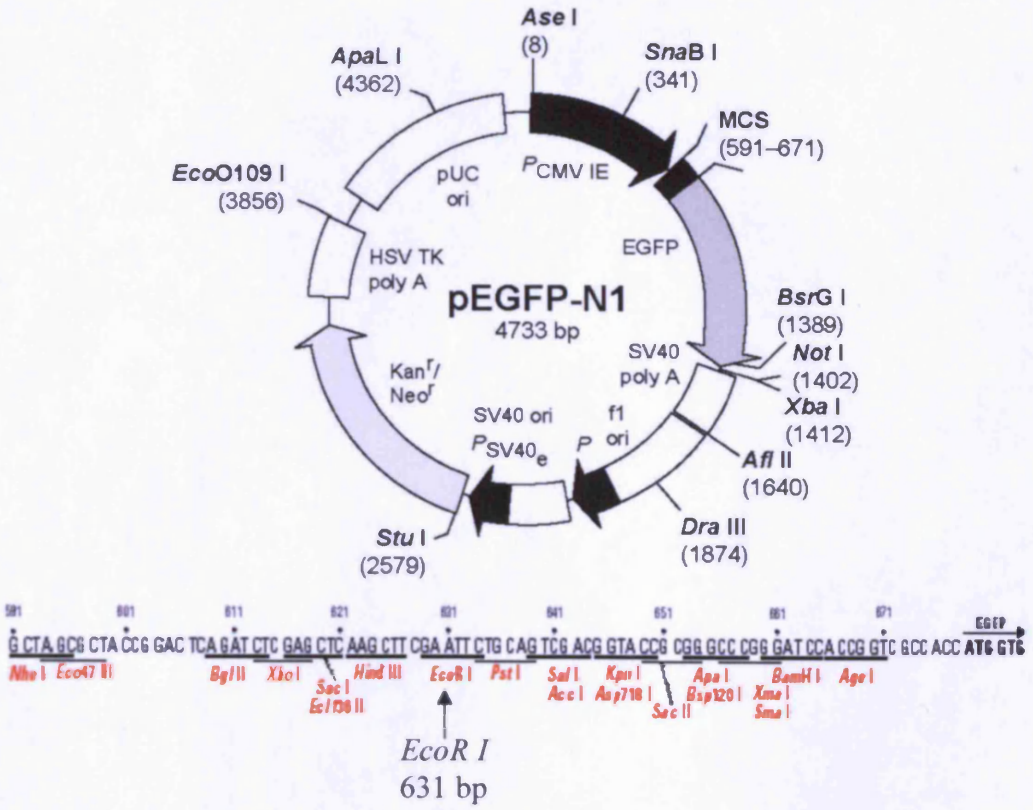


**Figure 3.2 Restriction map and multiple cloning site of pEGFP-N1.** Adapted from Clontech (1999).

pDNA was incubated with *EcoR I* and/ *Not I* restriction enzymes for a single digest and a double digest (Table 3.1).

Table 3.1 Single digest and double digest components.

| Component | Single digest | Single digest | Double digest |
|---|---|---|---|
| Restriction enzyme | *EcoR I* | *Not I* | *EcoR I* & *Not I* |
| | 0.5 µl | 0.5 µl | **2 x 0.5 µl** |
| Digest buffer | 10x buffer H | 10x buffer SH | 10x buffer H |
| | 2 µl | 2 µl | 2 µl |
| pEGFP-N1 | 2 µg | 2 µg | 2 µg |
| Sterile water | up to 20 µl | up to 20 µl | up to 20 µl |

Typically, 2 µl of 10x digest buffer was pipetted into a sterile microcentrifuge tube containing autoclaved water (to a final volume of 20 µl). To this solution

2 μg of pDNA was introduced, followed by the addition of 0.5 μl of the restriction enzyme. The tube was gently mixed and incubated at 37°C for 2 hr. Three digestions were performed (Table 3.1), the first containing *EcoR I* as the restriction enzyme, the second containing *Not I* as the restriction enzyme with the third being a double digest using both restriction enzymes.

After the incubation period, aliquots of 15 μl from each digest mix were made up to 20 μl with 5x coloured loading buffer. A sample of the purified pDNA diluted to 2 μg/ 15 μl using TE buffer pH 8.0 was also prepared and made up to 20 μl using 5x coloured loading buffer blue. The 20 μl aliquots of each sample were then carefully pipetted into the wells of an EtBr agarose gel (prepared as in Section 3.2.3.1). A DNA 2-log ladder was also pipetted into a well (no dilution was required). The gel was developed for 2 hr at 150 volts using an electrophoresis power supply and analysed using Molecular Analyst® software and Bio-Rad Gel Doc 1000 (Bio-Rad Laboratories Ltd., Hertfordshire, UK).

### 3.2.4 Investigating the Effect of Lyoprotectant and Freezing Rate on Lyophilised pDNA

Prior to forming surfactant-coated pDNA particles, an initial pilot study was performed to investigate optimal lyoprotectants and rates of freezing for retaining pDNA integrity during lyophilisation.

Investigating Alternative Lyoprotectants

Six sugars were investigated for pDNA lyoprotection; disaccharides; sucrose, lactose, maltose and trehalose; a monosaccharide glucose and a sugar alcohol mannitol. pDNA (50 μg) was added to six freeze-drying vials (Fisher Scientific Ltd., Loughborough, UK) containing 5 ml of deionised water and sugar 3% (w/v) which was deemed a sufficient lyoprotectant concentration to maintain pDNA integrity (Cherng *et al* 1997; Seville *et al* 2002; Li *et al* 2005a). A seventh vial containing 50 μg of pDNA in 5 ml of deionised water (sugar was excluded) was prepared as a negative control. All seven vials were gently vortexed to ensure a good mix before being frozen using one of two freezing rates (below) prior to lyophilisation.

Investigating Alternative Freezing Rates

In order to identify any effect freezing rate may have on the integrity of pDNA through freeze-drying, vials containing pDNA and the various sugars (prepared above) were frozen using one of two methods:

Rapid Freezing: pDNA samples were snap-frozen by submerging vials in liquid nitrogen prior to lyophilisation.

Controlled Freezing: Samples were frozen using a cryopreservation technique typically used in freezing and storing cells. pDNA samples were placed in a polystyrene container and frozen at -20°C for 2 hr, and then placed into deep freeze at -80°C for 16 hr. Samples were then submerged in liquid nitrogen prior to lyophilisation.

All frozen samples were subsequently lyophilised for 24 hr using the Heto Drywinner freeze-drier (Heto-Holten, Alleroed, Denmark) with the condenser chamber set at -110°C.

Freeze-dried pDNA samples were diluted to a final concentration of 2 μg/ 15 μl using TE buffer pH 8.0 and made up to 20 μl using 5x coloured loading buffer blue. A control sample of the unprocessed pDNA diluted to 2 μg/ 15 μl using TE buffer was also prepared and mixed with gel-loading dye. The 20 μl aliquots of each sample were then carefully pipetted into the wells of a 1% (w/v) agarose gel containing EtBr (Section 3.2.3.1). The gel was developed for 30 min at 200 volts using an electrophoresis power supply and analysed using Molecular Analyst® software and Bio-Rad Gel Doc 1000 (Bio-Rad Laboratories Ltd., Hertfordshire, UK).

### 3.2.5 Preparation of pDNA Particles

Microemulsions of previously optimised constituent ratios were prepared as outlined in Section 2.2.1. pDNA was added to the aqueous phase (26% w/w of microemulsion) containing sucrose (3% w/v) as lyoprotectant and agitated using a vortex mixer to form a solution prior to addition into the surfactant

(lecithin: propan-2-ol (1:3)) (52% w/w of microemulsion) and iso-octane (22% w/w of microemulsion) mixture. Various pDNA concentrations were investigated in order to establish the maximum quantity of pDNA that could be successfully incorporated into a microemulsion.

Optimised pDNA microemulsions were subjected to one of two drying methods to form pDNA particles.

Freeze-Drying

Pre-weighed centrifuge tubes containing pDNA loaded microemulsions were sealed with perforated Parafilm and snap-frozen by submersion in liquid nitrogen. Snap-frozen microemulsions were placed into a tray filled with dry ice in order to maintain their solid state, ensuring sublimation rather than melting occurred, and lyophilised for 24 hr using a Heto Drywinner freeze-drier (Heto-Holten, Alleroed, Denmark) with the condenser chamber set at -110°C. After the drying procedure, centrifuge tubes were re-weighed to determine percentage yield.

Spray-Drying

Centrifuge tubes containing pDNA loaded microemulsions were placed under the feed hose of a Büchi B-191 mini spray dryer (Büchi Labortechnik, Flawil, Switzerland). The spray dryer was operated under the following conditions; inlet temperature 120°C; spray flow rate 600 l/hr; aspirator 100%; pump 20%. These conditions resulted in an outlet temperature of 80°C. Spray-dried particles were removed from the collection vessel using a spatula. The recovered formulation was weighed to determine percentage yield.

### 3.2.6 Analysis of pDNA Particles

#### 3.2.6.1 Integrity of pDNA Particles

Agarose gel electrophoresis, with EtBr staining, was used to determine the physical integrity of the processed pEGFP-N1. Following the microemulsion and drying stages, surfactant from the freeze-dried and spray-dried surfactant-coated pEGFP-N1 particles was removed using a Wizard® DNA Clean-Up kit.

This was deemed necessary as excess surfactant in the microemulsion and resulting particulates could hinder the pDNA migration across the agarose gel.

Sample Preparation Using a Wizard® DNA Clean-Up System

An in-depth protocol for surfactant clean up is available on the Promega (2006) web site. The sample was taken through a three stage process: binding, washing and elution briefly explained below.

Binding Stage: 28 mg of surfactant-coated pDNA particles were weighed out into a microcentrifuge tube containing 1 ml Wizard® DNA Clean-Up resin and mixed by inversion. The resin/ pDNA mix was pipetted into a syringe barrel which was attached to a minicolumn. A syringe plunger was then used to slowly push the resin/DNA mix into the minicolumn.

Washing Stage: 2 ml of propan-2-ol was pipetted into the syringe barrel and slowly pushed through the minicolumn using a plunger. The minicolumn was then transferred to a microcentrifuge tube and centrifuged at 13,000 rpm for 2 min using a Sanyo MSE Micro Centaur microcentrifuge (Sanyo Electric Co., Ltd., Hertfordshire, UK) to dry the resin.

Elution Stage: 50 µl of pre-warmed de-ionised water (65-70°C) was pipetted into the minicolumn and left for 1 min. The minicolumn was then transferred to a new microcentrifuge tube and centrifuged as before for 20 sec. Centrifugation at this stage eluted the bound pDNA.

Aliquots of 15 µl eluted pDNA and a control sample of the unprocessed pDNA (2 µg/ 15 µl) were made up to 20 µl with 5x coloured loading buffer and ran through an EtBr agarose gel as previously outlined in Section 3.2.3.1.

### 3.2.6.2 Microscopic Characterisation of pDNA particles

Excess surfactant in the microemulsion and resulting particulates could potentially cause particle aggregation and hinder surface morphology characterisation. For this reason a solvent-wash procedure was utilised to

remove excess surfactant from the surfactant-coated pDNA particles. Freeze-dried surfactant-coated pDNA particles (500 mg) and spray-dried surfactant-coated pDNA particles (9 mg) were solvent-washed using the optimised sequential wash Method Two using propan-2-ol (outlined in Chapter 2, Section 2.2.3).

Solvent-washed pDNA formulations were sputter coated with gold (gold sputter coater, EM Scope, Kent, UK) and viewed using a Philips XL-200 Scanning Electron Microscope (TEI Company, Eindhoven, The Netherlands) (previously outlined in Section 2.2.3).

### 3.2.6.3 Integrity of Solvent-Washed pDNA Particles

Following the microemulsion and solvent removal stages, surfactant from the lyophilised surfactant-coated pEGFP-N1 (28 mg) and solvent-washed pEGFP-N1 (0.8 mg) was removed using a Wizard® DNA Clean-Up System (Section 3.2.6.1). Aliquots of 15 µl eluted pDNA and a control sample of the unprocessed pDNA (2 µg/ 15 µl) were made up to 20 µl with 5x coloured loading buffer and ran through an EtBr agarose gel as previously outlined in Section 3.2.3.1.

### 3.2.6.4 Measurement of Particle Size

The mean diameter of the solvent-washed pDNA particles was determined by photon correlation spectroscopy using a Coulter® N4 Plus (Coulter Electronics Ltd., Luton, UK). Particles of lyophilised pEGFP-N1 (2 mg) were dispersed in iso-octane (5 ml) and agitated using a vortex mixer for ~ 3 min. Samples were transferred into a clear sided disposable cuvette, which was sealed using Parafilm to prevent evaporation. Measurements were expressed using the unimodal size distribution model and repeated six times.

## 3.3 Results

### 3.3.1 Bacterial Transformation

pEGFP-N1 was introduced into a bacterial vector using the process of bacterial transformation. In order to assure that the transformation was successful, three controls were also prepared. Agar plate A streaked with pEGFP-N1 transformed DH5α *E. coli* cells without the presence of antibiotic shows an abundant growth of bacterial colonies (Figure 3.3A). The appearance of colonies acted as a marker to indicate that heat shocking did not result in total cell death. Agar plate B which was streaked with DH5α *E. coli* transformed with pUC19 in the presence of ampicillin and X-gal, reveals the presence of discreet blue colonies. For visual purposes the blue colonies were highlighted on the figure using circles (Figure 3.3B). The blue colonies observed on plate B were the result of X-gal cleaved by β-galactosidase an enzyme coded for by the lacZ gene contained within the plasmid vector, which acted as a visual marker to confirm that the process resulted in cells successfully transformed with pUC19. Agar plate C streaked with non-transformed DH5α *E. coli* cells in the presence of kanamycin reveals a blank plate, showing no bacterial colonies. The absence of colonies is due to antibiotic induced cell death. Agar plate D which was streaked with pEGFP-N1 transformed DH5α *E. coli* cells in the presence of kanamycin reveals multiple discrete colonies. These colonies were a result of successfully transformed bacteria with pEGFP-N1 as untransformed bacteria would succumb to antibiotic induced cell selection.

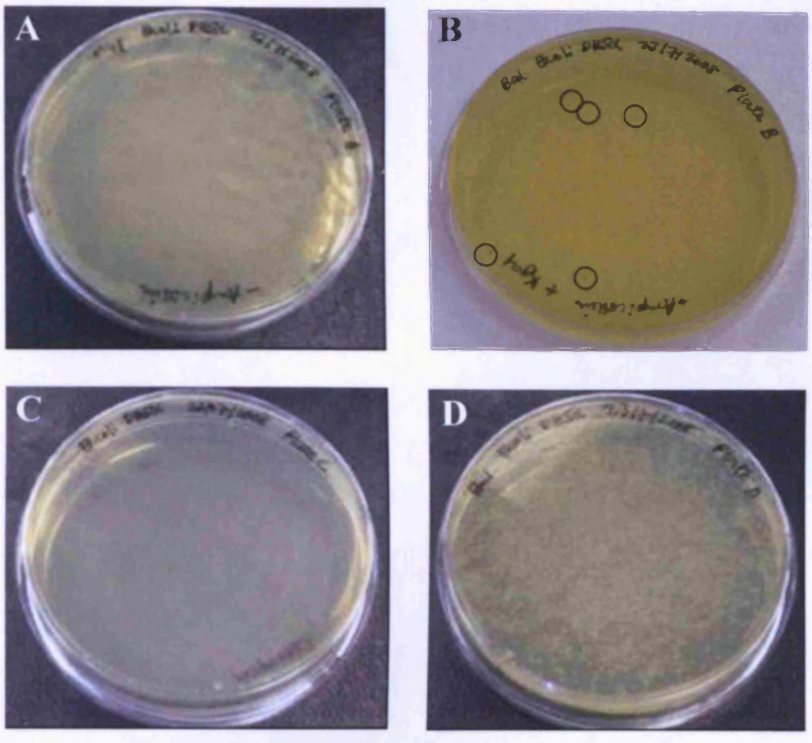


**Figure 3.3 Photographs taken of treated Luria agar plates during bacterial transformation. A:** Control A plate containing no antibiotic, streaked with pEGFP-N1 transformed DH5α *E. coli* cells. **B:** Control B plate containing ampicillin and X-gal, streaked with pUC19 transformed DH5α *E. coli* cells. The circles indicate the presence of blue colonies. **C:** Control C plate containing kanamycin, streaked with non-transformed DH5α *E. coli* cells. **D:** agar plate containing kanamycin streaked with pEGFP-N1 transformed DH5α *E. coli* cells.

### 3.3.2 Assessment of pDNA Quality

#### 3.3.2.1 Gel Electrophoresis – Analysis of pDNA Purification Procedure

The success of the plasmid purification procedure was monitored on an analytical gel (Figure 3.4).

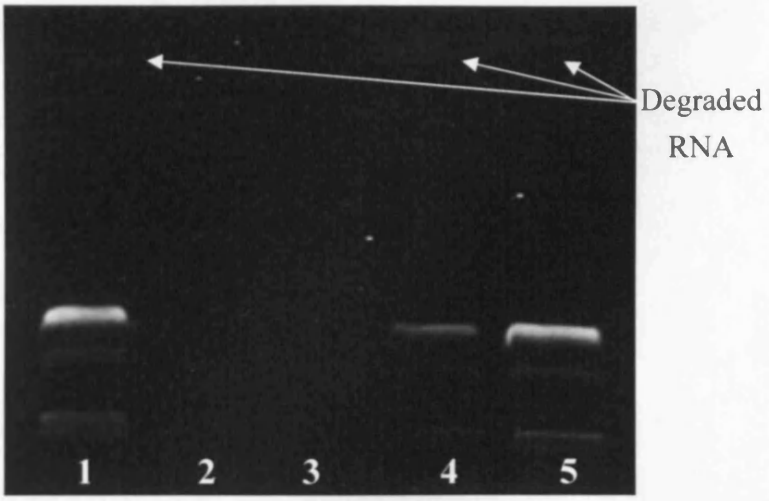


**Figure 3.4 A typical agarose gel analysis of the pEGFP-N1 purification procedure.** Sample (**1**) cleared bacterial lysate. Sample (**2**) pDNA supernatant flow through column. (**3**) buffer wash through column. Sample (**4**) column eluate containing pure pDNA sample. Sample (**5**) stock pDNA. The arrows indicate degraded RNA.

The original bacterial lysate (lane 1, Figure 3.4) contained supercoiled and open circular pDNA as well as a small band of degraded RNA (visible as a faint band at the top of the lane highlighted by an arrow). The pDNA supernatant flow through column and the buffer wash used to remove contaminants from the pDNA bound column (lanes 2 and 3 respectively, Figure 3.4) show no bands, indicating that there was no pDNA flow through the column and that the pDNA remained bound to the column during the wash step of the purification procedure. The absence of pDNA bands during these two stages revealed that there was no excessive loss of pDNA which could result in a low yield. The column eluate (lane 4, Figure 3.4) contained pure pDNA as well as a faint band at the top of the lane indicating a small band of degraded RNA. Both the eluate and the purified pDNA (lane 4 and 5 respectively, Figure 3.4) had three bands present in the DNA profile. The presence of the intense supercoiled band in the samples containing pDNA

(lanes 1,4 and 5) verify that the pDNA remained intact throughout the procedure. The results shown here confirm the efficiency of the techniques used and are representative of the many batches of pDNA produced throughout the time course of the project.

### 3.3.2.2 Determination of pDNA Yield and Purity

Purified pDNA was routinely quantified by UV-vis spectrophotometric analysis using an Eppendorf Biophotometer. Typical pDNA yields ranged from 2 mg to 3.5 mg which was within the expected range for high copy plasmids (Qiagen® 2005). The pDNA absorbance $^{260}/_{280}$ ratio was typically in the region of 1.8 indicating the samples were free from salt and protein contamination with 100% purity.

### 3.3.2.3 pEGFP-N1 Restriction Enzyme Double Digest – Determination of Plasmid Identity

A restriction enzyme double digest was carried out to confirm the identity of the amplified and purified pDNA (Section 3.2.2). As indicated on the pEGFP-N1 restriction map (Figure 3.2), there is one specific restriction site for each restriction enzyme; *EcoR I* and *Not I*. Incubation with each of these enzymes caused the linearization of the plasmid at a single site visualised in lanes labelled *EcoR I* and *Not I* (Figure 3.5). The bands in each of these two lanes correspond to the linearised form of pEGFP-N1 made up of 4,700 base pairs, which is confirmed by the 2-log ladder (Figure 3.5). The last lane on the gel is the result of the double digest using both restriction enzymes *EcoR I* and *Not I*. The difference between the *EcoR I* and *Not I* restriction site on the plasmid map (Figure 3.2), is approximately 770 base pairs. This linear piece is visualised at the top of the lane (Fragment 1, Digest x2, Figure 3.5) confirmed with reference to the 2-log ladder. The larger second band, approximately 3,930 base pairs (Fragment 2), produced by the double digest is visible at the expected range for pEGFP-N1.

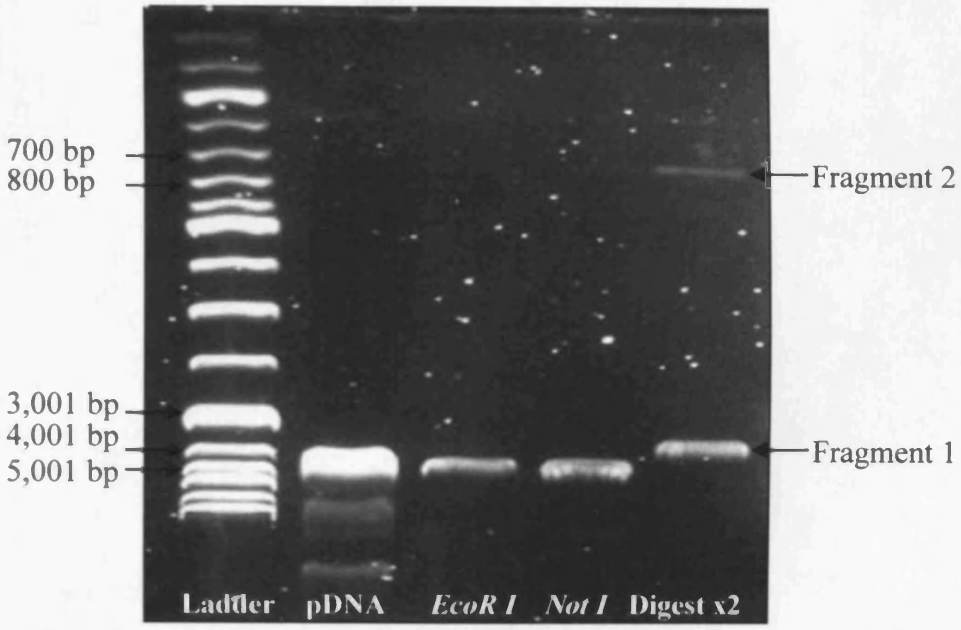


**Figure 3.5 A typical gel electrophoresis image of pEGFP-N1 after a single and double digest. Ladder:** 2-log ladder. **pDNA:** pure pDNA. ***EcoR I*:** single digest of pDNA by *EcoR I* restriction enzyme. ***Not I*:** single digest of pDNA by *Not I* restriction enzyme. **Digest x2:** double digest of pDNA using both *EcoR I* and *Not I*.

### 3.3.3 Investigating the Effect of Lyoprotectant and Freezing Rate on Lyophilised pDNA

Comparisons were made between the physical integrity of pDNA lyophilised in the presence of various lyoprotectants and freezing rates in order to optimise pDNA retained integrity post-lyophilisation. The integrity of the tertiary structure of pEGFP-N1 post-lyophilisation can be determined by the presence of a supercoiled band in line with that shown by the unprocessed pEGFP-N1. Figure 3.6 and Figure 3.7 show the supercoiled signal band relating to pEGFP-N1 lyophilised in the presence of various lyoprotectants and freeze-dried using the rapid freezing and controlled freezing methods respectively (Section 3.2.4). In all but one case, pEGFP-N1 lyophilised using mannitol as the lyoprotectant, the integrity of pEGFP-N1 was clearly maintained throughout processing with maintenance of the supercoiled band. A partial reduction in pDNA signal intensity was, however, observed when comparing the supercoiled bands of the processed pDNA samples to the unprocessed positive control. pDNA lyophilised in the presence of mannitol (lane 'Man', Figure 3.6 and Figure 3.7) appeared to migrate at a slower rate than unprocessed pDNA (+ve Control,

Figure 3.6 and Figure 3.7). In respect to the pDNA freeze-dried using the fast freezing method without the presence of a lyoprotectant (-ve Control, Figure 3.6) the supercoiled band, although present, shows a partial reduction in the signal intensity. pDNA frozen using the controlled freezing method and lyophilised without the presence of a lyoprotectant (-ve Control, Figure 3.7) displays a supercoiled band with a signal intensity equivalent with that emitted from unprocessed pDNA (+ve Control, Figure 3.7).

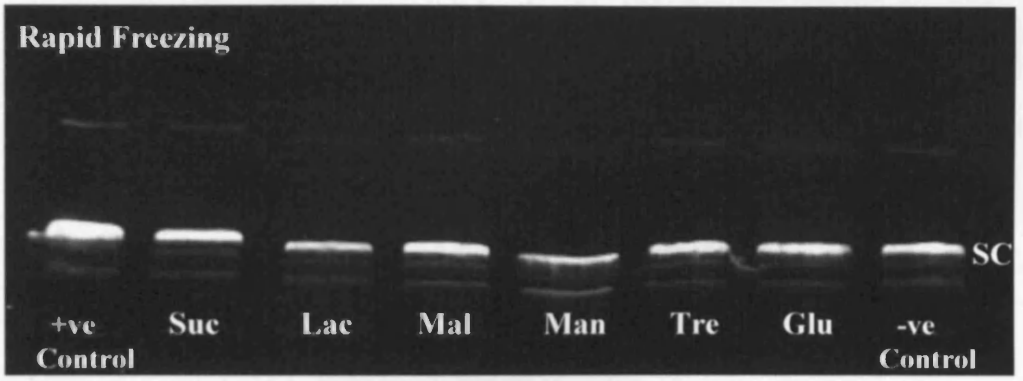


**Figure 3.6 Gel electrophoresis image of pEGFP-N1 after rapid freezing and lyophilisation in the presence of various lyoprotectants. +ve Control**: unprocessed pDNA, **Suc:** sucrose, **Lac:** Lactose. **Mal:** maltose, **Man:** mannitol, **Tre:** trehalose, **Glu:** glucose, **–ve Control:** pDNA freeze-dried without a lyoprotectant. (n = 1) (**SC:** supercoiled fraction).

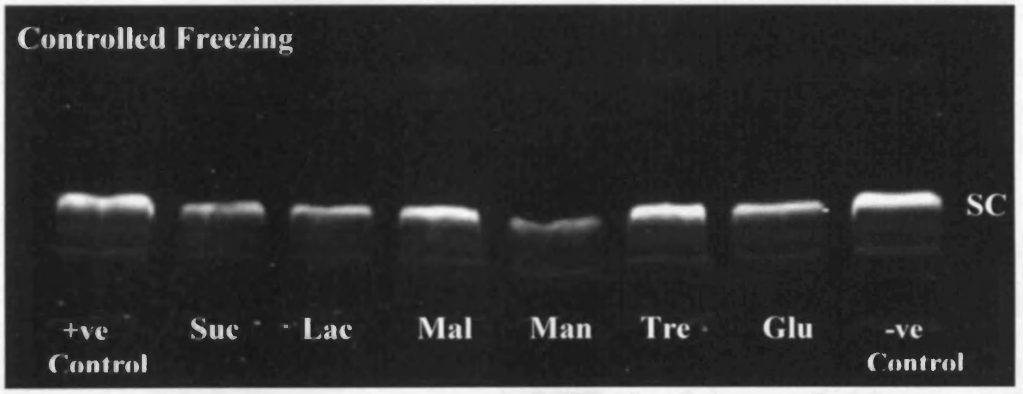


**Figure 3.7 Gel electrophoresis image of pEGFP-N1 after controlled freezing and lyophilisation in the presence of various lyoprotectants. +ve Control**: unprocessed pDNA, **Suc:** sucrose, **Lac:** Lactose. **Mal:** maltose, **Man:** mannitol, **Tre:** trehalose, **Glu:** glucose, **–ve Control:** pDNA freeze-dried without a lyoprotectant. (n = 1) (**SC:** supercoiled fraction).

Semi-quantitative signal analysis was used to compare fluorescence emission

(Figure 3.8). The percentage of fluorescence attributable to the supercoiled fraction of pDNA that was maintained post-lyophilisation (Figure 3.8) was calculated by comparing the intensity of the supercoiled band from the processed pDNA samples against that of the unprocessed pDNA. The fluorescence emitted from the supercoiled band of the unprocessed pDNA in this analysis (+ve Control, Figure 3.6 and Figure 3.7) was taken as 100%.

The percentage of fluorescence maintained by the pDNA supercoiled fraction was reduced in all pDNA samples that had undergone the lyophilisation process (Figure 3.8).

Rapid Freezing:

pDNA lyophilised in the presence of sucrose and maltose maintained the highest percentage of supercoiled signal intensity of all the lyoprotectant samples (70% and 75% respectively). Mannitol performed the poorest as a pDNA lyoprotectant, the percentage fluorescence emitted from the supercoiled band was taken to be 0% (lane 'Man', Figure 3.8) as the top most band from this sample did not migrate as far as the supercoiled band from the unprocessed pDNA (Figure 3.6). In most cases the presence of a lyoprotectant maintained either the same (lactose 48%) or a higher percentage of fluorescence emitted from the supercoiled fraction than pDNA lyophilised without the presence of a lyoprotectant (48%).

Controlled Freezing:

The highest percentage of supercoiled fluorescence that was maintained using the controlled freezing method was achieved when maltose or trehalose were used as lyoprotectants (79% and 86% respectively). The worst performing lyoprotectant once again was found to be mannitol (0% pDNA supercoiled fluorescence maintained). The relative percentage of signal intensity afforded by supercoiled pDNA lyophilised without the presence of a lyoprotectant was higher (89%) than for any pDNA samples lyophilised in the presence of a lyoprotectant.

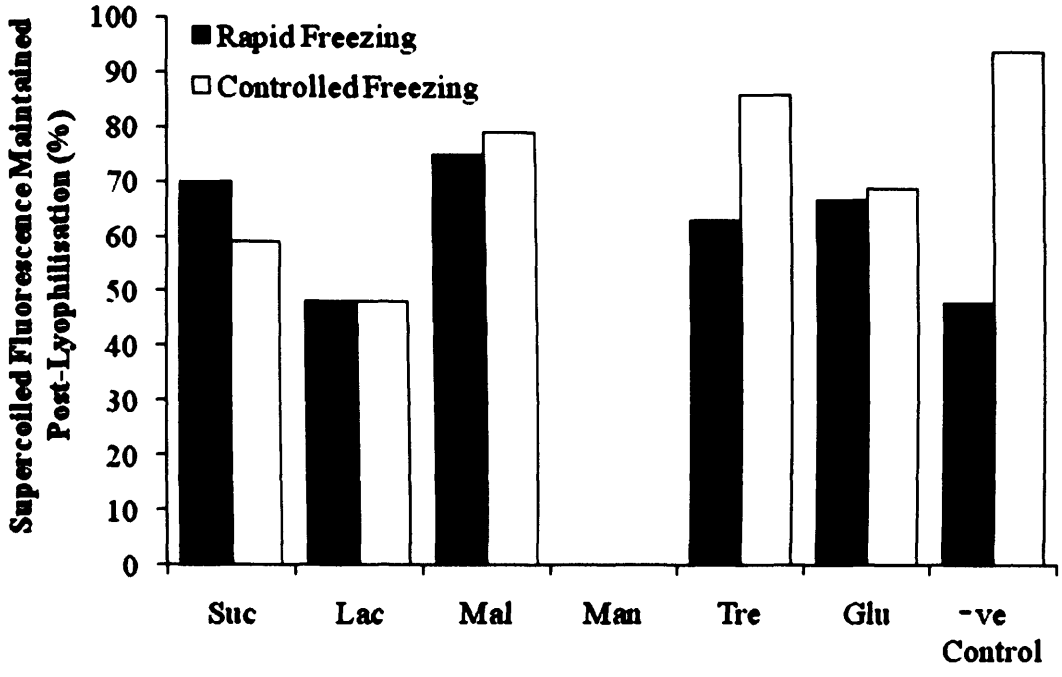


**Figure 3.8 A comparison of pDNA lyoprotection conferred using sugars and freezing rates.** The values represent a semi-quantitative analysis of the ratio of fluorescence emitted from the supercoiled band of lyophilised pDNA compared to unprocessed pDNA. **Suc:** sucrose, **Lac:** Lactose. **Mal:** maltose, **Man:** mannitol, **Tre:** trehalose, **Glu:** glucose, **–ve Control:** pDNA freeze-dried without a lyoprotectant. (n = 1).

### 3.3.4 Preparation of pDNA Particles

Visual observation revealed that pDNA incorporated into the aqueous phase of an optimised microemulsion (Section 2.2.1) at concentrations above approximately 0.048% (w/v) resulted in a biphasic microemulsion (Table 3.2). The incorporation of pDNA at concentrations of 0.048% (w/v) and below produced isotropic microemulsions.

Table 3.2 Investigating the maximum quantity of pDNA that can be successfully incorporated into the aqueous phase of an optimised microemulsion system (n = 3).

| pEGFP-N1 (% w/v) | Observation |
|---|---|
| 0.096 | Cloudy microemulsion with a biphasic system forming 10 min after pDNA addition |
| 0.048 | Isotropic microemulsion |
| 0.028 | Isotropic microemulsion |

### 3.3.5 Investigating the Effect of Freeze-Drying versus Spray-Drying During pDNA Processing

Solvent and water present in pDNA microemulsions was removed using either freeze-drying or spray-drying resulting in the production of surfactant-coated pDNA particles (Table 3.3). The surfactant-coated pDNA particles produced from either method had an amorphous yellow appearance and a sticky texture. pDNA particles were almost completely recovered after undergoing the freeze-drying process 94 ± 5% (mean ± sd; n = 3) (Table 3.3). Product recovery after spray-drying was lower at 20 ± 10%.

Table 3.3 Percentage yield of surfactant-coated pDNA particles recovered from the freeze-drying and spray-drying process (mean ± sd; n = 3).

| Process | Yield (%) | Observed product |
|---|---|---|
| Freeze-drying | 94 ± 5 | Yellow surfactant with a sticky texture |
| Spray-drying | 20 ± 10 | Yellow surfactant with a sticky texture |

#### 3.3.5.1 Integrity of pDNA Particles

The integrity of pDNA was assessed following drying and removal of the surfactant (Section 3.2.6.1). Figure 3.9 shows the fluorescent pDNA signal, prior to and post freeze-drying or spray-drying. The integrity of pEGFP-N1, as evidenced by similar band intensity for supercoiled fraction, was maintained through either drying process.

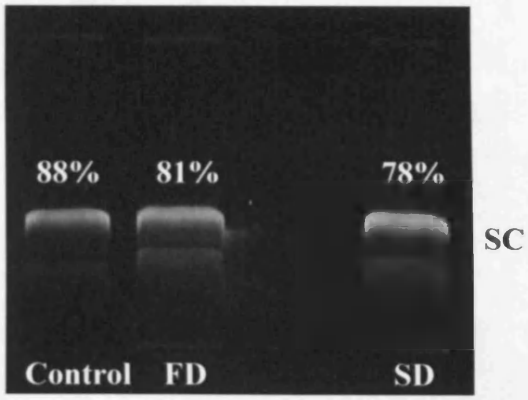


**Figure 3.9 A typical gel electrophoresis image of pEGFP-N1 after freeze-drying and spray-drying. Control:** unprocessed pEGFP-N1, **FD:** Freeze-dried pEGFP-N1, **SD:** Spray-dried pEGFP-N1. The percentage values represent a semi-quantitative analysis of the ratio of fluorescence emitted from the supercoiled band compared to the total pDNA. All percentages are mean of n = 3 (**SC:** supercoiled fraction).

A semi-quantitative signal analysis was used to compare the fluorescence emission between the samples. The percentage supercoiled fluorescence was calculated by comparing the intensity of the supercoiled band against the fluorescence emitted from the total pDNA signal. The supercoiled band of unprocessed pDNA contributed 88 ± 7% (mean ± sd; n = 3) of emitted fluorescence from the total pDNA (Control, Figure 3.9). Once the pEGFP-N1 had been incorporated into a microemulsion and freeze-dried, fluorescence from the supercoiled fraction was reduced to 81 ± 12% (FD, Figure 3.9). Removing solvent from pDNA incorporated in a microemulsion using the spray-drying process caused a reduction in the supercoiled fraction to 78 ± 19% of the total fluorescence emitted from the whole pDNA (SD, Figure 3.9).

### 3.3.5.2 Microscopic Characterisation of pDNA particles

SEM was utilised to characterise any differences between the pDNA formulations dried using one of the two methods, freeze-drying or spray-drying.

Freeze-Dried:

SEM images of unwashed surfactant-coated freeze-dried pDNA particles revealed a continuous matrix with no visible particle outline (Figure 3.10).

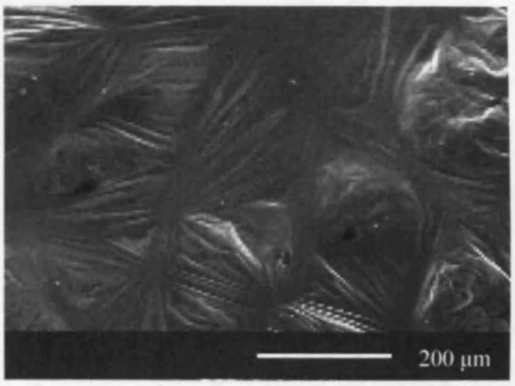


**Figure 3.10 Scanning electron micrograph of unwashed surfactant-coated freeze-dried pDNA formulation containing lecithin, pEGFP-N1 and sucrose.** Scale bar = 200 µm.

Excess surfactant was removed from the lyophilised pDNA samples using a developed wash method which utilised propan-2-ol solvent and repeated vortexing and centrifugation cycles (outlined in Section 2.2.3) (Figure 3.11). SEM images of washed samples (Figure 3.11A) conferred aggregates of pDNA-lyoprotectant particles. Figure 3.11B shows the presence of a heterogeneous, in both size and shape, population made up of near spherical and cuboidal particles. Although particle sizes vary, all particles are generally less than 10 µm in size.

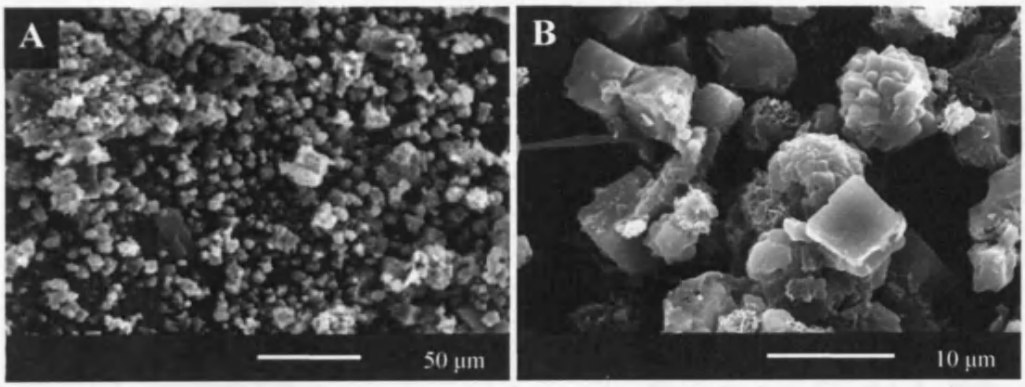


**Figure 3.11 Scanning electron micrographs of solvent-washed freeze-dried pDNA formulation containing pEGFP-N1 and sucrose.** Scale bar = 50 µm (A) and 10 µm (B).

Spray-dried:

SEM images, of unwashed surfactant-coated spray-dried pDNA particles, revealed a continuous matrix with no clear particle outline visible (Figure 3.12).

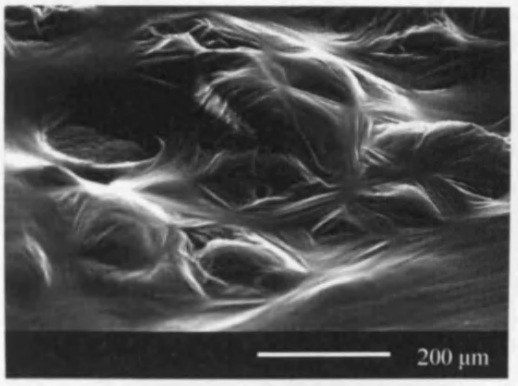


**Figure 3.12 Scanning electron micrograph of unwashed surfactant-coated spray-dried pDNA formulation containing lecithin, pEGFP-N1 and sucrose.** Scale bar = 200 µm.

As earlier a wash method utilising propan-2-ol solvent (Section 2.2.3) was used to remove excess surfactant from the spray-dried pDNA samples (Figure 3.13). SEM images of solvent-washed spray-dried pDNA particles (Figure 3.13A) revealed a general population of particle clusters residing in a continuous matrix. On closer inspection, Figure 3.13B revealed the continuous matrix interspersed with a heterogeneous particle population comprising of angular particles. Although the particle size is variable visible particles are smaller than 10 µm.

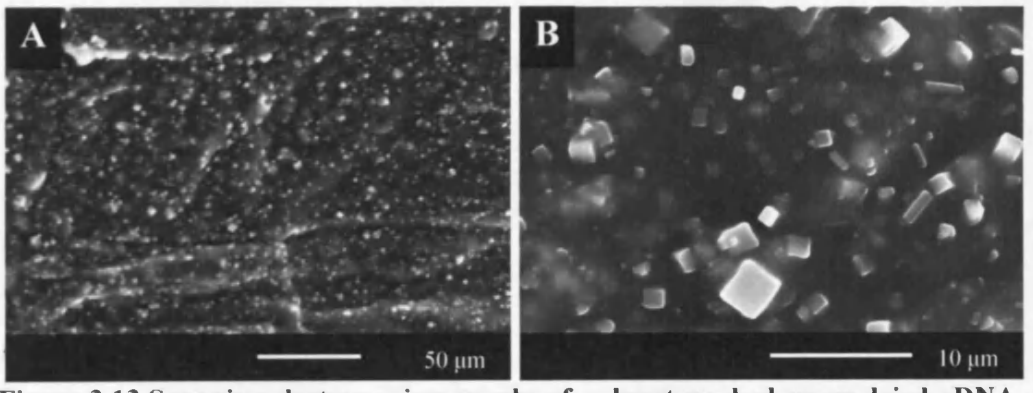


**Figure 3.13 Scanning electron micrographs of solvent-washed spray-dried pDNA formulation containing pEGFP-N1 and sucrose.** Scale bar = 50 µm (A) and 10 µm (B).

### 3.3.6 Analysis of Solvent-Washed pDNA Particles

#### 3.3.6.1 Integrity of Solvent-Washed pDNA Particles

The integrity of pDNA following processing was assessed using Figure 3.14. Figure 14 shows the supercoiled signal band relating to pEGFP-N1, prior to and following freeze-drying and solvent-wash cycles. The integrity of pEGFP-N1 was maintained through processing, although a partial reduction in pDNA signal intensity was observed.

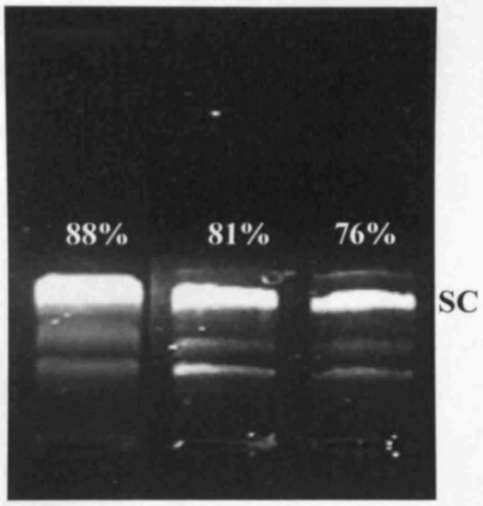


**Figure 3.14 A typical gel electrophoresis image of pEGFP-N1 before and after freeze-drying and solvent-washes.** The percentage values represent a semi-quantitative analysis of the ratio of fluorescence emitted from the supercoiled band compared to the total pDNA. All percentages are mean of n = 3 (**SC:** supercoiled fraction).

The fluorescence emitted from pDNA samples was compared using semi-quantitative signal analysis. The percentage supercoiled fluorescence was calculated by comparing the intensity of the supercoiled band against the fluorescence emitted from the corresponding whole pDNA. The supercoiled band of unprocessed pDNA contributed 88 ± 7% (mean ± sd; n = 3) of emitted fluorescence from the total pDNA (Figure 3.14). Once the pEGFP-N1 had been incorporated into a microemulsion and freeze-dried, fluorescence from the supercoiled fraction was reduced to 81 ± 12% and then further reduced to

76 ± 14% of the total after solvent-wash.

### 3.3.6.2 Measurement of Particle Size

Particle size analysis using photon correlation spectroscopy was performed on solvent-washed lyophilised particles. Analysis revealed particles with a mean diameter of 1.9 ± 0.8 μm (mean ± sd; n = 6). The average particle size distribution shown by the polydispersity index was 1.0 indicating a polydisperse population of particles.

## 3.4 Discussion

### 3.4.1 Choice of lyoprotectant

Ethidium bromide (EtBr) gel electrophoresis and semi-quantitative signal analysis were used to assess the physical integrity of processed pDNA and compare the supercoiled fluorescence emission respectively. The disaccharides sucrose and maltose (during rapid freezing) and trehalose (during controlled freezing) conferred the greatest pDNA stability (70%, 75% and 86% fluorescence maintained from the supercoiled fraction respectively). The superiority of disaccharides in maintaining macromolecule stability during freeze-drying has been reported due to their ability to promote glass formation (Crowe *et al* 1994) and by substituting water by hydrogen bonding with the macromolecule (Carpenter *et al* 1987; Carpenter and Crowe 1989).

The monosaccharide glucose maintained a lower pDNA supercoiled fraction than most of the disaccharides. Glucose is known to have a lower glass transition temperature and a fewer number of hydroxyl groups for hydrogen bonding than the disaccharides which could be a feasible reason for its poorer performance in maintaining pDNA integrity (Carpenter *et al* 1987; Allison and Anchordoquy 2000).

Mannitol, in particular, was found least effective at maintaining pDNA supercoiled fraction during freeze-drying. Gel electrophoresis images, for both rapid and controlled freezing, reveal that the migration of the top most band was slower than the supercoiled band of the unprocessed pDNA. This led to the belief that the pDNA freeze-dried in the presence of mannitol had predominantly degraded into its linearised and nicked open circular conformations. This increased pDNA degradation maybe attributable to the tendency for mannitol to crystallize during freeze-drying (Izutsu *et al* 1993). Excipients that crystallize rather than remain amorphous during freeze-drying, tend to separate from the macromolecule causing the macromolecule to concentrate in the uncrystallised fraction (Izutsu *et al* 1993; Allison and Anchordoquy 2000). This concentration effect causes the macromolecule to aggregate and consequently have reduced biological activity (Anchordoquy *et*

*al* 1997). The use of mannitol may have augmented pDNA degradation, which could explain the reason why a clear pDNA supercoiled fraction was not observed on the electrophoresis gels.

Comparisons between sugar induced pDNA protection during freeze-drying, using either rapid or controlled freezing, conferred no major differences between the freezing methods. Semi-quantitative signal analysis of pDNA processed without a lyoprotectant, however, revealed that an increased supercoiled fraction was maintained in controlled freezing conditions (89%) compared to rapid freezing conditions (48%). These results are contrary to the published literature which indicates the converse to be true as rapid freezing should be more efficient at minimising pDNA aggregation and therefore degradation (Anchordoquy *et al* 1998; Heller *et al* 1999).

The increased degradation of pDNA subjected to rapid freezing without a lyoprotectant compared to controlled freezing could however be explained by a cryolysis mechanism (Lyscov and Moshkovsky 1969). Lyscov and Moshkovsky (1969) described a mechanism of DNA degradation (cryolysis) that resulted from the formation of cracks within the ice during freezing. These cracks and therefore DNA degradation was shown to be more prevalent in rapidly cooled samples. This mechanism of cryolysis also offers an explanation as to why there were no major differences in the extent of pDNA degradation between the two freezing rates in the presence of a lyoprotectant. Glass formation caused by the addition of a sugar may have inhibited the cracking that is implicated in the DNA degradation during rapid freezing (Lyscov and Moshkovsky 1969; Franks *et al* 1991).

The data generated in this study revealed that during controlled freezing, a larger supercoiled pDNA signal was conferred from the pDNA sample processed without a sugar (89%) compared to with a disaccharide (trehalose 86%). This is contrary to the data generated for the pDNA frozen using rapid freezing methods and published data, where pDNA processed in the absence of a sugar has been reported to result in an increased degradation (Ando *et al*

1999; Allison and Anchordoquy 2000). Although a maintenance of up to 75% of pDNA supercoiled fraction post freezing-drying without a lyoprotectant has been reported, the use of a lyoprotectant has always been of benefit (Ando *et al* 1999). Considering the limitations of this study, as these sets of experiments were not repeated (n = 1), any significant conclusions should not be drawn. The results however do provide an insight into the applicability of rapid freezing and the disaccharides sucrose, in maintaining pDNA stability which was confirmed by published data (Carpenter and Crowe 1989; Crowe *et al* 1994; Allison and Anchordoquy 2000). As this study revealed that rapid freezing pDNA in the presence of sucrose during freeze-drying was able to sufficiently maintain pDNA stability, this method was utilised for preparing surfactant-coated pDNA particles for subsequent studies in this thesis.

### 3.4.2 Preparation of pDNA Particles

Varying quantities of pDNA were incorporated into the aqueous phase of an optimised microemulsion system comprising water phase: surfactant: organic phase 26:52:22 w/w/w (Section 2.3.1). Investigations revealed that incorporating pDNA up to a concentration of 0.048% (w/v) resulted in an isotropic system, indicating that the microemulsion had retained its stability. Increasing the pDNA concentration above 0.048% (w/v) resulted in a biphasic system, indicating that the microemulsion stability had been compromised. These results infer that the presence of the pDNA may have changed the microemulsion characteristics. To date there is a limited amount of work investigating how the presence of a drug affects microemulsion phase behaviour. However, the general consensus is that on addition of the hydrophilic drug, initially the microemulsion droplet size may reduce as the drug interacts with the hydrophilic portion of the surfactant (Lawrence and Rees 2000). However, further addition of the drug results in an increase in the droplet size (Park and Kim 1999). As the surfactant interacts with an increasing concentration of hydrophilic drug, this could alter the surfactant characteristics leading to changes in its ability to stabilise the system (Kelley and McClements 2003). It is therefore possible that as the droplet size increases, eventually the interfacial area will increase beyond the surfactants capability to maintain a

stable microemulsion, causing the system to phase separate.

### 3.4.2.1 Investigating the Effect of Freeze-Drying versus Spray-Drying During pDNA Processing

A comparative study between freeze-drying and spray-drying was carried out in order to determine the effectiveness of the drying method. The method of freeze-drying was compared to spray-drying as both have proved to be effective methods to prepare pDNA particles whilst maintaining pDNA integrity for lipid:protamine:pDNA (LPD) dry powders (Seville *et al* 2002; Li *et al* 2005a; Colonna *et al* 2008). The drying processes have not however, been evaluated in terms of their ability to form pDNA particles from microemulsion formulations.

In this comparative study the recovered percentage yield of the pDNA formulation was considered an important parameter. The reason for this was that each formulated microemulsion could only contain a maximum of 0.048% (w/v) pDNA in the aqueous phase whilst maintaining a stable isotropic state. Therefore, a low recovery of the pDNA particle formulation post-drying would result in a high wastage of pDNA that is relatively expensive and labour intensive to prepare. This would be detrimental from a large scale manufacturing perspective as well was for the progression of this project.

The recovered yields revealed a relatively large difference between the freeze-drying (94 ± 5%) and spray-drying process (20 ± 10%). The relatively high yield of recovered surfactant-coated pDNA particles from the freeze-dried procedure was to be expected as the formulation was dried *in situ* within its collection vessel (Liao *et al* 2004; Maitani *et al* 2008). Recovery from the spray-dried formulation however was deemed more difficult as the product was atomised and carried to the collection vessel using air flow. Typical yields of spray-dried samples are in the range of 40% to 70% (Maa *et al* 1998; Nguyen *et al* 2004; Li and Birchall 2006). This low yield is related to the fact that often small quantities of samples are spray-dried using relatively large spray-driers causing an increase in the possibility of sample loss throughout the apparatus.

In comparison to these reported typical yields, the quantity of pDNA formulation recovered in this study using spray-drying was exceptionally low. A possible reason for this was that as the pDNA particles were coated in surfactant which had a sticky texture, these particles had a tendency to stick to the various parts of spray-drying apparatus leading to a reduced sample recovery in the collection vessel. The low yield conferred from the spray-drying process is also a problem typically seen with cohesive powders for the same reason mentioned (Li *et al* 2005b; Li and Birchall 2006).

DNA integrity, assessed by gel electrophoresis, was studied following the drying of pDNA incorporated microemulsions using either freeze-drying or spray-drying methods. pDNA samples were analysed for their transfection competent supercoiled fraction as degradation of this fraction may have detrimental effects on the transfection efficiency of the pDNA (Cherng *et al* 1999; Chancham and Hughes 2001). Analysis of the unprocessed pDNA (control, Figure 3.9) indicated that 88% (± 7%) was in the supercoiled form which is within the expected range (80-90%) for small-scale, freshly made pDNA preparations (Middaugh *et al* 1998). Further analysis of freeze-dried and spray-dried preparations, showed a reduction in the supercoiled fraction (to approximately 81 (± 12%) and 78 (± 19%) respectively). This reduction may have possible adverse implications on the pDNA gene expression efficiency as, although linear DNA forms have been found to be transfection competent (Chancham and Hughes 2001; von Groll *et al* 2006), most published literature supports the opinion that pDNA supercoiled structure should be retained to optimise cellular transfection efficiency (Cherng *et al* 1999; Remaut *et al* 2006) and to comply with regulatory requirements on product quality (Arulmuthu *et al* 2007). However, in comparison to published reports, the results in this study infer that the process of either freeze-drying or spray-drying the pDNA-loaded microemulsion had a comparatively small adverse effect on the supercoiled form. The relatively small change in supercoiled fraction observed through processing is similar to that previously observed for freeze-dried and spray-dried lipid:protamine:pDNA (LPD) dry powders for inhalation prepared in the presence of a lyoprotectant (Seville *et al* 2002; Li *et*

*al* 2005a).

Freeze-dried pDNA samples were expected to retain their supercoiled fraction as the method works on the principle of sublimation using low temperatures and reduced pressures and is therefore suited to preparing thermolabile powders (Maitani *et al* 2008; Prego *et al* 2010). However, the relatively small reduction in the supercoiled fraction detected post spray-drying could initially be deemed as surprising, as spray-drying has demonstrated degradation of thermolabile macromolecules through shear-induced and thermal stress (Mumenthaler *et al* 1994; Ståhl *et al* 2002). The reason for this degradation is related to the fact that DNA denaturation is reported to occur at temperatures as low as 65°C (Lasic and Templeton 1996; Blake and Delcourt 1998). The elevated temperatures involved in the spray-drying procedure (inlet temperature 120°C, outlet temperature of 80°C) are therefore able to adversely affect the pDNA integrity. This said, the pDNA sample temperature may have remained significantly less than the drying air due to evaporative cooling and the final product may have been protected from overheating by its rapid removal from the drying zone (Johnson 1997). Also the presence of a lyoprotectant such as sucrose has been reported to aid in macromolecule preservation during spray-drying as a thermal and dehydration stress stabiliser (Tzannis and Prestrelski 1999; Colonna *et al* 2008).

The dimensions and surface morphology of processed pDNA particles were visualised using SEM. Microscopic characterisation of dried pDNA-lyoprotectant incorporated microemulsions revealed a continuous matrix, which may be the sticky surfactant system, covering the particles. A relatively high concentration of surfactant is required to stabilise microemulsion systems due to the large interfacial area between the disperse phase and the continuous phase (Shinoda *et al* 1991; Zarur *et al* 2000). However, the large quantity of surfactant used at the microemulsion stage leads to an excess of surfactant covering the pDNA particles resulting in the observed hindered surface morphology characterisation.

A solvent-wash technique developed in the previous chapter (Section 2.2.3) was used to remove the excess surfactant in order to visualise particles as the shape and size of the dried particles might differ depending on the drying condition used. Spray-drying for instance offers the potential to produce particles that are homogenous and smaller in size due to the atomisation and evaporation methods used during this process (Maa *et al* 1997; Seville *et al* 2002). These features, however, may not be observed in this study as the use of a microemulsion template should dictate the size of the resulting particles (Dickinson *et al* 2001).

Solvent-washed freeze-dried particle formulations revealed a reduction of excess surfactant so that individual particles could be visualised. The SEM images revealed a heterogeneous particle population comprising angular particles, likely to be the sucrose lyoprotectant, and more rounded particles, possibly including surfactant-coated pEGFP-N1 particles. SEM images of solvent-washed spray-dried pDNA particles revealed a continuous matrix, possibly the surfactant system, interspersed with protrusions of a heterogeneous particle population comprising of angular particles, likely to be the pDNA particle formulation.

A stark difference between the freeze-dried and spray-dried SEM images was observed due to the presence of the surfactant continuous matrix in the latter image. The presence of surfactant in the spray-dried SEM images may have been due to the fact that the spray-dried sample was put through a smaller number of wash cycles (3 wash cycles) compared to the freeze-dried sample (6 wash cycles). The reason for this being that a smaller quantity of the spray-dried sample was used in the solvent-wash, due to the low yield recovered Table 3.3, and so too many wash cycles may have resulted in total loss of the sample. The insufficient solvent-wash of spray-dried pDNA particles makes particle characterisation and any comparisons against the freeze-dried sample difficult. However, as the freeze-drying technique was found to successfully prepare transfection competent pDNA particles, and the solvent-wash procedure was able to remove some of the excess surfactant from the pDNA

particles, repeating this study for the spray-dried particles was not deemed necessary.

### 3.4.3 Analysis of Solvent-Washed pDNA Particles

The relatively high concentration of surfactant required to formulate a stable microemulsion system, in addition to hindering particle characterisation (Section 3.3.5.2), could also potentially adversely affect pDNA cellular functionality (Duncan *et al* 1997), an issue investigated in later chapters, and formulation dispersibility and physical stability in a pMDI due to the poor solubility of surfactants in HFA propellants (Blondino and Byron 1998). Although SEMs of the sequentially washed freeze-dried samples was found to successfully remove some of the excess surfactant (Section 3.3.5.2), it is important to assess pDNA integrity following solvent–washing from a pDNA functionality perspective. As mentioned earlier, a reduction in the transfection competent supercoiled fraction may have detrimental effects on the transfection efficiency of the pDNA (Cherng *et al* 1999; Chancham and Hughes 2001).

Analysis of freeze-dried and freeze-dried then solvent-washed preparations, did show a small reduction in the supercoiled fraction (from 88% (± 7%) unprocessed pDNA to approximately 81% (± 12%) and 76% (± 14%) respectively). This data highlights a possible limitation of the developed technology and the need for further optimisation of the process in order to maintain pDNA integrity and maximise cellular transfection efficiency. This said, comparisons of these results with those previously published infer that the process of freeze-drying the pDNA-loaded microemulsion had a comparatively small adverse effect on the supercoiled form and that further processing, via solvent-washing, was not particularly detrimental. The relatively small change in supercoiled fraction observed through processing, i.e. 88% to 76%, is similar to that previously observed for spray-dried lipid:protamine:pDNA (LPD) dry powders for inhalation prepared in the presence of a lyoprotectant (Seville *et al* 2002; Li *et al* 2005a). These results were not particularly surprising as although there are no published reports on the effect of solvent-washing pDNA particles,

solvent-washing protein particles to remove excess surfactant was found not to be detrimental (Nyambura *et al* 2009b).

Particle size analysis of solvent-washed lyophilised particles revealed particles with a mean diameter of 1.9 ± 0.8 μm. Photon correlation spectroscopy data supports the SEM images of lyophilised solvent-washed pDNA particles, as the particle sizing technique verifies that particles are smaller than 10 μm. Although the technology explored in this thesis was originally reported to generate particles of the nanoparticle size range (Dickinson *et al* 2001), such discrete particles were not detected. A possible reason for the larger particle size could be due to the particles being aggregated, which is certainly observed in the SEM images (Section 3.3.5.2). Nevertheless the particles generated from the developed technology was a significant advancement, as previous reports of lyophilised powders have often shown particles with diameters unsuitable for pulmonary delivery and generally require further processing using a milling step prior to incorporation into an inhaler (Seville *et al* 2002; Shoyele and Cawthorne 2006). It is generally acknowledged that particles require an aerodynamic diameter ≤ 5 μm to allow efficient penetration and deposition in the peripheral pulmonary regions (Hickey 1993). Solvent-washed lyophilised particles, although not in the nanoparticle size range, are still in the respirable size range for deposition in the bronchiolar and alveolar region.

## 3.5 Conclusion

This chapter aimed to further develop a nanotechnology process, previously used for small molecular weight drugs, and investigate its feasibility to formulate pDNA particles with the potential for incorporation into a pMDI.

Studies investigating the maintenance of pDNA integrity during freeze-drying demonstrated that pDNA freeze-dried in the presence of a disaccharide retained the supercoiled fraction which was confirmed by published data. Comparative studies between freeze-dried and spray-dried pDNA particles revealed that although in both cases the integrity of pDNA was maintained to a similar extent, freeze-drying was a more efficient process in terms of the recovered pDNA yield. Characterisation of solvent-washed freeze-dried pDNA particles, using SEM, and analysis of its retained integrity, using agarose gel electrophoresis, revealed that the developed washing procedure served to successfully remove some of the excess surfactant from the pDNA particles with a relatively small reduction in the pDNA integrity. Although the pDNA particles remained aggregated post-washing, particle sizing using photon correlation spectroscopy revealed pDNA particles were in the respirable size range for peripheral pulmonary deposition.

The data generated in this chapter highlight the feasibility of this developed technology, which utilises a low energy microemulsion lyophilisation process, to formulate pDNA particles with potential for incorporation into a pMDI system.

# CHAPTER FOUR

# Characterisation, Transfection and Cellular Toxicity of pDNA Delivered by pMDI

## 4.1 Introduction

The former chapter demonstrated that pDNA integrity could be maintained after processing to form pDNA particles using the outlined technology. This chapter will attempt to investigate the feasibility of incorporating these pDNA particles into a pMDI system and assess the pDNA biological functionality, using *in vitro* cellular transfection studies. Such studies will provide evidence of retained stability from a gene expression perspective.

Published reports have demonstrated that cellular uptake of naked DNA in its native form remains relatively inefficient (Zabner *et al* 1997; Remaut *et al* 2006). As a consequence, gene transfer vectors are employed in cellular transfection studies to promote cellular uptake and processing of the nucleic acid cargo (Remaut *et al* 2006; Davies *et al* 2008; Jiang *et al* 2008). Gene transfer vectors are generally split into two groups; viral gene vectors and non-viral gene vectors. Of the two, non-viral gene vectors are regarded to be the more clinically accepted form of vector from a safety perspective as they do not face the inherent safety and immunogenicity issues often associated with viral vectors (Thomas *et al* 2003; Li and Huang 2007). There are a number of non-viral gene vectors available including the polysaccharide chitosan (Guang Liu and De Yao 2002), polyethyleneimines (Densmore *et al* 2000) and dendrimers (Haensler and Szoka 1993; Jeong *et al* 2007). Also in this category of non-viral agents are cationic lipids and liposomes which have demonstrated proof-of-principle for gene transfer to the airway for almost two decades (Stribling *et al* 1992; Alton *et al* 1993; McDonald *et al* 1998).

### 4.1.1 Cationic Liposomes

Liposomes are structures composed of single or multiple concentric bilayers resulting from the assembly of amphiphilic molecules, such as phospholipids, in aqueous medium (Bangham and Horne 1964; Schuber *et al* 1998). Cationic lipids, which may form liposomes in aqueous media, can be divided into three main sections, a hydrophobic lipid anchor group which interacts with the cell membrane, a linker group which is responsible for the lipids chemical stability

and biodegradability and a positively charged head group which interacts with the plasmid and promotes condensation (Figure 4.1).

Felgner *et al* (1987) introduced the idea of using cationic liposomes as efficient pDNA carriers for intracellular delivery using N-[1-(2,3-dioleoyloxy) propyl]-N,N,N, trimethylammonium chloride (DOTMA). Since then other lipids such as 1,2 dioleoyloxypropyl-3 (trimethylammonium)- propane (DOTAP), 2,3 dioleyloxy-*N*-[2(sperminecarboxaminino)ethyl]-*N*,*N*-dimethyl-1 propanaminium (DOSPA) and cetyltrimethylammoniumbromide (CTAB) have been synthesised. Transfection studies in this chapter will focus on using DOTAP as this readily available lipid has been shown to be effective at delivering pDNA *in vitro* (Birchall *et al* 1999) and *in vivo* (Porteous *et al* 1997). In addition DOTAP has been suggested to have reduced cell toxicity compared to other lipids, such as DOTMA. This is because, unlike DOTMA, DOTAP contains readily cleavable ester bonds, which link the cationic headgroup to the lipid anchor, facilitating its degradation in eukaryotic cells (Leventis and Silvius 1990; Pedroso de Lima *et al* 2001) (Figure 4.1).

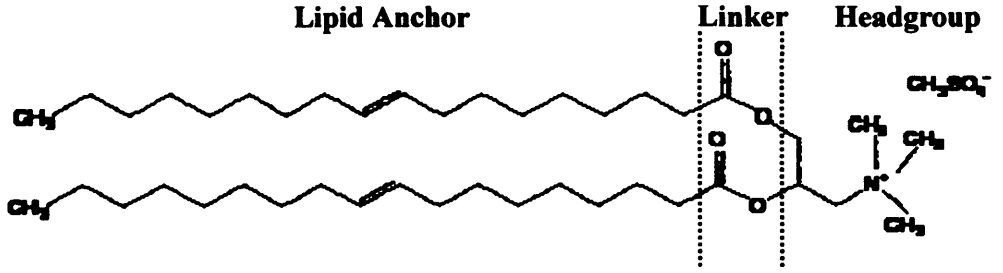


**Figure 4.1 Schematic illustration of the chemical structure of 1,2 dioleoyloxypropyl-3 (trimethylammonium)- propane methylsulphate (DOTAP).** Highlighting the hydrophilic head-group, linker region and hydrophobic lipid anchor.

### 4.1.1.1 Preparation of Cationic Liposomes

Several methods are available to prepare liposomes including, vortexing, sonication, and extrusion. These techniques are used to prepare small unilamellar vesicles (SUV), consisting of a single bilayer, from multilamellar vesicles (MLV) which consist of multiple concentric lipid bilayers. Liposomes

in this project were prepared by extrusion as this method offers greater batch to batch reproducibility of vesicle size and size distribution than the other methods, due to the physical processing involved (Lapinski *et al* 2007). Briefly, the extrusion process involves a technique in which the lipid suspension, prepared by the hydration of a thin lipid film in an aqueous solution, is forced through a polycarbonate filter with a defined pore size. Extrusion causes the concentric layers of MLVs to deform so that they can pass though the filter pore. As the MLVs pass through the pores breaking and re-sealing of the membranes occurs. If the liposome preparation is repeatedly cycled through the extrusion process a SUV population with a mean diameter that is comparable to the diameter of the filter pore can be produced (Hope *et al* 1985; Mayer *et al* 1986). The size of the liposome used to complex with the pDNA is important as it has been shown to affect resulting pDNA cell transfection (Templeton *et al* 1997). The extrusion of cationic liposomes through filters results in the conversion of MLV, which may be tens of microns in size, into SUV which may be only tens of nanometres in size. The overall increase in the surface area of the liposomes by extrusion results in more efficient complexing with the pDNA which is essential for transfection (Hope *et al* 1985; Templeton *et al* 1997).

#### 4.1.1.2 Liposomal Gene Delivery

Due to the difference in electrostatic charge, cationic liposomes are able to interact with DNA to form deliverable complexes so as to promote pDNA transfection into cells (Felgner *et al* 1987; Gao and Huang 1995). The electrostatic interactions between the anionic phosphate backbone of pDNA molecules and the positively charged polar amino- head group of the cationic lipids result in the pDNA self–assembling with the lipid to form lipoplexes (lipid-DNA complexes) of condensed pDNA. The condensation of DNA, which involves a decrease in the volume occupied by a DNA molecule, is of immense biological importance as it serves as a platform for enhancing the cellular delivery of DNA and protection from degradation by nucleases (Bloomfield 1996; Crook *et al* 1996). The formation of lipoplexes with an

overall positive charge facilitates the association of the lipoplex with the negatively charged cell membrane, and therefore entry of the complex into the cell primarily via the endocytotic route (Felgner *et al* 1987; Zabner *et al* 1995; Xu and Szoka 1996).

Although lipoplexes are widely used to transfect DNA into cells both *in vitro* and *in vivo* (Xu and Szoka 1996), lipoplexes that are microinjected directly into the nucleus do not induce high expression levels of the transgene (Zabner *et al* 1995). This implies that during the normal transfection process, plasmid DNA is released from the lipoplex before entering the nucleus (Xu and Szoka 1996). The mechanism by which DNA dissociates from the lipoplex is poorly understood, especially because there is a strong interaction between the cationic lipid and DNA (Gershon *et al* 1993).

Many researchers have found that destabilising the endosome membrane, by which the lipoplex enters the cell, plays a key role in catalysing DNA dissociation from its lipoplex and its subsequent release into the cytoplasm. When the cationic lipoplex comes into close contact with the negatively charged membrane of the endosome, the lipoplex fuses with the membrane causing membrane asymmetry to be lost resulting in its destabilisation (Stamatatos *et al* 1988; Bevers *et al* 1994). The destabilisation of the endosome membrane results in an influx of anionic lipids, which are located on the cytoplasmic face of the membrane, via a 'flip-flop' mechanism (Xu and Szoka 1996). The anionic lipids compete with the DNA for the cationic lipid, resulting in DNA displacement to form charge-neutralized ion pairs with the cationic lipids. The dissociated DNA is then permitted to enter the cell cytoplasm.

The cytoplasmic pDNA must then enter the cell nucleus for transcription to occur. In dividing cells pDNA entry into the nucleus is considered to occur predominantly during the cell mitosis stage during which the nuclear membrane disintegrates, allowing cytoplasmic pDNA entry into the nuclear

compartment (Wilke *et al* 1996; Brunner *et al* 2000). However, in non-dividing cells pDNA entry into the nucleus of such cells is suggested to also be via transport through the nuclear pore complex which spans the nuclear envelope (Dowty *et al* 1995; Dean 1997).

### 4.1.2 Cell Culture of a Mammalian Cell Line

The A549 cell line, used for the cell culture experiments in this chapter, originates from human lung carcinoma cells of a 58 year old Caucasian male (Lieber *et al* 1976). The A549 cells are a continuous epithelial cell line. Continuous cell lines are transformed from primary cells by a series of mutational events resulting in their capacity to multiply indefinitely *in vitro*.

The use of *in vitro* cell culture models to assess pDNA transfection can be advantageous in the sense that *in vitro* experiments are generally more economical than *in vivo*, the usage of animals is reduced if preliminary proof-of-principle studies are carried out *in vitro* and *in vitro* studies can offer more rapid results with better experimental control (Forbes 2000). However *in vitro* models are often based on cells with two dimensional growth characteristics (A549 cells) which do not mimic the complex three-dimensional geometry of cell interactions *in vivo*. Additionally *in vitro* cells tend to display a more constant rate of growth than cells *in vivo*, and as gene transfer occurs predominantly during the mitotic stage a significant variation between pDNA transfection efficiency can often be observed between the two models (Wilke *et al* 1996). More specifically to inhalation therapy, the lungs possess numerous biological barriers and mechanisms which *in vitro* models do not possess. Examples of this include the mucus layer and the mucociliary escalator that contribute to the clearance of foreign particles and therefore hinder their ability to exert any therapeutic effect (Farr *et al* 1985; Barker *et al* 1994; Weers *et al* 2009). In spite of this, A549 cells possess some of the morphological and biochemical features of the pulmonary alveolar type II cells typified by their endogenous ability to synthesise and secrete phosphatidylcholine, a constituent of lung surfactant (Lieber *et al* 1976; Smith

1977).

The use of cell cultures in laboratory investigations requires prior knowledge of growth characteristics for the specific cell line. Growth studies which involve plotting a growth curve are an essential prerequisite for ensuring that transfection studies are carried out on cells which are at their most viable and uniform state (cells in their log phase) (Freshney 2000).

### 4.1.3 Specific Aims and Objectives of the Chapter

The primary aim of this chapter is to report the potential for incorporating solvent-washed pDNA particles, prepared using methods developed in previous chapters, into a pMDI system. This chapter's secondary aims are to detail whether it is viable to aerosolise and deliver these pDNA particles via a pMDI using a standard valve and actuator and preliminary assess any formulation toxicity issues.

The experimental objectives are to:

1. Culture A549 human lung epithelial cells and establish growth characteristics.
2. Prepare DOTAP liposomes via solvent evaporation and extrusion methods and characterise liposomes in terms of particle size.
3. Identify the optimum DOTAP:pDNA constituent ratio by quantifying transfection efficiency on A549 cells using flow cytometry.
4. Assess the transfection competency of lyophilised pDNA particulates (before loading into pMDI) on A549 cells using flow cytometry.
5. Characterise the aerosolised solvent-washed pDNA particles using SEM of particles deposited at various stages of the ACI.
6. Verify stability of pDNA particles post pMDI aerosolisation through maintenance of the supercoiled fraction.
7. Assess pDNA functionality following pMDI aerosolisation via gene expression efficiency in A549 cells.
8. Investigate cytotoxic effects of the aerosolised pDNA pMDI formulation on the A549 cell line.

## 4.2 Materials and Methods

All reagents were used as received and were purchased from Fisher Scientific UK Ltd. (Loughborough, UK) unless otherwise stated.

Deionised water was obtained from an Elga reservoir (High Wycombe, UK). Phosphate buffered saline pH 7.4 ($Mg^{2+}$ and $Ca^{2+}$ free), trypan blue, Chloroform $\geq$ 99.8% spectrophotometric grade and MTT-based assay kit were purchased from Sigma-Aldrich Ltd. (Poole, UK). Agarose (LE analytical grade) was purchased from Promega Ltd. (Southampton, UK). Dulbecco's Modified Eagle's Medium (DMEM), foetal bovine serum, penicillin G 5000 units/ml, streptomycin sulphate 5000 μg/ml and trypsin-EDTA were purchased from Invitrogen Ltd. (Paisley, UK). 5x coloured loading buffer blue was purchased from Bioline Ltd. (London, UK). A549 mammalian cell line was purchased from ECACC (Salisbury, UK); 1,2- Dioleoyl- 3-Trimethylammonium propane (methyl sulphate salt) (DOTAP) was purchased from Avanti Polar Lipids Inc. (Alabama, USA). HFA 134a was a generous gift of INEOS Fluor Ltd. (Runcorn, UK). Brilliant Blue pMDIs were obtained courtesy of 3M Healthcare Ltd (Loughborough, UK).

### 4.2.1 Cell culture

Cell culture was carried out in a Class II laminar flow cabinet. The laminar flow cabinet and any cell culture equipment placed in the cabinet were sprayed with 70% (v/v) absolute ethanol in water prior to use. All media was sterile and pre-warmed to 37°C using a water bath to avoid any contamination and thermal damage to the cells respectively.

All cell investigations were performed using A549 human lung epithelial cells following at least two passages post-thawing. Cells were maintained as adherent monolayer cultures in 25 $cm^2$ angled neck, cell culture flasks (T25) (Corning Costar Ltd., High Wycombe, UK) in 5 ml growth media (10% fetal bovine serum, 2% penicillin/streptomycin 5000 iu/ml and Dulbecco's Modified Eagle's Medium (DMEM) to 100%). Cells were stored in a humidified

incubator at 37°C containing 5% $CO_2$. Once the cell line was confluent (every 72 hr) the growth media was removed using a pipette and washed twice with 5 ml pre-warmed phosphate buffered saline (PBS pH 7.4). The adherent cells were then released enzymatically by incubating them (37°C/ 5% $CO_2$) for 5 min with 1ml trypsin-EDTA. After 5 min the flask containing the cells was gently tapped on the bench top to ensure all the cells were released from the surface of the flask. The cells were then re-suspended using 10 ml growth media, pipetted into a 50 ml centrifuge tube and centrifuged at 1000 rpm for 5 min (20°C) using an Avanti J-20 XP Beckman Coulter centrifuge with J-14 head (Beckman Coulter, London, UK). The resultant supernatant was gently removed from the centrifuged cells using a pipette, the pellet formed during centrifugation was re-suspended using 10 ml growth media. Pipetting action was used to disperse the cell pellet throughout the growth media ensuring a homogenous cell suspension. A 50 µl aliquot of the cell suspension was taken and a cell count using a neubauer double net ruling bright lined haemocytometer (Fisher Scientific Ltd., Loughborough, UK) was performed. A549 cells were reseeded at 1 x $10^6$ cells/ T25 flask in 5 ml of growth media and returned to the humidified incubator (37°C/ 5% $CO_2$).

Cells were counted using a haemocytometer and trypan blue dye. Trypan blue is a stain used to selectively colour dead cells with damaged plasma membranes as live cells with an intact cell membrane exclude the stain. During cell counting non-viable cells, stained blue, were excluded from the cell counts with the aid of the exclusion dye. An equal volume (50 µl) of 0.4% trypan blue was pipetted into an eppendorf tube containing the cell suspension and incubated (37°C/ 5% $CO_2$) for 5 min.

A precision ground cover slip was pressed gently onto the top of the haemocytometer until Newton rings were visible. Approximately 10 µl of the incubated cell suspension was pipetted onto the haemocytometer at either end of the cover slip. Capillary action caused the cell suspension to be drawn into the haemocytometer counting chamber. The haemocytometer was then placed

under a light microscope so that number of living cells present on the grids engraved on the haemocytometer could be counted.

The haemocytometer is made up of two counting chambers. Each counting chamber contains an engraved grid. The total volume of cell suspension found on each square is $10^{-4}$ ml (Figure 4.2). The number of cells present in 1 ml of the cell suspension was therefore calculated using the following formula:

**No of cells per ml = (Average No of cells counted in 1 square x 2) x $10^4$**

(Note: the number of cells counted was multiplied by a factor of two to allow for the dilution of cell suspension with trypan blue).

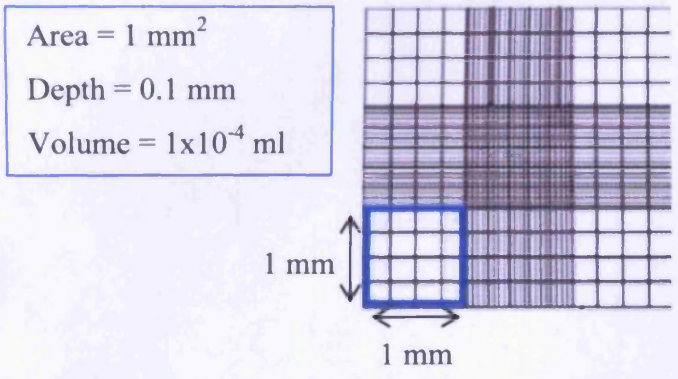


**Figure 4.2 Schematic drawing of one haemocytometer counting chamber.**

### 4.2.2 A549 Cell Growth Study

A549 cells prepared for the growth study were seeded into 24-well plates at a density of 4 x $10^4$ cells/cm$^2$ and submerged under 1 ml growth media. The seeding time was noted and cells were stored in a humidified incubator (37°C/ 5% $CO_2$). Cells were counted twice daily for a period of four days. During the growth study, cells were washed twice with 1 ml pre-warmed PBS pH 7.4, enzymatically released from the 24-well plate using 125 µl trypsin-EDTA and re-suspended in 875 µl growth media. The cell suspension was then prepared for counting using trypan blue as outlined earlier (Section 4.2.1). A growth curve was then plotted for the A549 cells in order to monitor cell growth over time.

### 4.2.3 DOTAP Liposome Preparation

To prepare DOTAP liposomes, 10 mg of DOTAP was weighed into a 100 ml round bottom flask and 5 ml of chloroform was added to dissolve the lipid. Once the lipid was dissolved, the round bottom flask was securely attached to a rotary evaporator set at approximately 1 revolution per second under negative pressure and 37°C. Once the chloroform had evaporated, rotary evaporation was carried on for a further 90 min in an attempt to remove solvent residues and produce a thin lipid film. A 1 mg/ml solution of DOTAP was prepared by adding 10 ml pre-warmed (37°C) sterile water. The flask was agitated using a vortex mixer to remove the lipid film from the glass to produce a multilamellar liposome solution. The round bottom flask was incubated for 30 min in a water bath (37°C) to aid annealing of the liposomes.

An extrusion process was used to form unilamellar vesicles from the multilamellar DOTAP vesicles. DOTAP was pipetted slowly into the central chamber of an Extruder ™ (Lipex Biomembranes Inc., Vancouver, Canada) and extruded through a 100 nm polycarbonate filter (Millipore, Watford, UK) using nitrogen pressure set between a 5-10 bar range. In order to obtain a vesicle population with a narrow size distribution the liposome suspension was cycled through the extrusion process a total of ten times (Hope *et al* 1985; Mayer *et al* 1986).

The mean diameter of liposomes was determined by photon correlation spectroscopy using a Coulter® N4 Plus (Coulter Electronics Ltd., Luton, UK). Liposomes (200 µl) were dispersed in sterile water (1800 µl). Samples were transferred into a clear sided disposable cuvette, which was sealed using Parafilm to prevent evaporation. Measurements were expressed using the unimodal size distribution model and repeated three times.

### 4.2.4 Optimising DOTAP: pDNA Ratio for Transfection Studies

Prior to assessing the transfection competency of lyophilised pDNA particles (Section 3.2.5), a pilot study was carried out to investigate the optimum

DOTAP: pDNA ratio in order to maximise cell transfection.

DOTAP: pDNA complexes were prepared by adding 18 μg of unprocessed pEGFP-N1 to DMEM (up to 6 ml). Extruded DOTAP ranging from a DOTAP liposome: pDNA ratio of 4:1 w/w increasing in two unit increments up to 12:1 w/w was slowly pipetted into the DMEM-pDNA solution. The various DOTAP liposome: pDNA ratio treatments were gently vortexed and then left to stand for 20 min to promote complexation.

Cellular transfection and gene expression performance was assessed in A549 cells seeded into 24-well plates at a density of 4 x $10^4$ cells/$cm^2$ and cultured under the specified culture conditions (Section 4.2.1) for 48 hr (68% confluency) as determined by the cell growth study (Section 4.2.2). Cells contained in 6 wells of the 24-well plates were each subjected to treatment with either 1 ml DMEM alone or up to 1 ml DMEM containing DOTAP liposome: pDNA complexes ranging from 4:1 w/w to 12:1 w/w ratios. Cells were then returned to the humidified incubator (37°C/ 5% $CO_2$) for 6 hr. After 6 hr the DMEM containing the treatments was removed, cells were washed once with 1 ml pre-warmed PBS pH 7.4 and replenished with 1 ml growth media. Cells were then returned to the humidified incubator (37°C/ 5% $CO_2$).

#### 4.2.4.1 Analysis of Gene Expression

42 hr after treatment cells were surface rinsed twice with 1 ml cold PBS pH 7.4 and trypsinised with 150 μl trypsin-EDTA solution. After 1 min the trypsin-EDTA was removed from the cells using a pipette and the cells were incubated (37°C/ 5% $CO_2$) for 10 min. Cells were then resuspended in 600 μl growth media. The cell suspension was then transferred from the well into an appropriately labelled flow cytometry tube (Falcon® Becton, Dickinson Biosciences, Oxford, UK) and placed on ice prior to analysis. The percentage of cells displaying GFP-associated fluorescence (FL1-H) was quantified by flow cytometry (FACSCalibur™ system Becton, Dickinson Biosciences, Oxford, UK) with analysis by WinMDI™ Software (Joseph Trotter, The

Scripps Institute, California, USA), as described previously (Seville *et al* 2002). Untreated control cells were used to establish a 'gated' region which excluded the fluorescence detected due to the natural autofluorescence of cells. The percentage of EGFP positive cells (fluorescent cells) was measured from the cells in this established 'gated' region.

### 4.2.5 Assessing the Transfection Competency of Lyophilised pDNA Particulates

The biological functionality of lyophilised pDNA particles (Section 3.2.5) was assessed in A549 cells seeded into 24-well plates at a density of $4 \times 10^4$ cells/cm$^2$ and cultured under the specified culture conditions (Section 4.2.1) to 68% confluency (cells were in their log phase).

Cells were subjected to one of seven treatments (Figure 4.3): (i) DMEM alone (no pDNA), (ii) unprocessed pEGFP-N1 (positive control), (iii) an unwashed formulation of lyophilised DNA-loaded particles, (iv) a solvent-washed variant of formulation (iii). In the case of (ii), (iii) and (iv) the formulations were added directly onto cells covered with (A) DMEM alone or (B) DMEM containing extruded DOTAP liposomes (Section 4.2.3). A549 cells, in each well of a 24-well plate, were treated with the equivalent of 5 μg pEGFP-N1. In the case of cells treated in the presence of DOTAP, a 6:1 w/w DOTAP liposome: DNA ratio was used. All treatments were conducted in serum-free DMEM. Treated cells were stored in a humidified incubator (37°C/ 5% $CO_2$). After a period of 6 hr, cells were washed once with 1 ml PBS, pH 7.4, replenished with 1 ml of growth media and returned to the humidified incubator (37°C/ 5% $CO_2$).

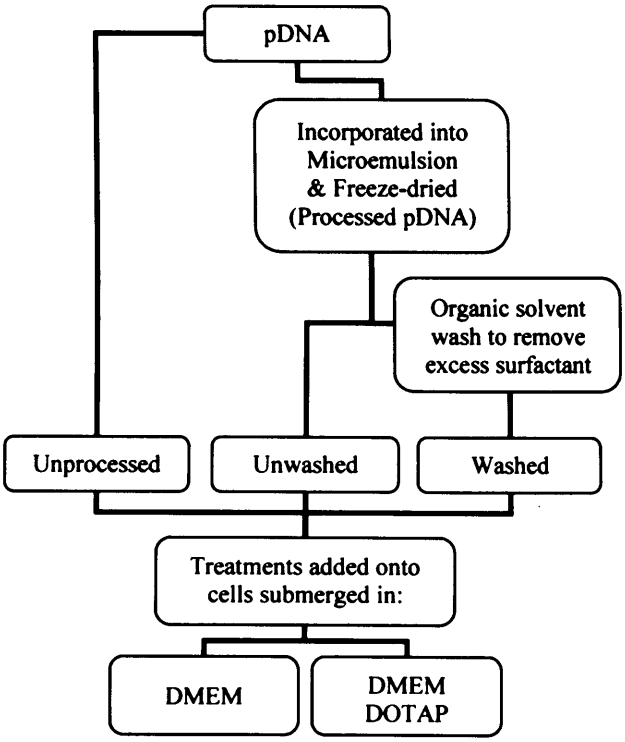


**Figure 4.3 Diagrammatic representation of the production of samples for subsequent *in vitro* analysis.**

The biological functionality of lyophilised pDNA particles was assessed qualitatively at 42 hr post-treatment, using fluorescent microscopy and quantitatively by flow cytometry (FACSCalibur™ system Becton, Dickinson Biosciences, Oxford, UK) with analysis by WinMDI™ Software (Joseph Trotter, The Scripps Institute, California, USA) (Section 4.2.4.1).

### 4.2.6 Production of pDNA pMDI Formulations

Two pMDI formulations were aerosolised and investigated for pEGFP-N1 biological functionality with the aim to determine whether you could detect gene expression based upon a loadable quantity. The first "unwashed" formulation used unwashed surfactant-coated, lyophilised pEGFP-N1 particles (25 mg, which was a quantity of formulation that would disperse in the propellant). The second "washed" formulation (16 mg) used the same batch of particles after solvent-washing to remove excess surfactant (the wash method was outlined Section 2.2.3). Particles were weighed directly into fluorinated ethylene propylene (FEP) coated aluminium canisters (3M Drug Delivery Systems, Loughborough, UK) and dispersed in absolute ethanol a co-solvent

(0.5 ml) using a vortex mixer. Spraymiser™ 50 µl retention valves (3M Drug Delivery Systems, Loughborough, UK) were crimped onto the aluminium canisters and 6 ml HFA 134a was added using a Pamasol® semi-automatic filling and crimping machine model P2005/2 (Pamasol Willi Mäder AG, Pfäffikon SZ, Switzerland). Washed formulations were also prepared in plastic polyethylene terephthalate (PET) pMDI vials (3M Drug Delivery Systems, Loughborough, UK), for visual assessment of physical stability and dispersion homogeneity. pMDI vials were stored at room temperature with visual observation at 24 hr and 5 months.

### 4.2.7 Assessment of pDNA pMDI Formulations

#### 4.2.7.1 Integrity of pDNA Particles Following Aerosolisation from a pMDI

Agarose gel electrophoresis, with EtBr staining, was used to determine the physical integrity of the processed pEGFP-N1 following aerosolisation from a pMDI system. Following the incorporation of the unwashed and washed processed pDNA into a pMDI formulation, the formulations were actuated onto glass slides with the equivalent of 2 µg aerosolised pEGFP-N1. The pDNA formulation deposited on the glass slides was reconstituted with 15 µl of TE buffer pH 8.0 and made up to 20 µl with 5x coloured loading buffer. A control sample of the unprocessed pDNA diluted to 2 µg/ 15 µl using TE buffer was also prepared and made up to 20 µl using 5x coloured loading buffer blue. The 20 µl aliquots of each sample were then carefully pipetted into the wells of an EtBr agarose gel (gel preparation was carried out as outlined in Section 3.2.3.1). The gel was developed for 50 min at 200 volts and analysed using Molecular Analyst® software and Bio-Rad Gel Doc 1000 (Bio-Rad Laboratories Ltd., Hertfordshire, UK).

#### 4.2.7.2 Aerosolised Delivery to Cell Culture Flask

Initial pilot studies, using pMDIs containing Brilliant Blue dye, were carried out to determine the most efficient orientation for delivery to cell culture medium (Figure 4.4). Brilliant Blue incorporated into a pMDI was primed by actuating five shots to waste using an actuator with a 0.5 mm orifice diameter

(3M Drug Delivery Systems, Loughborough, UK). The Brilliant Blue pMDI was then actuated 5 times into a T25 cell culture flask, containing 6 ml of water, by either spraying vertically or horizontally (with regards to the plane of the aerosolised spray) (Figure 4.4). For actuations carried out by spraying vertically a hole was cut out from the top of a T25 flask using a hot copper pipe which had been fabricated into the dimensions of the actuator mouthpiece. Also during actuations from the vertical orientation, the metering chamber of the valve was allowed to fill in the upright position between actuations. Following visual observation, the coloured liquid at the bottom of the T25 flask was transferred into a UV quartz cuvette (Hellma Worldwide Precision Cells, Essex, UK) and assayed by UV absorbance at 629 nm. Data from the two actuation orientations were compared to a positive control. Control absorbance data was generated by actuating the Brilliant Blue pMDI into a conical flask containing 6 ml of water and swirling the water around the flask to collect the total emitted dye present in the flask.

The relative deposition efficiency of the Brilliant Blue dye actuated from the two orientations was calculated by comparing the UV absorbance data of deposited dye against that of the control. As the UV absorbance detected from control was a measure of the total emitted dye collected from the flask, the deposition efficiency for the control was taken as 100%.

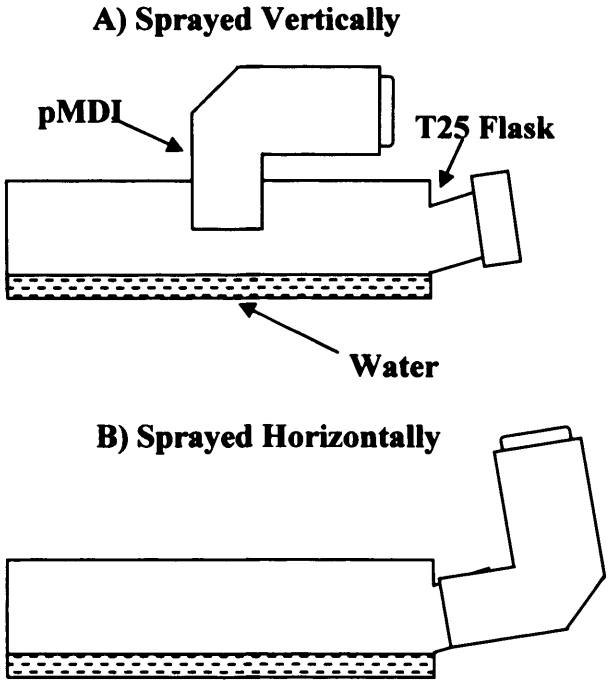


**Figure 4.4 Schematic representation of aerosolisation into a cell culture flask. A) Sprayed Vertically:** pMDI actuated with the aerosol directed onto liquid; **B) Sprayed Horizonatally:** pMDI actuated with aerosolisation across the liquid.

#### 4.2.7.3 Assessment of pDNA Functionality Following Aerosolisation from a pMDI

Biological functionality of pDNA actuated from the pMDI formulation was assessed in A549 cells seeded into T25 flasks with seeding densities previously outlined in Section 4.2.5.

Cells were subjected to the following treatments: (i) DMEM (negative control), (ii) an unwashed formulation of lyophilised DNA-loaded microemulsion incorporated into a pMDI, (iii) a solvent-washed variant of formulation (ii). In the case of (ii) and (iii) the formulations were actuated from pMDI canisters directly onto cells covered with (A) DMEM, and (B) DMEM containing extruded DOTAP liposomes (Section 4.2.3). Each T25 flask was treated with the equivalent of 15 μg aerosolised pEGFP-N1. In the case of cells treated in the presence of DOTAP, a ratio of 6:1 w/w DOTAP: washed DNA was used, based on the assumption that 15 μg of pDNA would be successfully expelled

from the pMDI. pMDIs were primed by firing five shots to waste using an actuator with a 0.5 mm orifice diameter (3M Drug Delivery Systems, Loughborough, UK). To reduce any cell death, due to aerosol cold freon effect, the T25 flasks were placed on pre-warmed saline infusion bags with 30 sec intervals between actuations. All treatments were conducted in serum-free DMEM. Treated cells were stored in a humidified incubator (37°C/ 5% $CO_2$). After a period of 6 hr, cells were washed once with 5 ml PBS, pH 7.4, replenished with 5 ml of growth media and returned to the humidified incubator (37°C/ 5% $CO_2$).

The biological functionality of lyophilised pDNA particles was assessed qualitatively at 42 hr post-treatment using fluorescent microscopy. Following microscopy, cells were surface rinsed twice with 5 ml cold PBS, trypsinised with 1 ml trypsin-EDTA solution and then resuspended in 6 ml growth media. Cells were assessed for fluorescence using flow cytometry (FACSCalibur™ system Becton, Dickinson Biosciences, Oxford, UK) with analysis by WinMDI™ Software (Joseph Trotter, The Scripps Institute, California, USA) (Section 4.2.4.1).

#### 4.2.7.4 Microscopic Characterisation of Particles

The solvent-washed pDNA pMDI formulation (Section 4.2.6) was actuated 80 times into a Volumatic™ spacer (Allen and Hanburys, Middlesex, UK) connected to an ACI (Westech Instrument Services Ltd., Bedfordshire, UK) operating at 28.3 l/min. Double sided carbon tape was attached at various points on the wall of the spacer and the plates in the ACI using tweezers. Particles that had deposited on the carbon tape, post-actuation, were mounted onto SEM aluminium stubs and sputter coated with gold (gold sputter coater, EM Scope, Kent, UK) before being viewed using a Philips XL-200 Scanning Electron Microscope (TEI Company, Eindhoven, The Netherlands).

### 4.2.8 Cell Toxicity Assay

*In vitro* toxicity of treatments was assessed using the colorimetric 3-[4, 5–

dimethylthiazol-2-yl]-2, 5-diphenyl tetrazolium bromide (MTT) based assay kit. In vitro cytotoxicity was determined by spectrophotometrically measuring the activity of living cells post-treatment via their mitochondrial activity.

Initially A549 cells were seeded into T25 flasks at a density of $4 \times 10^4$ cells/cm$^2$ and cultured under the specified culture conditions (Section 4.2.1) to 68% confluency. Cells were surface-treated with: (i) DMEM, (negative control), (ii) Nine actuations of a solvent-washed pEGFP-N1 pMDI formulation (produced in Section 4.2.6) actuated into DMEM alone, (iii) Nine actuations of a solvent-washed pEGFP-N1 pMDI formulation actuated onto DMEM containing DOTAP, (iv) Nine actuations of placebo pMDI formulation containing 6 ml HFA 134a and absolute ethanol (8% v/v) actuated onto DMEM alone, (v) Nine actuations of placebo pMDI formulation containing 6ml HFA 134a and absolute ethanol (8% v/v) actuated onto DMEM containing DOTAP, (vi) Eighty actuations of placebo pMDI formulation containing 6 ml HFA 134a and absolute ethanol (8% v/v) actuated onto DMEM containing DOTAP. In the case where pDNA loaded pMDI formulations were used, each T25 flask was treated with the equivalent of 15 μg aerosolised pEGFP-N1. A quantity of 90 μg extruded DOTAP liposomes (1 mg/ml) (Section 4.2.3) (ratio of 6:1 w/w DOTAP: washed DNA) was used in all cases where cells were treated in the presence of DOTAP.

pMDIs were primed by firing five shots to waste using an actuator with a 0.5 mm orifice diameter (3M Drug Delivery Systems, Loughborough, UK). To reduce any cell death, due to aerosol cold freon effect, the T25 flasks were placed on pre-warmed saline infusion bags with 30 sec intervals between actuations. All treatments were conducted in serum-free DMEM. Treated cells were stored in a humidified incubator (37°C/ 5% $CO_2$). After a period of 6 hr, cells were washed once with 5 ml PBS pH 7.4, replenished with 5 ml of growth media and returned to the humidified incubator (37°C/ 5% $CO_2$). 42 hr post-treatment, cells were washed twice with 5 ml aliquots of cold PBS, then PBS was removed and 1 ml trypsin-EDTA added to the cell surface. After 1 min,

the trypsin was removed from the wells and the T25 flasks stored in a humidified incubator at 37°C containing 5% $CO_2$ for 10 min. After 10 min incubation, cells were re-suspended in 6 ml growth media.

Reconstituted MTT (5mg/ml PBS) was added at 10% of the 100 µl culture medium volume in a 96-well plate and agitated using a bench top shaker to ensure mix. Samples were incubated (37°C/ 5% $CO_2$) for 4 hr after which the reconstituted MTT was removed using a syringe needle with care taken not to disturb the cells. Subsequently, formazan crystals were dissolved using 100 µl of MTT solubilisation solution. Cell culture samples were incubated (37°C/ 5% $CO_2$) for a further 30 min and assayed by UV absorbance at 570 nm using a Sunrise™ microplate reader (Tecan Trading AG, Männedorf, Switzerland). Background absorbance, measured at 690 nm, was subtracted from the 570 nm readings automatically using Magellan™ data reduction software (Tecan Trading AG, Männedorf, Switzerland).

### 4.2.9 Statistical Analysis

Statistical analysis was carried out using a statistical package, SPSS 16®. One-way analysis of variance (ANOVA) was followed by a Duncan's multiple range test, to compare multiple groups, or Dunnett's test, used to compare groups against a reference group with significant differences indicated by p-values $<0.05$ or $<0.001$. Results are summarised as mean ± sd.

## 4.3 Results

### 4.3.1 A549 Cell Growth Study

The A549 cell growth curve was plotted as cell number against time so that a clear understanding of the state of cell growth at any given time could be gained (Figure 4.5). The growth curve generally followed a sigmoidal pattern of cell proliferation, where cell exponential growth (log phase) commenced after a 23 hr lag period. At 71 hr after cell seeding, the cells entered their plateau phase of cell growth followed by a decline in cell number.

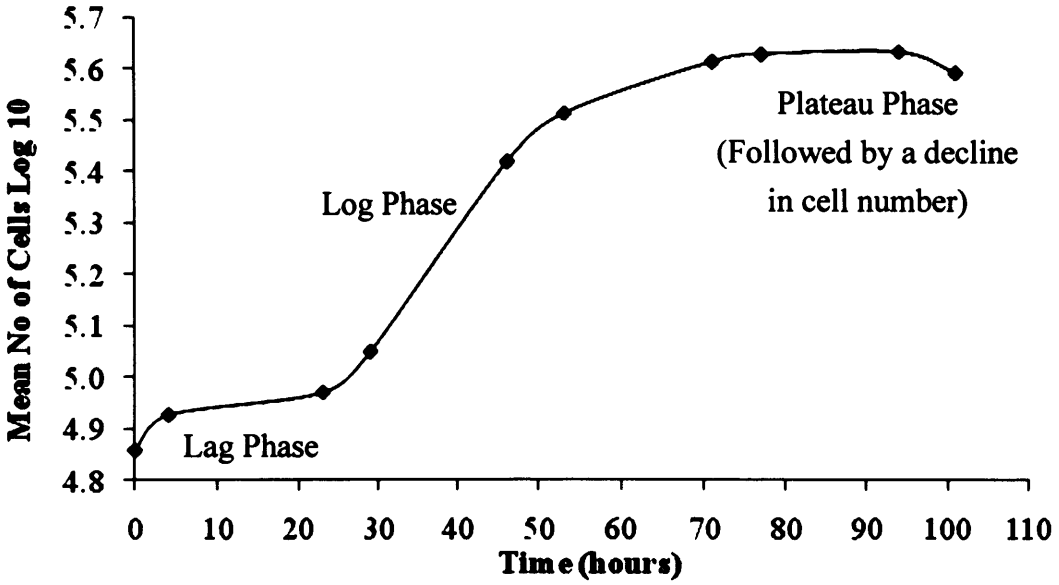


**Figure 4.5 A549 cell growth curve with annotations of the cell growth phases** (mean n = 4).

### 4.3.2 Measurement of DOTAP Liposome Size

Liposome size analysis using photon correlation spectroscopy was routinely performed on extruded DOTAP liposomes prior to transfection studies. Analysis revealed liposomes had a mean diameter of 119.4 ± 23.2 nm (mean ± sd; n = 3). The average vesicle size distribution shown by the polydispersity index was 0.046 indicating a monodisperse suspension of particles.

### 4.3.3 Optimising DOTAP: pDNA Ratio for Transfection Studies

Prior to experiments assessing the biological functionality of pDNA following processing into particles, a pilot study was carried out using flow cytometry to determine the most transfection efficient ratio of DOTAP: pDNA (Figure 4.6).

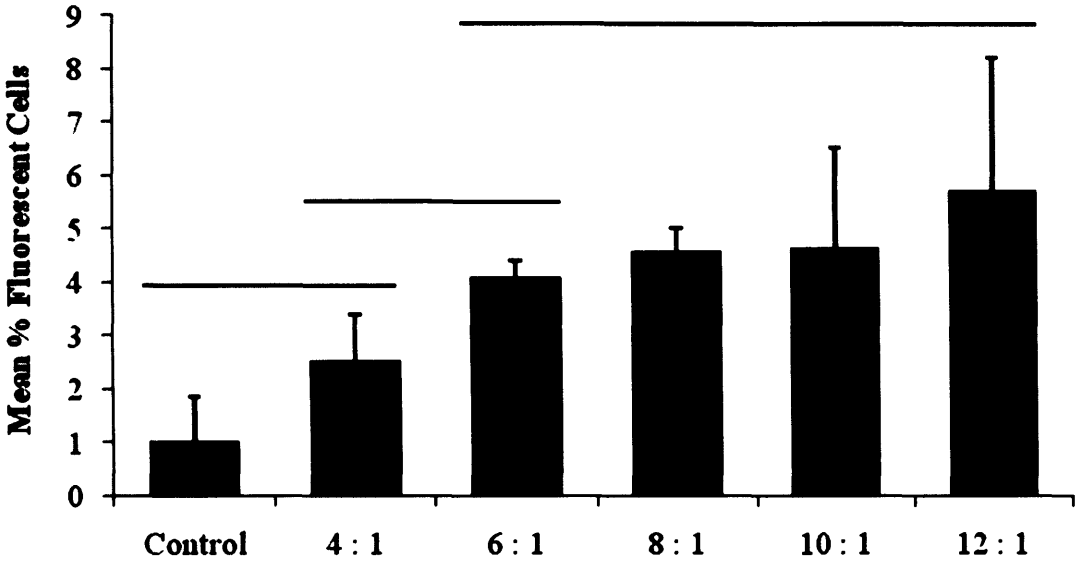


**Figure 4.6 Quantitative gene expression of pDNA particles using various ratios of DOTAP liposome: pDNA.** A549 cells were surface-treated with **Control:** DMEM alone, **4:1, 6:1, 8:1, 10:1, 12:1** represented the w/w DOTAP liposome: pDNA ratios. Data are presented as mean ± sd; n = 3. The bars represent no significant difference between treatments ($p>0.05$).

Gene expression analysis (Figure 4.6) revealed no statistical increase in reporter gene expression when using 4:1 w/w DOTAP liposome: pDNA ratio (2.51 ± 0.87% ($p>0.05$)) compared to the control (0.99 ± 0.87%). However increasing the ratio to 6:1 w/w resulted in a significantly increased percentage of cells emitting GFP fluorescence (4.09 ± 0.30% ($p<0.05$)) compared to control. Figure 4.6 revealed that any further increase in the DOTAP liposome: pDNA ratio beyond 6:1 w/w to 8:1, 10:1 or 12:1 w/w did not confer any further significant increase in the percentage of cells emitting GFP fluorescence (4.59 ± 0.44%, 4.63 ± 1.90%, 5.72 ± 2.50% respectively ($p>0.05$)) when compared to the 6:1 w/w treatment.

### 4.3.4 Assessing the Transfection Competency of Lyophilised pDNA Particulates

Figure 4.7 shows the result of an *in vitro* transfection experiment to assess the biological functionality of pDNA following processing into particles, but before loading into a pMDI canister and subsequent aerosolisation. DOTAP cationic lipid was added to selected cell culture flasks to form an electrostatic complex with the pDNA and enable cell transfection. A significant increase ($p<0.001$) in the percentage of fluorescent cells, attributed to expression of GFP, was observed when A549 cells were treated with unprocessed (positive control) pEGFP-N1 in the presence of DOTAP (14.49 ± 1.76%). The unwashed surfactant-coated pDNA particles did not mediate any gene expression, regardless of whether DOTAP was present (0.59 ± 0.11%) or not (0.67 ± 0.31%). Gene expression was however statistically comparable ($p>0.05$) to the positive control in DOTAP-supplemented samples that had undergone the washing procedure to remove excess surfactant (14.28 ± 1.82%). Formulations treated in the absence of DOTAP, showed no significant increase ($p>0.05$) in cell fluorescence against the negative control. Fluorescent microscopy inserts confirmed the presence of fluorescent protein in transfection-positive cells.

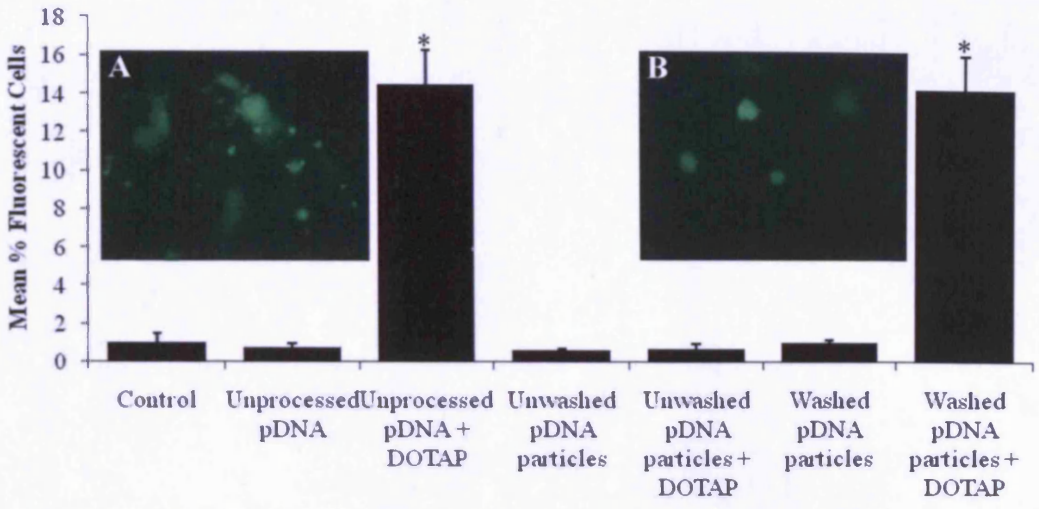


**Figure 4.7 Quantitative gene expression of pDNA particles.** A549 Cells were surface-treated with **(i)** Control– DMEM alone, **(ii)** Unprocessed pEGFP-N1 into DMEM alone, **(iii)** Unprocessed pEGFP-N1 into DMEM containing DOTAP, **(iv)** Unwashed pEGFP-N1 particles into DMEM alone, **(v)** Unwashed pEGFP-N1 particles into DMEM containing DOTAP, **(vi)** Solvent-washed pEGFP-N1 particles into DMEM alone, **(vii)** Solvent-washed pEGFP-N1 particles into DMEM containing DOTAP.

Data are presented as mean ± sd; n = 6. *denotes a significant difference from the control ($p<0.001$).

**Insert:** Fluorescence microscopy image of A549 cells following treatment with (A) unprocessed pEGFP-N1 into media containing DOTAP, and (B) solvent-washed pEGFP-N1 formulation into media containing DOTAP.

### 4.3.5 Assessment of pDNA pMDI Formulations

#### 4.3.5.1 Integrity of pDNA Particles Following Aerosolisation from a pMDI

Agarose gel electrophoresis with EtBr staining was used to assess the physical integrity of processed pDNA actuated from a pMDI formulation. The integrity of pEGFP-N1 post-aerosolisation can be determined by the presence of a supercoiled band that is in line with that shown by the unprocessed pEGFP-N1 (Figure 4.8). Figure 4.8 shows that the integrity of the washed pDNA formulation was maintained post-actuation from a pMDI with the maintenance of the supercoiled fraction. The unwashed formulation however reveals a streaked band with the top most band not migrating as far as the unprocessed pDNA supercoiled band.

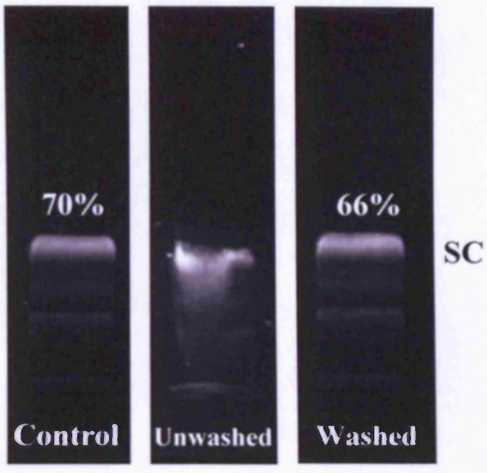


**Figure 4.8 Gel electrophoresis of unwashed and solvent-washed freeze-dried pEGFP-N1 particles actuated from a pMDI formulation. Control:** unprocessed pEGFP-N1, **Unwashed:** surfactant-coated pDNA pMDI formulation, **Washed:** solvent-washed pDNA pMDI formulation. The percentage values represent a semi-quantitative analysis of the ratio of fluorescence emitted from the supercoiled band compared to the total pDNA. (n = 1) (**SC**: supercoiled fraction).

A semi-quantitative signal analysis was used to compare the fluorescence emission from the supercoiled pDNA bands. The supercoiled band of unprocessed pDNA contributed 70% of emitted fluorescence from the total pDNA (Control, Figure 4.8). Once the solvent-washed pDNA had been actuated from a pMDI system fluorescence from the supercoiled fraction was reduced to 66% (washed, Figure 4.8). A semi-quantitative analysis was not carried out on the unwashed actuated pDNA sample as a clear supercoiled band was not visible.

#### 4.3.5.2 Aerosol Delivery to Cell Culture Flask

Prior to experiments assessing biological functionality of aerosolised pDNA particles, pilot studies using Brilliant Blue dye were performed to ascertain the most efficient orientation to actuate processed pDNA formulations to capture aerosol output onto adherent cells *in vitro*.

Visual observations revealed spraying vertically resulted in the majority of the

dye depositing in the water coating the bottom of the flask (Figure 4.9A). Spraying horizontally (Figure 4.9B) resulted in deposition of dye at the neck of the flask as well as into the water at the bottom of the flask. A partial reduction in the dye intensity was observed when aerosolisation from the horizontal orientation was compared with that from the vertical orientation. The intensity of colour was further analysed quantitatively in Figure 4.10.

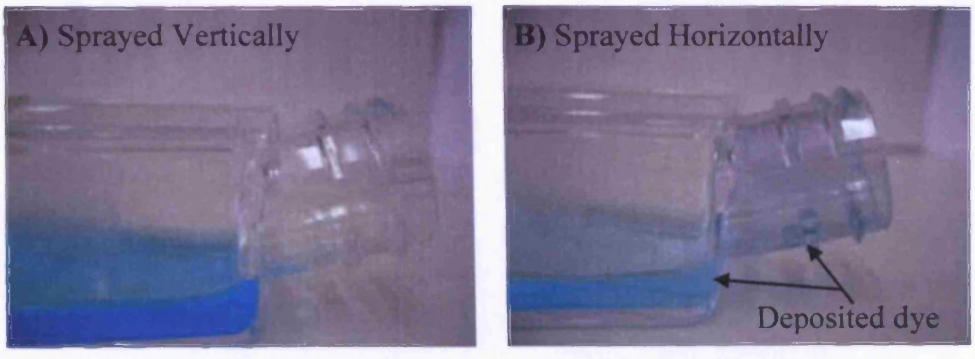


**Figure 4.9 A typical photograph taken of Brilliant Blue pMDI actuated into a cell culture flask. A) Sprayed Vertically:** pMDI actuated with the aerosol directed onto liquid; **B) Sprayed Horizontally:** pMDI actuated with aerosolisation across the liquid.

Figure 4.10 shows the relative UV-vis absorbance of the liquid at the base of the flask following actuation of the Brilliant Blue pMDI. The vertically sprayed pMDI gave a greater relative collection efficiency (78% of the actuated dye was deposited into the collection medium at the bottom of the flask) than horizontally spraying into a flask (19% deposition). Statistical analysis confirmed no significant reduction ($p>0.05$) in the concentration of deposited dye from the vertically sprayed pMDI (0.15 μg/6 ml ± 0.04 μg) compared to the control (0.19 ± 0.01 μg).

As a result of this pilot study, pDNA loaded pMDI formulations were actuated onto A549 cells directly from above (vertically sprayed).

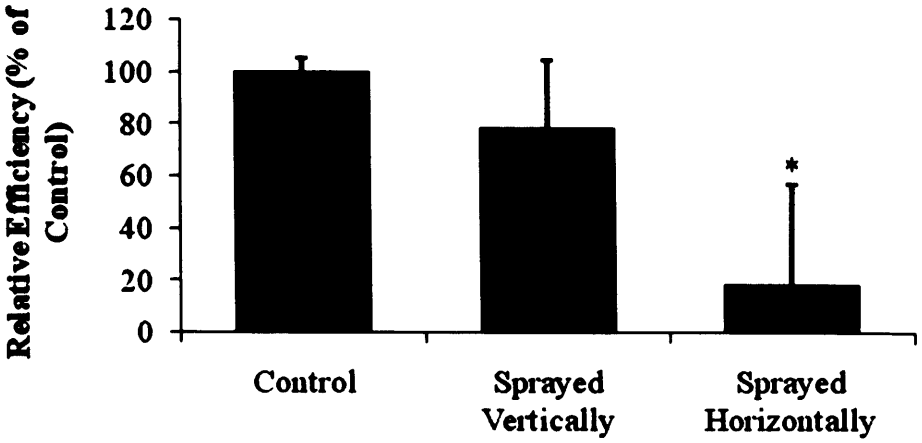


**Figure 4.10 Relative deposition efficiency of Brilliant Blue when actuated from a pMDI in the vertical and horizontal orientation relative to the control. Control:** positive control where the total pMDI emitted dose is collected, **Sprayed Vertically:** pMDI actuated with the aerosol directed onto liquid; **Sprayed Horizontally:** pMDI actuated with aerosolisation across the liquid. Data are presented as mean ± sd; n = 3. *denotes a significant difference from the control (using one-way analysis of variance and Dunnett's multiple range test $p<0.05$).

### 4.3.5.3 Assessment of pDNA Functionality Following Aerosolisation from a pMDI

Flow cytometry was used to determine whether pEGFP-N1 remained biologically active subsequent to particle processing, propellant dispersion and aerosolisation from a pMDI (Figure 4.11). As previously, DOTAP cationic lipid was added to selected cell culture flasks to facilitate *in vitro* cell transfection. No increase in gene expression was observed for the unwashed aerosolised formulation ($p>0.05$) regardless of whether it was actuated in the presence (1.35 ± 0.33%) or absence (1.16 ± 0.94%) of DOTAP. Aerosolising the washed formulation onto cells in normal media also conferred no significant rise in the percentage of cells emitting GFP fluorescence (1.74 ± 0.67%, $p>0.05$). However, a significant increase in the percentage of cells expressing GFP ($p<0.001$) was apparent following aerosolisation of the washed pEGFP-N1 particulates into DOTAP containing media (24.75 ± 2.35%) compared with control cells (0.96 ± 0.30%).

Fluorescence microscopy (Figure 4.11 insert) further confirmed gene expression in cells following aerosolisation of the washed formulation onto cells in DOTAP-supplemented media.

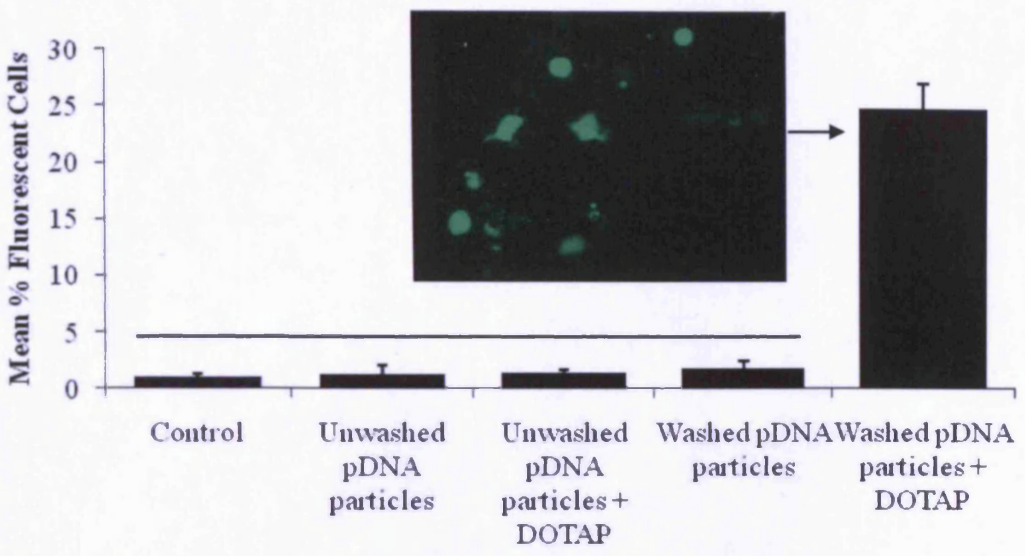


**Figure 4.11 Quantitative gene expression of aerosolised pDNA particles.** A549 cells were surface-treated with **(i)** Control- DMEM alone, **(ii)** Unwashed pEGFP-N1 particles into DMEM alone, **(iii)** Unwashed pEGFP-N1 particles into DMEM containing DOTAP, **(iv)** Solvent-washed pEGFP-N1 particles into DMEM alone, **(v)** Solvent-washed pEGFP-N1 particles into DMEM containing DOTAP.
Data are presented as mean ± sd; n = 4. The bar represents no significant difference ($p$>0.05). **Insert:** Fluorescence microscopy image of A549 cells following treatment with solvent-washed pEGFP-N1 formulation into media containing DOTAP.

#### 4.3.5.4 Visual Assessment of Washed lyophilised pDNA pMDI Formulations

Visual observations of the washed pDNA particulate formulation, in transparent PET pMDI vials, provided a simple indication of the gross physical stability of the formulation *in situ* (Figure 12). When the surfactant-coated lyophilised pDNA particles were subjected to six cycles of the solvent-wash procedure, excess surfactant was removed to leave an off-white powder. Upon addition of the washed pEGFP-N1 particles into a pMDI vial, initial observations showed that particles were suspended throughout the propellant ethanol mix. After a 24 hr period, suspended particles were still visible,

although most particles had formed loose sedimented floccules at the base of the canister. These floccules were easily dispersed by one inversion of the PET vial. Redispersible floccules were also observed after a storage period of 5 months.

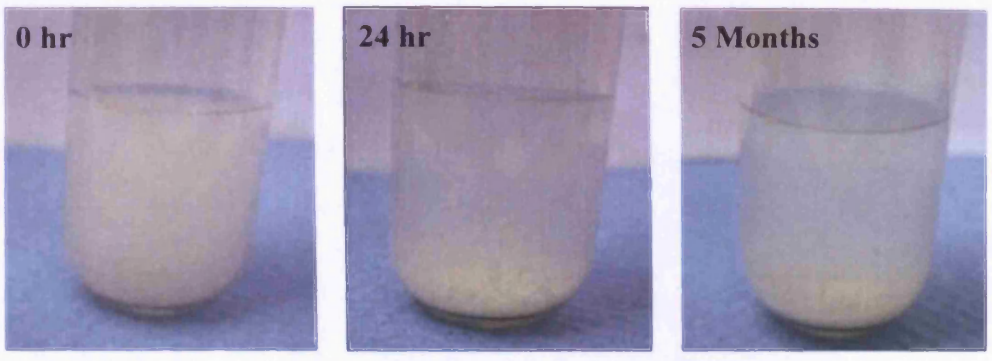


**Figure 4.12 Photograph of PET pMDI vials containing solvent-washed freeze-dried pEGFP-N1 particles in HFA 134a propellant with absolute ethanol as a co-solvent.** Images were taken 0 hr, 24 hr and 5 months after producing the formulation stored at room temperature.

#### 4.3.5.5 Microscopic Characterisation of Particles

SEM images of material aerosolised from the pMDI formulation and collected on Stages 4 and 5 of an ACI indicate the presence of a heterogeneous population of particles comprising rounded and angular particle protrusions from a continuous matrix (Figure 4.13) Although variable in size, all of these particle protrusions were less than 10 μm in diameter. Microscopic observations indicated that ACI Stages 4 (Figure 4.13A) and 5 (Figure 4.13B) with cut-off diameters of 2.1 μm and 1.1 μm respectively contained the greatest number of particle protrusions, potentially indicating that the majority of the aerosolised material is within the respirable size range. However, SEM images (Figure 4.13A and Figure 4.13B) also reveal the presence of particle protrusions larger than the quoted cut-off diameters.

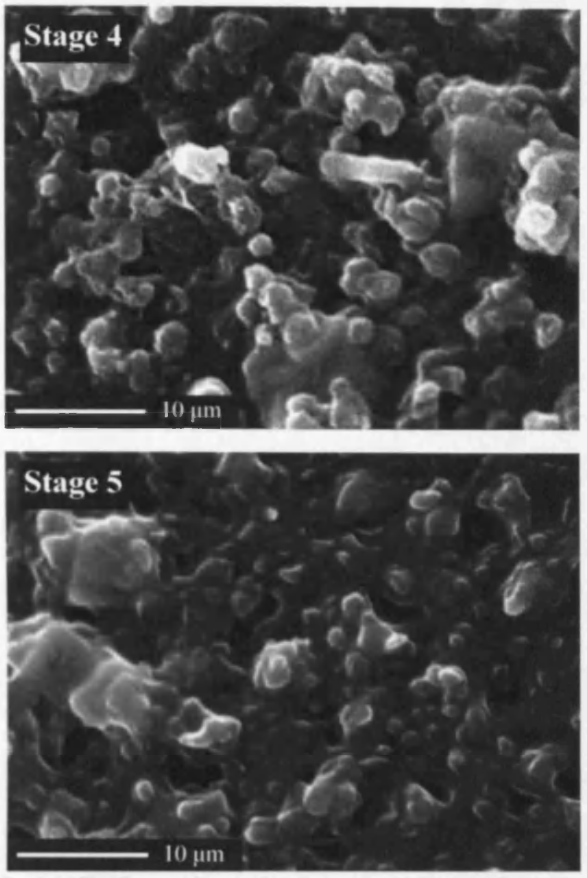


**Figure 4.13A and 4.13B Scanning electron micrographs of a solvent-washed freeze-dried pMDI formulation containing pEGFP-N1 and sucrose collected at Stage 4 and 5 of an ACI.** Scale bar = 10 µm.

### 4.3.6 Cell Toxicity Assay

The *in vitro* MTT toxicity assay, performed on A549 cells (Figure 4.14), showed no significant loss in cell viability ($p>0.05$) between blank, untreated cells and cells treated with the washed, aerosolised pDNA formulation. A significant reduction in cell viability ($p<0.05$) was however observed when DOTAP was added to the cell culture medium. The MTT assay was also used to ascertain the effect of number of actuations on cell viability. Statistical analysis showed a significant reduction ($p<0.05$) in cell viability when cells bathed in DMEM plus DOTAP were exposed to 80 compared to 9 actuations of 8%v/v ethanol in HFA134a. This demonstrates the sensitivity of the MTT assay and is likely due to the cold-freon effect of repeated aerosolisations or increased exposure to ethanol.

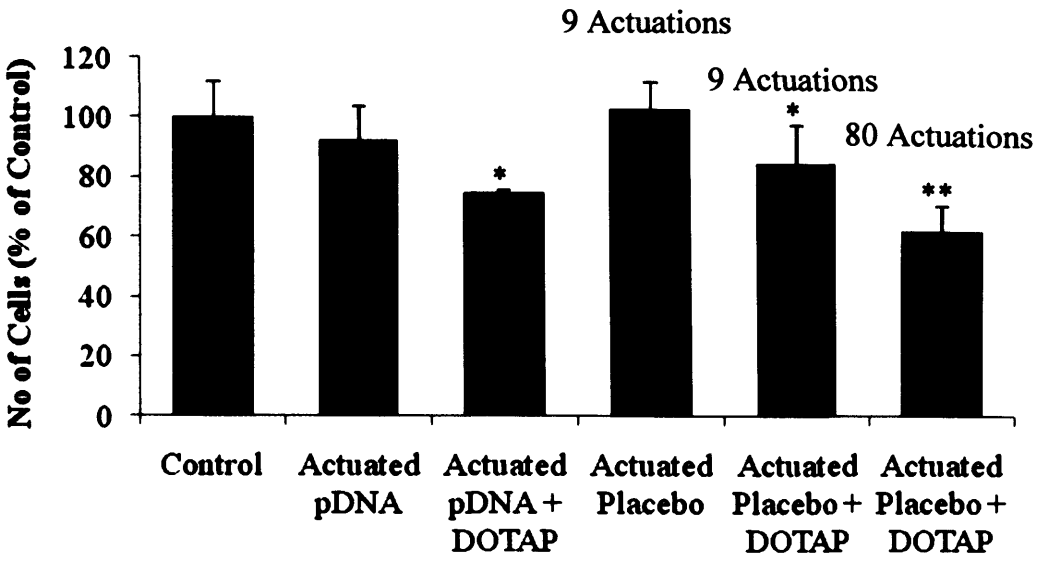


**Figure 4.14 Percentage cell viability of cells following aerosolisation of treatments.** Cells were surface-treated with: **(i)** DMEM, (control cells; 100% viability), **(ii)** Nine actuations of a solvent-washed pEGFP-N1 pMDI formulation actuated into DMEM alone, **(iii)** Nine actuations of a solvent-washed pEGFP-N1 pMDI formulation actuated onto DMEM containing DOTAP, **(iv)** Nine actuations of placebo pMDI formulation containing HFA 134a and absolute ethanol actuated onto DMEM alone, **(v)** Nine actuations of placebo pMDI formulation containing HFA 134a and absolute ethanol actuated onto DMEM containing DOTAP, **(vi)** Eighty actuations of placebo pMDI formulation containing HFA 134a and absolute ethanol actuated onto DMEM containing DOTAP. Data are presented as mean ± sd; n = 3. *denotes a significant difference from the control ($p<0.05$). **denotes a significant difference from both the control and the treatment with nine actuations ($p<0.05$).

## 4.4 Discussion

### 4.4.1 A549 Cell Growth Study

The cell growth study demonstrated that A549 cells followed a sigmoidal pattern of cell proliferation (Figure 4.5) (Davis 2002). Transfection studies were performed on cultures during the exponential log phase of cell growth as this is considered the optimal time to treat cells as transfection efficiency is increased in dividing cells due to the compromised cell membranes (Wilke *et al* 1996). Also the cell population in this phase is at its most uniform and cell viability is high (Freshney 2000). For this reason, knowledge of the A549 growth curve played a critical role in the transfection studies carried out in this chapter. In addition, as the percentage cell confluency at any given time could be calculated from the growth curve, all transfection studies could be carried out at a predetermined cell confluency to facilitate consistency in results between investigations. Cells in this study were treated at 68% confluency, 48 hr post seeding, as cells were in their log phase and this was considered an appropriate time period from an operational perspective.

### 4.4.2 Optimising DOTAP: pDNA Ratio for Transfection Studies

In the pilot study to determine the most transfection efficient DOTAP: pDNA ratio (Section 4.3.3), the data revealed that a 6:1 w/w ratio of DOTAP: pDNA was the minimum required to obtain a significant increase in the percentage of cells emitting GFP fluorescence compared to the control (Figure 4.6). This could be due to the fact that a 6:1 w/w ratio may contain an excess of lipid leading to the formation of complexes with an overall positive charge which is critical for efficient cell entry (Felgner *et al* 1987; Zabner *et al* 1995; Xu and Szoka 1996). Higher DOTAP: pDNA ratios, i.e. from 8:1, 10:1 and 12:1 w/w did not yield any further significant increase in the percentage of fluorescent cells. As lipid toxicity is concentration dependent, (Felgner *et al* 1987; Chiaramoni *et al* 2007) the lowest transfection efficient ratio of DOTAP: pDNA was used in order to minimise any cationic lipid induced cell toxicity. As DOTAP: pDNA ratios of 6:1 w/w delivered DNA to A549 cells at least as efficiently as did treatments containing higher proportions of cationic lipids,

the 6:1 w/w ratio was deemed a suitable treatment ratio for the transfection studies (Section 4.2.5 and Section 4.2.7.3).

However, the percentages of cells expressing GFP fluorescence in this study are relatively low, for example a 6:1 w/w ratio conferred 4.59% gene expression. By comparison, Birchall *et al* (2000) reported GFP expression of approximately 29% in A549 cells treated with a 6:1w/w DOTAP: pDNA ratio. Possible reasons for the reduced absolute levels observed could have been due to the quality of the lipid. As the DOTAP used in this study had been stored for a long period of time and was past its expiry date, the lipid used may not have been of sufficient quality. Nevertheless, this study was not repeated using newly purchased DOTAP. The reason for this being that the general trend observed in this study was reflective of published work, in the sense that gene expression increased with DOTAP: pDNA ratios up to approximately 6:1 w/w ratio after which expression levels tended to plateau (Birchall *et al* 2000). Although this study was not repeated, all subsequent studies conducted in this thesis were performed using newly purchased DOTAP.

### 4.4.3 Assessing the Transfection Competency of Lyophilised pDNA Particulates

Initial transfection results revealed no significant difference in the expression of reporter gene in cells treated with unprocessed pDNA and solvent-washed lyophilised pDNA (Figure 4.7). These data demonstrate the utility of the developed nanotechnology processes to deliver biologically active pDNA particles. The transfection data also highlight that a washing stage is essential to maintain pDNA functionality, by removing the excess surfactant, as treating the cells with pDNA particles coated in an excess of surfactant revealed no significant increase in the expression of the reporter gene compared to the control (Figure 4.7). This suggests that the excess of surfactant present in the unwashed samples may have reduced the formation of the electrostatic lipid:pDNA complex and/or affected interactions of the lipid:pDNA complex with the cell surface.

Lecithin surfactant, used during processing the pDNA particles, is composed of various substances including anionic lipids. Given the charge of the surfactant, it is feasible that an excess of surfactant coating the pDNA particles may have electrostatically interacted with the DOTAP, preventing the lipid:DNA complexes from forming. Also as anionic lipids have been shown to have a strong ability to displace pDNA from cationic lipid:pDNA complexes (Xu and Szoka 1996), a reduction in transfection in the presence of surfactant may have been anticipated. Additionally, previous research has shown that anionic surfactants have the ability to reduce transfection efficiency by inducing release of DNA from cationic lipid:DNA complexes before it reaches the target cell (Duncan *et al* 1997; Tsan *et al* 1997).

### 4.4.4 Assessment of pDNA pMDI Formulations

DNA integrity, assessed by electrophoresis, was studied following incorporation of processed pDNA into a pMDI formulation and aerosolisation (Figure 4.8). Aerosolised pDNA was assessed for retention of the transfection competent supercoiled band, as most published literature supports the opinion that degradation of this fraction may have detrimental effects on the transfection efficiency of the pDNA (Chancham and Hughes 2001; Remaut *et al* 2006). Analysis of unprocessed pDNA indicated that 70% was in the supercoiled form, providing the baseline for subsequent samples. Analysis of the aerosolised solvent-washed pDNA particles showed a reduction in the supercoiled fraction to 66% (Figure 4.8). Placing this result in context with the extant literature in the pulmonary gene delivery field, previous research has demonstrated that jet nebulisation can result in much greater losses of pDNA with only 5 to 60% (Birchall *et al* 2000; Kleemann *et al* 2004; Lentz *et al* 2005) of supercoiled pDNA, of a similar size to that of pEGFP-N1, being recoverable after nebulisation compared with non-nebulised control. Our results infer that the formulation processes of preparing, solvent-washing, incorporating into a co-solvent propellant mixture and aerosolising of the pDNA particulates had a comparatively small adverse effect on the tertiary structure of the pDNA.

Analysis of the aerosolised unwashed pDNA pMDI formulation revealed a sample that did not migrate as far as the supercoiled fraction from the unprocessed pDNA (Figure 4.8). As sample migration during electrophoresis is size driven as well as charge driven, a possible reason for the reduced mobility of the surfactant-coated pDNA particles may have been due to the increase in the size or change in the net charge of the pDNA composite due to the surfactant coating.

Cellular transfection and gene expression studies, using aerosolised pDNA formulations were carried out by actuating treatments onto cells seeded in flasks. Treatments were actuated directly into cell seeded flasks as this technique would allow a closer simulation of *in vivo* delivery, rather than collection and then treatment of aerosolised pDNA on to cells (Stern *et al* 1998). Guided by the results from a preliminary study using coloured dye (Figure 4.10), pDNA loaded pMDI formulations were actuated from above onto A549 cells seeded in a cell culture flask. Data from the transfection studies, using various aerosolised formulations, revealed that only the solvent-washed pDNA particles conferred a significant rise in the percentage of fluorescent cells in the presence of DOTAP Figure 4.11. This suggests that the solvent-washed pEGFP-N1 particulates remained functionally active following formulation processing, dispersion in propellant and aerosolisation from a pMDI. Statistical analysis showed no significant difference in the percentage of cells expressing GFP following treatment with the washed pEGFP-N1 formulation actuated onto cells without the presence of DOTAP compared with control cells. This data substantiates previous research that a transfection agent is essential in conferring efficient gene expression *in vitro* (Zabner *et al* 1995; Gao and Huang 1996; Remaut *et al* 2006), and acts as a control to confirm that the fluorescence detected during FACS analysis was indeed due to intact pEGFP-N1 transfecting cells with the aid of a transfection agent.

These *in vitro* cell culture studies establish that pDNA can be formulated to remain transfection competent when actuated from a pMDI. However whilst *in*

*vitro* studies are necessary to demonstrate proof-of-concept, a clear understanding of the barriers encountered *in vivo* is required to progress this work towards clinical therapy. The lungs possess numerous biological barriers and mechanisms that all contribute to the clearance of foreign particles and therefore hinder their ability to exert any therapeutic effect. The presence of a mucus layer and the mucociliary escalator are crucial in trapping and removing foreign particles in the upper airways. Lung surfactant at the air-water interface not only causes macromolecule aggregation and thus promotes particle removal by macrophage engulfment, but has also been shown to interact with cationic lipid:pDNA complexes to reduce pDNA transfection (Duncan *et al* 1997; Tsan *et al* 1997). Therefore if the lipid DNA treatment is administered separately, endogenous anionic surfactants have the potential for interacting with the DOTAP preventing the lipid:DNA complexes from forming in situ. In addition, due to the mechanism of gene transfer, the differences between cell proliferation rates *in vitro* and *in vivo* has revealed significant variation in pDNA transfection efficiency (Wilke *et al* 1996; Brunner *et al* 2000; Remaut *et al* 2006). Nevertheless, our data provides early proof-of-concept of this approach and more research through *in vivo* assessment is now warranted.

Visual observations of solvent-washed pDNA formulations in PET vials with time highlighted a number of points (Figure 4.12) Solvent-washing the surfactant-coated pDNA particles removed the excess surfactant to produce an off-white powder which initially dispersed in the propellant-cosolvent mixture. Sedimentation of the particles did occur after 24 hr but the sedimented particles were readily redispersed by one inversion of the vial confirming the presence of loose floccules. This flocculated system showed no signs of caking following storage at ambient temperatures for 5 months. Surfactants are often incorporated into suspensions to stabilise the drug dispersion by reducing the electrostatic charge of the drug. Observations of a dispersible flocculated system indicated that drug aggregation of the formulation was suitably controlled within the 5 month time span. The lack of solubility of hydrophobic surfactants (e.g. lecithin) in HFA 134a propellant is well documented

(Blondino and Byron 1998; Vervaet and Byron 1999) and commonly requires the use of a co-solvent in commercial formulations. The observations of a dispersed system (Figure 4.12) suggested that the quantity of surfactant in the solvent-washed formulation fell within the range of that which could be solubilised into the propellant with the aid of ethanol as co-solvent (8% v/v).

Scanning electron microscopy of the aerosolised, solvent-washed pEGFP-N1 formulation revealed a continuous matrix (which may be the sticky surfactant system) interspersed with protrusions of a heterogeneous particle population comprising of angular particles (likely to be the sucrose lyoprotectant) and more rounded particles (possibly including surfactant-coated pEGFP-N1 particles) (Figure 4.13). Although micrographs showed that more of these particle protrusions were present at Stage 5 of the ACI (cut-off diameter 1.1 μm), the observed larger particle dimensions suggest that particle agglomeration was prevalent. Whilst particles were solvent-washed to remove excess surfactant, the presence of the surfactant, even at a minimal quantity, may have caused the particles to agglomerate as they impacted on the ACI plate. Additionally as the formulation was actuated into the ACI a total of 80 times, particle overload on the ACI stages could have resulted, another significant reason as to why particle agglomeration may have been observed. It is also possible that sample heating during SEM processing and analysis may have caused particle agglomeration. Further characterisation of discrete particles may have been possible at higher magnifications, however, due to the magnifying limitations of the SEM the particles could not be viewed at higher magnifications without a significant loss in the image resolution.

The MTT toxicity assay was used to assess the cytotoxicity of the aerosolised pDNA treatments (Figure 4.14). The assay showed a significant reduction in the percentage cell viability in the presence of DOTAP. The significant reduction in cell viability in the presence of DOTAP concurs with previously published reports (Choi *et al* 2004; Chiaramoni *et al* 2007). More promisingly however, the toxicity assay revealed an absence of effect of washed,

aerosolised pEGFP-N1 formulation (without DOTAP) on cell viability. This result confirms that the washed pEGFP-N1 aerosolised formulation *per se* exerted no significant toxic effect on cells. As diminished cell viability occurred with DOTAP, it may be appropriate to explore the use of alternative transfection agents (Choi *et al* 2004; Jiang *et al* 2008; Prata *et al* 2008) and 'helper' lipids (Felgner *et al* 1994; Bennett *et al* 1995). Indeed, *in vivo* gene expression has been achieved in the past without the use of a transfection agent, although transfection efficiency was found to be relatively low (Zabner *et al* 1997; Xenariou *et al* 2007).

The toxicity assay also highlighted that increasing the number of actuations from 9 to 80 caused a significant reduction in the percentage cell viability. This reduction in cell viability is likely to be a result of the cold freon effect, a phenomenon that has been used to describe the cessation of inhalation in patients in reaction to the high velocity strike and evaporative cooling of the propellant plume (Pedersen *et al* 1986; Crompton 1990). However, in the context of this study increased actuations would expose the cells to an increase in the cold freon effects. As cells are notoriously fragile and sensitive to temperature, an increased number of high velocity strikes on the cell monolayer and the evaporative cooling effects may have been the cause for cell damage and stress. Additionally the increase in actuations would cause cells to be exposed to an increased concentration of aerosolised ethanol. Ethanol is known for its ability to induce cell death (Ewald and Shao 1993; Jacobs and Miller 2001) and so the loss of cell viability observed with increasing the number of actuations may have also been attributed to effect of ethanol. Although these actuation effects would not be significant *in vivo*, as the concentration of aerosolised ethanol administered would be relatively low, this data does however provide important information for maintaining cell viability in further *in vitro* studies carried out in the subsequent chapter.

## 4.5 Conclusion

This chapter aimed to investigate the feasibility of dispersing and aerosolising pDNA particles from a pMDI system whilst maintaining the pDNA biological functionality.

Analysis of aerosolised solvent-washed pDNA particles, using agarose gel electrophoresis, showed that the formulation could be incorporated into a HFA 134a system and aerosolised using a standard valve and actuator with a relatively small reduction in the pDNA integrity. A549 cellular gene expression studies revealed that the biological functionality of solvent-washed pDNA particulates remained functionally active following formulation processing, dispersion in propellant and aerosolisation from a pMDI. The presence of excess surfactant coating the unwashed pDNA formulation, however, was found to hinder pDNA functionality.

A549 cellular cytotoxicity, investigated using the MTT assay, demonstrated that any loss of cell viability was a cumulative effect between the number of actuations used and the use of DOTAP. Promisingly the data revealed an absence of effect of washed, aerosolised pEGFP-N1 formulation (without DOTAP) on A549 cell viability. Subsequent characterisation of solvent-washed pDNA particles aerosolised into an ACI revealed that particles were in the respirable size range.

The data generated from this chapter highlights that particles prepared by this low-energy microemulsion process may have the potential for stable and efficient delivery of pDNA to cells in the lower respiratory tract via pMDIs.

# CHAPTER FIVE

# Characterisation, Transfection and Stability of DOTAP-pDNA pMDI Formulation

## 5.1 Introduction

The previous chapter focussed on characterising pDNA pMDI formulations actuated onto cells immersed in DOTAP transfection agent. This chapter will attempt to incorporate the DOTAP transfection agent into the pDNA pMDI system and characterise the aerosolised formulation.

The need for a transfection agent to confer efficient cellular DNA delivery has been previously reported (Gao and Huang 1996; Zabner *et al* 1997). However, preparing the complexes to ensure effective cellular transfection is a process that is poorly defined and can be difficult to control. Factors including liposome:DNA concentrations and mixing rate have been found to affect complex formation efficiency resulting in variations in cellular transfection (Gershon *et al* 1993; Hirota *et al* 1999; Birchall *et al* 2000). Successfully incorporating DOTAP, the model transfection agent used in this thesis, into our pDNA pMDI formulation to form a single dosing unit would reduce the likelihood of encountering variations in complex formation which may occur if for example the DOTAP and pDNA were administered separately, even if this were possible. In a clinical setting, variations in complexing efficiency would lead to inconsistent pDNA transfection and possible variations in therapeutic effect between doses. Administering the DOTAP and pDNA separately would open the formulations up to a number of challenges and barriers. Great care would be required to ensure both components had similar aerodynamic particle size diameters so that they deposited in close proximity *in vivo* to ensure complexing. Also the presence of endogenous anionic surfactants, which have been shown to induce the release of DNA from cationic lipid:DNA complexes (Duncan *et al* 1997; Tsan *et al* 1997), may preferentially complex to the lipid preventing DNA complexes from even forming in the first place. Preparing the DOTAP:pDNA formulation prior to administration would overcome some of these challenges.

Freshly preparing the lipid:DNA complex prior to administration, a technique used with nebulisers due to the aqueous instability of lipoplexes, requires

specialist skill from a clinician (Hyde *et al* 2000; Ruiz *et al* 2001). The use of a formulation which incorporates both the transfection agent and pDNA, such as the formulation investigated in this chapter, would have an added advantage in terms of patient autonomy as it would be feasible for patients to administer their treatment after initial consultations on good inhaler technique.

### 5.1.1 Envisaged Formulation Challenges

Incorporating a transfection agent such as DOTAP into a pDNA pMDI system is relatively novel and to date there is extremely little published work in this field. The plausibility of preparing such a formulation and the challenges envisaged are therefore difficult to fully predict. However, delivery of liposomes from a pMDI system has been investigated for a number of decades. The preparation of lipid formulations in a pMDI has been developed as a drug delivery vehicle (Farr *et al* 1987, 1989). The limitations of such a formulation have, however, been reported. The incorporation of phospholipids into a CFC pMDI system has been found to increase the aerosolised droplet size, with a reduction in the respirable fraction (Farr *et al* 1987). The tendency of aerosolised lipids to associate at the droplet-air interface, retarding propellant evaporation, to result in larger droplets and an increased deposition in the upper airways is well documented (Snead and Zung 1968; Otani and Wang 1984;). This adverse effect on the formulation deposition profile is a challenge that will be faced in this chapter during the incorporation of a lipid transfection agent into a pDNA pMDI system. Nevertheless, Farr *et al* (1987) demonstrated that a lipid could be incorporated into the nonpolar environment of a pMDI system and form liposomes upon aerosolisation into a aqueous environment such as the pulmonary epithelial lining fluid.

pMDI formulations prepared in this thesis utilised HFA propellant, due to the phase out of CFC propellants (United Nations Environment Programme 2006). HFAs are relatively polar compared to CFCs, and have insufficient capacity to solubilise lipids that would be soluble in CFCs (Blondino and Byron 1998; Vervaet and Byron 1999). Incorporation of DOTAP lipid into our pDNA pMDI

formulation would therefore be challenging in terms of ensuring its dispersibility and therefore stability in HFA propellant. The use of a co-solvent such as ethanol, to facilitate lipid solubility may offer a potential solution to such a problem (Smyth 2003). Other possible ways of incorporating the transfection agent into the pDNA pMDI formulation include coating the pDNA particles with the lipid prior to incorporation into the pMDI. Spray-drying or freeze-drying lipids in the presence of a hydrophilic drug in either an aqueous or emulsion environment has been reported to yield lipid coated particles that can be dispersed and aerosolised from a HFA based pMDI system (Tarara *et al* 2004; Cook *et al* 2005; Nyambura *et al* 2009b).

### 5.1.2 Characterising Liposome-DNA Complex Structure

DNA cellular transfection is promoted by the formation of lipoplexes with a net positive charge (Felgner *et al* 1987; Gao and Huang 1995). The formation of these lipoplexes is driven by the difference in electrostatic charge between the anionic phosphate backbone of pDNA molecules and the positively charged polar amino- head group of cationic liposomes. This interaction can cause the formation of structures which can exist as one or more possible geometries and is related to the lipid:pDNA ratio (Dan 1998). Cationic liposomes bind initially to the DNA molecule to form clusters of aggregated vesicles along the nucleic acid strand in a 'beads on a string' type of structure (Gershon *et al* 1993; Sternberg *et al* 1994). At a critical lipid:pDNA ratio (1:1 w/w) any further increase in the lipid was found to cause a DNA induced liposome fusion, where the negatively charged DNA appears to act as a fusogenic agent, drawing together the positively charged liposomes (Felgner *et al* 1995). During the fusion process, a lipid induced DNA collapse has been observed which results in the formation of a condensed DNA structure that can be completely encapsulated within the fused lipid bilayer (Gershon *et al* 1993). Similar observations were also made by Sternberg *et al* (1994) who, using freeze-fracture electron microscopy, identified lipoplexes as aggregates surrounding the DNA strand co-existing with tubular structures composed of DNA molecules coated by lipid bilayers, giving rise to the 'spaghetti and meatballs'

analogy. Additionally, the presence of flat lamellar structures have also been identified, where the DNA adsorbs between the liposome layers forming an alternating multilamellar structure as the condensed DNA is sandwiched between layers (Radler *et al* 1997). These transfection competent lipid:DNA multilamellar complexes have been reported to have a characteristic 'fingerprint' like appearance when viewed using transmission electron microscopy (TEM) (Tomlinson and Rolland 1996; Birchall *et al* 2000).

### 5.1.3 Characterising Aerosolised Particles

Characterisation of aerosolised particles, through aerodynamic particle size distribution profiles, has been typically carried out using instruments recognised in the compendia such as the non-viable ACI (British Pharmacopoeia 2010b). The Andersen viable sampler may be used as an alternative to such methods with possible applications in determining the aerodynamic size distribution of particles emitted from a pMDI.

The six stage Andersen viable sampler (AVS) was first developed in 1958 (Andersen 1958) and was originally designed to measure the concentration and particle size distribution of viable aerobic bacteria and fungi. Since then it has been utilised as an *in vitro* model in predicting and assessing the health hazard or infection potential of biological aerosols to humans (Wendt *et al* 1980; Weis *et al* 2002; Fennelly *et al* 2004) (Section 1.4.2). In this chapter the AVS is used to characterise the aerodynamic particle size distribution of aerosolised pDNA pMDI formulations. To date the use of a viable sampler for characterising aerosolised particles emitted from an inhaler system has not been reported in published work. The viable sampler is deemed to be advantageous over other particle sizing methods, for the work carried out in this chapter, for a number of reasons. The viable sampler is designed to minimise 'wall loss' so that particle impaction is predominantly on the media contained in petri dishes as opposed to the walls of the apparatus as in the glass impinger (Andersen 1958). Sample collection from the viable sampler does therefore not require any wash methods, which is labour intensive and if carried out insufficiently can lead to

poor sample collection (Andersen 1958) For this reason the use of a viable sampler can be deemed advantageous over other particle sizing apparatus such as the glass impinger, which requires washing of the overall inner surface of the apparatus, or ACI, where impaction plates require washing (British Pharmacopoeia 2010b). Often cascade impactors using impaction plates can have a reduced efficiency due to particle bounce and re-entrainment effects (Ranz and Wong 1952). However, this effect is reduced in a viable sampler as an impaction medium is used for particle collection (Andersen 1958). Additionally in particle sizing instruments where the particles are deposited directly into impaction medium, the viable sampler requires the use of a lower quantity of medium per stage (approximately 8 ml with total volume of 48 ml for the six impingement stages) compared to the MSLI (20 ml per stage and 80 ml total volume for the four impingement stages) (British Pharmacopoeia 2010b). Maintaining a low volume of impaction medium is crucial to prevent any dilution effect during quantification of deposited pDNA particles using cellular transfection methods.

The viable sampler is also commercially available as an abbreviated system comprising a reduced number of stages; typically single stage (Thermo Scientific 2009a) or two stage (Thermo Scientific 2009b; Westech Instruments 2009). These labour saving abbreviated systems have been designed and used for applications in the characterisation of biological aerosol particles in terms of the respirable and non-respirable fraction rather than particle size distribution (Trout *et al* 2001; Thermo Scientific 2009b). They have been shown to produce characterisation data comparable with the standard six stage Andersen viable sampler in terms of both their precision and accuracy (Jensen *et al* 1992; Jones *et al* 1985). To date there is no published data available on the utility of an abbreviated viable sampler for collection of particles deposited from a pMDI. However, a two stage viable impactor based on the Andersen six stage viable sampler (Andersen 1958) has been developed by Westech Instruments Ltd. for determining the fine particle dose of pMDI using coated petri dishes.

In order to assess the use of the abbreviated viable sampler for characterising particles emitted from a pMDI, investigations will be carried out in this chapter to compare the FPF generated from the ACI, six stage Andersen viable sampler (AVS) and the abbreviated Andersen viable sampler (AAVS) using the commercially available formulation Airomir® which comprises SS a molecule which can be relatively easily assayed.

### 5.1.4 Specific Aims and Objectives of the Chapter

This chapter aims to investigate the feasibility of incorporating DOTAP into a pMDI system containing solvent-washed pDNA particles. One of the aims of this chapter is to assess the potential for delivering the DOTAP-pDNA formulation to cells via a pMDI using a standard valve and actuator. Subsequent aims of this chapter are to determine the deposition pattern of the aerosolised DOTAP-pDNA formulation and to assess its stability after a four week storage period.

The experimental objectives are to:

1. Investigate different methods to incorporate DOTAP transfection agent into pDNA pMDI systems. The optimum system will be identified by quantifying transfection efficiency of aerosolised formulations on A549 cells using flow cytometry.
2. Characterise structure of lipid:pDNA lipoplexes formed from aerosolised DOTAP-pDNA formulations using TEM.
3. Determine deposition patterns of aerosolised DOTAP-pDNA pMDI using *in vitro* cascade impaction methods.
4. Assess the stability of the DOTAP-pDNA pMDI system subjected to accelerated storage conditions through quantifying gene expression in A549 cells treated with the aerosolised formulation.
5. Characterise DOTAP-pDNA dispersion behaviour in pMDI canisters.

## 5.2 Materials and Methods

All reagents were used as received and were purchased from Fisher Scientific UK Ltd. (Loughborough, UK) unless otherwise stated.

Deionised water was obtained from an Elga reservoir (High Wycombe, UK). Phosphate buffered saline pH 7.4 ($Mg^{2+}$ and $Ca^{2+}$ free) and Chloroform ≥ 99.8% spectrophotometric grade were purchased from Sigma-Aldrich Ltd. (Poole, UK). Dulbecco's Modified Eagle's Medium (DMEM), foetal bovine serum, penicillin G 5000 units/ml and streptomycin sulphate 5000 μg/ml were purchased from Invitrogen Ltd. (Paisley, UK). A549 mammalian cell line was purchased from ECACC (Salisbury, UK); 1,2- Dioleoyl- 3-Trimethylammonium propane (methyl sulphate salt) (DOTAP) was purchased from Avanti Polar Lipids Inc. (Alabama, USA). HFA 134a was a generous gift of INEOS Fluor Ltd. (Runcorn, UK). Airomir® pMDI was obtained courtesy of 3M Healthcare Ltd (Loughborough, UK).

### 5.2.1 Incorporation of DOTAP into a pDNA pMDI System

Investigations were carried out to assess whether DOTAP could be incorporated into a pMDI containing the solvent-washed pDNA particle formulation and successfully aerosolised to confer pDNA transfection and gene expression.

To achieve this goal the following DOTAP–pDNA formulations were produced and investigated for cellular gene expression post-actuation from a pMDI system;

In all formulations the equivalent of 79 μg pDNA and a DOTAP (474 μg) equivalent to a DOTAP:DNA 6:1 w/w ratio was incorporated into the pMDI system.

- Liposomal DOTAP + pDNA particles:

Extruded DOTAP (1 mg/ml) (prepared in Section 4.2.3) liposomes were

pipetted directly into a fluorinated ethylene propylene (FEP) coated aluminium canister (3M Drug Delivery Systems, Loughborough, UK) containing 5 mg (equivalent to 79 μg pDNA) of solvent-washed pDNA particles. The pDNA-DOTAP formulation was then vortexed for 5 min and left to stand at room temperature for 20 min to promote lipoplex formation. Absolute ethanol (0.5 ml) was then pipetted into the canister after which the formulation was vortexed for another 5 min.

- DOTAP in pDNA particle formulation:

DOTAP lipid (6 mg) was weighed and added to the surfactant phase during the production of an optimised microemulsion system comprising water phase: surfactant: organic phase, 26:52:22 w/w/w (preparation previously outlined in Section 2.2.1) containing 1 mg pDNA. The microemulsion was left to stand at room temperature for 20 min to promote lipoplex formation. After 20 min the microemulsion was freeze-dried (Section 2.2.2) and put through the solvent-wash procedure using propan-2-ol (Section 2.2.3). Once solvent-washing was completed, 5 mg of the pDNA sample was then weighed into a FEP coated canister and dispersed in 0.5 ml of absolute ethanol by vortexing for 5 min.

- DOTAP + pDNA particles:

DOTAP lipid was weighed into a FEP coated canister containing 5 mg of solvent-washed pDNA particles (equivalent to 79 μg pDNA). Absolute ethanol (0.5 ml) was pipetted into the canister and the formulation was dispersed by vortexing for 5 min.

- DOTAP coated canister + pDNA particles:

The inside of an FEP coated canister was coated with DOTAP by dissolving 474 μg DOTAP lipid in 1 ml chloroform, adding to the canister and then evaporating the solvent using rotary evaporation methods outlined previously (Section 4.2.3). Solvent-washed pDNA particles (equivalent to 79 μg pDNA) were then weighed into the canister and dispersed using 0.5 ml absolute ethanol and vortexing for 5 min.

All formulations were left to stand at room temperature for 20 min in order to allow DOTAP:pDNA complex formation to proceed prior to the addition of HFA 134a propellant. Spraymiser™ 50 µl retention valves (3M Drug Delivery Systems, Loughborough, UK) were crimped onto the aluminium canisters and 6 ml HFA 134a was added using a Pamasol® semi-automatic filling and crimping machine model P2005/2 (Pamasol Willi Mäder AG, Pfäffikon SZ, Switzerland).

The pMDI formulations were actuated from the vertical orientation (Section 4.2.7.2) onto A549 cells seeded in T25 flasks (Corning Costar Ltd., High Wycombe, UK) at a density of 4 x $10^4$ cells/$cm^2$ and cultured under the culture conditions outlined in Section 4.2.1 to 68% confluency. Each T25 flask was treated with the equivalent of 15 µg aerosolised pEGFP-N1. pMDIs were primed by firing five shots to waste using an actuator with a 0.5 mm orifice diameter (3M Drug Delivery Systems, Loughborough, UK). To reduce any cell death, due to aerosol cold freon effect, the T25 flasks were placed on pre-warmed saline infusion bags with 30 sec intervals between actuations. All treatments were conducted in serum-free DMEM. Treated cells were stored in a humidified incubator (37°C/ 5% $CO_2$). After a period of 6 hr, cells were washed once with 5 ml PBS, pH 7.4, replenished with 5 ml of growth media (10% fetal bovine serum, 2% penicillin/streptomycin 5000 iu/ml and DMEM to 100%) and returned to the humidified incubator (37°C/ 5% $CO_2$). The percentage of cells displaying GFP-associated fluorescence (FL1-H) was quantified 42 hr post-treatment by flow cytometry (FACSCalibur™ system Becton, Dickinson Biosciences, Oxford, UK) with analysis by WinMDI™ Software (Joseph Trotter, The Scripps Institute, California, USA), as described previously (Section 4.2.4.1).

#### 5.2.1.1 Microscopic Characterisation of Aerosolised DOTAP-pDNA Formulation

A Philips 208 transmission electron microscope (TEM) (Philips, Eindhoven, The Netherlands) was used to characterise the actuated DOTAP-pDNA

formulations. The method used to visualise the presence of any DOTAP:pDNA complexes was adapted from Zabner *et al* (1995). Freshly prepared DOTAP-pDNA formulations were actuated ten times into a 50 ml centrifuge tube containing 25 ml deionised waster. A pioloform-coated 200 mesh nickel grid was fixed between the tips of metal forceps and 5 µl of the actuated sample in water was pipetted onto the 'dull side' of the grid. After a contact time of 5 min the excess formulation was wicked from the grid using filter paper. Aqueous uranyl acetate (2% w/w), used as the negative stain, was centrifuged for 2 min at 13,000 rpm prior to use. The grid surface was then placed on the surface of a 2% aqueous uranyl acetate drop for 30 sec. After 30 sec the stain was wicked from the grid and the grid was rinsed twice in drops of deionised water, ensuring that the grid was wicked between washes, prior to analysis by TEM.

### 5.2.2 Assessment of DOTAP-pDNA Deposition Following Aerosolisation from a pMDI

Initial experiments were carried out to assess the minimum quantity of the aerosolised DOTAP-pDNA formulation required to ensure a detectable deposition result. Using the DOTAP coated canister formulation (Section 5.2.1) three quantities of solvent-washed pDNA were investigated, 5 mg, 10 mg and 20 mg, which were actuated with the assumption that an equivalent of 79 µg, 158 µg and 316 µg pEGFP-N1 respectively would be successfully expelled from the pMDI.

The *in vitro* deposition performance of aerosolised DOTAP-pDNA formulation was characterised using an Andersen six stage viable sampler (AVS) (Andersen Samplers Inc., Georgia, USA) fitted with a 90° aluminium USP-2 induction port (throat), to act as an inlet to the device, and operated at 28.3 l/min in a 20°C temperature controlled room. Prior to use all sampler components were sprayed with 70% (v/v) absolute ethanol in water and dried. Each stage of the AVS consisted of a sterile petri dish containing 8 ml of sterile serum-free DMEM as the impaction medium.

DOTAP-pDNA pMDIs were primed by firing five shots to waste using an actuator with a 0.5 mm orifice diameter (3M Drug Delivery Systems, Loughborough, UK). During priming and testing pMDIs were shaken for 5 sec between actuations, as specified in compendia procedures (British Pharmacopoeia 2010b). Following priming each inhaler was fixed into the testing position using a rubber mouthpiece attached to the throat of the AVS. The vacuum was then turned on and the canister was depressed and held for five sec. Once the pMDI formulation had been actuated to completion (approximately 130 actuations), flow through the AVS was maintained for an additional 30 sec. The sampler was then disassembled and the deposited DOTAP-pDNA formulation was recovered quantitatively from the throat by washing with 8 ml DMEM. 1 ml aliquots of aerosolised DOTAP-pDNA deposited on the throat and in the petri dishes containing DMEM were used to treat A549 cells seeded into 24-well plates at a density of $4 \times 10^4$ cells/cm$^2$ and cultured under the conditions outlined in Section 4.2.1 to 68% confluency. A total of 6 wells were treated with sample aliquots taken from each stage of the AVS.

After a period of 6 hr, cells were washed once with 1 ml PBS, pH 7.4, replenished with 1 ml of growth media and returned to the humidified incubator (37°C/ 5% $CO_2$). The percentage of cells displaying GFP-associated fluorescence (FL1-H) was quantified 42 hr post-treatment by flow cytometry (FACSCalibur™ system Becton, Dickinson Biosciences, Oxford, UK) with analysis by WinMDI™ Software (Joseph Trotter, The Scripps Institute, California, USA), as described previously (Section 4.2.4.1).

### 5.2.2.1 Validation of the Abbreviated Andersen Viable Sampler

In order to maximise the detection of any DOTAP-pDNA aerosolised sample deposition, the AVS was abbreviated by reducing the number of deposition stages. Initial experiments using Airomir® (Salbutamol Sulphate 100 µg Inhalation Aerosol) pMDI were carried out to validate the use of the abbreviated viable sampler (AAVS). The AAVS was constructed from the six

stage AVS (full stack) using only Stages 2, 5 and 6. The AAVS was operated as before at 28.3 l/min in a 20°C temperature controlled room. Each stage of the AAVS consisted of a petri dish containing 8 ml internal standard (IS) prepared as outlined previously (Section 2.2.4). Airomir® pMDIs were initially primed by firing five shots to waste. Following priming the pMDIs were actuated twice into the sampler with a 5 sec shaking interval between actuations using the technique outlined in Section 5.2.2. After actuation, the AAVS was then disassembled and the deposited SS from the Airomir® pMDI was recovered quantitatively from the throat and inlet by washing with 8 ml IS. Aliquots of the samples were then analysed quantitatively for SS using the HPLC protocol (previously outlined in Section 2.2.4) and compared against SS deposition data generated from the full stack AVS and an ACI (Westech Instrument Services Ltd., Bedfordshire, UK) (protocol for use in Section 2.2.6). The FPF parameter generated from the ACI, full stack AVS and AAVS was used during equipment validation. The FPF referred to the proportion of particles with an aerodynamic diameter smaller than 4.7 μm. This parameter was calculated as a ratio of the aerosolised fine particle mass to the total mass of drug emitted.

Following validation with regard to the FPF, the AAVS was utilised for *in vitro* deposition performance assessment of aerosolised DOTAP-pDNA. Using the formulation which conferred the greatest cellular gene expression, 20 mg of solvent-washed pDNA was incorporated into a pMDI system (Section 5.2.1). The formulation was primed and actuated into the validated AAVS with the assumption that an equivalent of 316 μg pEGFP-N1 would be successfully expelled from the pMDI. The samples deposited in petri dishes at the various stages of the AAVS were analysed for transfection competency using cell culture methods outlined in Section 5.2.2.

The $FPF_{4.7\ \mu m}$ was calculated for the AAVS as the level of gene expression observed for particles with an aerodynamic diameter smaller than 4.7 μm (deposited on Stages 5 and 6 of the AVS, as Stages 3 and 4 had been removed)

as a percentage of total gene expression observed (throat to Stage 6). The $EPF_{1.1\ \mu m}$ was also calculated which referred to the ratio of gene expression observed for particles with an aerodynamic diameter smaller than 1.1 μm (Stage 6) compared to total gene expression.

### 5.2.3 Investigating the Stability of DOTAP-pDNA pMDI Formulation Following Accelerated Storage

DOTAP-pDNA pMDI formulations using DOTAP coated canisters and 5 mg solvent–washed pDNA were prepared as previously outlined (Section 5.2.1). Following preparation, the pMDI canisters were stored in the valve down position at accelerated storage conditions 40 ± 2°C /75 ± 5% relative humidity (ICH Expert Working Group 2003) using a Sanyo stability chamber (Sanyo Gallenkamp plc., Loughborough, UK). The valve down position was used as pharmaceutical pMDIs are often stored and used in this position. Three canisters were removed from the stability chamber and tested for cell transfection at pre-determined time points, 0 week (freshly prepared pMDI), 1 week, 2 weeks and 4 weeks after the pMDI formulations had been stored in accelerated conditions.

Canisters were actuated using a 0.5 mm orifice diameter actuator (3M Drug Delivery Systems, Loughborough, UK), from the vertical orientation (Section 4.2.7.2) onto A549 cells seeded in T25 flasks at a density of $4 \times 10^4$ cells/cm$^2$ and cultured under conditions outlined in Section 4.2.1. Each T25 flask was treated with the equivalent of 15 μg aerosolised pEGFP-N1, assumed to be successfully expelled, in the presence of serum-free DMEM. Treated cells were then stored in a humidified incubator (37°C/ 5% $CO_2$) and further handling of the cells was carried out as outlined above (Section 5.2.1). The percentage of cell fluorescence was quantified 42 hr post-treatment by flow cytometry (FACSCalibur™ system Becton, Dickinson Biosciences, Oxford, UK) with analysis by WinMDI™ Software (Joseph Trotter, The Scripps Institute, California, USA), as described previously (Section 4.2.4.1).

Formulations were also prepared in plastic polyethylene terephthalate (PET) pMDI vials (3M Drug Delivery Systems, Loughborough, UK) and stored in the stability chamber under accelerated conditions, for visual assessment of physical stability and dispersion homogeneity.

### 5.2.4 Statistical Analysis

Statistical analysis was carried out using a statistical package, SPSS 16®. One-way analysis of variance (ANOVA) followed by a Duncan's multiple range test used to compare multiple groups was used with significant difference indicated by the p-value $<0.05$. Results are summarised as mean ± sd.

## 5.3 Results

### 5.3.1 Incorporation of DOTAP into a pDNA pMDI System

The various DOTAP-pDNA formulations (Section 5.2.1) were aerosolised onto A549 cells in order to assess which formulation conferred the greatest cellular gene expression. Figure 5.1 highlights the significant increases ($p<0.05$) in fluorescent cells following aerosolisation of formulations that incorporated DOTAP into pMDI canisters as either a lipid powder (5.09 ± 3.83% fluorescent cells) or coating the canister with DOTAP (9.01 ± 3.98% fluorescent cells) compared with control cells (1.03 ± 0.51%). Formulations using liposomal DOTAP (1.83 ± 0.27%) or the incorporation of DOTAP lipid at the microemulsion stage (2.31 ± 2.31%) did not mediate any significant gene expression. Out of the four DOTAP-pDNA formulations investigated, the DOTAP coated canister formulation led to the largest significant increase in the percentage of fluorescent cells.

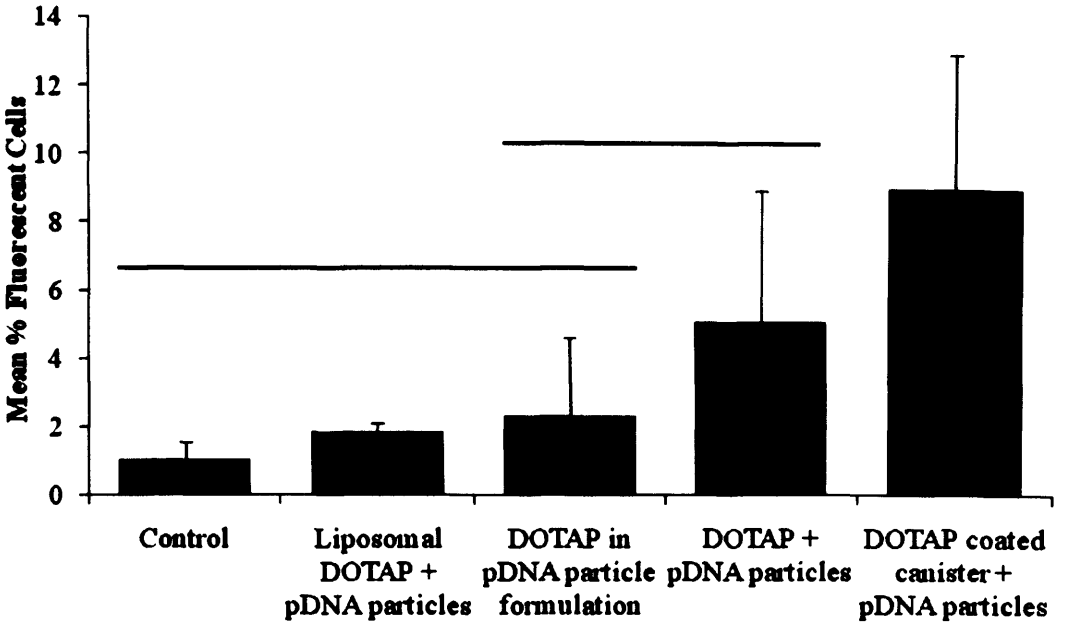


**Figure 5.1 Quantitative gene expression of aerosolised DOTAP–pDNA formulations.** A549 cells were surface-treated with **(i)** Control- DMEM alone, or aerosolised: **(ii)** Extruded DOTAP liposomes and solvent-washed pEGFP-N1 particles, **(iii))** DOTAP lipid incorporated into the pDNA microemulsion prior to freeze-drying and solvent–washing, **(iv)** DOTAP lipid and solvent-washed pEGFP-N1 particles, **(v)** DOTAP coating pMDI canister and solvent-washed pEGFP-N1 particles. Data are presented as mean ± sd; n = 3. The bar represents no significant difference ($p$>0.05).

### 5.3.1.1 Microscopic Characterisation of Aerosolised DOTAP-pDNA Formulation

TEM analysis was performed on actuated DOTAP-pDNA formulations to characterise the structural properties of the aerosolised products. DOTAP liposomes prepared by solvent evaporation and extrusion and added to the pDNA particles in the canister, revealed the presence of indistinguishable disperse bodies (Figure 5.2, Micrograph A). Lamellar structures indicating the presence of either liposomes or lipoplexes were not observed.

DOTAP lipid in powder form incorporated into a pMDI system containing solvent-washed pDNA, revealed a heterogeneous population made up of spherical and aggregated complexes (Figure 5.2, Micrograph B). The spherical complex was approximately 100 nm in diameter. Aggregates varied in

diameter but were generally larger than 100 nm.

When DOTAP was pre-coated onto the canister wall prior to addition of the pDNA particles, TEM revealed a population of multilamellar lipoplexes indicated by the 'finger print' like structures. These lipoplexes were generally larger than 100 nm (Figure 5.2, Micrograph C).

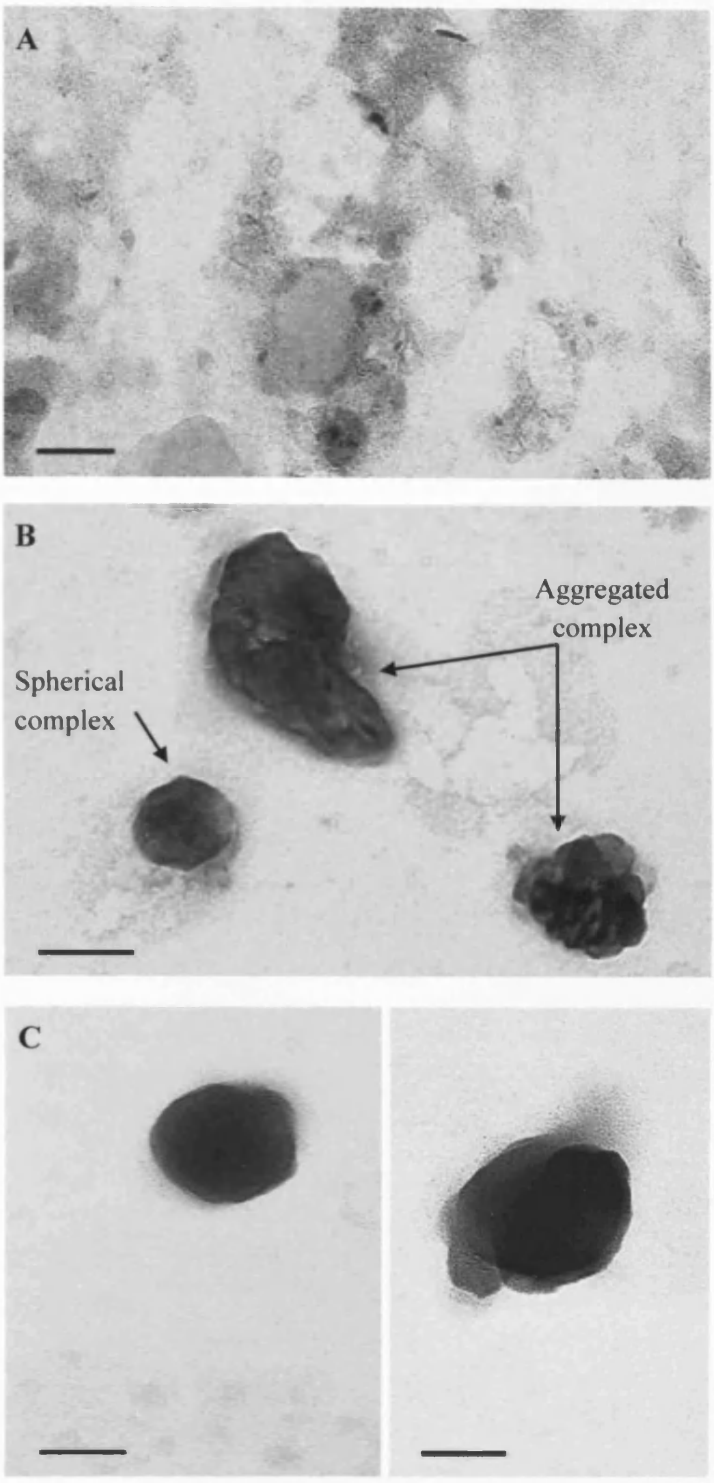


**Figure 5.2 Typical transmission electron microscopy of aerosolised DOTAP-pDNA formulations. A:** Liposomal DOTAP + pDNA particles, **B:** DOTAP + pDNA particles, **C:** DOTAP coated canister + pDNA particles. Scale bar = 100 nm.

### 5.3.2 Assessment of DOTAP-pDNA Deposition Following Aerosolisation from a pMDI

Prior to assessing aerosolised DOTAP-pDNA deposition, an initial study (n = 2) was carried out to assess the minimum quantity of aerosolised formulation required to ensure a detectable deposition result in an AVS. This study was carried out using the DOTAP coating canister-pDNA formulation as this formulation conferred the greatest cellular gene expression. Aerodynamic particle size distribution data (Figure 5.3) revealed that actuating 79 μg or 158 μg of pDNA led to relatively low levels of gene expression with maximum gene expression detected from particles deposited in the throat (1.54% and 1.80% respectively). Increasing the aerosolised pDNA quantity to 316 μg did confer a greater gene expression however even at this dose the maximum gene expression was 3.12%, detected from pDNA deposited in the throat.

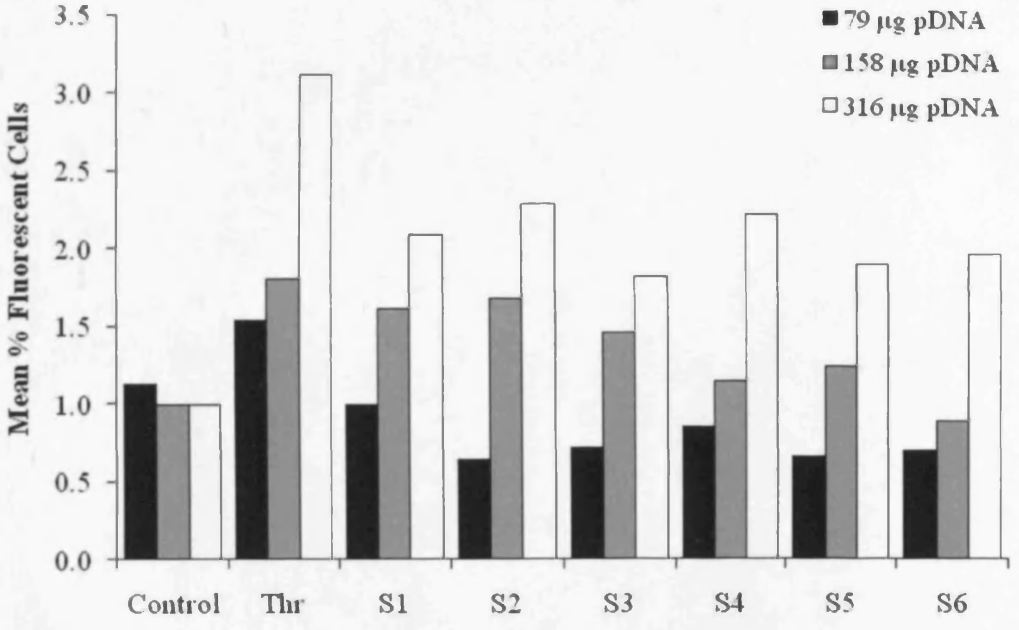


**Figure 5.3 Aerodynamic particle size distribution of transfection competent aerosolised DOTAP coating canister-pDNA formulation.** The equivalent of 79 μg, 158 μg and 316 μg pEGFP-N1 was expelled from the pMDI into an Andersen six stage viable sampler. A549 cells were surface-treated with **Control:** DMEM alone, or aerosolised DOTAP-pDNA formulation deposited on the: **Thr:** throat, **S1 to S6:** Stages 1 to 6 of the viable sampler (n = 2).

### 5.3.2.1 Validation of the Abbreviated Andersen Viable Sampler

In order to maximise the detection of any DOTAP-pDNA aerosolised sample deposition, the number of stages in the AVS was reduced to construct the AAVS. Initial deposition experiments, using a commercially available formulation Airomir®, were carried out to validate the AAVS by comparing the $FPF_{4.7\ \mu m}$ data generated from the ACI, AVS and AAVS (Figure 5.4).

Figure 4 reveals no significant difference ($p>0.05$) in FPF between the ACI non-viable sampler (61.3 ± 1.00%), AVS (55.3 ± 10.8%) and AAVS (53.6 ± 8.60%).

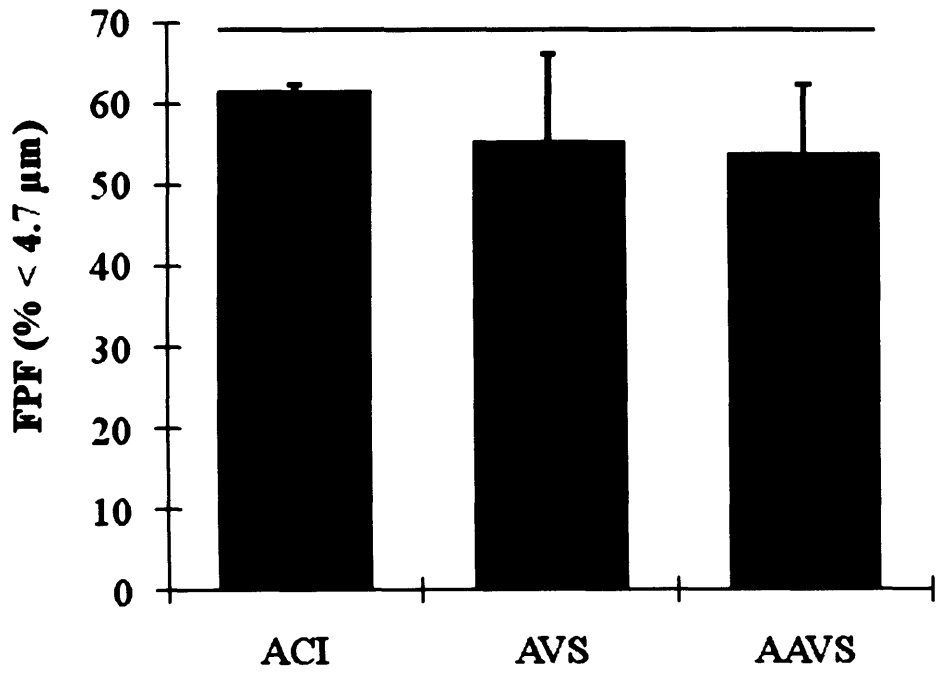


**Figure 5.4 A comparison of fine particle fraction ($FPF_{4.7\ \mu m}$, ex-actuator) measured from an ACI, AVS and AAVS using an Airomir® pMDI. ACI:** eight stage non-viable Andersen cascade impactor, **AVS:** six stage Andersen viable sampler, **AAVS:** three stage Andersen viable sampler. Data are presented as mean ± sd; n = 3. Bar represents no significant difference in $FPF_{4.7\ \mu m}$ ($p>0.05$).

Once validated, with regard to the $FPF_{4.7\ \mu m}$, the AAVS was used to assess aerosolised DOTAP-pDNA deposition using the DOTAP coating canister-pDNA formulation (Figure 5.5). DOTAP-pDNA actuated from a pMDI system

into the AAVS was assessed by quantifying gene expression of cells treated with the samples deposited on the various parts of the AAVS (Figure 5.5). No significant increase ($p>0.05$) in gene expression from samples deposited in the throat (5.65 ± 3.92%), inlet (4.57 ± 3.54%) or Stage 5 (5.60 ± 4.66%) was detected compared to the control (1.00 ± 0.23%) (Figure 5.5). Significantly enhanced cellular gene expression, however, did result from DOTAP-pDNA deposition on Stage 2 (9.17 ± 4.50%, $p<0.05$) and Stage 6 (8.54 ± 5.68%). The DOTAP-pDNA formulation had a $FPF_{4.7\ \mu m}$ (ex-actuator) of 44.6 ± 18.0% and an $EPF_{1.1\ \mu m}$ (ex-actuator) of 26.9 ± 9.37%.

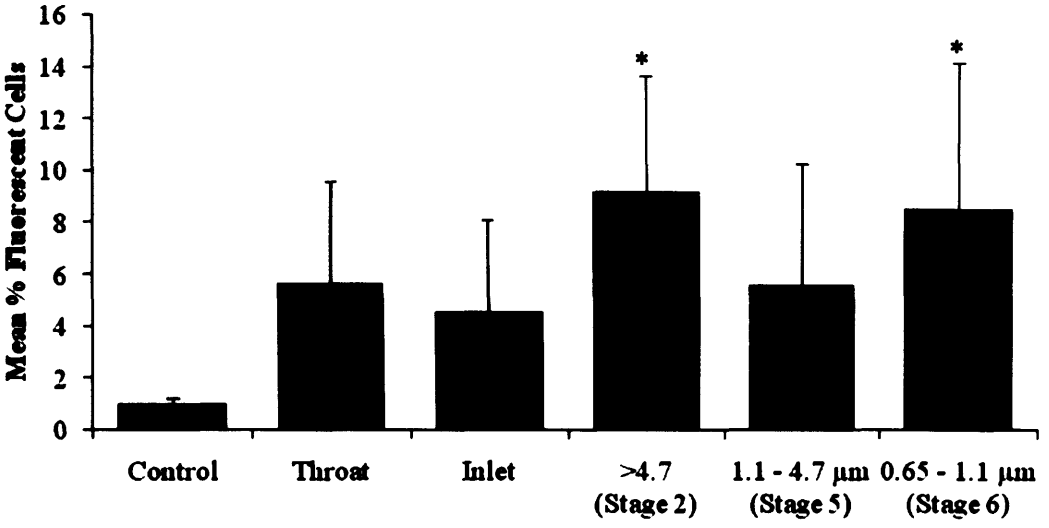


**Figure 5.5 Aerodynamic particle size of transfection competent aerosolised DOTAP coating canister–pDNA formulation deposited in a validated abbreviated Andersen viable sampler.** A549 cells were surface-treated with **Control:** DMEM alone, or aerosolised DOTAP-pDNA formulation deposited on the various stages of the sampler. Data are presented as mean ± sd; n = 3. *denotes a significant difference from the control ($p<0.05$).

### 5.3.3 Investigating the Stability of DOTAP-pDNA pMDI Formulation Following Accelerated Storage

Cellular gene expression conferred by aerosolised DOTAP-pDNA formulations was assessed following storage in order to investigate the formulation stability over time. Due to stability chamber breakdown, the freshly prepared DOTAP-pDNA formulations were stored in accelerated conditions for less than 24 hr prior to an eleven day break during which time

formulations were stored at room temperature (Figure 5.6). This time at ambient conditions is not accounted for in the analysis.

The reduction in gene expression after storing DOTAP-pDNA pMDI formulations under accelerated testing conditions is graphically presented in (Figure 5.6). The percentage of fluorescent cells, i.e. gene expression efficiency, was significantly reduced after treatment with aerosolised DOTAP-pDNA formulation stored under accelerated conditions for one week at 40°C/75RH (6.31 ± 2.87%, $p<0.05$) compared to that which was freshly prepared (9.15 ± 2.73%). A further significant reduction in the gene expression was observed from the formulation stored in accelerated conditions for two weeks at 40°C/75RH (4.96 ± 1.25%). At four weeks, however, gene expression (4.55 ± 0.64%). was statistically comparable ($p>0.05$) to the formulation tested at two weeks. Overall the data revealed that gene expression up to four weeks storage was significantly higher than compared to the control (0.94 ± 1.14%).

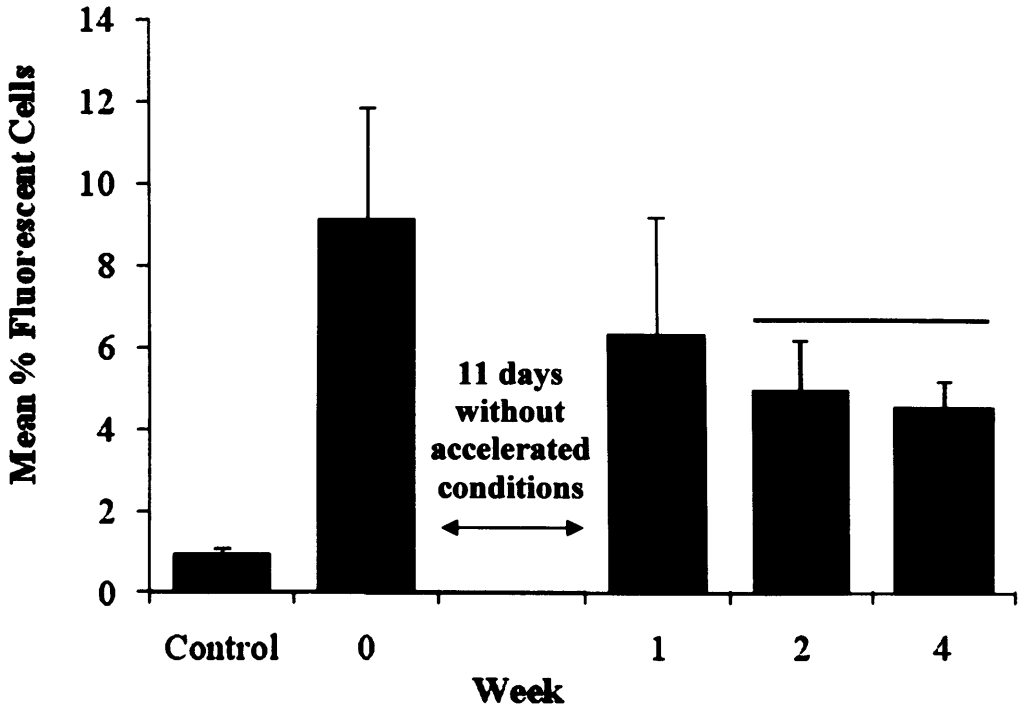


**Figure 5.6 Quantitative gene expression of aerosolised DOTAP coating canister–pDNA formulation stored under accelerated storage conditions.** A549 cells were surface-treated with **Control:** DMEM alone, or aerosolised DOTAP-pDNA formulation: **Week 0:** Freshly prepared pMDI formulation, **Week 1, 2 and 4:** pMDI formulations were stored in accelerated conditions for one, two and four weeks prior to actuation onto cells. Formulations were subjected to an interval of eleven days before which accelerated conditions were applied to the freshly prepared formulation due to stability chamber breakdown. Data are presented as mean ± sd; n = 3. The bar represents no significant difference ($p$>0.05).

Visual observation of DOTAP-pDNA formulations loaded into PET vials was used to determine gross visual changes in the properties of the dispersion (Figure 5.7). Freshly prepared formulations (Week 0) consisted of white particles suspended in the liquid propellant continuous phase. After 1, 2 and 4 weeks storage in accelerated conditions most of the formulation had sedimented to the bottom of the canister. Sedimented particles were readily re-dispersed upon one inversion of the vial. A stark difference between the re-dispersed formulations was observed when comparing the formulation at Week 0 to Week 4. The initial opaque dispersion observed at Week 0 gradually turned clearer throughout the duration of storage until it was relatively clear

with few suspended particles at Week 4. Visual observations of the particles suspended in the propellant at Week 4 appeared to be larger compared to the particles at Week 0 implying the possibility of aggregation.

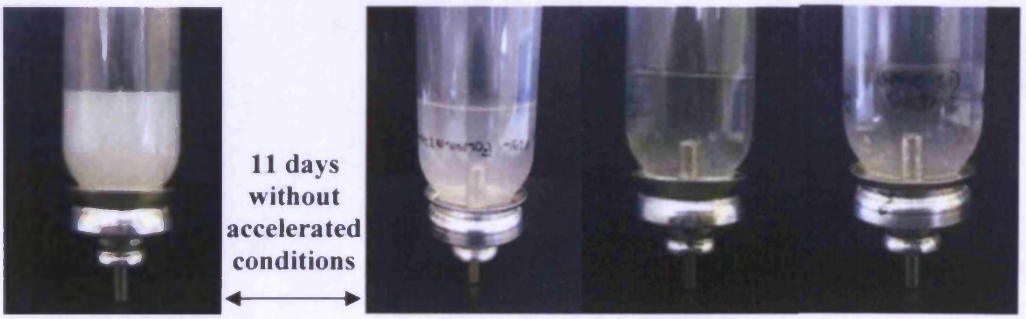


**Figure 5.7 Photograph of plastic PET pMDI vials containing DOTAP coating canister–pDNA formulation in HFA 134a propellant with absolute ethanol as a co-solvent. Images were taken Week 0:** Freshly prepared pMDI formulation, **Week 1, 2 and 4:** pMDI formulations were stored in accelerated conditions for one, two and four weeks. Photographs were taken of vials after one inversion of the vial. Formulations were subjected to an interval of eleven days at ambient conditions before exposure to accelerated conditions.

## 5.4 Discussion

### 5.4.1 Incorporation of DOTAP into a pDNA pMDI System

A549 cellular gene expression data revealed that pEGFP-N1 transfection could be successfully conferred using aerosolised DOTAP-pDNA particle pMDI formulations. However, the success of transfection was found to be reliant on the method used to incorporate DOTAP into the pDNA pMDI formulation. Incorporating a transfection agent such as DOTAP into a pDNA pMDI system is relatively novel and to date there is little published work in this field (Birchall 2007).

Brown and Chowdhury (1997) demonstrated gene expression in the respiratory epithelial cells of aerosol exposed mice using pDNA lyophilised in the presence of both non-ionic surfactant (Tween 40) and ionic transfection agent (lipofectin or lipofectamine) suspended in dimethylether propellant pMDI system. In the study carried out in this chapter however, aerosolisation of a DOTAP-pDNA formulation using pDNA lyophilised in the presence of DOTAP, incorporated at the microemulsion stage, resulted in no significant transfection. A possible reason for the lack of transfection could be due to the presence of lecithin surfactant used to stabilise the microemulsion. Lecithin is composed of anionic lipids and is able to compete with the pDNA on an electrostatic level to displace any DOTAP:pDNA complexes that may have formed prior to lyophilisation (Xu and Szoka 1996; Duncan *et al* 1997). DOTAP:pDNA complex displacement was not observed by Brown and Chowdhury (1997) as they used a non-ionic surfactant. Additionally, as DOTAP is freely soluble in solvents such as alcohol (Merck 2007), the solvent-wash procedure utilised in this thesis following lyophilisation may have also caused the removal of DOTAP. As *in vitro* cellular uptake of pDNA without the use of a transfection agent is relatively inefficient (Zabner *et al* 1997), the possible loss of DOTAP through solvent-washing may have led to the poor pDNA transfection observed.

Aerosolisation of formulations using preformed liposomal DOTAP added to

the pDNA particles also resulted in no significant cell transfection. The effect of water in pMDI systems is known to promote chemical instability, particle cohesion and particle adhesion onto canister walls (Vervaet and Byron 1999; James *et al* 2008). The presence of 7.6% v/v water in the pMDI system, from the DOTAP liposomes, may have had a detrimental effect on the formulation stability causing a loss in formulation activity, reduced aerosolisation efficiency and consequently poor gene expression.

Transfection competent DOTAP:pDNA multilamellar complexes have a typical characteristic 'fingerprint' like appearance (Tomlinson and Rolland 1996; Birchall *et al* 2000). TEM analysis, of the aerosolised liposome DOTAP formulation, revealed DOTAP:pDNA multilamellar complexes were not present.

The addition of DOTAP, by either coating the canister or using the lipid in powder form, to pMDIs containing pDNA particles did confer a significant increase in gene expression. As it is well known that pDNA complexed to the transfection agent is a prerequisite for successful *in vitro* and *in vivo* transfection (Gao and Huang 1995; Zabner *et al* 1997), the significant gene expression demonstrated by these formulations suggests the formation of functional lipoplexes. However, as there is no published work on this topic, the mechanism of complex formation in the non-aqueous pMDI environment is unclear.

The DOTAP coating canister formulation was prepared using a solvent evaporation method commonly used to form lipid films originally described by Bangham *et al* (1965). As DOTAP is soluble in alcohol (Merck 2007), agitation of this film in the presence of ethanol would have caused the DOTAP film to disperse into the solvent. In the presence of HFA 134a propellant, based on its chemistry, the DOTAP hydrophobic lipid anchor group may have orientated towards the propellant whilst the cationic head group electrostatically interacted with the pDNA to form a lipoplex with a reverse

micelle like structure (Brown 1996). Introducing the DOTAP in the form of a lipid powder may have also lead to the dispersion of the lipid and interaction with pDNA in the same way. Also, as it is well known that liposomes interact spontaneously with pDNA to form lipoplexes in aqueous conditions (Felgner *et al* 1987), lipoplexes may have formed post-aerosolisation of the DOTAP-pDNA formulation into an aqueous environment.

TEM of formulations utilising DOTAP lipid in powder form revealed a heterogeneous population of spherical complexes, similar to those seen with the DOTAP coating canister formulation, and aggregated complexes. This infers that DOTAP:pDNA complexation may not have been complete (Birchall *et al* 2000). The DOTAP coating canister formulation generally revealed a population of DOTAP:pDNA complexes, as neither free DOTAP nor pDNA was observed. It is possible therefore that the aerosolised pDNA may have been completely condensed which could be a possible reason for the observed superior cell transfection (Zabner *et al* 1995; Birchall *et al* 2000).

As a result of this transfection study, further investigations in this chapter to assess aerosolised particle size distribution and storage stability were carried out using the DOTAP coated canister formulation.

### 5.4.2 Assessment of DOTAP-pDNA Deposition Following Aerosolisation from a pMDI

Aerodynamic particle size distribution data generated from the three doses of aerosolised pDNA, 79 μg, 158 μg and 316 μg, into the AVS revealed the maximum percentage cell fluorescence was 3.12% detected from an estimated 316 μg dose. Dry powder inhalation (DPI) pDNA formulations containing transfection agents actuated into a MSLI, at a dose of 133 μg, revealed A549 cell fluorescence percentages at various stages ranging from approximately 2% to 22% (Li *et al* 2005a). The relatively low percentage cell fluorescence detected, from the stages of the AVS, in this chapter using more than double the pDNA dose to that used in the DPI studies could be due to the variations

between the formulations, as a transfection agent may be more stable as a dry powder than in the propellant environment of a pMDI. The aerosolisation of pDNA using 130 successive actuations, in this study, may also have affected the viability of the temperature sensitive DNA due to the cold freon effect which would cause the formulation to rapidly cool, however as evidence of a dose response was observed this effect may have been minimal.

In an attempt to generate significant deposition data with a more pronounced percentage gene expression, DOTAP-pDNA formulations were actuated into a viable sampler (AVS) after reducing the number of stages and validating the system as an abbreviated viable sampler (AAVS). During validation with regards to the FPF, the AAVS generated an FPF that was not significantly different from the AVS and the Andersen cascade impactor (ACI). This was to be expected as although the number of stages in the AAVS were reduced, the cut-off stage (Stage 2) which defined the $FPF_{4.7\ \mu m}$ parameter remained in place. Although the data generated from the AAVS is limited as it would not provide a particle size distribution profile, it would however characterise particles in terms of the respirable and non-respirable fractions.

Particle deposition in the AAVS revealed significant gene expression from particles deposited in Stage 2 (particle diameter cut-off 4.7 μm) as well as Stage 6 (cut-off 0.65 μm) compared to control. No significant difference between these two stages was detected. It is generally acknowledged that particles require an aerodynamic diameter of $\leq$ 5 μm to allow efficient penetration and deposition in the peripheral pulmonary regions (Hickey 1993). The data generated from the AVS therefore predicted that aerosolised DOTAP-pDNA formulation may significantly deposit in the lower respiratory tract as well as the upper respiratory tract.

The $FPF_{4.7\ \mu m}$ (ex-actuator) is a ratio often used as a guide to understanding the portion of the aerosolised drug that is likely to reach the lung (the respirable portion). Example FPF data from commercially available inhalers intended for

localised pulmonary delivery include Proventil® HFA $FPF_{4.7\ \mu m}$ is approximately 45% (Harris *et al* 2006) and Airomir® $FPF_{5.8\ \mu m}$ approximately 64% (Dubus *et al* 2001). Aerosolised DOTAP-pDNA had a $FPF_{4.7\ \mu m}$ 44.6 ± 18.0%. Although the DOTAP-pDNA formulation has yet to be optimised, comparisons between the FPF data demonstrate the potential of this formulation for localised pulmonary delivery. It is important to remember that the FPF data generated from this study was a measure of cellular gene expression conferred by the pDNA formulation deposited on the various stages of the AAVS. The FPF generated may therefore have been an underestimate of the actual deposited pDNA. This is because, given the sensitive nature of conferring gene expression, not all the pDNA deposited in the AVS would have gone on to successfully transfect the cells and express GFP.

Published reports in the aerosolised gene therapy field reveal $FPF_{6.8\ \mu m}$ data for DPI formulations, containing freeze-dried or spray-dried lipid:protamine:pDNA (LPD) complexes in the presence of cryoprotectants, in the range of approximately 7% to 16% (Li *et al* 2003, 2005a). The $FPF_{6.8\ \mu m}$ was only increased to between approximately 38% to 58% when dispersibility enhancers and cellular uptake enhancers were incorporated into the formulations (Li *et al* 2003; Li and Birchall 2006). The FPF data generated from the unoptimised DOTAP-pDNA pMDI formulation in this chapter ($FPF_{4.7\ \mu m}$ 44.6 ± 18.0%),compared to DPI LPD formulations, reveals the utility of a pMDI system for the pulmonary delivery of transfection competent DOTAP-pDNA. A possible avenue of further work to optimise the formulation and confer greater gene expression values includes exploring the utility of newer transfection agents. Nevertheless, stability data is critical in order to assess the feasibility for use of the DOTAP-pDNA pMDI formulation over extended periods of time.

### 5.4.3 Investigating the Stability of DOTAP-pDNA pMDI Formulation Following Accelerated Storage

Stability data generated from aerosolised DOTAP-pDNA formulation stored

under accelerated conditions revealed that gene expression was reduced over time. However significant gene expression, although reduced, was maintained for up to four weeks. As accelerated storage conditions expose the formulation to harsh conditions which can accelerate degradation (ICH Expert Working Group 2003), maintenance of a transfection competent formulation for up to four weeks provides an insight into the potential use of this formulation after storage in less extreme conditions. Nevertheless gene expression was reduced and as there is a lack of published data reporting the long-term stability of pDNA formulations in pMDI systems, the mechanism for the loss in transfection is poorly understood. Generally, as macromolecules are hydrophilic they have a low solubility in non-polar HFA propellants causing them to aggregate and denature (Byron 1990). More recently however, macromolecules have been demonstrated to have maintained stability and biological activity after storage for up to six months at room temperature with the use of formulation excipients such as polysaccharides and the polymeric surfactant polyvinyl alcohol (Liao *et al* 2005; Jones *et al* 2006; Li and Seville 2009). Such formulation excipients have been used to coat protein using drying methods and shown to prevent denaturation by protection from the external propellant conditions and reducing particle aggregation (Liao *et al* 2005).

Visual observations (Figure 5.7) of freshly prepared DOTAP-pDNA pMDI formulations revealed a physically stable readily dispersible flocculated system. The presence of surfactant excipient coating the pDNA particles may have prevented any irreversible sedimenting due to sterically conferred repulsive forces between the surfactant tails which extend into the propellant (Vervaet and Byron 1999). However, although the freshly prepared formulation appeared to be physically stable, as it did not rapidly sediment, the observed increase in aggregated particles over time (Figure 5.7) could be a possible reason for the loss in gene expression (Figure 5.6). The phenomenon of aggregation and resulting loss in gene expression could have occurred due to the inherent instability of lipid-pDNA complexes (Felgner *et al* 1995) or the ingress of water during storage in accelerated conditions.

The aggregation of lipoplex formulations in aqueous environments is a known phenomenon which has been shown to be exacerbated at heightened temperatures causing a reduction in the pDNA transfection activity over time (de Lima *et al* 2003). Additionally unextruded liposomes have been reported to form heterogeneous lipoplexes which have exhibited a greater tendency to aggregate leading to poor transfection compared to extruded homogenous liposomes (Zelphati *et al* 1998). As any liposomes formed from the DOTAP coated canister formulation would be of the unextruded form, these reports shed some light on possible reasons for the reduction in cellular gene expression observed after exposure to accelerated storage conditions. However as previous reports have only been carried out in an aqueous environment, it may not be appropriate to extrapolate this data to non-aqueous environments found in pMDI systems.

Stability of pMDI formulations is reliant upon the strict control over impurities such as water (Vervaet and Byron 1999). Possible sources of water in the DOTAP coating canister-pDNA formulation include; water residues left behind after chloroform rotary evaporation during formulation preparation, or moisture ingress through seals and valve components during stability testing using accelerated storage conditions (Reynolds and McNamara 1996; Williams III and Hu 2000). The presence of trace amounts of water in a pMDI system has been shown to influence the stability of drug formulations causing aggregation of the formulation components (Williams III *et al* 1997; Blondino and Byron 1998). The interfacial tension between the relatively non-polar HFA 134a propellant and water can cause the water to accumulate and adsorb onto the surface of drug particles and canister components rather than mix with the propellant (Peguin *et al* 2006; James *et al* 2008). These adsorbed water layers interact with each other by hydrogen bonding and have been shown, using atomic force microscopy, to cause adhesion between the drug particles and interior of the pMDI components (James *et al* 2008).

The presence of water in a pMDI system can influence formulation stability

over time by increasing interparticulate attraction causing particle aggregation (Williams III and Hu 2000) and drug adhesion onto the walls of the canister (Vervaet and Byron 1999; James *et al* 2008). These interactions could result in the loss of DOTAP-pDNA biological activity and inefficient device performance, both of which are possible reasons to explain the observed reduction in gene expression.

Although this stability study did give an indication as to the biological activity of DOTAP-pDNA formulations in a pMDI system, using accelerated storage conditions over a period of four weeks, this study was limited for a number of reasons. Due to breakdown of the stability chamber, the freshly prepared DOTAP-pDNA formulations were stored under accelerated conditions for less than 24 hr prior to an eleven day break during which time formulations were stored at room temperature. As fluctuations in the storage temperature are known to intensify degradation (Kommanaboyina and Rhodes 1999), the enforced eleven day break from accelerated storage conditions may have caused a further reduction in the formulation biological activity. However, these fluctuations in temperature would have had minimal additional degradative effect on the formulation, as exacerbated degradation is normally only observed if the product is subjected to repetitive temperature cycling (Carstensen and Rhodes 1993). Additionally, moisture uptake into the pMDI, which is known to affect formulation stability, is temperature and humidity dependent (Williams III and Hu 2000). As any degradation of the formulation is hastened due to increased temperature and humidity conditions used during accelerated storage, it is likely that any loss of formulation biological activity would have been relatively minimal during the eleven days the formulation was kept at room temperature (Kommanaboyina and Rhodes 1999; ICH Expert Working Group 2003).

Accelerated storage conditions are typically carried out for a minimum of six months, in order to generate any clear conclusions as to the stability of the formulation (ICH Expert Working Group 2003). This time period and

conditions used are used to reflect a sufficient time to cover duration for storage, shipment and use in the pharmaceutical industry. The stability study carried out in this chapter provides limited information as it was carried out only over a four week period. However, as a preliminary study, relevant information was generated regarding whether transfection competency of a formulation stored in a propellant environment could be maintained for subsequent weeks after being freshly prepared.

Although reductions in the biological activity of the formulation was assessed over time during the stability study, assessing other important factors such as changes in the aerodynamic particle size distribution and emitted dose would have been of benefit. As formulation stability can be reduced through adhesion and cohesion, the utility of *in vitro* cascade impaction tests and emitted dose studies would have been invaluable in confirming and evaluating the presence of aggregation, a possible avenue for further work.

## 5.5 Conclusion

This chapter aimed to investigate the potential for incorporating DOTAP into a pDNA pMDI formulation and delivering the formulation to cells via a pMDI using a standard valve and actuator.

Gene expression studies demonstrated that a transfection agent can be incorporated into the pDNA pMDI formulation, successfully actuated to confer gene expression and remain functional for up to four weeks in accelerated storage conditions. The incorporation of a transfection agent into a pDNA HFA pMDI system to successfully confer gene expression is novel and to date there is no published work in this field. Although further optimisation is required to maximise transfection efficiency, the work carried out in this chapter demonstrated an important concept that a transfection agent can be incorporated into a pDNA pMDI system to form a single dosing unit with gene expression capability.

# CHAPTER SIX

# General Discussion

## 6.1 Discussion

The incorporation of pDNA into a pMDI system for pulmonary administration is a relatively unexplored area of research due to the inherent challenges of formulating and maintaining pDNA stability. The aim of this thesis was to research the potential of developing a low-energy process (Dickinson *et al* 2001), previously used for small molecules, to formulate surfactant-coated pDNA particles suitable for incorporation into a pMDI system. Subsequently, this thesis aimed to investigate whether it is viable to aerosolise these particles and determine their deposition characteristics.

Development work began with the optimisation of the microemulsion stage of the process. An optimised microemulsion with a surfactant to water ratio of 2.0 was found to yield a stable isotropic system whilst maximising the volume of the aqueous phase and maintaining the minimum surfactant concentration possible. The incorporation of a model drug, salbutamol sulphate (SS), into the aqueous phase led to the formation of a stable drug-loaded microemulsion which, upon lyophilisation, resulted in the production of surfactant-coated SS particles.

The presence of excess surfactant after the lyophilisation stage of the process could potentially cause particle aggregation, hinder surface morphology characterisation and potentially adversely affect particulate dispersibility and stability in a pMDI (Blondino and Byron 1998). For this reason a washing technique was developed which served to successfully remove some of the excess surfactant from the SS particles with a 10-fold reduction in surfactant content. The utility of this additional procedure was shown when handling surfactant-coated pDNA particles. The wash procedure was successful in removing some of the excess surfactant from the pDNA particles whilst maintaining a relatively small reduction in the pDNA integrity.

In both cases, even though some of the excess surfactant was removed, particles remained aggregated post-washing. This aggregation was of concern,

as the aerosolisation of such aggregates could adversely affect pulmonary deposition (Berry *et al* 2004; Traini *et al* 2007). However, particle sizing prior to incorporation into a pMDI system revealed that in either case, using SS or pDNA, the solvent-washed aggregated particles were in the respirable size range. Additionally, aerodynamic particle size data for aerosolised solvent-washed SS particles confirmed that the developed technology had generated smaller SS particles than commercially available formulations with significant improvements in the MMAD, FPF and EPF. Aerosolised particle characterisation highlights the potential for the use of this novel low-energy microemulsion process technology in delivering macromolecules to the lower respiratory tract. Although the technology explored was originally reported to generate particles of the nanoparticle size range (Dickinson *et al* 2001), such particles were not detected in this thesis. A possible reason for this may due to the observed aggregation caused by the presence of a sticky surfactant. Nevertheless the particles were observed to be of smaller dimensions than those that can be prepared using other procedures; previous reports of lyophilised powders have often shown particles with diameters unsuitable for pulmonary delivery and generally require further processing using a milling step prior to incorporation into an inhaler (Seville *et al* 2002; Shoyele and Cawthorne 2006).

The next series of experiments presented in this thesis related to investigating the utility of the developed technology for the preparation of pDNA particles. As the native structure of the macromolecule is susceptible to damage during processing conditions (Carpenter and Crowe 1988a; Anchordoquy *et al* 1997), applying the developed technology to pDNA invariably brought about new formulation challenges previously not faced when dealing with the small molecular weight model drug SS.

Investigations revealed that the developed technology, which utilised the low energy microemulsion lyophilisation process in the presence of a sugar lyoprotectant, was capable of preparing surfactant-coated pDNA particles.

Analysis of the integrity of the processed pDNA revealed that there was, however, a reduction in the pDNA supercoiled fraction. Although linear DNA forms have been found to be transfection competent (Chancham and Hughes 2001; von Groll *et al* 2006), most published literature supports the opinion that pDNA supercoiled structure should be retained to optimise cellular transfection efficiency (Cherng *et al* 1999; Remaut *et al* 2006) and to comply with regulatory requirements on product quality (Arulmuthu *et al* 2007). The observed reduction in the supercoiled fraction may therefore have adverse implications on the pDNA gene expression efficiency. This data highlights a possible limitation of the developed technology and the need for further optimisation of the process in order to maintain pDNA integrity and maximise cellular transfection efficiency.

That said, the observed reduction in the supercoiled fraction is considered to be relatively small as it was found to be similar to previously published reports observed for spray-dried lipid:protamine:pDNA (LPD) dry powders for inhalation prepared in the presence of a lyoprotectant (Seville *et al* 2002; Li *et al* 2005a). Furthermore, despite observing a reduction in the supercoiled fraction, initial transfection results showed no significant difference in expression of reporter gene in cells treated with unprocessed pDNA and pDNA following processing. This data demonstrates the ability of this developed process to generate biologically active pDNA particles.

Experiments involving quantifying pDNA gene expression confirmed the importance of the wash procedure developed for the removal of excess surfactant. Although the integrity of the unwashed surfactant-coated pDNA particles remain intact post-lyophilisation, this formulation was unable to confer significant cellular gene expression. This lack of significant gene expression may have been due to the adverse effect of excess surfactant on pDNA functionality which has been discussed in previous studies (Xu and Szoka 1996; Duncan *et al* 1997; Tsan *et al* 1997). Gene expression however, was observed in cells which were treated with the solvent-washed variant of

the lyophilised pDNA formulation.

The biological activity of the solvent-washed pDNA after incorporation and aerosolisation from a pMDI was also investigated. Prior to *in vitro* analysis of gene expression, the maintenance of pDNA integrity post-aerosolisation was confirmed. Cellular gene expression studies revealed that the solvent-washed pDNA particles conferred a significant rise in the percentage of fluorescent cells in the presence of DOTAP. This suggests that solvent-washed pDNA particulates remained functionally active following formulation processing, dispersion in propellant and aerosolisation from a pMDI. These data demonstrate proof-of-concept that the developed technology can successfully formulate pDNA suitable for a pMDI system with potential for pulmonary gene delivery. This is of importance as the incorporation of pDNA into a pMDI for pulmonary administration is a sparsely explored area of research. The anticipated challenges include ensuring the stability and preventing aggregation of the pDNA particles in the pMDI propellant environment through effective formulation. As conventional delivery devices such as nebulisers can be inefficient, the investigations carried out in this thesis reveal pMDIs to offer a potential alternative. However, due to the differences between the *in vitro* and *in vivo* environments, including the difference in cellular proliferation rate which has been reported to effect gene transfer efficiency (Wilke *et al* 1996; Brunner *et al* 2000; Remaut *et al* 2006), understanding the barriers encountered *in vivo* is required to progress this work towards clinical therapy.

Regarding the topic of clinical therapy, the studies in this thesis demonstrated that 316 μg of pDNA can be aerosolised from a pMDI system to successfully confer gene expression. As pre-clinical and clinical research studies in pulmonary gene therapy have required larger doses of pDNA (often mg quantities) (Alton *et al* 1999; Ruiz *et al* 2001), 316 μg may not be a sufficient dose to confer a therapeutic effect. However, these clinical trials used nebulisers to deliver the pDNA where a larger dose of pDNA is often required as nebulisers can cause instability to the nucleic acid cargo, resulting in a 40 to

75% reduction in supercoiled pDNA post-nebulisation compared to a non-nebulised control (Kleemann *et al* 2004; Lentz *et al* 2005; Arulmuthu *et al* 2007). Also as this pMDI technology is not yet optimised, increasing the deliverable dose further is highly probable. Additionally as gene therapy vectors continue to improve, the dose of deliverable pDNA is likely to reduce.

The work carried out in this thesis substantiates previous research that transfection of naked DNA *in vitro* is relatively inefficient and that a transfection agent must be employed to promote the cellular uptake of the nucleic acid (Zabner *et al* 1997; Davies *et al* 2008). Due to this, the feasibility of incorporating the transfection agent DOTAP into the pDNA pMDI system to form a pre-complexed single dosing unit was therefore investigated. A number of approaches were used in this thesis to incorporate DOTAP into the pDNA pMDI formulation. Investigations demonstrated that coating the pMDI canister with DOTAP prior to the incorporation of the solvent-washed pDNA resulted in a significant level of gene expression. However, the level of gene expression was less than half of that conferred from previous experiments which aerosolised the pDNA formulation onto cells treated with DOTAP i.e. DOTAP was pipetted onto cells. The lower expression level generated from cells treated with the aerosolised DOTAP-pDNA formulation may have been due to inefficient DOTAP-pDNA complexing in the non-aqueous propellant environment. Nevertheless the incorporation of any transfection agent into a pDNA pMDI system is relatively novel and to date there is little published work in this field. Although further optimisation is required to maximise transfection efficiency, through the use of perhaps different transfection agents, the work carried out in this thesis demonstrated an important concept that a transfection agent can be incorporated into a pDNA pMDI system to form a single dosing unit with gene expression capability. Particle sizing of the aerosolised formulation demonstrated that a significant proportion of the formulation had the potential for gene expression in the lower respiratory tract.

Stability experiments involving the DOTAP-pDNA formulation revealed that

although there was a reduction in the gene expression, the formulation remained functional for up to four weeks in accelerated storage conditions. This study was limited in the sense that accelerated storage conditions are typically carried out for a minimum of six months in order to generate any clear conclusions as to the stability of the formulation (ICH Expert Working Group 2003). However, as a preliminary study, this experiment revealed that the transfection and biological activity of the DOTAP-pDNA formulation stored in a propellant environment could be retained for subsequent weeks after being freshly prepared.

The various experiments conducted during the course of this thesis demonstrate the feasibility of preparing a DOTAP-pDNA formulation suitable for incorporation into a generic HFA134a pMDI system and aerosolised using a standard valve and actuator with potential for pulmonary gene delivery. These studies however highlight the need for process optimisation in order for the developed technology to be realised in a clinical setting.

## 6.2 Further Work

In view of the findings described above, further research is suggested which may optimise the technology and lead to a greater understanding of the potential of this technology in delivering aerosolised pDNA capable of eliciting a therapeutic response.

**Optimise the formulation:** The developed technology has demonstrated its utility in preparing pDNA particles suitable for delivery by a pMDI system to confer significant gene expression. However, further development of the process may result in maximising gene expression levels through a number of ways. pDNA degradation during freeze-drying conditions has been shown to be related to lyoprotectant concentration (Anchordoquy *et al* 1997; Cherng *et al* 1997). It may therefore be viable to investigate optimal lyoprotectant concentrations to effectively maintain pDNA integrity. The use of a transfection agent has been shown to promote efficient cellular uptake of the nucleic acid (Zabner *et al* 1997). As newer transfection agents are being developed, it may be appropriate to explore the use of these alternative transfection agents (Choi *et al* 2004; Jiang *et al* 2008; Prata *et al* 2008) and 'helper' lipids (Felgner *et al* 1994; Bennett *et al* 1995) which have the potential for enhancing pDNA transfection and subsequently gene expression whilst minimising cellular toxicity. Investigating the maximum capacity of processed pDNA that can be incorporated into a pMDI system would also be worthy of further work in order to ascertain the feasibility of delivering a manageable therapeutic dose using the pMDI in a clinical setting.

**Assess formulation stability:** Although a four week stability test was carried out, increasing the test period to the generally accepted six months in accelerated conditions would give a better understanding of the formulation stability (ICH Expert Working Group 2003). Additionally formulation instability can manifest itself in a number of ways other than a reduction in the pDNA biological activity which was the criteria tested in this thesis. One such form of instability includes particle aggregation in the pMDI system. A

possible avenue of further work could therefore entail assessing the pMDI formulation for susceptibility to aggregation, by examining any changes in the aerodynamic particle size distribution and emitted dose, through the use of *in vitro* cascade impaction tests.

**Alternative vectors:** Plasmid constructs used in pre-clinical and clinical research studies are larger than the 4.7 kb pEGFP-N1 plasmid used in this thesis (Hyde *et al* 2000; Ruiz *et al* 2001). Although to date there are no published reports on the size dependent effects of plasmid aerosolisation via a pMDI, size dependent degradation of pDNA exposed to shear forces has been previously demonstrated in nebulisers (Arulmuthu *et al* 2007). Investigations are required to understand whether the developed technology can be used to prepare larger plasmids with the potential for incorporation and aerosolisation from a pMDI system.

***In vivo* studies:** The *in vitro* experimental work described in this thesis has demonstrated proof-of-concept that the developed technology can formulate pDNA suitable for a pMDI system with potential for pulmonary gene delivery. However, there is a need to move these studies into animal models as a clear understanding of the barriers encountered *in vivo* is required to progress this work towards clinical therapy. An example of an appropriate model to use for further work would be the mouse (Grosse *et al* 2008). The *in vivo* study could entail aerosolising the DOTAP-pDNA pMDI formulation into a chamber containing the mouse, causing the mouse to inhale the pDNA therapy.

## References

Aboofazeli, R. and Lawrence, M. J. 1993. Investigations into the formation and characterization of phospholipid microemulsions. I. Pseudo-ternary phase diagrams of systems containing water-lecithin-alcohol-isopropyl myristate. *International Journal of Pharmaceutics* 93(1-3), pp. 161-175.

Agu, R. U., Ugwoke, M. I., Armand, M., Kinget, R. and Verbeke, N. 2001. The lung as a route for systemic delivery of therapeutic proteins and peptides. *Respiratory Research* 2(4), pp. 198-209.

Alexander, D. J. and Libretto, S. E. 1995. An overview of the toxicology of HFA-134a (1,1,1,2-tetrafluoroethane). *Human & Experimental Toxicology* 14(9), pp. 715-720.

Allison, S. D. and Anchordoquy, T. J. 2000. Mechanisms of protection of cationic lipid-DNA complexes during lyophilization. *Journal of Pharmaceutical Sciences* 89(5), pp. 682-691.

Allison, S. D., Chang, B., Randolph, T. W. and Carpenter, J. F. 1999. Hydrogen bonding between sugar and protein is responsible for inhibition of dehydration-induced protein unfolding. *Archives of Biochemistry and Biophysics* 365(2), pp. 289-298.

Alton, E., Middleton, P. G., Caplen, N. J., Smith, S. N., Steel, D. M., Munkonge, F. M., Jeffery, P. K., Geddes, D. M., Hart, S. L., Williamson, R., Fasold, K. I., Miller, A. D., Dickinson, P., Stevenson, B. J., McLachlan, G., Dorin, J. R. and Porteous, D. J. 1993. Non-invasive liposome-mediated gene delivery can correct the ion transport defect in cystic fibrosis mutant mice. *Nature Genetics* 5(2), pp. 135-142.

Alton, E., Stern, M., Farley, R., Jaffe, A., Chadwick, S. L., Phillips, J., Davies, J., Smith, S. N., Browning, J., Davies, M. G., Hodson, M. E., Durham, S. R., Li, D., Jeffery, P. K., Scallan, M., Balfour, R., Eastman, S. J., Cheng, S. H., Smith, A. E., Meeker, D. and Geddes, D. M. 1999. Cationic lipid-mediated CFTR gene transfer to the lungs and nose of patients with cystic fibrosis: A double-blind placebo-controlled trial. *The Lancet* 353(9157), pp. 947-954.

Amorij, J. P., Huckriede, A., Wischut, J., Frifflink, H. W. and Hinrichs, W. L. J. 2008. Development of stable influenza vaccine powder formulations: Challenges and possibilities. *Pharmaceutical Research* 25(6), pp. 1256-1273.

Anchordoquy, T. J., Carpenter, J. F. and Kroll, D. J. 1997. Maintenance of transfection rates and physical characterization of lipid/DNA complexes after freeze-drying and rehydration. *Archives of Biochemistry and Biophysics* 348(1), pp. 199-206.

Anchordoquy, T. J., Girouard, L. G., Carpenter, J. F. and Kroll, D. J. 1998. Stability of lipid/DNA complexes during agitation and freeze-thawing. *Journal of Pharmaceutical Sciences* 87(9), pp. 1046-1051.

Andersen 1985. *1 ACFM non-viable sampler operating manual.* Smyrna, Georgia: Thermo Andersen Inc.

Andersen, A. A. 1958. New sampler for the collection, sizing, and enumeration of viable airborne particles. *Journal of Bacteriology* 76(5), pp. 471-484.

Andersen, A. A. 1966. A sampler for respiratory health hazard assessment. *American Industrial Hygiene Association journal* 27(2), pp. 160-165.

Ando, S., Putnam, D., Pack, D. W. and Langer, R. 1999. PLGA microspheres containing plasmid DNA: Preservation of supercoiled DNA via cryopreparation and carbohydrate stabilization. *Journal of Pharmaceutical Sciences* 88(1), pp. 126-130.

Arulmuthu, E. R., Williams, D. J., Baldascini, H., Versteeg, H. K. and Hoare, M. 2007. Studies on aerosol delivery of plasmid DNA using a mesh nebulizer. *Biotechnology and Bioengineering* 98(5), pp. 939-955.

Attwood, D. 2008. Disperse systems. In: Aulton, M.E. ed. *Pharmaceutics the science of dosage form design.* Edinburgh: Churchill Livingstone, pp. 70-98.

Attwood, D., Mallon, C. and Taylor, C. J. 1992. Phase studies on oil-in-water phospholipid microemulsions. *International Journal of Pharmaceutics* 84(2), pp. R5-R8.

Bancroft, W. D. 1912. The theory of emulsification. I. *Journal of Physical Chemistry* 16(3), pp. 177-233.

Bangham, A. D. and Horne, R. W. 1964. Negative staining of phospholipids and their structural modification by surface-active agents as observed in the electron microscope. *Journal of Molecular Biology* 8(5), pp. 660-668.

Bangham, A. D., Standish, M. M. and Watkins, J. C. 1965. Diffusion of univalent ions across the lamellae of swollen phospholipids. *Journal of Molecular Biology* 13(1), pp. 238-252,.

Barker, S. A., Taylor, K. M. G. and Short, M. D. 1994. The deposition and clearance of liposome entrapped 99mTc-DTPA in the human respiratory tract. *International Journal of Pharmaceutics* 102(1-3), pp. 159-165.

Bennett, M. J., Nantz, M. H., Balasubramaniam, R. P., Gruenert, D. C. and Malone, R. W. 1995. Cholesterol enhances cationic liposome-mediated DNA transfection of human respiratory epithelial cells. *Bioscience Reports* 15(1), pp. 47-53.

Berry, J., Kline, L. C., Sherwood, J. K., Chaudhry, S., Obenauer-Kutner, L., Hart, J. L. and Sequeira, J. 2004. Influence of the size of micronized active pharmaceutical ingredient on the aerodynamic particle size and stability of a metered dose inhaler. *Drug Development and Industrial Pharmacy* 30(7), pp. 705-714.

Bevers, E. M., Smeets, E. F., Comfurius, P. and Zwaal, R. F. A. 1994. Physiology of membrane lipid asymmetry. *Lupus* 3(4), pp. 235-240.

Birchall, J. 2007. Pulmonary delivery of nucleic acids. *Expert Opinion on Drug Delivery* 4(6), pp. 575-578.

Birchall, J. C., Kellaway, I. W. and Gumbleton, M. 2000. Physical stability and in-vitro gene expression efficiency of nebulised lipid-peptide-DNA complexes. *International Journal of Pharmaceutics* 197(1-2), pp. 221-231.

Birchall, J. C., Kellaway, I. W. and Mills, S. N. 1999. Physico-chemical characterisation and transfection efficiency of lipid-based gene delivery complexes. *International Journal of Pharmaceutics* 183(2), pp. 195-207.

Bitterle, E., Keller, M., Tservistas, M., Lang, G., Meyers, R., Elbashir, S., DeVincenzo, J., Radesca, L. and Cehelsky, J. 2006. *Integrity, in-vitro activity and aerosol delivery performance of RSV specific siRNA (ALN-RSV01) inhalation solutions nebulised by an eFlow® electronic nebuliser.* Available at: <URL: http://www.paripharma.com/studies2a.htm> [Accessed: 20/1/2010].

Bivas-Benita, M., Ottenhoff, T. H. M., Junginger, H. E. and Borchard, G. 2005. Pulmonary DNA vaccination: Concepts, possibilities and perspectives. *Journal of Controlled Release* 107(1), pp. 1-29.

Bivas-Benita, M., van Meijgaarden, K. E., Franken, K. L. M. C., Junginger, H. E., Borchard, G., Ottenhoff, T. H. M. and Geluk, A. 2004. Pulmonary delivery of chitosan-DNA nanoparticles enhances the immunogenicity of a DNA vaccine encoding HLA-A*0201-restricted T-cell epitopes of Mycobacterium tuberculosis. *Vaccine* 22(13-14), pp. 1609-1615.

Blake, R. D. and Delcourt, S. G. 1998. Thermal stability of DNA. *Nucleic Acids Research* 26(14), pp. 3323-3332.

Blondino, F. E. and Byron, P. R. 1998. Surfactant dissolution and water solubilization in chlorine-free liquified gas propellants. *Drug Development and Industrial Pharmacy* 24(10), pp. 935-945.

Bloomfield, V. A. 1996. DNA condensation. *Current Opinion in Structural Biology* 6(3), pp. 334-341.

Bosquillon, C., Préat, V. and Vanbever, R. 2004. Pulmonary delivery of growth hormone using dry powders and visualization of its local fate in rats. *Journal of Controlled Release* 96(2), pp. 233-244.

Boyd, J., Parkinson, C. and Sherman, P. 1972. Factors affecting emulsion stability, and the HLB concept. *Journal of Colloid and Interface Science* 41(2), pp. 359-370.

Brantly, M. L., Spencer, L. T., Humphries, M., Conlon, T. J., Spencer, C. T., Poirier, A., Garlington, W., Baker, D., Song, S. H., Berns, K. I., Muzyczka, N., Snyder, R. O., Byrne, B. J. and Flotte, T. R. 2006. Phase I trial of intramuscular injection of a recombinant adeno-associated virus serotype 2 alpha(1)-antitrypsin (AAT) vector in AAT-deficient adults. *Human Gene Therapy* 17(12), pp. 1177-1186.

Brigham, K. L., Lane, K. B., Meyrick, B., Stecenko, A. A., Strack, S., Cannon, D. R., Caudill, M. and Canonico, A. E. 2000. Transfection of nasal mucosa with a normal alpha(1)-antitrypsin gene in alpha(1)-antitrypsin-deficient subjects: Comparison with protein therapy. *Human Gene Therapy* 11(7), pp. 1023-1032.

British Pharmacopoeia 2010a. *British Pharmacopoeia* London: The Stationery Office pp. 2300-2304.

British Pharmacopoeia 2010b. *British Pharmacopoeia* London: The Stationery Office pp. A324-A337.

Broadhead, J., Rouan, S. K. E. and Rhodes, C. T. 1992. The spray drying of pharmaceuticals. *Drug Development and Industrial Pharmacy* 18(11-12), pp. 1169-1206.

Brown, A. R. 1996. Propellant-driven aerosols of proteins. *Aerosol Science and Technology* 24(1), pp. 45-56.

Brown, A. R. and Chowdhury, S. I. 1997. Propellant-driven aerosols of DNA plasmids for gene expression in the respiratory tract. *Journal of Aerosol Medicine* 10(2), pp. 129-146.

Brown, A. R. and George, D. W. 1997. Tetrafluoroethane (HFC 134A) propellant-driven aerosols of proteins. *Pharmaceutical Research* 14(11), pp. 1542-1547.

Brunner, S., Sauer, T., Carotta, S., Cotten, M., Saltik, M. and Wagner, E. 2000. Cell cycle dependence of gene transfer by lipoplex, polyplex and recombinant adenovirus. *Gene Therapy* 7(5), pp. 401-407.

Burch, W. M., Sullivan, P. J. and McLaren, C. J. 1986. Technegas - a new ventilation agent for lung scanning. *Nuclear Medicine Communications* 7(12), pp. 865-871.

Bustami, R. T., Chan, H. K., Sweeney, T., Dehghani, F. and Foster, N. R. 2003. Generation of fine powders of recombinant human deoxyribonuclease using the aerosol solvent extraction system. *Pharmaceutical Research* 20(12), pp. 2028-2035.

Byron, P. R. 1990. Determinants of drug and polypeptide bioavailability from aerosols delivered to the lung. *Advanced Drug Delivery Reviews* 5(1-2), pp. 107-132.

Byron, P. R. 1994. Dosing reproducibility from experimental albuterol suspension metered-dose inhalers. *Pharmaceutical Research* 11(4), pp. 580-584.

Byron, P. R. 1997. Performance characteristics of pressurized metered dose inhalers in vitro. *Journal of Aerosol Medicine: The official journal of the International Society for Aerosols in Medicine* 10 Suppl 1, pp. S3-6.

Canonico, A. E., Conary, J. T., Meyrick, B. O. and Brigham, K. L. 1994. Aerosol and intravenous transfection of human alpha-1-antitrypsin gene to lungs of rabbits. *American Journal of Respiratory Cell and Molecular Biology* 10(1), pp. 24-29.

Capek, I. 2004. Degradation of kinetically-stable o/w emulsions. *Advances in Colloid and Interface Science* 107(2-3), pp. 125-155.

Carpenter, J. F. and Crowe, J. H. 1988a. The mechanism of cryoprotection of proteins by solutes. *Cryobiology* 25(3), pp. 244-255.

Carpenter, J. F. and Crowe, J. H. 1988b. Modes of stabilization of a protein by organic solutes during desiccation. *Cryobiology* 25(5), pp. 459-470.

Carpenter, J. F. and Crowe, J. H. 1989. An infrared spectroscopic study of the interactions of carbohydrates with dried proteins. *Biochemistry* 28(9), pp. 3916-3922.

Carpenter, J. F., Crowe, L. M. and Crowe, J. H. 1987. Stabilization of phosphofructokinase with sugars during freeze-drying: Characterization of enhanced protection in the presence of divalent cations. *Biochimica et Biophysica Acta* 923(1), pp. 109-115.

Carstensen, J. T. and Rhodes, C. T. 1993. Cyclic temperature stress-testing of pharmaceuticals *Drug Development and Industrial Pharmacy* 19(3), pp. 401-403.

Chalfie, M., Tu, Y., Euskirchen, G., Ward, W. W. and Prasher, D. C. 1994. Green fluorescent protein as a marker for gene expression. *Science* 263(5148), pp. 802-805.

Chan, J., Maghraby, G. M. M. E., Craig, J. P. and Alany, R. G. 2007. Phase transition water-in-oil microemulsions as ocular drug delivery systems: In vitro and in vivo evaluation. *International Journal of Pharmaceutics* 328(1), pp. 65-71.

Chancham, P. and Hughes, J. A. 2001. Relationship between plasmid DNA topological forms and in vitro transfection. *Journal of Liposome Research* 11(2-3), pp. 139-152.

Chen, H., Chang, X., Du, D., Li, J., Xu, H. and Yang, X. 2006. Microemulsion-based hydrogel formulation of ibuprofen for topical delivery. *International Journal of Pharmaceutics* 315(1-2), pp. 52-58.

Cherng, J. Y., Schuurmans-Nieuwenbroek, N. M. E., Jiskoot, W., Talsma, H., Zuidam, N. J., Hennink, W. E. and Crommelin, D. J. A. 1999. Effect of DNA topology on the transfection efficiency of poly((2-dimethylamino)ethyl methacrylate)-plasmid complexes. *Journal of Controlled Release* 60(2-3), pp. 343-353.

Cherng, J. Y., van de Wetering, P., Talsma, H., Crommelin, D. J. and Hennink, W. E. 1997. Freeze-drying of poly((2-dimethylamino)ethyl methacrylate)-based gene delivery systems. *Pharmaceutical Research* 14(12), pp. 1838-1841.

Chiaramoni, N. S., Speroni, L., Taira, M. C. and Alonso, S. D. V. 2007. Liposome/DNA systems: Correlation between association, hydrophobicity and cell viability. *Biotechnology Letters* 29, pp. 1637-1644.

Choi, S. H., Jin, S. E., Lee, M. K., Lim, S. J., Park, J. S., Kim, B. G., Ahn, W. S. and Kim, C. K. 2008. Novel cationic solid lipid nanoparticles enhanced p53 gene transfer to lung cancer cells. *European Journal of Pharmaceutics and Biopharmaceutics* 68(3), pp. 545-554.

Choi, W. J., Kim, J. K., Choi, S. H., Park, J. S., Ahn, W. S. and Kim, C.-K. 2004. Low toxicity of cationic lipid-based emulsion for gene transfer. *Biomaterials* 25(27), pp. 5893-5903.

Chokshi, U., Selvam, P., Porcar, L. and da Rocha, S. R. P. 2009. Reverse aqueous emulsions and microemulsions in HFA227 propellant stabilized by non-ionic ethoxylated amphiphiles. *International Journal of Pharmaceutics* 369(1-2), pp. 176-184.

Cilek, A., Celebi, N. and Tirnaksiz, F. 2006. Lecithin-based microemulsion of a peptide for oral administration: Preparation, characterization, and physical stability of the formulation. *Drug Delivery* 13(1), pp. 19-24.

Clark, A. R. 1996. MDIs: Physics of aerosol formation. *Journal of Aerosol Medicine-Deposition Clearance and Effects in the Lung* 9, pp. S19-S26.

Clontech. 1999. *pEGFP-N1 Vector Information.* Available at: <URL: http://www.pkclab.org/PKC/vector/pEGFPN1.pdf> [Accessed: 2/10/2006].

Colonna, C., Conti, B., Genta, I. and Alpar, O. H. 2008. Non-viral dried powders for respiratory gene delivery prepared by cationic and chitosan loaded liposomes. *International Journal of Pharmaceutics* 364(1), pp. 108-118.

Cook, R. O., Pannu, R. K. and Kellaway, I. W. 2005. Novel sustained release microspheres for pulmonary drug delivery. *Journal of Controlled Release* 104(1), pp. 79-90.

Crompton, G. K. 1990. The adult patient's difficulties with inhalers. *Lung* 168 Suppl, pp. 658-662.

Crook, K., McLachlan, G., Stevenson, B. J. and Porteous, D. J. 1996. Plasmid DNA molecules complexed with cationic liposomes are protected from degradation by nucleases and shearing by aerosolisation. *Gene Therapy* 3(9), pp. 834-839.

Crowe, J. H., Leslie, S. B. and Crowe, L. M. 1994. Is vitrification sufficient to preserve liposomes during freeze-drying? *Cryobiology* 31(4), pp. 355-366.

Cui, Z., Qiu, F. and Sloat, B. R. 2006. Lecithin-based cationic nanoparticles as a potential DNA delivery system. *International Journal of Pharmaceutics* 313(1-2), pp. 206-213.

Cunningham, S., Meng, Q. H., Klein, N., McAnulty, R. J. and Hart, S. L. 2002. Evaluation of a porcine model for pulmonary gene transfer using a novel synthetic vector. *Journal of Gene Medicine* 4(4), pp. 438-446.

Cyr, T. D., Graham, S. J., Li, K. Y. and Lovering, E. G. 1991. Low first-spray drug content in albuterol metered-dose inhalers. *Pharmaceutical Research* 8(5), pp. 658-660.

Dalby, R. N. and Byron, P. R. 1988. Comparison of output particle-size distribution from pressurized aerosols formulated as solutions or suspensions. *Pharmaceutical Research* 5(1), pp. 36-39.

Dan, N. 1998. The structure of DNA complexes with cationic liposomes - cylindrical or flat bilayers? *Biochimica Et Biophysica Acta-Biomembranes* 1369(1), pp. 34-38.

Danielsson, I. and Lindman, B. 1981. The definition of microemulsion. *Colloids and Surfaces* 3(4), pp. 391-392.

Davies, L. A., Hannavy, K., Davies, N., Pirrie, A., Coffee, R. A., Hyde, S. C. and Gill, D. R. 2005. Electrohydrodynamic comminution: A novel technique for the aerosolisation of plasmid DNA. *Pharmaceutical Research* 22(8), pp. 1294-1304.

Davies, L. A., McLachlan, G., Sumner-Jones, S. G., Ferguson, D., Baker, A., Tennant, P., Gordon, C., Vrettou, C., Baker, E., Zhu, J., Alton, E., Collie, D. D. S., Porteous, D. J., Hyde, S. C. and Gill, D. R. 2008. Enhanced lung gene expression after aerosol delivery of concentrated pDNA/PEI complexes. *Molecular Therapy* 16(7), pp. 1283-1290.

Davis, J. 2002. *Basic cell culture: A practical approach.* 2 ed. New York: Oxford University Press Inc.

de Boer, A. H., Gjaltema, D., Hagedoorn, P. and Frijlink, H. W. 2002. Characterization of inhalation aerosols: A critical evaluation of cascade impactor analysis and laser diffraction technique. *International Journal of Pharmaceutics* 249(1-2), pp. 219-231.

de Gennes, P. G. and Taupin, C. 1982. Microemulsions and the flexibility of oil/water interfaces. *Journal of Physical Chemistry* 86(13), pp. 2294-2304.

de Lima, M. C. P., Neves, S., Filipe, A., Duzgunes, N. and Simoes, S. 2003. Cationic liposomes for gene delivery: From biophysics to biological applications. *Current Medicinal Chemistry* 10(14), pp. 1221-1231.

de Martimprey, H., Vauthier, C., Malvy, C. and Couvreur, P. 2009. Polymer nanocarriers for the delivery of small fragments of nucleic acids: Oligonucleotides and siRNA. *European Journal of Pharmaceutics and Biopharmaceutics* 71(3), pp. 490-504.

Dean, D. A. 1997. Import of plasmid DNA into the nucleus is sequence specific. *Experimental Cell Research* 230(2), pp. 293-302.

Densmore, C. L., Orson, F. M., Xu, B., Kinsey, B. M., Waldrep, J. C., Hua, P., Bhogal, B. and Knight, V. 2000. Aerosol delivery of robust polyethyleneimine-DNA complexes for gene therapy and genetic immunization. *Molecular Therapy* 1(2), pp. 180-188.

Dickinson, P. A., Howells, S. W. and Kellaway, I. W. 2001. Novel nanoparticles for pulmonary drug administration. *Journal of Drug Targeting* 9(4), pp. 295-302.

Dolovich, M. B., Ahrens, R. C., Hess, D. R., Anderson, P., Dhand, R., Rau, J. L., Smaldone, G. C. and Guyatt, G. 2005. Device selection and outcomes of aerosol therapy: Evidence-based guidelines. *Chest* 127(1), pp. 335-371.

Donaldson, K., Stone, V., Gilmour, P. S., Brown, D. M. and MacNee, W. 2000. Ultrafine particles: Mechanisms of lung injury. *Philosophical Transactions of the Royal Society of London Series a-Mathematical Physical and Engineering Sciences* 358(1775), pp. 2741-2748.

Donnell, D., Harrison, L. I., Ward, S., Klinger, N. M., Ekholm, B. P., Cooper, K. M., Porietis, I. and McEwen, J. 1995. Acute safety of the CFC-free propellant HFA-134a from a pressurized metered dose inhaler. *European Journal of Clinical Pharmacology* 48(6), pp. 473-477.

Dowty, M. E., Williams, P., Zhang, G. F., Hagstrom, J. E. and Wolff, J. A. 1995. Plasmid DNA entry into postmitotic nuclei of primary rat myotubes. *Proceedings of the National Academy of Sciences of the United States of America* 92(10), pp. 4572-4576.

Driskell, R. A. and Engelhardt, J. F. 2003. Current status of gene therapy for inherited lung diseases. *Annual Review of Physiology* 65, pp. 585-612.

Dubus, J. C., Rhem, R. and Dolovich, M. 2001. Delivery of HFA and CFC salbutamol from spacer devices used in infancy. *International Journal of Pharmaceutics* 222(1), pp. 101-108.

Dunbar, C. and Mitchell, J. 2005. Analysis of cascade impactor mass distributions. *Journal of Aerosol Medicine-Deposition Clearance and Effects in the Lung* 18(4), pp. 439-451.

Duncan, J. E., Whitsett, J. A. and Horowitz, A. D. 1997. Pulmonary surfactant inhibits cationic liposome-mediated gene delivery to respiratory epithelial cells in vitro. *Human Gene Therapy* 8(4), pp. 431-438.

Ecanow, B., Webster, J. M. and Blake, M. I. 1986. Particle aggregation states and aerosol clogging. *Drug Development and Industrial Pharmacy* 12(6), pp. 867-874.

El-Aneed, A. 2004. An overview of current delivery systems in cancer gene therapy. *Journal of Controlled Release* 94(1), pp. 1-14.

EMEA. 2002. *Note for guidance on requirements for pharmaceutical documentation for pressurised metered dose inhalation products.* Available at: <URL: http://www.emea.europa.eu/pdfs/human/qwp/284500en.pdf> [Accessed: 1/10/09].

Even-Chen, S. and Barenholz, Y. 2000. DOTAP cationic liposomes prefer relaxed over supercoiled plasmids. *Biochimica et Biophysica Acta (BBA) - Biomembranes* 1509(1-2), pp. 176-188.

Ewald, S. J. and Shao, H. 1993. Ethanol increases apoptotic cell death of thymocytes in vitro. *Alcoholism-Clinical and Experimental Research* 17(2), pp. 359-365.

Farr, S. J., Kellaway, I. W. and Carman-Meakin, B. 1987. Assessing the potential of aerosol-generated liposomes from pressurised pack formulations. *Journal of Controlled Release* 5(2), pp. 119-127.

Farr, S. J., Kellaway, I. W. and Carman-Meakin, B. 1989. Comparison of solute partitioning and efflux in liposomes formed by a conventional and an aerosolised method. *International Journal of Pharmaceutics* 51(1), pp. 39-46.

Farr, S. J., Kellaway, I. W., Parry-Jones, D. R. and Woolfrey, S. G. 1985. 99m-Technetium as a marker of liposomal deposition and clearance in the human lung. *International Journal of Pharmaceutics* 26(3), pp. 303-316.

Felgner, J. H., Kumar, R., Sridhar, C. N., Wheeler, C. J., Tsai, Y. J., Border, R., Ramsey, P., Martin, M. and Felgner, P. L. 1994. Enhanced gene delivery and mechanism studies with a novel series of cationic lipid formulations. *Journal of Biological Chemistry* 269(4), pp. 2550-2561.

Felgner, P. L., Gadek, T. R., Holm, M., Roman, R., Chan, H. W., Wenz, M., Northrop, J. P., Ringold, G. M. and Danielsen, M. 1987. Lipofection: A highly efficient, lipid-mediated DNA-transfection procedure. *Proceedings of the National Academy of Sciences of the United States of America* 84(21), pp. 7413-7417.

Felgner, P. L., Tsai, Y. J., Sukhu, L., Wheeler, C. J., Manthorpe, M., Marshall, J. and Cheng, S. H. 1995. Improved cationic lipid formulations for in vivo gene therapy. *Annals of New York Academy of Sciences* 772, pp. 126-139.

Fennelly, G. J., Khan, S. A., Abadi, M. A., Wild, T. F. and Bloom, B. R. 1999. Mucosal DNA vaccine immunization against measles with a highly attenuated Shigella flexneri vector. *Journal of Immunology* 162(3), pp. 1603-1610.

Fennelly, K. P., Martyny, J. W., Fulton, K. E., Orme, I. M., Cave, D. M. and Heifets, L. B. 2004. Cough-generated aerosols of Mycobacterium tuberculosis - A new method to study infectiousness. *American Journal of Respiratory and Critical Care Medicine* 169(5), pp. 604-609.

Ferrari, S., Geddes, D. M. and Alton, E. W. 2002. Barriers to and new approaches for gene therapy and gene delivery in cystic fibrosis. *Advanced Drug Delivery Reviews* 54(11), pp. 1373-1393.

Ferrari, S., Griesenbach, U., Geddes, D. M. and Alton, E. 2003. Immunological hurdles to lung gene therapy. *Clinical and Experimental Immunololgy* 132(1), pp. 1-8.

Forbes, B. 2000. Human airway epithelial cell lines for in vitro drug transport and metabolism studies. *Pharmaceutical Science & Technology Today* 3(1), pp. 18-27.

Fowler, K. 2006. *Handbook of pharmaceutical excipients.* London: Pharmaceutical Press.

Franks, F., Hatley, R. H. M. and Mathias, S. F. 1991. Materials science and the production of shelf-stable biologicals. *Biopharm* 4(9), pp. 38-55.

Freshney, I. 2000. *Culture of animal cells: A manual of basic technique.* 4 ed. USA: Wiley-Liss Inc.

Gabrio, B. J., Stein, S. W. and Velasquez, D. J. 1999. A new method to evaluate plume characteristics of hydrofluoroalkane and chlorofluorocarbon metered dose inhalers. *International Journal of Pharmaceutics* 186(1), pp. 3-12.

Gao, X. and Huang, L. 1995. Cationic liposome-mediated gene transfer. *Gene Therapy* 2(10), pp. 710-722.

Gao, X. and Huang, L. 1996. Potentiation of cationic liposome-mediated gene delivery by polycations. *Biochemistry* 35(3), pp. 1027-1036.

Gershon, H., Ghirlando, R., Guttman, S. B. and Minsky, A. 1993. Mode of formation and structural features of DNA-cationic liposome complexes used for transfection. *Biochemistry* 32(28), pp. 7143-7151.

Gillberg, G., Lehtinen, H. and Friberg, S. 1970. NMR and IR investigation of the conditions determining the stability of microemulsions. *Journal of Colloid and Interface Science* 33(1), pp. 40-53.

Gonda, I. 1985. Development of a systematic theory of suspension inhalation aerosols. I. A framework to study the effects of aggregation on the aerodynamic behaviour of drug particles. *International Journal of Pharmaceutics* 27(1), pp. 99-116.

Gonda, I. 2000. Therapeutic aerosols. In: Aulton, M.E. ed. *Pharmaceutics the science of dosage form design.* Edinburgh: Churchill Livingstone, pp. 341-358.

Grenha, A., Seijo, B. and Remunan-Lopez, C. 2005. Microencapsulated chitosan nanoparticles for lung protein delivery. *European Journal of Pharmaceutical Sciences* 25(4-5), pp. 427-437.

Griesenbach, U. and Alton, E. W. F. W. 2009. Gene transfer to the lung: Lessons learned from more than 2 decades of CF gene therapy. *Advanced Drug Delivery Reviews* 61(2), pp. 128-139.

Griffin, W. C. 1949. Classification of suface active-agents by "HLB". *Journal of the Society of Cosmetic Chemists* 1, pp. 311-326.

Grosse, S., Thévenot, G., Aron, Y., Duverger, E., Abdelkarim, M., Roche, A. C., Monsigny, M. and Fajac, I. 2008. In vivo gene delivery in the mouse lung with lactosylated polyethylenimine, questioning the relevance of in vitro experiments. *Journal of Controlled Release* 132(2), pp. 105-112.

Guang Liu, W. and De Yao, K. 2002. Chitosan and its derivatives- A promising non-viral vector for gene transfection. *Journal of Controlled Release* 83(1), pp. 1-11.

Gupta, A., Stein, S. W. and Myrdal, P. B. 2003. Balancing ethanol cosolvent concentration with product performance in 134a-based pressurized metered dose inhalers. *Journal of Aerosol Medicine-Deposition Clearance and Effects in the Lung* 16(2), pp. 167-174.

Haensler, J. and Szoka, F. C. 1993. Polyamidoamine cascade polymers mediate efficient transfection of cells in culture. *Bioconjugate Chemistry* 4(5), pp. 372-379.

Hallworth, G. W. and Westmoreland, D. G. 1987. The twin impinger: A simple device for assessing the delivery of drugs from metered dose pressurized aerosol inhalers. *Journal of Pharmacy and Pharmacology* 39(12), pp. 966-972.

Harcourt, J. L., Anderson, L. J., Sullender, W. and Tripp, R. A. 2004. Pulmonary delivery of respiratory syncytial virus DNA vaccines using macroaggregated albumin particles. *Vaccine* 22(17-18), pp. 2248-2260.

Harris, J. A., Stein, S. W. and Myrdal, P. B. 2006. Evaluation of the TSI aerosol impactor 3306/3321 system using a redesigned impactor stage with solution and suspension metered-dose inhalers. *AAPS Pharmscitech* 7(1), pp. E138-E145.

Heller, M. C., Carpenter, J. F. and Randolph, T. W. 1999. Protein formulation and lyophilization cycle design: Prevention of damage due to freeze-concentration induced phase separation. *Biotechnology and Bioengineering* 63(2), pp. 166-174.

Hickey, A. J. 1993. Lung deposition and clearance of pharmaceutical aerosols: What can be learned from inhalation toxicology and industrial hygiene? *Aerosol Science and Technology* 18(3), pp. 290-304.

Hickey, A. J., Dalby, R. N. and Byron, P. R. 1988. Effects of surfactants on aerosol powders in suspension. Implications for airborne particle size. *International Journal of Pharmaceutics* 42(1-3), pp. 267-270.

Hirota, S., de Ilarduya, C. T., Barron, L. G. and Szoka, F. C. 1999. Simple mixing device to reproducibly prepare cationic lipid-DNA complexes (lipoplexes). *Biotechniques* 27(2), pp. 286-290.

Hope, M. J., Bally, M. B., Webb, G. and Cullis, P. R. 1985. Production of large unilamellar vesicles by a rapid extrusion procedure. Characterization of size distribution, trapped volume and ability to maintain a membrane potential. *Biochimica et Biophysica Acta (BBA) - Biomembranes* 812(1), pp. 55-65.

Hyde, S. C., Gill, D. R., Higgins, C. F., Trezise, A. E. O., Macvinish, L. J., Cuthbert, A. W., Ratcliff, R., Evans, M. J. and Colledge, W. H. 1993. Correction of the ion-transport defect in cystic-fibrosis transgenic mice by gene-therapy. *Nature* 362(6417), pp. 250-255.

Hyde, S. C., Southern, K. W., Gileadi, U., Fitzjohn, E. M., Mofford, K. A., Waddell, B. E., Gooi, H. C., Goddard, C. A., Hannavy, K., Smyth, S. E., Egan, J. J., Sorgi, F. L., Huang, L., Cuthbert, A. W., Evans, M. J., Colledge, W. H., Higgins, C. F., Webb, A. K. and Gill, D. R. 2000. Repeat administration of DNA/liposomes to the nasal epithelium of patients with cystic fibrosis. *Gene Therapy* 7(13), pp. 1156-1165.

ICH Expert Working Group. 2003. *Stability Testing of New Drug Substances and Products Q1A(R2).* Available at: <URL: http://www.ich.org/LOB/media/MEDIA419.pdf> [Accessed: 28/2/2010].

Invitrogen. 2003. *Transformation Procedure.* Available at: <URL: http://tools.invitrogen.com/content/sfs/manuals/18263012.pdf> [Accessed: 1/1/2010].

Israelachvilli, J. N., Mitchell, D. J. and Ninham, B. W. 1976. Theory of self-assembly of hydrocarbon amphiphiles into micelles and bilayers. *Journal of the Chemical Society, Faraday Transactions 2: Molecular and Chemical Physics* 72(9), pp. 1525-1568.

Izutsu, K., Yoshioka, S. and Terao, T. 1993. Decreased protein-stabilising effects of cryoprotectants due to crystallization. *Pharmaceutical Research* 10(8), pp. 1232-1237.

Jacobs, J. S. and Miller, M. W. 2001. Proliferation and death of cultured fetal neocortical neurons: Effects of ethanol on the dynamics of cell growth. *Journal of Neurocytology* 30(5), pp. 391-401.

James, J., Davies, M., Toon, R., Jinks, P. and Roberts, C. J. eds. 2008. *Studying the Effect of Water Ingress on API Adhesion in Suspension Metered Dose Inhalers using AFM.* Drug Delivery to the Lungs 19. Edinburgh: The Aerosol Society.

Jensen, P. A., Todd, W. F., Davis, G. N. and Scarpino, P. V. 1992. Evaluation of 8 Bioaerosol Samplers Challenged with Aerosols of Free Bacteria. *American Industrial Hygiene Association journal* 53(10), pp. 660-667.

Jeong, J. H., Kim, S. W. and Park, T. G. 2007. Molecular design of functional polymers for gene therapy. *Progress in Polymer Science* 32(11), pp. 1239-1274.

Jiang, H. L., Arote, R., Jere, D., Kim, Y. K., Cho, M. H. and Cho, C. S. 2008. Degradable polyethylenimines as gene carriers. *Materials Science and Technology* 24(9), pp. 1118-1126.

Johnson, K. A. 1997. Preparation of peptide and protein powders for inhalation. *Advanced Drug Delivery Reviews* 26(1), pp. 3-15.

Jones, S. A., Martin, G. P. and Brown, M. B. 2006. Stabilisation of deoxyribonuclease in hydrofluoroalkanes using miscible vinyl polymers. *Journal of Controlled Release* 115(1), pp. 1-8.

Jones, W., Morring, K., Morey, P. and Sorenson, W. 1985. Evaluation of the Andersen viable impactor for single stage sampling *American Industrial Hygiene Association journal* 46(5), pp. 294-298.

Kay, M. A., Glorioso, J. C. and Naldini, L. 2001. Viral vectors for gene therapy: The art of turning infectious agents into vehicles of therapeutics. *Nature Medicine* 7(1), pp. 33-40.

Kelley, D. and McClements, D. J. 2003. Interactions of bovine serum albumin with ionic surfactants in aqueous solutions. *Food Hydrocolloids* 17(1), pp. 73-85.

Kleemann, E., Dailey, L. A., Abdelhady, H. G., Gessler, T., Schmehl, T., Roberts, C. J., Davies, M. C., Seeger, W. and Kissel, T. 2004. Modified polyethylenimines as non-viral gene delivery systems for aerosol gene therapy: Investigations of the complex structure and stability during air-jet and ultrasonic nebulization. *Journal of Controlled Release* 100(3), pp. 437-450.

Kommanaboyina, B. and Rhodes, C. T. 1999. Trends in stability testing, with emphasis on stability during, with emphasis on stability during distribution and storage. *Drug Development and Industrial Pharmacy* 25(7), pp. 857-868.

Lang, N. and Tuel, A. 2004. A fast and efficient ion-exchange procedure to remove surfactant molecules from MCM-41 materials. *Chemistry of Materials* 16(10), pp. 1961-1966.

Lapinski, M. M., Castro-Forero, A., Greiner, A. J., Ofoli, R. Y. and Blanchard, G. J. 2007. Comparison of liposomes formed by sonication and extrusion: Rotational and translational diffusion of an embedded chromophore. *Langmuir* 23, pp. 11677-11683.

Lasic, D. D. and Templeton, N. S. 1996. Liposomes in gene therapy. *Advanced Drug Delivery Reviews* 20(2-3), pp. 221-266.

Lawrence, M. J. and Rees, G. D. 2000. Microemulsion-based media as novel drug delivery systems. *Advanced Drug Delivery Reviews* 45(1), pp. 89-121.

Lentz, Y. K., Anchordoquy, T. J. and Lengsfeld, C. S. 2006a. DNA acts as a nucleation site for transient cavitation in the ultrasonic nebulizer. *Journal of Pharmaceutical Sciences* 95(3), pp. 607-619.

Lentz, Y. K., Anchordoquy, T. J. and Lengsfeld, C. S. 2006b. Rationale for the selection of an aerosol delivery system for gene delivery. *Journal of Aerosol Medicine* 19(3), pp. 372-384.

Lentz, Y. K., Worden, L. R., Anchordoquy, T. J. and Lengsfeld, C. S. 2005. Effect of jet nebulization on DNA: Identifying the dominant degradation mechanism and mitigation methods. *Journal of Aerosol Science* 36(8), pp. 973-990.

Leventis, R. and Silvius, J. R. 1990. Interactions of mammalian cells with lipid dispersions containing novel metabolizable cationic amphiphiles. *Biochimica et Biophysica Acta* 1023(1), pp. 124-132.

Levine, H. and Slade, L. 1992. Another view of trehalose for drying and stabilizing biological materials. *BioPharm* 5, pp. 36-40.

Li, H. Y. and Seville, P. C. 2009. Novel pMDI formulations for pulmonary delivery of proteins. *International Journal of Pharmaceutics* 385(1-2), pp. 73-78.

Li, H. Y. and Birchall, J. 2006. Chitosan-modified dry powder formulations for pulmonary gene delivery. *Pharmaceutical Research* 23(5), pp. 941-950.

Li, H. Y., Neill, H., Innocent, R., Seville, P., Williamson, I. and Birchall, J. C. 2003. Enhanced dispersibility and deposition of spray-dried powders for pulmonary gene therapy. *Journal of Drug Targeting* 11(7), pp. 425-432.

Li, H. Y., Seville, P. C., Williamson, I. J. and Birchall, J. C. 2005a. The use of absorption enhancers to enhance the dispersibility of spray-dried powders for pulmonary gene therapy. *The Journal of Gene Medicine* 7(8), pp. 1035-1043.

Li, H. Y., Seville, P. C., Williamson, I. J. and Birchall, J. C. 2005b. The use of amino acids to enhance the aerosolisation of spray-dried powders for pulmonary gene therapy. *The Journal of Gene Medicine* 7(3), pp. 343-353.

Li, S. D. and Huang, L. 2007. Non-viral is superior to viral gene delivery. *Journal of Controlled Release* 123(3), pp. 181-183.

Liao, Y. H., Brown, M. B., Jones, S. A., Nazir, T. and Martin, G. P. 2005. The effects of polyvinyl alcohol on the in vitro stability and delivery of spray-dried protein particles from surfactant-free HFA 134a-based pressurised metered dose inhalers. *International Journal of Pharmaceutics* 304(1-2), pp. 29-39.

Liao, Y. H., Brown, M. B. and Martin, G. P. 2004. Investigation of the stabilisation of freeze-dried lysozyme and the physical properties of the formulations. *European Journal of Pharmaceutics and Biopharmaceutics* 58(1), pp. 15-24.

Lieber, M., Smith, B., Szakal, A., Nelsonrees, W. and Todaro, G. 1976. A continuous tumor-cell line from a human lung carcinoma with properties of type II alveolar epithelial cells. *International Journal of Cancer* 17(1), pp. 62-70.

Limberis, M., Anson, D. S., Fuller, M. and Parsons, D. W. 2002. Recovery of airway cystic fibrosis transmembrane conductance regulator function in mice with cystic fibrosis after single-dose lentivirus-mediated gene transfer. *Human Gene Therapy* 13(16), pp. 1961-1970.

Logan, J. J., Bebok, Z., Walker, L. C., Peng, S. Y., Felgner, P. L., Siegal, G. P., Frizzell, R. A., Dong, J. Y., Howard, M., Matalon, S., Lindsey, J. R., Duvall, M. and Sorscher, E. J. 1995. Cationic lipids for reporter gene and CFTR transfer to rat pulmonary epithelium. *Gene Therapy* 2(1), pp. 38-49.

Lu, D. and Hickey, A. J. 2007. Pulmonary vaccine delivery. *Expert Review of Vaccines* 6(2), pp. 213-226.

Lv, F. F., Zheng, L. Q. and Tung, C. H. 2005. Phase behavior of the microemulsions and the stability of the chloramphenicol in the microemulsion-based ocular drug delivery system. *International Journal of Pharmaceutics* 301(1-2), pp. 237-246.

Lyscov, V. N. and Moshkovsky, Y. S. 1969. DNA cryolysis. *Biochimica et Biophysica Acta (BBA) - Nucleic Acids and Protein Synthesis* 190(1), pp. 101-110.

Maa, Y. F., Costantino, H. R., Nguyen, P. A. and Hsu, C. C. 1997. The effect of operating and formulation variables on the morphology of spray-dried protein particles. *Pharmaceutical Development and Technology* 2(3), pp. 213-223.

Maa, Y. F., Nguyen, P. A., Andya, J. D., Dasovich, N., Sweeney, T. D., Shire, S. J. and Hsu, C. C. 1998. Effect of spray drying and subsequent processing conditions on residual moisture content and physical/biochemical stability of protein inhalation powders. *Pharmaceutical Research* 15(5), pp. 768-775.

Maa, Y. F., Nguyen, P. A., Sweeney, T., Shire, S. J. and Hsu, C. C. 1999. Protein inhalation powders: Spray drying vs spray freeze drying. *Pharmaceutical Research* 16(2), pp. 249-254.

Maitani, Y., Aso, Y., Yamada, A. and Yoshioka, S. 2008. Effect of sugars on storage stability of lyophilized liposome/DNA complexes with high transfection efficiency. *International Journal of Pharmaceutics* 356(1-2), pp. 69-75.

Makino, K., Yamamoto, N., Higuchi, K., Harada, N., Ohshima, H. and Terada, H. 2003. Phagocytic uptake of polystyrene microspheres by alveolar macrophages: Effects of the size and surface properties of the microspheres. *Colloids and Surfaces B-Biointerfaces* 27(1), pp. 33-39.

Marple, V. A., Olson, B. A. and Miller, N. C. 1998. The role of inertial particle collectors in evaluating pharmaceutical aerosol delivery systems. *Journal of Aerosol Medicine-Deposition Clearance and Effects in the Lung* 11, pp. S139-S153.

Mayer, L. D., Hope, M. J. and Cullis, P. R. 1986. Vesicles of variable sizes produced by a rapid extrusion procedure. *Biochimica et Biophysica Acta (BBA) - Biomembranes* 858(1), pp. 161-168.

Maynard, A. D. and Kuempel, E. D. 2005. Airborne nanostructured particles and occupational health. *Journal of Nanoparticle Research* 7(6), pp. 587-614.

McDonald, R. J., Liggitt, H. D., Roche, L., Nguyen, H. T., Pearlman, R., Raabe, O. G., Bussey, L. B. and Gorman, C. M. 1998. Aerosol delivery of lipid:DNA complexes to lungs of rhesus monkeys. *Pharmaceutical Research* 15(5), pp. 671-679.

Mendonça, C. R. B., Silva, Y. P., Böckel, W. J., Simó-Alfonso, E. F., Ramis-Ramos, G., Piatnicki, C. M. S. and Bica, C. I. D. 2009. Role of the co-surfactant nature in soybean w/o microemulsions. *Journal of Colloid and Interface Science* 337(2), pp. 579-585.

Merck. 2007. *Product Data Sheet: DOTAP.* Available at: <URL: http://www.merck.ru/servlet/PB/show/1770230/MBA_PDS_071123_DOTAP%20Chloride.pdf> [Accessed: 17/4/2008].

Middaugh, C. R., Evans, R. K., Montgomery, D. L. and Casimiro, D. R. 1998. Analysis of plasmid DNA from a pharmaceutical perspective. *Journal of Pharmaceutical Sciences* 87(2), pp. 130-146.

Miller, N. C. and Purrington, A. R. 1996. A cascade impactor entry port for MDI sprays with collection characteristics imitating a physical model of the human throat. *Pharmaceutical Research* 13(3), pp. 391-397.

Mitchell, D. J. and Ninham, B. W. 1981. Micelles, vesicles and microemulsions. *Journal of the Chemical Society, Faraday Transactions 2: Molecular and Chemical Physics* 77, pp. 601-629.

Mitchell, J. P. and Nagel, M. W. 2003. Cascade impactors for the size characterization of aerosols from medical inhalers: Their uses and limitations. *Journal of Aerosol Medicine* 16(4), pp. 341-377.

Mitchell, J. P., Nagel, M. W., Nichols, S. and Nerbrink, O. 2006. Laser diffractometry as a technique for the rapid assessment of aerosol particle size from inhalers. *Journal of Aerosol Medicine-Deposition Clearance and Effects in the Lung* 19(4), pp. 409-433.

Morén, F. 1978. Drug deposition of pressurized inhalation aerosols II. Influence of vapour pressure and metered volume. *International Journal of Pharmaceutics* 1(4), pp. 213-218.

Moss, R. B., Milla, C., Colombo, J., Accurso, F., Zeitlin, P. L., Clancy, J. P., Spencer, L. T., Pilewski, J., Waltz, D. A., Dorkin, H. L., Ferkol, T., Pian, M., Ramsey, B., Carter, B. J., Martin, D. B. and Heald, A. E. 2007. Repeated aerosolized AAV-CFTR for treatment of cystic fibrosis: A Randomized placebo-controlled phase 2B trial. *Human Gene Therapy* 18(8), pp. 726-732.

Moss, R. B., Rochman, D., Spencer, L. T., Aitken, M. L., Zeitlhi, P. L., Waltz, D., Milla, C., Brody, A. S., Clancy, J. P., Ramsey, B., Hamblett, N. and Heald, A. E. 2004. Repeated adeno-associated virus serotype 2 aerosol-mediated cystic fibrosis transmembrane regulator gene transfer to the lungs of patients with cystic fibrosis - A multicenter, double-blind, placebo-controlled trial. *Chest* 125(2), pp. 509-521.

Muller, J., Huaux, F. and Lison, D. 2006. Respiratory toxicity of carbon nanotubes: How worried should we be? *Carbon* 44(6), pp. 1048-1056.

Mumenthaler, M., Hsu, C. C. and Pearlman, R. 1994. Feasibility study on spray-drying protein pharmaceuticals: Recombinant human growth hormone and tissue-type plasminogen activator *Pharmaceutical Research* 11(1), pp. 12-20.

Murnane, D., Marriott, C. and Martin, G. P. 2008. Polymorphic control of inhalation microparticles prepared by crystallization. *International Journal of Pharmaceutics* 361(1-2), pp. 141-149.

Newman, S. P. 1998. How well do in vitro particle size measurements predict drug delivery in vivo? *Journal of Aerosol Medicine-Deposition Clearance and Effects in the Lung* 11, pp. S97-S104.

Nguyen, X. C., Herberger, J. D. and Burke, P. A. 2004. Protein powders for encapsulation: A comparison of spray-freeze drying and spray drying of darbepoetin alfa. *Pharmaceutical Research* 21(3), pp. 507-514.

Nyambura, B. K., Kellaway, I. W. and Taylor, K. M. G. 2009a. Insulin nanoparticles: Stability and aerosolization from pressurized metered dose inhalers. *International Journal of Pharmaceutics* 375(1-2), pp. 114-122.

Nyambura, B. K., Kellaway, I. W. and Taylor, K. M. G. 2009b. The processing of nanoparticles containing protein for suspension in hydrofluoroalkane propellants. *International Journal of Pharmaceutics* 372(1-2), pp. 140-146.

O'Callaghan, C. and Wright, P. 2002. The metered-dose inhaler. In: O'Callaghan, C. and Smaldone, G.C. eds. *Drug Delivery to the Lung.* Vol. 162. New York: Marcel Dekker, pp. 337-370.

Oberdorster, G. 2000. Toxicology of ultrafine particles: In vivo studies. *Philosophical Transactions of the Royal Society of London Series a-Mathematical Physical and Engineering Sciences* 358(1775), pp. 2719-2739.

Oberdorster, G., Oberdorster, E. and Oberdorster, J. 2005. Nanotoxicology: An emerging discipline evolving from studies of ultrafine particles. *Environ Health Perspect* 113(7), pp. 823-839.

Otani, Y. and Wang, C. S. 1984. Growth and deposition of saline droplets covered with a monolayer of surfactant. *Aerosol Science and Technology* 3(2), pp. 155-166.

Park, K. M. and Kim, C. K. 1999. Preparation and evaluation of flurbiprofen-loaded microemulsion for parenteral delivery. *International Journal of Pharmaceutics* 181(2), pp. 173-179.

Patel, N., Marlow, M. and Lawrence, M. J. 2003. Fluorinated ionic surfactant microemulsions in hydrofluorocarbon 134a (HFC 134a). *Journal of Colloid and Interface Science* 258(2), pp. 354-362.

Patil, S. D., Rhodes, D. G. and Burgess, D. J. 2005. DNA-based therapeutics and DNA delivery systems: A comprehensive review. *AAPS Journal* 7(1), pp. E61-77.

Patton, J. S. and Byron, P. R. 2007. Inhaling medicines: Delivering drugs to the body through the lungs. *Nature Reviews Drug Discovery* 6(1), pp. 67-74.

Pedersen, S., Frost, L. and Arnfred, T. 1986. Errors in inhalation technique and efficiency in inhaler use in asthmatic children. *Allergy* 41(2), pp. 118-124.

Pedroso de Lima, M. C., Simões, S., Pires, P., Faneca, H. and Düzgünes, N. 2001. Cationic lipid-DNA complexes in gene delivery: From biophysics to biological applications. *Advanced Drug Delivery Reviews* 47(2-3), pp. 277-294.

Peguin, R. P., Selvam, P. and da Rocha, S. R. 2006. Microscopic and thermodynamic properties of the HFA134a-water interface: Atomistic computer simulations and tensiometry under pressure. *Langmuir* 22(21), pp. 8826-8830.

Perricone, M. A., Morris, J. E., Pavelka, K., Plog, M. S., O'Sullivan, B. P., Joseph, P. M., Dorkin, H., Lapey, A., Balfour, R., Meeker, D. P., Smith, A. E., Wadsworth, S. C. and St George, J. A. 2001. Aerosol and lobar administration of a recombinant adenovirus to individuals with cystic fibrosis. II. Transfection efficiency in airway epithelium. *Human Gene Therapy* 12(11), pp. 1383-1394.

Porteous, D. J., Dorin, J. R., McLachlan, G., DavidsonSmith, H., Davidson, H., Stevenson, B. J., Carothers, A. D., Wallace, W. A. H., Moralee, S., Hoenes, C., Kallmeyer, G., Michaelis, U., Naujoks, K., Ho, L. P., Samways, J. M., Imrie, M., Greening, A. P. and Innes, J. A. 1997. Evidence for safety and efficacy of DOTAP cationic liposome mediated CFTR gene transfer to the nasal epithelium of patients with cystic fibrosis. *Gene Therapy* 4(3), pp. 210-218.

Poxon, S. W. and Hughes, J. A. 2000. The effect of lyophilization on plasmid DNA activity. *Pharmaceutical Development and Technology* 5(1), pp. 115-122.

Prasher, D. C., Eckenrode, V. K., Ward, W. W., Prendergast, F. G. and Cormier, M. J. 1992. Primary structure of the Aequorea victoria green-fluorescent protein. *Gene* 111(2), pp. 229-233.

Prata, C. A., Zhang, X. X., Luo, D., McIntosh, T. J., Barthelemy, P. and Grinstaff, M. W. 2008. Lipophilic peptides for gene delivery. *Bioconjugate Chemistry* 19(2), pp. 418-420.

Prego, C., Paolicelli, P., Díaz, B., Vicente, S., Sánchez, A., González-Fernández, Á. and Alonso, M. J. 2010. Chitosan-based nanoparticles for improving immunization against hepatitis B infection. *Vaccine* 28(14), pp. 2607-2614.

Promega. 2006. *Wizard® DNA Clean-Up System- Technical Bulletin.* Available at: <URL: http://www.promega.com/tbs/tb141/tb141.pdf> [Accessed: 3/11/2006].

Qiagen®. 2005. *Qiagen® Plasmid Purification Handbook.* Available at: <URL: http://www1.qiagen.com/Search/Search.aspx?SearchTerm=plasmid+purification&category=0> [Accessed: 10/9/2006].

Radler, J. O., Koltover, I., Salditt, T. and Safinya, C. R. 1997. Structure of DNA-cationic liposome complexes: DNA intercalation in multilamellar membranes in distinct interhelical packing regimes. *Science* 275(5301), pp. 810-814.

Ranz, W. E. and Wong, J. B. 1952. Jet impactors for determining the particle-size distributions of aerosols. *A.M.A Archives of Industrial Hygiene and Occupational Medicine* 5(5), pp. 464-477.

Ratjen, F. 2008. Recent advances in cystic fibrosis. *Paediatric Respiratory Reviews* 9(2), pp. 144-148.

Remaut, K., Sanders, N. N., Fayazpour, F., Demeester, J. and De Smedt, S. C. 2006. Influence of plasmid DNA topology on the transfection properties of DOTAP/DOPE lipoplexes. *Journal of Controlled Release* 115(3), pp. 335-343.

Reynolds, J. M. and McNamara, D. P. 1996. Model for moisture transport into inhalation aerosols. *Pharmaceutical Research* 13(5), pp. 809-811.

Rich, D. P., Anderson, M. P., Gregory, R. J., Cheng, S. H., Paul, S., Jefferson, D. M., McCann, J. D., Klinger, K. W., Smith, A. E. and Welsh, M. J. 1990. Expression of cystic-fibrosis transmembrane conductance regulator corrects defective chloride channel regulation in cystic-fibrosis airway epithelial-cells. *Nature* 347(6291), pp. 358-363.

Riordan, J. R. 2008. CFTR function and prospects for therapy. *Annual Review of Biochemistry* 77, pp. 701-726.

Riordan, J. R., Rommens, J. M., Kerem, B. S., Alon, N., Rozmahel, R., Grzelczak, Z., Zielenski, J., Lok, S., Plavsic, N. 1989. Identification of the cystic fibrosis gene: Cloning and characterization of complementary DNA. *Science* 245(4922), pp. 1066-1073.

Robinson, B. W. S., Erle, D. J., Jones, D. A., Shapiro, S., Metzger, W. J., Albelda, S. M., Parks, W. C. and Boylan, A. 2000. Recent advances in molecular biological techniques and their relevance to pulmonary research. *Thorax* 55(4), pp. 329-339.

Rogueda, P. G. A. and Traini, D. 2007a. The nanoscale in pulmonary delivery. Part 1: Deposition, fate, toxicology and effects. *Expert Opinion on Drug Delivery* 4(6), pp. 595-606.

Rogueda, P. G. A. and Traini, D. 2007b. The nanoscale in pulmonary delivery. Part 2: Formulation platforms. *Expert Opinion on Drug Delivery* 4(6), pp. 607-620.

Rosenfeld, M. A., Yoshimura, K., Trapnell, B. C., Yoneyama, K., Rosenthal, E. R., Dalemans, W., Fukayama, M., Bargon, J., Stier, L. E., Stratfordperricaudet, L., Perricaudet, M., Guggino, W. B., Pavirani, A., Lecocq, J. P. and Crystal, R. G. 1992. In vivo transfer of the human cystic-fibrosis transmembrane conductance regulator gene to the airway epithelium. *Cell* 68(1), pp. 143-155.

Ruckenstein, E. 1996. Microemulsions, macroemulsions, and the Bancroft rule. *Langmuir* 12(26), pp. 6351-6353.

Ruiz, F. E., Clancy, J. P., Perricone, M. A., Bebok, Z., Hong, J. S., Cheng, S. H., Meeker, D. P., Young, K. R., Schoumacher, R. A., Weatherly, M. R., Wing, L., Morris, J. E., Sindel, L., Rosenberg, M., van Ginkel, F. W., McGhee, J. R., Kelly, D., Lyrene, R. K. and Sorscher, E. J. 2001. A clinical inflammatory syndrome attributable to aerosolized lipid-DNA administration in cystic fibrosis. *Human Gene Therapy* 12(7), pp. 751-761.

Saint Ruth, H., Attwood, D., Ktistis, G. and Taylor, C. J. 1995. Phase studies and particle size analysis of oil-in-water phospholipid microemulsions. *International Journal of Pharmaceutics* 116(2), pp. 253-261.

Schuber, F., Kichler, A., Boeckler, C. and Frisch, B. 1998. Liposomes: From membrane models to gene therapy. *Pure and Applied Chemistry* 70(1), pp. 89-96.

Schulman, J. H. and Cockbain, E. G. 1940. Molecular interactions at oil/water interfaces. Part I. Molecular complex formation and the stability of oil in water emulsions. *Transactions of the Faraday Society* 35(3), pp. 0651-0660.

Schulman, J. H., Stoeckenius, W. and Prince, L. M. 1959. Mechanism of formation and structure of micro emulsions by electron microscopy. *Journal of Physical Chemistry* 63(10), pp. 1677-1680.

Schurtenberger, P., Peng, Q., Leser, M. E. and Luisi, P. L. 1993. Structure and phase behavior of lecithin-based microemulsions: A study of the chain length dependence. *Journal of Colloid and Interface Science* 156(1), pp. 43-51.

Seville, P. C., Kellaway, I. W. and Birchall, J. C. 2002. Preparation of dry powder dispersions for non-viral gene delivery by freeze-drying and spray-drying. *The Journal of Gene Medicine* 4(4), pp. 428-437.

Shinoda, K., Araki, M., Sadaghiani, A., Khan, A. and Lindman, B. 1991. Lecithin-based microemulsions: Phase behavior and microstructure. *Journal of Physical Chemistry* 95(2), pp. 989-993.

Shinoda, K. and Lindman, B. 1987. Organized surfactant systems-microemulsions. *Langmuir* 3(2), pp. 135-149.

Shoyele, S. A. and Cawthorne, S. 2006. Particle engineering techniques for inhaled biopharmaceuticals. *Advanced Drug Delivery Reviews* 58(9-10), pp. 1009-1029.

Smith, B. T. 1977. Cell line A549 – a model system for the study of alveolar type II cell function. *American Review of Respiratory Disease* 115(2), pp. 285-293.

Smyth, H. D. 2003. The influence of formulation variables on the performance of alternative propellant-driven metered dose inhalers. *Advanced Drug Delivery Reviews* 55(7), pp. 807-828.

Smyth, H. D. C., Mejia-Milan, E. A. and Hickey, A. J. 2002. The effect of ethanol on solvency vapor pressure, and emitted droplet size of solution metered dose inhalers containing HFA 134a. In: Dalby, R.N., Byron, P.R., Peart, J. and Farr, S.J. eds. *Respiratory Drug Delivery VIII.* pp. 735-738.

Snead, C. C. and Zung, J. T. 1968. The effects of insoluble films upon the evaporation kinetics of liquid droplets. *Journal of Colloid and Interface Science* 27(1), pp. 25-31.

Ståhl, K., Claesson, M., Lilliehorn, P., Lindén, H. and Bäckström, K. 2002. The effect of process variables on the degradation and physical properties of spray dried insulin intended for inhalation. *International Journal of Pharmaceutics* 233(1-2), pp. 227-237.

Stamatatos, L., Leventis, R., Zuckermann, M. J. and Silvius, J. R. 1988. Interactions of cationic lipid vesicles with negatively charged phospholipid vesicles and biological membranes. *Biochemistry* 27(11), pp. 3917-3925.

Steckel, H. and Müller, B. W. 1998. Metered-dose inhaler formulations with beclomethasone-17,21-dipropionate using the ozone friendly propellant R 134a. *European Journal of Pharmaceutics and Biopharmaceutics* 46(1), pp. 77-83.

Stein, S. W. 1999. Size distribution measurements of metered dose inhalers using Andersen Mark II cascade impactors. *International Journal of Pharmaceutics* 186(1), pp. 43-52.

Stein, S. W. and Myrdal, P. B. 2006. The relative influence of atomization and evaporation on metered dose inhaler drug delivery efficiency. *Aerosol Science and Technology* 40(5), pp. 335-347.

Stern, M., Sorgi, F., Hughes, C., Caplen, N. J., Browning, J. E., Middleton, P. G., Gruenert, D. C., Farr, S. J., Huang, L., Geddes, D. M. and Alton, E. W. 1998. The effects of jet nebulisation on cationic liposome-mediated gene transfer in vitro. *Gene Therapy* 5(5), pp. 583-593.

Sternberg, B., Sorgi, F. L. and Huang, L. 1994. New structures in complex formation between DNA and cationic liposomes visualized by freeze-fracture electron microscopy. *FEBS Letters* 356(2-3), pp. 361-366.

Stribling, R., Brunette, E., Liggitt, D., Gaensler, K. and Debs, R. 1992. Aerosol gene delivery in vivo. *Proceedings of the National Academy of Sciences of the United States of America* 89(23), pp. 11277-11281.

Talsma, H., Cherng, J. Y., Lehrmann, H., Kursa, M., Ogris, M., Hennink, W. E., Cotten, M. and Wagner, E. 1997. Stabilization of gene delivery systems by freeze-drying. *International Journal of Pharmaceutics* 157(2), pp. 233-238.

Tarara, T. E., Hartman, M. S., Gill, H., Kennedy, A. A. and Weers, J. G. 2004. Characterization of suspension-based metered dose inhaler formulations composed of spray-dried budesonide microcrystals dispersed in HFA-134a. *Pharmaceutical Research* 21(9), pp. 1607-1614.

Task group on lung dynamics 1966. Deposition and retention models for internal dosimetry of the human respiratory tract. . *Health Physics* 12(2), pp. 173-207.

Taylor, G. and Kellaway, I. 2001. Pulmonary drug delivery. In: Hillery, A., Lloyd, A. and Swarbrick, J. eds. *Drug Delivery and Targeting for Pharmacists and Pharmaceutical Scientsts*. New York: Taylor & Francis, pp. 269-300.

Templeton, N. S., Lasic, D. D., Frederik, P. M., Strey, H. H., Roberts, D. D. and Pavlakis, G. N. 1997. Improved DNA: Liposome complexes for increased systemic delivery and gene expression. *Nature Biotechnology* 15(7), pp. 647-652.

Thermo Scientific. 2009a. *Single stage N6, Andersen cascade impactor.* Available at: <URL: http://www.thermo.com/com/cda/product/detail/1,,22503,00.html> [Accessed: 1/2/2010].

Thermo Scientific. 2009b. *Two stage viable, Andersen cascade impactor.* Available at: <URL: http://www.thermo.com/com/cda/product/detail/0,1055,22538,00.html> [Accessed: 1/2/2010].

Thomas, C. E., Ehrhardt, A. and Kay, M. A. 2003. Progress and problems with the use of viral vectors for gene therapy. *Nature Reviews Genetics* 4(5), pp. 346-358.

Tomlinson, E. and Rolland, A. P. 1996. Controllable gene therapy. Pharmaceutics of non-viral gene delivery systems. *Journal of Controlled Release* 39(2,3), pp. 357-372.

Traini, D., Young, P. M., Rogueda, P. and Price, R. 2007. In vitro investigation of drug particulates interactions and aerosol performance of pressurised metered dose inhalers. *Pharmaceutical Research* 24(1), pp. 125-135.

Trout, D., Bernstein, J., Martinez, K., Biagini, R. and Wallingford, K. 2001. Bioaerosol lung damage in a worker with repeated exposure to fungi in a water-damaged building. *Environmental Health Perspectives* 109(6), pp. 641-644.

Tsan, M. F., Tsan, G. L. and White, J. E. 1997. Surfactant inhibits cationic liposome-mediated gene transfer. *Human Gene Therapy* 8(7), pp. 817-825.

Tzannis, S. T. and Prestrelski, S. J. 1999. Activity-stability considerations of trypsinogen during spray drying: Effects of sucrose. *Journal of Pharmaceutical Sciences* 88(3), pp. 351-359.

Tzou, T. Z., Pachuta, R. R., Coy, R. B. and Schultz, R. K. 1997. Drug form selection in albuterol-containing metered-dose inhaler formulations and its impact on chemical and physical stability. *Journal of Pharmaceutical Sciences* 86(12), pp. 1352-1357.

United Nations Environment Programme. 2006. *Handbook for the Montreal Protocol on Substances that Deplete the Ozone Layer* Available at: <URL: http://ozone.unep.org/Publications/MP_Handbook/Section_1.1_The_Montreal_Protocol/> [Accessed: 01/10/2009].

Van Oort, M. and Truman, K. 1998. What is a respirable dose? *Journal of Aerosol Medicine-Deposition Clearance and Effects in the Lung* 11, pp. S89-S96.

Vervaet, C. and Byron, P. R. 1999. Drug-surfactant-propellant interactions in HFA-formulations. *International Journal of Pharmaceutics* 186(1), pp. 13-30.

von Groll, A., Levin, Y., Barbosa, M. C. and Ravazzolo, A. P. 2006. Linear DNA low efficiency transfection by liposome can be improved by the use of cationic lipid as charge neutralizer. *Biotechnology Progress* 22(4), pp. 1220-1224.

Weers, J., Metzheiser, B., Taylor, G., Warren, S., Meers, P. and Perkins, W. R. 2009. A gamma scintigraphy study to investigate lung deposition and clearance of inhaled amikacin-loaded liposomes in healthy male volunteers. *Journal of Aerosol Medicine and Pulmonary Drug Delivery* 22(2), pp. 131-138.

Weis, C. P., Intrepido, A. J., Miller, A. K., Cowin, P. G., Durno, M. A., Gebhardt, J. S. and Bull, R. 2002. Secondary aerosolization of viable Bacillus anthracis spores in a contaminated US Senate Office. *Journal of the American Medical Association* 288(22), pp. 2853-2858.

Wendt, S. L., George, K. L., Parker, B. C., Gruft, H. and Falkinham, J. O. 1980. Epidemiology of infection by nontuberculous Mycobacteria .3. Isolation of potentially pathogenic Mycobacteria from aerosols. *American Review of Respiratory Disease* 122(2), pp. 259-263.

Wennerstrom, H., Soderman, O., Olsson, U. and Lindman, B. 1997. Macroemulsions versus microemulsions. *Colloids and Surfaces A: Physicochemical and Engineering Aspects* 123-124, pp. 13-26.

Westech Instruments. 2009. *Westech FPD Impactor.* Available at: <URL: http://www.westechinstruments.com/> [Accessed: 1/1/2009].

Wilke, M., Fortunati, E., vandenBroek, M., Hoogeveen, A. T. and Scholte, B. J. 1996. Efficacy of a peptide-based gene delivery system depends on mitotic activity. *Gene Therapy* 3(12), pp. 1133-1142.

Williams III, R. O. and Hu, C. J. 2000. Moisture uptake and its influence on pressurized metered-dose inhalers. *Pharmaceutical Development and Technology* 5(2), pp. 153-162.

Williams III, R. O. and Liu, J. 1999. Formulation of a protein with propellant HFA 134a for aerosol delivery. *European Journal of Pharmaceutical Sciences* 7(2), pp. 137-144.

Williams III, R. O., Liu, J. and Koleng, J. J. 1997. Influence of metering chamber volume and water level on the emitted dose of a suspension-based pMDI containing propellant 134a. *Pharmaceutical Research* 14(4), pp. 438-443.

Woelders, H. and Chaveiro, A. 2004. Theoretical prediction of `optimal' freezing programmes. *Cryobiology* 49(3), pp. 258-271.

Xenariou, S., Griesenbach, U., Liang, H. D., Zhu, J., Farley, R., Somerton, L., Singh, C., Jeffery, P. K., Ferrari, S., Scheule, R. K., Cheng, S. H., Geddes, D. M., Blomley, M. and Alton, E. 2007. Use of ultrasound to enhance nonviral lung gene transfer in vivo. *Gene Therapy* 14(9), pp. 768-774.

Xu, Y. and Szoka, F. C., Jr. 1996. Mechanism of DNA release from cationic liposome/DNA complexes used in cell transfection. *Biochemistry* 35(18), pp. 5616-5623.

Zabner, J., Cheng, S. H., Meeker, D., Launspach, J., Balfour, R., Perricone, M. A., Morris, J. E., Marshall, J., Fasbender, A., Smith, A. E. and Welsh, M. J. 1997. Comparison of DNA-lipid complexes and DNA alone for gene transfer to cystic fibrosis airway epithelia in vivo. *Journal of Clinical Investigation* 100(6), pp. 1529-1537.

Zabner, J., Fasbender, A. J., Moninger, T., Poellinger, K. A. and Welsh, M. J. 1995. Cellular and molecular barriers to gene transfer by a cationic lipid. *Journal of Biological Chemistry* 270(32), pp. 18997-19007.

Zarur, A. J., Mehenti, N. Z., Heibel, A. T. and Ying, J. Y. 2000. Phase behavior, structure, and applications of reverse microemulsions stabilized by nonionic surfactants. *Langmuir* 16(24), pp. 9168-9176.

Zelphati, O., Nguyen, C., Ferrari, M., Felgner, J., Tsai, Y. and Felgner, P. L. 1998. Stable and monodisperse lipoplex formulations for gene delivery. *Gene Therapy* 5(9), pp. 1272-1282.

Ziegler, J. and Wachtel, H. 2005. Comparison of cascade impaction and laser diffraction for particle size distribution measurements. *Journal of Aerosol Medicine-Deposition Clearance and Effects in the Lung* 18(3), pp. 311-324.

Zou, Y. Y., Tornos, C., Qiu, X., Lia, M. and Perez-Soler, R. 2007. p53 aerosol formulation with low toxicity and high efficiency for early lung cancer treatment. *Clinical Cancer Research* 13(16), pp. 4900-4908.

# Appendix

# Publications, Conferences and Meetings

## Publications

During my postgraduate studies the following peer-reviewed paper (attached) and abstracts were published:

**Journal Publications**

Bains, B.K. Birchall, J.C. Toon, R. Taylor, G. 2010. In vitro reporter gene transfection via plasmid DNA delivered by metered dose inhaler. *Journal of Pharmaceutical Sciences* 99(7), pp. 3089-3099.

**Conference Publications**

Bains, B.K. Taylor, G. Toon, R. Jinks, P. Birchall, J.C. 2008. Maintenance of pDNA viability following aerosolisation. In *Proceedings of Drug Delivery to the Lungs* 19, pp 67-70.

Bains, B.K. Birchall, J.C. Jinks, P. Toon, R. Taylor, G. 2008. In vitro reporter gene transfection via plasmid DNA delivered by metered dose inhaler. In *Proceedings of Respiratory Drug Delivery* 11, 2, pp 457-460.

Bains, B.K. Taylor, G. Toon, R. Birchall, J.C. 2007. Novel pDNA Particulates for Pulmonary Gene Delivery. In *Proceedings of Drug Delivery to the Lungs* 18, pp 196-199.

Bains, B.K. Taylor, G. Toon, R. Birchall, J.C. 2007. Novel nanoparticles for pulmonary gene delivery. *Journal of Pharmacy and Pharmacology* 59, pp. A31-A32.

James, J. Davies, M.C. Bains, B.K. Toon, R.C. Jinks, P. Roberts, C.J. 2007. The use of AFM to assess macromolecule suspension formulations for metered dose inhalers. *Journal of Pharmacy and Pharmacology* 59, pp. A45-A45.

## Conferences and Meetings

During my postgraduate studies I presented at the following conferences:

**Oral presentation**

The Academy of Pharmaceutical Sciences: Inhalation (APS), Nottingham 2009. (Prize winner for oral presentation)

Drug Delivery to the Lungs 19 (DDL), Edinburgh 2008.

**Poster presentation:**

Young Pharmaceutical Scientist, Nice (France) 2009.

Cellular Delivery of Therapeutic Macromolecules (CDTM), Cardiff 2008.

Respiratory Drug Delivery 11 (RDD), Arizona (USA) 2008.

Welsh School of Pharmacy Postgraduate Research Day, Cardiff 2008.
(Prize winner for poster presentation)

Drug Delivery to the Lungs 18 (DDL), Edinburgh 2007.
(Prize winner for poster presentation)

Formula V: Formulating across boundaries, Potsdam (Germany) 2007.

British Pharmaceutical Conference (BPC), Manchester 2007.

European Science Foundation Summer School in Nanomedicine (ESF), Cardiff 2007.

Academy of Pharmaceutical Sciences: Inhalation (APS), Bath 2007.

# *In Vitro* Reporter Gene Transfection via Plasmid DNA Delivered by Metered Dose Inhaler

BALJINDER K. BAINS,[1] JAMES C. BIRCHALL,[1] RICHARD TOON,[2] GLYN TAYLOR[1]

[1]Welsh School of Pharmacy, Cardiff University, Redwood Building, King Edward VII Avenue, Cardiff CF10 3NB, UK

[2]3M Drug Delivery Systems, Loughborough, UK

*Received 19 June 2009; revised 17 November 2009; accepted 22 December 2009*

*Published online in Wiley InterScience (www.interscience.wiley.com). DOI 10.1002/jps.22085*

**ABSTRACT:** Aerosolised DNA administration could potentially advance the treatment of inheritable lung diseases, lung malignancies and provide genetic immunisation against infection. Jet nebulisation, the current standard for introducing DNA formulations into the lung, is inherently inefficient. Pressurised metered dose inhalers (pMDIs) offer a potentially more efficacious and convenient alternative, especially for repeat administration. We aim to modify a novel low-energy nanotechnology process to prepare surfactant-coated pDNA nanoparticles for pulmonary gene delivery via a pMDI. Water-in-oil microemulsions containing green fluorescent protein reporter plasmid were snap-frozen and lyophilised. Lyophilised pDNA, in some cases following a surfactant wash, was incorporated into pMDIs with hydrofluoroalkane 134a (HFA134a) propellant and ethanol as cosolvent. To assess biological functionality, A549 human lung epithelial cells were exposed to aerosolised pDNA particles in the presence of dioleoyltrimethylammonium propane (DOTAP). Transfection studies demonstrated that pDNA biological functionality was maintained following aerosolisation. *In vitro* toxicity assays (MTT) showed no significant cell viability loss following aerosolised pDNA treatment. We have demonstrated that pDNA particles can be incorporated into an HFA134a formulation and aerosolised using a standard valve and actuator. Particles prepared by this novel process have potential for stable and efficient delivery of pDNA to the lower respiratory tract via standard pMDI technology. © 2010 Wiley-Liss, Inc. and the American Pharmacists Association J Pharm Sci

**Keywords:** pulmonary drug delivery; pressurised metered dose inhaler; aerosol; plasmid DNA; nonviral gene delivery; nanotechnology; formulation; microemulsion

## INTRODUCTION

Pulmonary administration of nucleic acids may be particularly relevant for treating localised lung disorders of genetic origin.[1,2] The pulmonary route would also be appropriate for the delivery of inhaled DNA vaccines, as this would follow the natural route of infection for many common airborne diseases,[3,4] such as measles,[5] *Mycobacterium tuberculosis*[6] and respiratory syncytial virus.[7] Cellular uptake of naked deoxyribonucleic acid (DNA) in its native form remains relatively inefficient.[8,9] As a consequence, gene transfer vectors are employed to promote cellular uptake and processing of the nucleic acid cargo.[8,10,11] Although viral gene delivery systems are often very efficient at stimulating cell transfection and can be modified to reduce both their pathogenicity and ability to replicate, they still face inherent safety and immunogenicity issues and are sometimes inappropriate for repeated use.[12] As an alternative, nonviral gene vectors employ synthetic carriers that complex with plasmid DNA (pDNA) to form particulates that are generally regarded as safer and less immunogenic,[13] although not as efficient.[14,15] In this category of nonviral agents, cationic lipids and liposomes have demonstrated proof of principle for gene transfer to the airway for over two decades.[16–18] Whilst impressive results have been achieved in some animal models including mice,[18,19] rats,[20,21] rabbits,[22] monkeys[17] and pigs,[23] nonviral gene transfer has yet to deliver a clear therapeutic benefit in human studies. For example, although the correction of the chloride transport defect in cystic fibrosis has been demonstrated to some extent in most clinical trials,[24,25] the level of effect has been found to be

*Correspondence to*: Glyn Taylor (Telephone: +44-29-208-75822; Fax: +44-29-208-74149; E-mail: taylorg@Cardiff.ac.uk)

Journal of Pharmaceutical Sciences

variable, usually lasting for <15 days,[26,27] and thus will require repeated administration. Clinical trials using gene therapy have also been undertaken in an attempt to restore normal α-1 antitrypsin deficiency (AAT) function. This involved either nasal instillation of the AAT gene with a cationic liposome,[28] or intramuscular injection of the gene with a viral vector.[29] As with the cystic fibrosis trials, although proof of principle of successful gene expression has been demonstrated, there was a notable lack of significant functional correction.

It is accepted, therefore, that the development of more efficient vectors is essential for the progression of gene delivery science towards the clinic.[25,30,31] Equally, however, the administration method selected to deliver the therapeutic material to the cellular target is of paramount importance, yet is often overlooked. The efficiency of delivery to the cell targets, the avoidance of biological barriers and clearance mechanisms,[32] the physical and chemical durability of the nucleic acid cargo during delivery[1] and the manageable dose are all critical parameters that require optimisation.[33]

To date, most preclinical and clinical research studies in pulmonary gene therapy have used nebulisers to deliver the gene 'cargo' in liquid suspension.[24,25,34] Nebulisation is, however, an inherently inefficient process for the delivery of large charged macromolecules[4,35] due to: adhesion of the formulated therapeutic agent to the device components, large residual dead volume, limitations on suspension concentration without causing precipitation, chemical degradation through high shearing forces[35–37] and evaporation.[19]

Conventional jet and ultrasonic nebulisers have both been reported to extensively damage naked pDNA due to the shearing forces generated on creation of the aerosol.[37–39] Recently, newer nebuliser technologies have claimed greater pDNA aerosolisation efficiency.[40] Aerosolisation, based on electrohydrodynamic (EHD) delivery for example, has been found to cause no detectable pDNA degradation or loss in transfection efficiency in plasmids up to 15 kb in size.[40] Whilst these encouraging new-generation nebuliser technologies are under development, pressurised metered dose inhalers (pMDIs) offer a sparsely investigated alternative to nebulisers. Potential advantages of pMDIs over other pulmonary delivery systems include their portability, low cost, rapid drug administration and disposability.[41] Many doses can be stored in a relatively small canister and the metering valve ensures reproducible dose delivery. pMDIs offer a more convenient alternative to nebulisers, especially for therapies requiring repeated administration.

To date, there has been very little published research on methods for incorporating pDNA into pMDIs.[42] Brown and Chowdhury[42] demonstrated that pDNA, lyophilised in the presence of a both nonionic (Tween 40) and ionic (lipofectin or lipofectamine) surfactant, could be incorporated into a metered dose inhaler resulting in suspended pDNA particles in dimethylether propellant. In addition, they demonstrated that gene expression could be obtained in the lungs of mice following exposure to the aerosolised pDNA formulation.[42] Clearly, further investigations in this area are warranted.

This study aims to explore the potential of adapting a formulation process to prepare surfactant-coated pDNA particulates suitable for pulmonary gene delivery.[43] Previously, this technology had only been investigated with low molecular weight drugs in nanoparticles in pMDI formulations. The approach utilises a reverse microemulsion as a 'template'. Reverse micelles containing the drug are subsequently reduced to solid surfactant-coated nanoparticles using lyophilisation, prior to pressure filling with HFA 134a propellant. This investigation aims to develop an optimised surfactant microemulsion system based on HLB and HFA solubility, to confer pDNA stability and propellant dispersion and retain pDNA biological activity on aerosolisation.

## MATERIALS AND METHODS

### Materials

Chemicals were used as received. Tris-borate EDTA buffer (TBE Buffer) electrophoresis grade, propan-2-ol, lecithin (egg ~90%), ethidium bromide (EtBr) solution and ethanol (absolute, analytical grade reagent) were from Fisher Scientific UK Ltd. (Loughborough, UK). Iso-octane (2,2,4-trimethylpentane 99+ %), sodium chloride (NaCl), trizma HCl, proteinase K, sucrose 99+ %, phosphate-buffered saline (PBS) pH 7.4 ($Mg^{2+}$ and $Ca^{2+}$ free), trypan blue and MTT-based assay kit were from Sigma-Aldrich Ltd. (Poole, UK). Agarose (LE analytical grade) and Wizard® DNA Clean-Up System product A7280 were from Promega UK Ltd. (Southampton, UK). Dulbecco's Modified Eagle's Medium (DMEM), foetal bovine serum, penicillin G 5000 units/mL, streptomycin sulphate 5000 μg/mL, trypsin-EDTA and Library Efficiency® DH5α Competent Cells were from Invitrogen Ltd. (Paisley, UK). Other reagents used were: 5× coloured loading buffer blue (Bioline Ltd., London, UK); A549 mammalian cell line (ECACC, Salisbury, UK); pEGFP-N1 (4.7 kb) reporter pDNA (Clontech Laboratories, Inc., Palo Alto, CA); Qiagen Plasmid Mega Kit (Qiagen, Crawley, UK); and 1,2-Dioleoyl- 3-Trimethylammonium propane (methyl sulphate salt) (DOTAP) (Avanti Polar Lipids, Inc., Alabaster, AL). HFA 134a was a generous gift of INEOS Fluor Ltd. (Runcorn, UK).


DOI 10.1002/jps

## Experimental Methods

### *Optimisation of Microemulsion Formulation Parameters*

Water-in-oil microemulsions were prepared at ambient temperatures using distilled water (aqueous phase), lecithin in propan-2-ol (1:3, w/w) (stabilising surfactant system) and iso-octane (organic phase). *iso*-octane was added to the surfactant: co-surfactant mixture in a 15 mL polypropylene centrifuge tube and gently agitated using a vortex mixer. Nineteen formulations were investigated with surfactant concentrations, based on previous studies, ranging from 30% to 64% (w/w). The water content was sequentially increased to determine the phase boundary between a clear micellar (isotropic) phase and an opaque (nonisotropic) multiphase system. Samples that were potentially isotropic were visually inspected at 10 min and 24 h, after the final water addition, to ensure that equilibrium had been fully established. Any visual changes over this period were noted. A pseudoternary phase diagram was constructed to show the phase boundary and identify optimum microemulsion formulation constituent ratios.

### *Preparation of pDNA Particles*

The 4.7 kb pDNA construct pEGFP-N1, encoding the enhanced green fluorescent protein (GFP) reporter gene under the control of a cytomegalovirus promoter, was amplified using a transformed DH5α strain of *Escherichia coli*, using kanamycin to ensure selective growth of transformed bacteria. The pDNA was purified using the Qiagen Plasmid Mega Kit. Prior to subsequent use, the pDNA concentration and purity were determined by the 260/280 UV absorbance ratio and plasmid integrity was assessed by agarose gel electrophoresis using a specific restriction enzyme digest.

The pEGFP-N1 and 3% (w/v) sucrose, as lyoprotectant, were incorporated into the aqueous phase of the optimised microemulsion system. The microemulsions were snap-frozen by submersion in liquid nitrogen and lyophilised for 24 h using a Heto Drywinner freeze-drier (Heto-Holten, Alleroed, Denmark) with the condenser chamber set at −110°C. The process of freeze-drying was carried out by applying temperatures and pressures below that of the sample triple point in order to promote sublimation and subsequent removal of solvent from the solid phase directly into the gaseous phase. Excess surfactant in the microemulsion and resulting particulates could potentially adversely affect particulate dispersibility, physical stability, toxicity and pDNA cellular functionality. A sequential washing method was therefore adapted from Dickinson et al.[43] for certain test samples, whereby excess surfactant was removed from the freeze-dried pEGFP-N1 particles using an organic solvent followed by centrifugation.

### *Analysis of Lyophilised pDNA Particles*

**Integrity of Lyophilised pDNA.** Agarose gel electrophoresis, with EtBr staining, was used to determine the physical integrity of the processed pEGFP-N1. Following the microemulsion and solvent removal stages, surfactant from the lyophilised surfactant-coated pEGFP-N1 was removed using a Wizard® DNA Clean-Up System. pDNA samples were mixed with gel-loading dye and loaded into the wells of a 1% (w/v) agarose gel. The gel was developed for 30 min at 200 V and analysed using Molecular Analyst® software and Bio-Rad Gel Doc 1000 (Bio-Rad Laboratories Ltd., Hertfordshire, UK) or Alpha DigiDoc™ RT (Alpha Innotech Corporation, San Leandro, CA, USA).

**Measurement of Particle Size.** The mean diameter of the solvent-washed pDNA particles was determined by photon correlation spectroscopy using a Coulter® N4 Plus (Coulter Electronics Ltd., Luton, UK). Particles of lyophilised pEGFP-N1 were dispersed in iso-octane and agitated using a vortex mixer for ~3 min. Samples were transferred into a quartz cuvette, which was sealed to prevent evaporation. Measurements were expressed using the unimodal size distribution model and repeated six times.

### *Assessing the Transfection Competency of Lyophilised pDNA Particulates (before Propellant Dispersion and Aerosolisation)*

**Cell Culture.** All cell investigations were performed using A549 human lung epithelial cells, which were maintained as adherent monolayer cultures in 25 $cm^2$ angled neck, cell culture flasks (T25) (Corning Costar Ltd., High Wycombe, UK) in growth medium (10% fetal bovine serum, 2% penicillin/streptomycin 5000 IU/mL and DMEM to 100%). Cells were incubated in a humidified incubator at 37°C containing 5% $CO_2$. Confluent adherent cells were released enzymatically (every 72 h) using trypsin-EDTA and reseeded at $1 \times 10^6$ cells/T25 flask. All cells used in the transfection studies were a result of at least two passages, post-thawing, and were in their log growth phase, as determined by previous cell growth studies. Cells were seeded into 24-well plates at a density of $4 \times 10^4$ cells/$cm^2$ and submerged under 1 mL growth media 48 h before transfection.

**Cell Treatment.** Cells were subjected to one of seven treatments (Fig. 1): (i) DMEM alone (no pDNA), (ii) unprocessed pEGFP-N1 (positive control), (iii) an unwashed formulation of lyophilised DNA-loaded

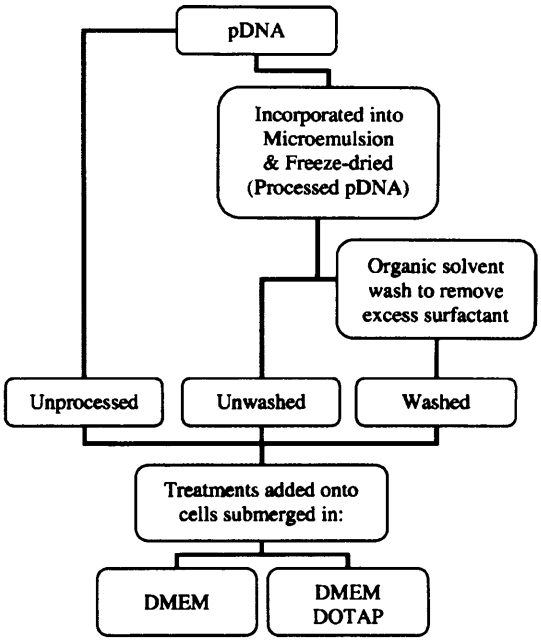


**Figure 1.** Diagrammatic representation of the production of samples for subsequent *in vitro* analysis.

particles and (iv) a solvent-washed variant of formulation (iii). In the case of (ii), (iii) and (iv), the formulations were added directly onto cells covered with (A) DMEM alone or (B) DMEM-containing dioleoyl-trimethylammonium proprane (DOTAP) liposomes, which had been previously prepared through solvent evaporation, resuspension in sterile water and membrane extrusion using 100 nm polycarbonate filters (Millipore, Watford, UK) and an Extruder™ (Lipex Biomembranes, Inc., Vancouver, Canada). A549 cells, in each well of a 24-well plate, were treated with the equivalent of 5 $\mu$g pEGFP-N1. In the case of cells treated in the presence of DOTAP, a 6:1 (w/w) DOTAP liposome:DNA ratio was used. All treatments were conducted in serum-free DMEM. Treated cells were incubated in a humidified incubator (37°C/5% $CO_2$). After a period of 6 h, cells were washed once with 1 mL PBS (pH 7.4) and replenished with 1 mL of growth media.

**Analysis of Gene Expression.** The biological functionality of the aerosolised reporter plasmid pEGFP-N1, was assessed qualitatively at 42 h post-treatment, using fluorescent microscopy. Following microscopy, cells were surface rinsed with 1 mL PBS, trypsinised with 150 $\mu$L trypsin–EDTA solution, and resuspended in 600 $\mu$L growth media. The percentage of cells displaying GFP-associated fluorescence (FL1-H) was quantified by flow cytometry (FACSCalibur™ system; Becton Dickinson Biosciences, Oxford, UK) with the analysis by WinMDI™ Software (Joseph Trotter, The Scripps Institute, La Jolla, CA), as described previously.[44]

### *Production of pMDI Formulations*

Two pMDI formulations were aerosolised and investigated for pEGFP-N1 biological functionality. The first 'unwashed' formulation used unwashed surfactant-coated, lyophilised pEGFP-N1 particles. The second 'washed' formulation used the same batch of particles after washing to remove excess surfactant. Particles were added directly to fluorinated ethylene propylene (FEP) coated aluminium canisters (3M Drug Delivery Systems, Loughborough, UK) and dispersed using ethanol as a cosolvent (8% v/v). Spraymiser™ 50 $\mu$L retention valves (3M Drug Delivery Systems) were crimped onto the aluminium canisters and HFA 134a was added using a Pamasol® semi-automatic filling and crimping machine (Pamasol Willi Mäder AG, Pfäffikon SZ, Switzerland). Washed formulations were also prepared in plastic polyethylene terephthalate (PET) pMDI vials (3M; Drug Delivery Systems), for visual assessment of physical stability and dispersion homogeneity. pMDI vials were stored at room temperature with visual observation at 24 h and 5 months.

### *Assessment of pDNA pMDI Formulations*

**Microscopic Characterisation of Particles.** The solvent-washed pDNA pMDI formulation was actuated into a Volumatic™ spacer (Allen and Hanburys, Middlesex, UK) connected to an eight-stage Andersen-type cascade impactor (ACI) (Westech Instrument Services Ltd., Bedfordshire, UK). Double-sided carbon tape was attached at various points on the wall of the spacer and the plates in the ACI. The ACI was operated at a flow rate of 28.3 L/min. Particles that had deposited on the carbon tape, postactuation, were mounted onto a scanning electron microscopy (SEM) aluminium stub and sputter coated with gold before being viewed using a Philips XL-200 Scanning Electron Microscope (TEI Company, Eindhoven, the Netherlands).

**Aerosol Delivery to Cell Culture Flask.** Initial pilot studies, using pMDIs containing Brilliant Blue dye, were carried out to determine the most efficient orientation for delivery to cell culture medium (Fig. 2). Brilliant Blue actuated from the pMDI five times into a T25 cell culture flask, containing 6 mL of water, was assayed by UV absorbance at 629 nm. Data from the two actuation orientations were compared with a positive control. Control absorbance data were generated by actuating the Brilliant Blue pMDI into a conical flask containing 6 mL of water and swirling the water around the flask to collect the total emitted dye present in the flask.


DOI 10.1002/jps

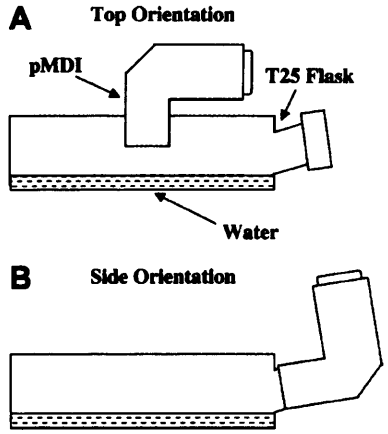


**Figure 2.** Schematic representation of actuation into a cell culture flask. (A) Top orientation with actuation depositing directly onto liquid; (B) side orientation with actuation depositing across the liquid.

**Assessment of pDNA Functionality Following Actuation from a pMDI.** Biological functionality of DNA actuated from the pMDI formulation was assessed in A549 cells seeded into T25 flasks at a density of $4 \times 10^4$ cells/cm$^2$ and cultured under the aforementioned culture conditions to 50% confluency. Cells were subjected to the following treatments: (i) DMEM (negative control), (ii) an unwashed formulation of lyophilised DNA-loaded microemulsion incorporated into a pMDI, (iii) a solvent-washed variant of formulation (ii). In the case of (ii) and (iii), the formulations were actuated from pMDI canisters directly onto cells covered with (A) DMEM, and (B) DMEM-containing extruded DOTAP liposomes. Each T25 flask was treated with the equivalent of 15 $\mu$g aerosolised pEGFP-N1. In the case of cells treated in the presence of DOTAP, a ratio of 6:1 (w/w) DOTAP:washed DNA was used, based on the assumption that 15 $\mu$g of pDNA would be successfully expelled from the pMDI. MDIs were primed by firing five shots to waste. To reduce any cell death, due to aerosol cold freon effect, the T25 flasks were placed on prewarmed saline infusion bags with 30 s intervals between actuations.

### *Cell Toxicity Assay*

*In vitro* toxicity of treatments was assessed using the colorimetric 3-[4,5–dimethylthiazol-2-yl]-2, 5-diphenyl tetrazolium bromide (MTT) based assay kit. Initially, A549 cells were treated with pEGFP-N1 from pMDI formulations in T25 flasks. After 42 h post-treatment, cells were washed twice with 5 mL aliquots of cold PBS (pH 7.4). PBS was removed and 1 mL trypsin–EDTA was added to the cell surface. After 1 min, the trypsin was removed from the wells and the T25 flasks incubated in a humidified incubator at 37°C containing 5% $CO_2$ for 10 min. After 10 min incubation, cells were re-suspended in growth media.

Reconstituted MTT was added at 10% of the culture medium volume in a 96-well plate. Samples were incubated (37°C/5% $CO_2$) for 4 h. Subsequently, formazan crystals were dissolved using 100 $\mu$L of MTT solubilisation solution. Cell culture samples were incubated (37°C/5% $CO_2$) for a further 30 min and assayed by UV absorbance at 570 nm using a Sunrise$^{TM}$ microplate reader (Tecan Trading AG, Männedorf, Switzerland). Background absorbance, measured at 690 nm, was subtracted from the 570-nm readings automatically using Magellan$^{TM}$ data reduction software (Tecan Trading AG).

### Statistical Analysis

One-way analysis of variance (ANOVA) was followed by either a Duncan's multiple range test, used to compare multiple groups, or Dunnett's test, used to compare groups against a reference group with significant differences indicated by $p$-values $<0.05$ or $<0.001$. Results are summarised as mean $\pm$ SD.

## RESULTS

Initial studies were aimed to identify optimised constituent ratios that form stable isotropic water-in-oil microemulsions. Microemulsions with a surfactant to water ratio of approximately 1.5 and greater formed stable isotropic systems. Unstable biphasic systems were formed when the surfactant to water ratio fell below 1.5. Stable microemulsion systems with the lowest surfactant to water ratio were deemed as optimal from a drug loading and surfactant content perspective. Optimised formulations resulted in effective incorporation of pDNA (1.2 mg) into the aqueous pool (2.08 g) of reverse micelles.

Agarose gel electrophoresis with EtBr staining was used to assess the physical integrity of processed pDNA. Figure 3 shows the supercoiled signal band relating to pEGFP-N1, prior to and following freeze-drying and solvent wash cycles. The integrity of pEGFP-N1 was maintained through processing, although a partial reduction in pDNA signal intensity was observed. Semi-quantitative signal analysis was used to compare fluorescence emission. The supercoiled band of unprocessed pDNA contributed $88 \pm 7\%$ (mean $\pm$ SD, $n = 3$) of emitted fluorescence from the total pDNA. Once the pEGFP-N1 had been incorporated into a microemulsion and freeze-dried, fluorescence from the supercoiled fraction was reduced to $81 \pm 12\%$ and then further reduced to $76 \pm 14\%$ of the total after solvent wash.

Figure 4 shows the result of an *in vitro* transfection experiment to assess the biological functionality of pDNA following processing into particles. DOTAP

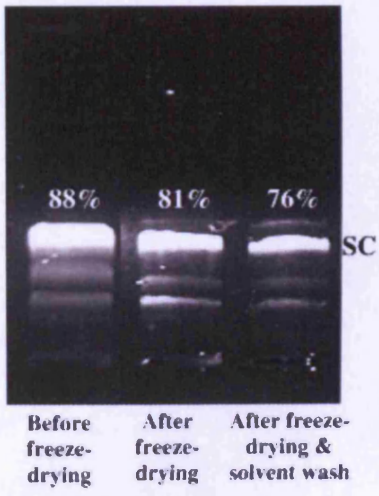


**Figure 3.** A typical gel electrophoresis image of pEGFP before and after freeze-drying and solvent washes. The percentage values represent a semi-quantitative analysis of the ratio of fluorescence emitted from the supercoiled band compared with the total pDNA. All percentages are mean of $n = 3$ (SC, supercoiled fraction).

cationic lipid was added to selected cell culture flasks to form an electrostatic complex with the pDNA and enable cell transfection. A significant increase ($p < 0.001$) in the percentage of fluorescent cells, attributed to expression of GFP, was observed when A549 cells were treated with unprocessed (control) pEGFP-N1 in the presence of DOTAP ($14.49 \pm 1.76\%$). The unwashed surfactant-coated pDNA particles did not mediate any gene expression, regardless of whether DOTAP was present ($0.59 \pm 0.11\%$) or not ($0.67 \pm 0.31\%$). Gene expression was, however, statistically comparable ($p > 0.05$) with the positive control in DOTAP-supplemented samples that had undergone the washing procedure to remove excess surfactant ($14.28 \pm 1.82\%$). Formulations treated in the absence of DOTAP showed no significant increase ($p > 0.05$) in cell fluorescence against the negative control. Fluorescent microscopy inserts confirmed the presence of fluorescent protein in transfection-positive cells.

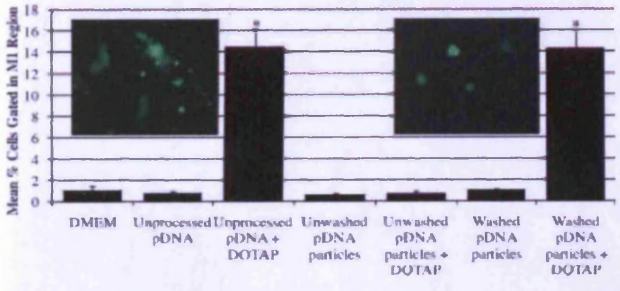


**Figure 4.** Quantitative gene expression of pDNA particles. A549 Cells were surface-treated with (i) DMEM, (ii) unprocessed pEGFP-N1 into DMEM alone, (iii) unprocessed pEGFP-N1 into DMEM-containing DOTAP, (iv) unwashed pEGFP-N1 particles into DMEM alone, (v) unwashed pEGFP-N1 particles into DMEM-containing DOTAP, (vi) solvent-washed pEGFP-N1 particles into DMEM alone and (vii) solvent-washed pEGFP-N1 particles into DMEM-containing DOTAP. Data are represented as mean ± SD, $n = 6$. * denotes a significant difference from the control ($p < 0.001$). Inset: Fluorescence microscopy image of A549 cells following treatment with (A) unprocessed pEGFP-N1 into media-containing DOTAP, and (B) solvent-washed pEGFP-N1 formulation into media-containing DOTAP.

SEM images of material aerosolised from the pMDI formulation and collected using an ACI showed the presence of DNA-lyoprotectant aggregates. The micrographs in Figure 5a and b confirm the presence of a heterogeneous population comprising rounded and angular particle protrusions from a continuous matrix. Although variable in size, all of these particle protrusions were <10 μm in diameter. Microscopic observations showed that ACI stages four (Fig. 5a) and five (Fig. 5b) with cut-off diameters of 2.1 and 1.1 μm respectively contained the greatest number of particle protrusions, potentially indicating that the majority of the aerosolised material is within the respirable size range. However, SEM images (Fig. 5a and b) revealed the presence of particle protrusions larger than the quoted cut-off diameters. Possible reasons for this could include particle agglomeration upon impaction onto each of the stages and changes in particle size through SEM analysis. Particle size analysis using photon correlation spectroscopy was also performed on solvent-washed

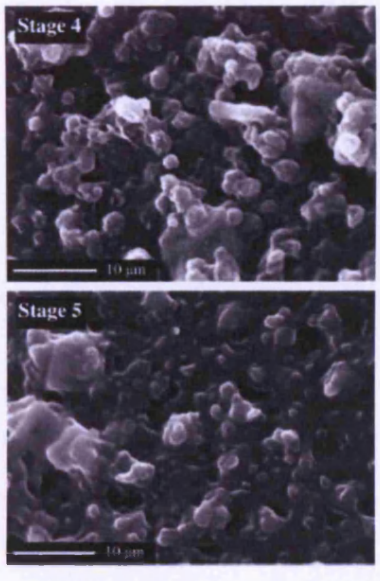


**Figure 5.** Scanning electron micrographs of a solvent-washed freeze-dried pMDI formulation containing pEGFP-N1 and sucrose collected at (a) Stage 4 and (b) Stage 5 of an ACI. Scale bar = 10 μm.


DOI 10.1002/jps

lyophilised particles prior to incorporation into propellant dispersions. Analysis revealed particles with a mean diameter of $1.9\,\mu m \pm 0.8$ (mean $\pm$ SD, $n = 6$).

Visual observations of the washed pDNA particulate formulation, in transparent PET pMDI vials, provided a simple indication to the physical stability of the formulation *in situ*. When the surfactant-coated lyophilised pDNA particles were subjected to eight cycles of the solvent-wash procedure, excess surfactant was removed to leave an off-white powder. Upon addition of the washed pEGFP-N1 particles into a pMDI vial, initial observations showed that particles were suspended throughout the propellant co-solvent mix. After a 24 h period, suspended particles were still visible, although most particles had formed loose sedimented floccules that were easily dispersed by one inversion of the PET vial. Redispersible floccules were also observed after a period of 5 months.

Prior to experiments assessing biological functionality of aerosolised pDNA particles, pilot studies, using Brilliant Blue dye actuated from a pMDI into T25 flasks, were performed to ascertain the most quantitatively efficient orientation to actuate processed pDNA formulations onto adherent cells *in vitro* (Fig. 6). Figure 6 shows that actuating the Brilliant Blue pMDI from the top orientation gave a greater relative collection efficiency (78% of the actuated dye was deposited into the collection medium at the bottom of the flask) than actuating onto a flask from the side orientation (19% deposition). In each case, the metering chamber of the valve was allowed to fill in the upright position prior to actuation. Statistical analysis confirmed no significant reduction ($p > 0.05$) in the concentration of deposited dye when actuated from the top orientation ($0.15\,\mu g/6\,mL \pm 0.04\,\mu g$, mean $\pm$ SD, $n = 3$) compared with the control ($0.19 \pm 0.01\,\mu g$).

As a result of the Brilliant Blue pilot study, pDNA-loaded pMDI formulations were actuated onto A549 cells directly from above. Flow cytometry was used to determine whether pEGFP-N1 remained biologically active subsequent to particle processing, propellant dispersion and actuation from a pMDI canister and valve (Fig. 7). As previously, DOTAP cationic lipid was added to selected cell culture flasks to facilitate *in vitro* cell transfection. No increase in gene expression was observed for the unwashed aerosolised formulation ($p > 0.05$) regardless of whether it was actuated in the presence ($1.35 \pm 0.33\%$) or absence ($1.16 \pm 0.94\%$) of DOTAP. Aerosolising the washed formulation onto cells in normal media also conferred no significant rise in the percentage of cells emitting GFP fluorescence ($1.74 \pm 0.67\%$, $p > 0.05$). However, a significant increase in the percentage of cells expressing GFP ($p < 0.001$) was apparent following aerosolisation of the washed pEGFP-N1 particulates into DOTAP-containing media ($24.75 \pm 2.35\%$, $n = 4$) compared with control cells ($0.96 \pm 0.30\%$).

Fluorescence microscopy (Fig. 7, inset) further confirmed the presence of gene expression in cells following actuation of the washed formulation from a pMDI onto cells in DOTAP-supplemented media.

An *in vitro* MTT toxicity assay was performed on A549 cells to determine whether any component of the pEGFP-N1 particulate pMDI formulation caused a reduction in cell viability (Fig. 8). Statistical analysis showed no significant loss in cell viability ($p > 0.05$) between blank, untreated cells and cells treated with the washed, aerosolised pDNA formulation. A significant reduction in cell viability ($p < 0.05$) was, however, observed when DOTAP was added to

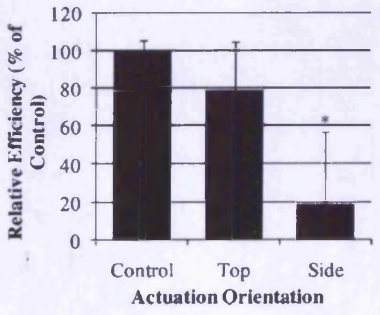


**Figure 6.** Relative deposition efficiency of Brilliant Blue when actuated from a pMDI in the top and side orientation relative to the control. Data are represented as mean $\pm$ SD, $n = 3$. * denotes a significant difference from the control ($p < 0.05$).

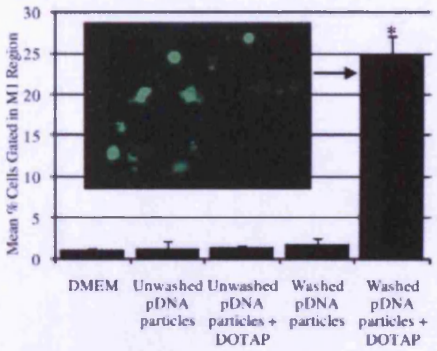


**Figure 7.** Quantitative gene expression of aerosolised pDNA particles. A549 cells were surface-treated with (i) DMEM, (ii) unwashed pEGFP-N1 particles into DMEM alone, (iii) unwashed pEGFP-N1 particles into DMEM-containing DOTAP, (iv) solvent-washed pEGFP-N1 particles into DMEM alone and (v) solvent-washed pEGFP-N1 particles into DMEM-containing DOTAP. Data are represented as mean $\pm$ SD, $n = 4$. * denotes a significant difference from the control ($p < 0.001$). Inset: Fluorescence microscopy image of A549 cells following treatment with solvent-washed pEGFP-N1 formulation into media-containing DOTAP.

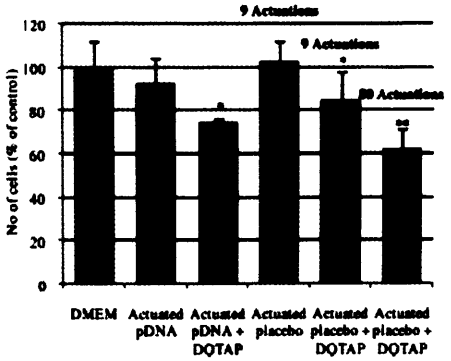


**Figure 8.** Percentage cell viability of cells following actuation of treatments. Cells were surface-treated with: (i) DMEM (control cells: 100% viability), (ii) nine actuations of a solvent-washed pEGFP-N1 pMDI formulation actuated into DMEM alone, (iii) nine actuations of a solvent-washed pEGFP-N1 pMDI formulation actuated onto DMEM-containing DOTAP, (iv) nine actuations of placebo pMDI formulation containing HFA 134a and ethanol actuated onto DMEM alone, (v) nine actuations of placebo pMDI formulation containing HFA 134a and ethanol actuated onto DMEM-containing DOTAP and (vi) eighty actuations of placebo pMDI formulation containing HFA 134a and ethanol actuated onto DMEM-containing DOTAP. Data are represented as mean ± SD, $n = 3$. * denotes a significant difference from the control ($p < 0.05$). ** denotes a significant difference from both the control and the treatment with nine actuations ($p < 0.05$).

the cell culture medium. The MTT assay was also used to ascertain the effect of actuation on cell viability. Statistical analysis showed a significant reduction ($p < 0.05$) in cell viability when cells were treated with 80 pMDI-aerosolised doses, compared with 9 doses of the same formulation; this demonstrates the sensitivity of the MTT assay and is likely due to the cold-freon effect of repeated aerosolisations.

## DISCUSSION

Ternary phase microemulsions are made up of three phases: an aqueous phase, organic phase and a surfactant system. In order to maximise the loading capacity of a water-soluble therapeutic molecule such as pDNA, an optimum microemulsion should consist of a large aqueous phase and a small volume of surfactant. Freeze-drying the microemulsion phase serves to remove solvent to leave surfactant-coated particles. If the concentration of surfactant coating the particles is high, the excess surfactant could potentially adversely affect cellular toxicity, particulate dispersibility, the physical stability of the formulation and, ultimately, pDNA transfection functionality. In this study, an optimum microemulsion was found to have a surfactant to water ratio of approximately 1.5. Controlled lyophilisation of the pDNA-incorporated microemulsions enabled the removal of solvent and water to produce surfactant-coated pDNA particles.

DNA integrity, assessed by electrophoresis, was studied following incorporation into the microemulsion, freeze-drying and solvent washing to remove excess surfactant. Although linear DNA forms have also been found to be transfection competent,[45,46] most published literature supports the opinion that pDNA-supercoiled structure should be retained to optimise cellular transfection efficiency[8,47,48] and to comply with regulatory requirements on product quality.[35,40] Analysis of our unprocessed pDNA indicated that 88% (±7%) was in the supercoiled form and this is within the expected range (80–90%) for small-scale, freshly made pDNA preparations.[49] Further analysis of freeze-dried, and freeze-dried then solvent-washed preparations, showed a reduction in the supercoiled fraction to approximately 81% (±12%) and 76% (±14%) respectively. Previous research has demonstrated that jet nebulisation can result in significant loss of pDNA with only 5–60% [36,38,39] of supercoiled pDNA, of a similar size to that of pEGFP-N1, being recoverable after nebulisation compared with non-nebulised control. Our results infer that the process of freeze-drying the pDNA-loaded microemulsion had a comparatively small adverse effect on the supercoiled form and that further processing, via solvent washing, was not particularly detrimental. The relatively small change in supercoiled fraction we observe through processing, that is 88–76%, is similar to that previously observed for spray-dried lipid:protamine:pDNA (LPD) dry powders for inhalation prepared in the presence of a cryoprotectant.[44,50]

Degradation of the supercoiled topology of the pDNA may have detrimental effects on both the safety and transfection efficiency of the pDNA.[35,45,48] Further work is required in optimising procedures to preserve the supercoiled pDNA structure, for example through the use of alternative lyoprotectants. Despite observing a reduction in the supercoiled fraction, initial transfection results showing no significant difference in expression of reporter gene in cells treated with unprocessed pDNA and pDNA following processing for incorporation into a pMDI formulation demonstrate the utility of our processes. Our transfection data also highlight that a washing stage is essential to maintain pDNA functionality, indicating that excess surfactant may reduce formation of the electrostatic lipid:pDNA complex and/or affect interactions of the lipid:pDNA complex with the cell surface. The lecithin surfactant is composed of various substances including anionic lipids. As anionic lipids have been shown to have a strong ability to displace pDNA from cationic lipid:pDNA


DOI 10.1002/jps

complexes,[51] a reduction in transfection may be anticipated. Previous research has shown that anionic surfactants have the ability to reduce transfection efficiency by inducing release of DNA from cationic lipid:DNA complexes before it reaches the target cell.[52,53]

SEM of the aerosolised, washed pEGFP-N1 formulation revealed a continuous matrix (which may be the sticky surfactant system) interspersed with protrusions of a heterogeneous particle population comprising of angular particles (likely to be the sucrose cryoprotectant) and more rounded particles (possibly including surfactant-coated pEGFP-N1 particles). Although micrographs showed that more of these particle protrusions were present at Stage 5 of the ACI (cut off diameter 1.1 μm), the observed larger particle dimensions suggest that particle agglomeration was prevalent. Whilst particles were solvent-washed to remove excess surfactant, the presence of the surfactant, even at a minimal quantity, may have caused the particles to agglomerate as they impacted on the ACI plate. It is also possible that sample heating during SEM processing and analysis may cause particle agglomeration. Further characterisation of discrete particles may have been possible at higher magnifications; however, increasing the magnification resulted in a reduction of the image resolution as the SEM was operating towards its limit.

Visual observations of solvent-washed pDNA formulations in PET vials with time highlighted a number of points. Solvent-washing the surfactant-coated pDNA particles removed the excess surfactant to produce an off-white powder, which initially dispersed in the propellant–cosolvent mixture. Sedimentation of the particles did occur after 24 h but the sedimented particles were readily redispersed by one inversion of the vial confirming the presence of loose floccules. This flocculated system showed no signs of caking following storage at ambient temperatures for 5 months. Surfactants are often incorporated into suspensions to stabilise the drug dispersion by reducing the electrostatic charge of the drug. Observations of a dispersible flocculated system indicate that drug aggregation of the formulation was suitably controlled within the 5-month time span. The lack of solubility of hydrophobic surfactants (e.g. lecithin) in HFA 134a propellant is well documented and commonly requires the use of a co-solvent in commercial formulations. Our observations of a dispersed system suggest that the quantity of surfactant in the solvent-washed formulation fell within the range of that which can be solubilised into the propellant with the aid of ethanol as cosolvent (8%, v/v).

Transfection studies, using various aerosolised formulations, revealed that only the solvent-washed pDNA particles conferred a significant rise in the percentage of fluorescent cells in the presence of DOTAP. This suggests that the solvent-washed pEGFP-N1 particulates remained functionally active following formulation processing, dispersion in propellant and aerosolisation from a pMDI. Statistical analysis showed no significant difference in the percentage of cells expressing GFP following treatment with the washed pEGFP-N1 formulation actuated onto cells without the presence of DOTAP compared with control cells. These data substantiate previous research that a transfection agent is essential in conferring gene expression *in vitro*[8] and acts as a control to confirm that the fluorescence detected during FACS analysis was indeed due to intact pEGFP-N1 transfecting cells with the aid of a transfection agent. These *in vitro* cell culture studies establish that pDNA can be formulated to remain transfection competent when actuated from a pMDI. However, whilst *in vitro* studies are necessary to demonstrate proof of concept, a clear understanding of the barriers encountered *in vivo* is required to progress this work towards clinical therapy. The lungs possess numerous biological barriers and mechanisms that all contribute to the clearance of foreign particles, and therefore hinder their ability to exert any therapeutic effect. The presence of a mucus layer and the mucociliary escalator are crucial in trapping and removing foreign particles in the upper airways. Lung surfactant at the air–water interface not only causes macromolecule aggregation and thus promote particle removal by macrophage engulfment, but has also been shown to interact with cationic lipid:pDNA complexes to reduce pDNA transfection.[52,53] In addition, due to the mechanism of gene transfer, the differences between cell proliferation rates *in vitro* and *in vivo* has revealed significant variation in pDNA transfection efficiency.[8,54]

The absence of effect of washed, aerosolised pEGFP-N1 formulation (without DOTAP) on cell viability is promising. The significant reduction in cell viability in the presence of DOTAP concurs with previously published reports[55,56] and it may be appropriate to explore the use of alternative transfection agents[10,56,57] and 'helper' lipids.[58,59] Indeed, *in vivo* gene expression has been achieved in the past without the use of a transfection agent, although transfection efficiency was found to be relatively low.[9,60]

## CONCLUSION

Methods have been developed and evaluated to freeze-dry pDNA microemulsions to produce surfactant-coated pDNA particles whilst successfully maintaining the integrity of the pDNA. Furthermore, we

have demonstrated that the pDNA particles can be incorporated into a HFA 134a formulation and aerosolised using a standard valve and actuator. The transfection studies demonstrated that the biological functionality of the pDNA can be maintained after aerosolisation from this type of pMDI formulation. Particles prepared by this novel low-energy microemulsion process may have the potential for stable and efficient delivery of pDNA to cells in the lower respiratory tract via pMDIs. Further studies will focus on the requirements for and the effects of transfection agents.

## ACKNOWLEDGMENTS

The authors are grateful to 3M Drug Delivery Systems for their financial support, Phil Jinks (3M) for suggesting and supplying Brilliant Blue pMDIs and to INEOS Fluor for the provision of HFA 134a.

## REFERENCES

1. Birchall J. 2007. Pulmonary delivery of nucleic acids. Expert Opin Drug Deliv 4:575–578.
2. Driskell RA, Engelhardt JF. 2003. Current status of gene therapy for inherited lung diseases. Ann Rev Physiol 65:585–612.
3. Bivas-Benita M, Ottenhoff THM, Junginger HE, Borchard G. 2005. Pulmonary DNA vaccination: Concepts, possibilities and perspectives. J Control Release 107:1–29.
4. Lu D, Hickey AJ. 2007. Pulmonary vaccine delivery. Expert Rev Vaccines 6:213–226.
5. Fennelly GJ, Khan SA, Abadi MA, Wild TF, Bloom BR. 1999. Mucosal DNA vaccine immunization against measles with a highly attenuated Shigella flexneri vector. J Immunol 162: 1603–1610.
6. Bivas-Benita M, van Meijgaarden KE, Franken KLMC, Junginger HE, Borchard G, Ottenhoff THM, Geluk A. 2004. Pulmonary delivery of chitosan-DNA nanoparticles enhances the immunogenicity of a DNA vaccine encoding HLA-A*0201-restricted T-cell epitopes of mycobacterium tuberculosis. Vaccine 22:1609–1615.
7. Harcourt JL, Anderson LJ, Sullender W, Tripp RA. 2004. Pulmonary delivery of respiratory syncytial virus DNA vaccines using macroaggregated albumin particles. Vaccine 22: 2248–2260.
8. Remaut K, Sanders NN, Fayazpour F, Demeester J, De Smedt SC. 2006. Influence of plasmid DNA topology on the transfection properties of DOTAP/DOPE lipoplexes. J Control Release 115:335–343.
9. Zabner J, Cheng SH, Meeker D, Launspach J, Balfour R, Perricone MA, Morris JE, Marshall J, Fasbender A, Smith AE, Welsh MJ. 1997. Comparison of DNA-lipid complexes and DNA alone for gene transfer to cystic fibrosis airway epithelia in vivo. J Clin Invest 100:1529–1537.
10. Jiang HL, Arote R, Jere D, Kim YK, Cho MH, Cho CS. 2008. Degradable polyethylenimines as gene carriers. Mater Sci Technol 24:1118–1126.
11. Davies LA, McLachlan G, Sumner-Jones SG, Ferguson D, Baker A, Tennant P, Gordon C, Vrettou C, Baker E, Zhu J, Alton E, Collie DDS, Porteous DJ, Hyde SC, Gill DR. 2008. Enhanced lung gene expression after aerosol delivery of concentrated pDNA/PEI complexes. Mol Ther 16:1283–1290.
12. De Smedt SC, Demeester J, Hennink WE. 2000. Cationic polymer based gene delivery systems. Pharm Res 17:113–126.
13. Li S-D, Huang L. 2007. Non-viral is superior to viral gene delivery. J Control Release 123:181–183.
14. Ferrari S, Griesenbach U, Geddes DM, Alton E. 2003. Immunological hurdles to lung gene therapy. Clin Exp Immunol 132:1–8.
15. El-Aneed A. 2004. An overview of current delivery systems in cancer gene therapy. J Control Release 94:1–14.
16. Stribling R, Brunette E, Liggitt D, Gaensler K, Debs R. 1992. Aerosol gene delivery in vivo. Proc Natl Acad Sci USA 89: 11277–11281.
17. McDonald RJ, Liggitt HD, Roche L, Nguyen HT, Pearlman R, Raabe OG, Bussey LB, Gorman CM. 1998. Aerosol delivery of lipid: DNA complexes to lungs of rhesus monkeys. Pharm Res 15:671–679.
18. Alton E, Middleton PG, Caplen NJ, Smith SN, Steel DM, Munkonge FM, Jeffery PK, Geddes DM, Hart SL, Williamson R, Fasold KI, Miller AD, Dickinson P, Stevenson BJ, McLachlan G, Dorin JR, Porteous DJ. 1993. Noninvasive liposome-mediated gene delivery can correct the ion-transport defect in cystic-fibrosis mutant mice. Nat Genet 5:135–142.
19. Hyde SC, Gill DR, Higgins CF, Trezise AEO, Macvinish LJ, Cuthbert AW, Ratcliff R, Evans MJ, Colledge WH. 1993. Correction of the ion-transport defect in cystic-fibrosis transgenic mice by gene-therapy. Nature 362:250–255.
20. Logan JJ, Bebok Z, Walker LC, Peng SY, Felgner PL, Siegal GP, Frizzell RA, Dong JY, Howard M, Matalon S, Lindsey JR, Duvall M, Sorscher EJ. 1995. Cationic lipids for reporter gene and CFTR transfer to rat pulmonary epithelium. Gene Ther 2:38–49.
21. Rosenfeld MA, Yoshimura K, Trapnell BC, Yoneyama K, Rosenthal ER, Dalemans W, Fukayama M, Bargon J, Stier LE, Stratfordperricaudet L, Perricaudet M, Guggino WB, Pavirani A, Lecocq JP, Crystal RG. 1992. In vivo transfer of the human cystic-fibrosis transmembrane conductance regulator gene to the airway epithelium. Cell 68:143–155.
22. Canonico AE, Conary JT, Meyrick BO, Brigham KL. 1994. Aerosol and intravenous transfection of human alpha-1-antitrypsin gene to lungs of rabbits. Am J Respir Cell Mol Biol 10: 24–29.
23. Cunningham S, Meng QH, Klein N, McAnulty RJ, Hart SL. 2002. Evaluation of a porcine model for pulmonary gene transfer using a novel synthetic vector. J Gene Med 4:438–446.
24. Alton E, Stern M, Farley R, Jaffe A, Chadwick SL, Phillips J, Davies J, Smith SN, Browning J, Davies MG, Hodson ME, Durham SR, Li D, Jeffery PK, Scallan M, Balfour R, Eastman SJ, Cheng SH, Smith AE, Meeker D, Geddes DM. 1999. Cationic lipid-mediated CFTR gene transfer to the lungs and nose of patients with cystic fibrosis: A double-blind placebo-controlled trial. Lancet 353:947–954.
25. Moss RB, Milla C, Colombo J, Accurso F, Zeitlin PL, Clancy JP, Spencer LT, Pilewski J, Waltz DA, Dorkin HL, Ferkol T, Pian M, Ramsey B, Carter BJ, Martin DB, Heald AE. 2007. Repeated aerosolized AAV-CFTR for treatment of cystic fibrosis: A randomized placebo-controlled phase 2B trial. Hum Gene Ther 18:726–732.
26. Ruiz FE, Clancy JP, Perricone MA, Bebok Z, Hong JS, Cheng SH, Meeker DP, Young KR, Schoumacher RA, Weatherly MR, Wing L, Morris JE, Sindel L, Rosenberg M, van Ginkel FW, McGhee JR, Kelly D, Lyrene RK, Sorscher EJ. 2001. A clinical inflammatory syndrome attributable to aerosolized lipid-DNA administration in cystic fibrosis. Hum Gene Ther 12:751–761.
27. Hyde SC, Southern KW, Gileadi U, Fitzjohn EM, Mofford KA, Waddell BE, Gooi HC, Goddard CA, Hannavy K, Smyth SE, Egan JJ, Sorgi FL, Huang L, Cuthbert AW, Evans MJ, Colledge

WH, Higgins CF, Webb AK, Gill DR. 2000. Repeat administration of DNA/liposomes to the nasal epithelium of patients with cystic fibrosis. Gene Ther 7:1156–1165.
28. Brigham KL, Lane KB, Meyrick B, Stecenko AA, Strack S, Cannon DR, Caudill M, Canonico AE. 2000. Transfection of nasal mucosa with a normal alpha(1)-antitrypsin gene in alpha(1)-antitrypsin-deficient subjects: Comparison with protein therapy. Hum Gene Ther 11:1023–1032.
29. Brantly ML, Spencer LT, Humphries M, Conlon TJ, Spencer CT, Poirier A, Garlington W, Baker D, Song SH, Berns KI, Muzyczka N, Snyder RO, Byrne BJ, Flotte TR. 2006. Phase I trial of intramuscular injection of a recombinant adeno-associated virus serotype 2 alpha(1)-antitrypsin (AAT) vector in AAT-deficient adults. Hum Gene Ther 17:1177–1186.
30. Ferrari S, Geddes DM, Alton EW. 2002. Barriers to and new approaches for gene therapy and gene delivery in cystic fibrosis. Adv Drug Deliv Rev 54:1373–1393.
31. Ratjen F. 2008. Recent advances in cystic fibrosis. Paediatr Respir Rev 9:144–148.
32. Agu RU, Ugwoke MI, Armand M, Kinget R, Verbeke N. 2001. The lung as a route for systemic delivery of therapeutic proteins and peptides. Respir Res 2:198–209.
33. Robinson BWS, Erle DJ, Jones DA, Shapiro S, Metzger WJ, Albelda SM, Parks WC, Boylan A. 2000. Recent advances in molecular biological techniques and their relevance to pulmonary research. Thorax 55:329–339.
34. Moss RB, Rochman D, Spencer LT, Aitken ML, Zeitlhi PL, Waltz D, Milla C, Brody AS, Clancy JP, Ramsey B, Hamblett N, Heald AE. 2004. Repeated adeno-associated virus serotype 2 aerosol-mediated cystic fibrosis transmembrane regulator gene transfer to the lungs of patients with cystic fibrosis—A multicenter, double-blind, placebo-controlled trial. Chest 125:509–521.
35. Arulmuthu ER, Williams DJ, Baldascini H, Versteeg HK, Hoare M. 2007. Studies on aerosol delivery of plasmid DNA using a mesh nebulizer. Biotechnol Bioeng 98:939–955.
36. Birchall JC, Kellaway IW, Gumbleton M. 2000. Physical stability and in-vitro gene expression efficiency of nebulised lipid-peptide-DNA complexes. Int J Pharm 197:221–231.
37. Lentz YK, Anchordoquy TJ, Lengsfeld CS. 2006. DNA acts as a nucleation site for transient cavitation in the ultrasonic nebulizer. J Pharm Sci 95:607–619.
38. Lentz YK, Worden LR, Anchordoquy TJ, Lengsfeld CS. 2005. Effect of jet nebulization on DNA: Identifying the dominant degradation mechanism and mitigation methods. J Aerosol Sci 36:973–990.
39. Kleemann E, Dailey LA, Abdelhady HG, Gessler T, Schmehl T, Roberts CJ, Davies MC, Seeger W, Kissel T. 2004. Modified polyethylenimines as non-viral gene delivery systems for aerosol gene therapy: Investigations of the complex structure and stability during air-jet and ultrasonic nebulization. J Control Release 100:437–450.
40. Davies LA, Hannavy K, Davies N, Pirrie A, Coffee RA, Hyde SC, Gill DR. 2005. Electrohydrodynamic comminution: A novel technique for the aerosolisation of plasmid DNA. Pharm Res 22:1294–1304.
41. Dolovich MB, Ahrens RC, Hess DR, Anderson P, Dhand R, Rau JL, Smaldone GC, Guyatt G. 2005. Device selection and outcomes of aerosol therapy: Evidence-based guidelines. Chest 127:335–371.
42. Brown AR, Chowdhury SI. 1997. Propellant-driven aerosols of DNA plasmids for gene expression in the respiratory tract. J Aerosol Med 10:129–146.
43. Dickinson PA, Howells SW, Kellaway IW. 2001. Novel nanoparticles for pulmonary drug administration. J Drug Target 9:295–302.
44. Seville PC, Kellaway IW, Birchall JC. 2002. Preparation of dry powder dispersions for non-viral gene delivery by freeze-drying and spray-drying. J Gene Med 4:428–437.
45. Chancham P, Hughes JA. 2001. Relationship between plasmid DNA topological forms and in vitro transfection. J Liposome Res 11:139–152.
46. von Groll A, Levin Y, Barbosa MC, Ravazzolo AP. 2006. Linear DNA low efficiency transfection by liposome can be improved by the use of cationic lipid as charge neutralizer. Biotechnol Prog 22:1220–1224.
47. Even-Chen S, Barenholz Y. 2000. DOTAP cationic liposomes prefer relaxed over supercoiled plasmids. Biochim Biophys Acta—Biomembranes 1509:176–188.
48. Cherng JY, Schuurmans-Nieuwenbroek NME, Jiskoot W, Talsma H, Zuidam NJ, Hennink WE, Crommelin DJA. 1999. Effect of DNA topology on the transfection efficiency of poly((2-dimethylamino)ethyl methacrylate)-plasmid complexes. J Control Release 60:343–353.
49. Middaugh CR, Evans RK, Montgomery DL, Casimiro DR. 1998. Analysis of plasmid DNA from a pharmaceutical perspective. J Pharm Sci 87:130–146.
50. Li HY, Seville PC, Williamson IJ, Birchall JC. 2005. The use of absorption enhancers to enhance the dispersibility of spray-dried powders for pulmonary gene therapy. J Gene Med 7: 1035–1043.
51. Xu Y, Szoka FC, Jr. 1996. Mechanism of DNA release from cationic liposome/DNA complexes used in cell transfection. Biochemistry 35:5616–5623.
52. Tsan MF, Tsan GL, White JE. 1997. Surfactant inhibits cationic liposome-mediated gene transfer. Hum Gene Ther 8:817–825.
53. Duncan JE, Whitsett JA, Horowitz AD. 1997. Pulmonary surfactant inhibits cationic liposome-mediated gene delivery to respiratory epithelial cells in vitro. Hum Gene Ther 8:431–438.
54. Wilke M, Fortunati E, vandenBroek M, Hoogeveen AT, Scholte BJ. 1996. Efficacy of a peptide-based gene delivery system depends on mitotic activity. Gene Ther 3:1133–1142.
55. Chiaramoni NS, Speroni L, Taira MC, Alonso SDV. 2007. Liposome/DNA systems: Correlation between association, hydrophobicity and cell viability. Biotechnol Lett 29:1637–1644.
56. Choi W-J, Kim J-K, Choi S-H, Park J-S, Ahn WS, Kim C-K. 2004. Low toxicity of cationic lipid-based emulsion for gene transfer. Biomaterials 25:5893–5903.
57. Prata CA, Zhang XX, Luo D, McIntosh TJ, Barthelemy P, Grinstaff MW. 2008. Lipophilic peptides for gene delivery. Bioconjug Chem 19:418–420.
58. Felgner JH, Kumar R, Sridhar CN, Wheeler CJ, Tsai YJ, Border R, Ramsey P, Martin M, Felgner PL. 1994. Enhanced gene delivery and mechanism studies with a novel series of cationic lipid formulations. J Biol Chem 269:2550–2561.
59. Bennett MJ, Nantz MH, Balasubramaniam RP, Gruenert DC, Malone RW. 1995. Cholesterol enhances cationic liposome-mediated DNA transfection of human respiratory epithelial cells. Biosci Rep 15:47–53.
60. Xenariou S, Griesenbach U, Liang HD, Zhu J, Farley R, Somerton L, Singh C, Jeffery PK, Ferrari S, Scheule RK, Cheng SH, Geddes DM, Blomley M, Alton E. 2007. Use of ultrasound to enhance nonviral lung gene transfer in vivo. Gene Ther 14:768–774.